

# CHAPTER III - SUMMARY OF WESTERN NORTH PACIFIC AND NORTH INDIAN OCEAN TROPICAL CYCLONES

## 1. GENERAL

During 1985, JTWC issued warnings on 27 western North Pacific tropical cyclones (1 tropical depression, 9 tropical storms, 16 typhoons and one super-typhoon). This was almost an average year when compared to the climatological mean of 27 for the frequency of tropical storms and typhoons. Six north Indian Ocean tropical cyclones, all of tropical storm intensity, developed as compared to the climatological average of four. In summary, JTWC issued warnings on 33 northern hemisphere tropical cyclones.

In 1985 for the western North Pacific there were 127 warning days - a warning day is defined as a day during which JTWC issues warnings on at least one tropical cyclone. For 38 of these 127 days, warnings were being issued on two tropical cyclones. There were also 2 three-cyclone days, 2 four-cyclone days, and one day in which JTWC issued warnings on five different WESTPAC tropical cyclones at the same time. When the north Indian Ocean tropical cyclones are included, there were 141 warning days, 41 two-cyclone days, 3 three-cyclone days, 3 four-cyclone days and 1 five-cyclone day.

Six hundred and fifteen warnings were issued on the 27 western North Pacific tropical cyclones and 54 were issued on the six north Indian Ocean tropical cyclones. There were 39 initial Tropical Cyclone Formation Alerts (TCFA) for WESTPAC and 8 for the north Indian Ocean. In WESTPAC, TCFAs were issued for all except one of the significant tropical cyclones that developed during 1985. The false alarm rate of 33% for WESTPAC seems fairly high, however, it did enable JTWC to provide the customer with an mean lead time of 27.5 hours on significant tropical cyclone development. For the North Indian Ocean TCFAs were issued for all but one of the significant tropical cyclones. The false alarm rate for TCFAs was 38% with a mean lead time of 20.2 hours.

## 2. WESTERN NORTH PACIFIC TROPICAL CYCLONES

There are several interesting aspects of the 1985 tropical cyclone activity. In general, it can be neatly divided into two periods: the early part, January to August and the late, September to December (see composite tropical cyclone best tracks on pages 15 and 16). The early 1985 composite best tracks show that the overwhelming majority of the tropical

cyclones during that period recurved, that is: 11 recurvers versus 3 west-northwest straight runners and one low-latitude tropical storm (Fabian) which behaved erratically. This is somewhat atypical since, normally, the majority of the recurvers occur during the later part of the year when breaks in the subtropical high pressure ridge develop as the influence of the mid-latitude troughs extends further south with the approach of fall. The Philippine Islands were spared during the first part of the year, except for a glancing blow from Typhoon Hal in June. However, during that period, no less than 8 tropical cyclones affected, or posed a direct threat to, Okinawa, Korea and Japan. In some cases the same tropical cyclone affected all three. Notice the point 200 nm (370km) south-southeast of Okinawa - four, and nearly five, different tropical cyclone tracks intersected at that location. The major generation areas during the first part of the year were: a two-to-three degree swath centered on six degrees north latitude, from the southeastern coast of the Philippine Islands to near Ponape; another area north of Guam; and a third area south of Okinawa.

A major shift in tropical cyclone activity occurred during the second part of the year (see composite best tracks on page 16). Notice that only 2 tropical cyclones recurved. Whereas, Japan and Korea received the brunt of the tropical cyclone activity the first half of the year, it was the Philippines and Vietnam which suffered most during the second. Three typhoons and one supertyphoon transited Luzon. In addition, one typhoon crossed the southern Philippine Islands. Three typhoons affected northern Vietnam and a total of 4 typhoons and 4 tropical storms struck the Asian mainland from southern Vietnam to the vicinity of Hong Kong. The major generation areas were: one west of Palawan Island in the South China Sea, and the other south and southeast of Guam. This contrasts with the first part of the year, when generation locations were more evenly distributed over WESTPAC.

In the western North Pacific, tropical cyclones reaching tropical storm intensity, or greater, are assigned names in alphabetical order from a list of alternating male/female names (refer to Appendix II). Table 3-1 provides a summary of key statistics for all western North Pacific tropical cyclones. Each tropical cyclone's maximum surface wind and minimum sea-level pressure (in millibars) were obtained from best estimates based on all available data. The distance traveled was calculated from the JTWC official best tracks (see Annex A).

Tables 3-2 through 3-5 provide further information on the monthly and yearly distribution of tropical cyclones, warnings and Tropical Cyclone Formation Alerts.

TABLE 3-1.

WESTERN NORTH PACIFIC  
1985 SIGNIFICANT TROPICAL CYCLONES

TROPICAL CYCLONE	PERIOD OF WARNING	CALENDAR DAYS OF WARNING	NUMBER OF WARNINGS ISSUED	MAXIMUM SURFACE WINDS-KT (M/S)	ESTIMATED MSLP- MB	BEST TRACK DISTANCE TRAVELED-NM (KM)
01W TS ELSIE	07 JAN - 09 JAN	3	9	40 (21)	995	976 (1808)
02W TS FABIAN	09 JAN - 13 JAN	5	16	55 (28)	989	507 (939)
03W TY GAY	21 MAY - 26 MAY	6	22	100 (51)	951	1464 (2711)
04W TD 04W	18 JUN - 20 JUN	3	10	30 (15)	992	441 (817)
05W TY HAL	19 JUN - 25 JUN	6	22	100 (51)	942	1305 (2417)
06W TY IRMA	25 JUN - 01 JUL	7	27	90 (46)	957	2413 (4469)
07W TY JEFF	22 JUL - 02 AUG	12	43	75 (39)	967	2668 (4941)
08W TY KIT	03 AUG - 11 AUG	9	33	85 (44)	959	1953 (3617)
09W TS LEE	11 AUG - 14 AUG	4	15	60 (31)	985	1326 (2456)
10W TY MAMIE	16 AUG - 20 AUG	5	17	70 (36)	975	1335 (2472)
11W TY NELSON	17 AUG - 24 AUG	8	27	95 (49)	961	1651 (3058)
12W TY ODESSA	23 AUG - 01 SEP	10	39	90 (46)	957	2328 (4311)
13W TY PAT	27 AUG - 01 SEP	6	23	95 (49)	961	1337 (2476)
14W TS RUBY	28 AUG - 01 SEP	5	19	55 (28)	982	1310 (2426)
02C TY SKIP	30 AUG - 08 SEP	10	34	80 (41)	974	1822 (3374)
15W TY TESS	01 SEP - 06 SEP	7	22	75 (39)	967	1470 (2722)
16W TS VAL	15 SEP - 18 SEP	4	14	50 (26)	992	1630 (3019)
17W TS WINONA	19 SEP - 22 SEP	4	11	50 (26)	990	518 (959)
18W TY ANDY	28 SEP - 02 OCT	5	16	70 (36)	970	705 (1306)
19W TY BRENDA	29 SEP - 05 OCT	7	25	90 (46)	964	1551 (2872)
20W TY CECIL	12 OCT - 16 OCT	5	16	100 (51)	944	1034 (1915)
21W STY DOT	13 OCT - 22 OCT	10	34	150 (77)	897	3074 (5693)
22W TS ELLIS	16 OCT - 20 OCT	5	19	50 (26)	995	1046 (1937)
23W TY FAYE	23 OCT - 01 NOV	10	39	100 (51)	960	1849 (3424)
24W TS GORDON	20 NOV - 26 NOV	7	23	45 (23)	997	797 (1476)
25W TY HOPE	17 DEC - 24 DEC	8	26	100 (51)	948	1444 (2674)
26W TS IRVING	18 DEC - 21 DEC	4	14	60 (31)	994	806 (1493)

1985 TOTALS: 127\* 715

\* OVERLAPPING DAYS INCLUDED ONLY ONCE IN SUM.

TABLE 3-2.

1985 SIGNIFICANT TROPICAL CYCLONES

WESTERN NORTH PACIFIC	JAN	FEB	MAR	APR	MAY	JUN	JUL	AUG	SEP	OCT	NOV	DEC	TOTAL	(1959-1985) AVERAGE	CASES
TROPICAL DEPRESSIONS	0	0	0	0	0	1	0	0	0	0	0	0	1	3.7	99
TROPICAL STORMS	2	0	0	0	0	0	0	2	2	1	1	1	9	9.9	268
TYPHOONS	0	0	0	0	1	2	1	5	3	4	0	1	17	17.3	468
ALL TROPICAL CYCLONES	2	0	0	0	1	3	1	7	5	5	1	2	27	30.9	835
1959 - 1985 AVERAGE	.6	.3	.7	.8	1.3	2.0	4.7	6.3	5.7	4.6	2.6	1.4	30.9		
CASES	15	8	18	22	34	54	128	170	153	124	71	38	835		

FORMATION ALERTS: 26 of 39 Formation Alerts developed into significant tropical cyclones. Tropical Cyclone Formation Alerts were issued for all except one of the significant tropical cyclones that developed in 1985.

WARNINGS: Number of calendar warning days: 127  
Number of calendar warning days with two tropical cyclones in region: 32  
Number of calendar warning days with three or more tropical cyclones in region: 6

TABLE 3-3.

## FREQUENCY OF TYPHOONS BY MONTH AND YEAR

YEAR	JAN	FEB	MAR	APR	MAY	JUN	JUL	AUG	SEP	OCT	NOV	DEC	TOTAL
(1945-1958) AVERAGE	.4	.1	.3	.4	.7	1.1	2.0	2.9	3.2	2.4	2.0	.9	16.3
1959	0	0	0	1	0	0	1	5	3	3	2	2	17
1960	0	0	0	1	0	2	2	8	0	4	1	1	19
1961	0	0	1	0	2	1	3	3	5	3	1	1	20
1962	0	0	0	1	2	0	5	7	2	4	3	0	24
1963	0	0	0	1	1	2	3	3	3	4	0	2	19
1964	0	0	0	0	2	2	6	3	5	3	4	1	26
1965	1	0	0	1	2	2	4	3	5	2	1	0	21
1966	0	0	0	1	2	1	3	6	4	2	0	1	20
1967	0	0	1	1	0	1	3	4	4	3	3	0	20
1968	0	0	0	1	1	1	1	4	3	5	4	0	20
1969	1	0	0	1	0	0	2	3	2	3	1	0	13
1970	0	1	0	0	0	1	0	4	2	3	1	0	12
1971	0	0	0	3	1	2	6	3	5	3	1	0	24
1972	1	0	0	0	1	1	4	4	3	4	2	2	22
1973	0	0	0	0	0	0	4	2	2	4	0	0	12
1974	0	0	0	0	1	2	1	2	3	4	2	0	15
1975	1	0	0	0	0	0	1	3	4	3	2	0	14
1976	1	0	0	1	2	2	2	1	4	1	1	0	15
1977	0	0	0	0	0	0	3	0	2	3	2	1	11
1978	0	0	0	1	0	0	3	2	4	3	2	0	15
1979	1	0	1	1	0	0	2	2	3	2	1	1	14
1980	0	0	0	0	2	0	3	2	5	2	1	0	15
1981	0	0	1	0	0	2	2	2	4	1	2	2	16
1982	0	0	2	0	1	1	2	5	3	3	1	1	19
1983	0	0	0	0	0	0	3	2	1	4	2	0	12
1984	0	0	0	0	0	0	4	2	1	5	3	1	16
1985	0	0	0	0	1	2	1	5	3	4	0	1	17
(1959 - 1985) AVERAGE	.2	.04	.2	.6	.8	.9	2.7	3.3	3.1	3.1	1.6	.6	17.3
CASES	6	1	6	15	21	25	74	90	85	85	43	17	468

TABLE 3-4.

## FREQUENCY OF TROPICAL STORMS AND TYPHOONS BY MONTH AND YEAR

YEAR	JAN	FEB	MAR	APR	MAY	JUN	JUL	AUG	SEP	OCT	NOV	DEC	TOTAL
(1945-1958) AVERAGE	.4	.1	.4	.5	.8	1.3	3.0	3.9	4.1	3.3	2.7	1.1	21.6
1959	0	1	1	1	0	0	3	6	6	4	2	2	26
1960	0	0	0	1	1	3	3	10	3	4	1	1	27
1961	1	1	1	1	3	2	5	4	6	5	1	1	31
1962	0	1	0	1	2	0	6	7	3	5	3	2	30
1963	0	0	0	1	1	3	4	3	5	5	0	3	25
1964	0	0	0	0	2	2	7	9	7	6	6	1	40
1965	2	2	1	1	2	3	5	6	7	2	2	1	34
1966	0	0	0	1	2	1	5	8	7	3	2	1	30
1967	1	0	2	1	1	1	6	8	7	4	3	1	35
1968	0	0	0	1	1	1	3	8	3	6	4	0	27
1969	1	0	1	1	0	0	3	4	3	3	2	1	19
1970	0	1	0	0	0	2	2	6	4	5	4	0	24
1971	1	0	1	3	4	2	8	4	6	4	2	0	35
1972	1	0	0	0	1	3	6	5	4	5	2	3	30
1973	0	0	0	0	0	0	7	5	2	4	3	0	21
1974	1	0	1	1	1	4	4	5	5	4	4	2	32
1975	1	0	0	0	0	0	2	4	5	5	3	0	20
1976	1	1	0	2	2	2	4	4	5	1	1	2	25
1977	0	0	1	0	0	1	4	1	5	4	2	1	19
1978	1	0	0	1	0	3	4	7	5	4	3	0	28
1979	1	0	1	1	1	0	4	2	7	3	2	2	24
1980	0	0	0	1	4	1	4	2	6	4	1	1	24
1981	0	0	1	2	0	2	5	7	4	2	3	2	28
1982	0	0	3	0	1	3	4	5	5	3	1	1	26
1983	0	0	0	0	0	1	3	5	2	5	5	2	23
1984	0	0	0	0	0	2	5	5	4	7	3	1	27
1985	2	0	0	0	1	2	1	7	5	5	1	2	26
(1959-1985) AVERAGE	.5	.3	.5	.8	1.1	1.6	4.3	5.4	4.9	4.1	2.4	1.2	27.3
CASES	14	7	14	21	30	44	117	147	131	112	66	33	736

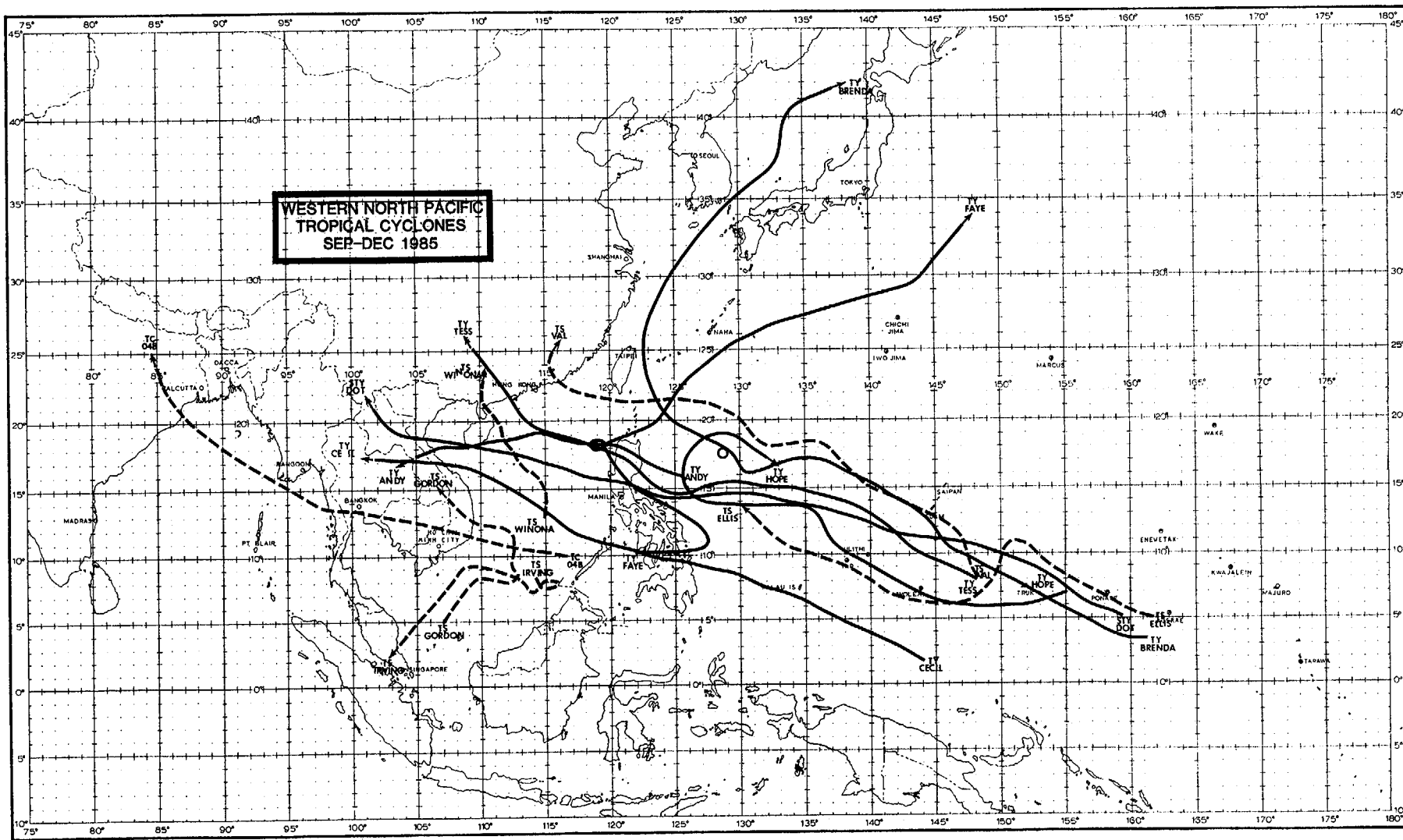
TABLE 3-5.

## FORMATION ALERT SUMMARY

## WESTERN NORTH PACIFIC

<u>YEAR</u>	<u>NUMBER OF ALERT SYSTEMS</u>	<u>ALERT SYSTEMS WHICH BECAME NUMBERED TROPICAL CYCLONES</u>	<u>TOTAL NUMBERED TROPICAL CYCLONES</u>	<u>DEVELOPMENT RATE</u>
1975	34	25	25	74%
1976	34	25	25	74%
1977	26	20	21	77%
1978	32	27	32	84%
1979	27	23	28	85%
1980	37	28	28	76%
1981	29	28	29	97%
1982	36	26	28	72%
1983	31	25	25	81%
1984	37	30	30	81%
1985	39	26	27	67%
(1975-1985) AVERAGE	32.9	25.7	27.1	78%
CASES	362	283	298	







Tropical Storm Elsie, the first tropical cyclone of the 1985 season, was also the first tropical storm to develop during January in six years. Warnings were issued for only two days and it never intensified beyond 40 kt (21 m/s).

During the first week of January the near-equatorial trough was quite active, and extended from the southern Philippines southeast to the vicinity of the Equator and 160E. Embedded in this trough were two weak circulations, one southwest of Guam which would later develop into Tropical Storm Fabian and another southeast of Guam which would eventually develop into Elsie. Enhanced convective activity persisted throughout the region.

The cloud system that was to become Elsie first appeared on 4 January as an area of weak convection southwest of Pohnpei (Ponape WMO 91348). The convection persisted through the 4th, and on the 5th began to increase in strength and organization. At 0000Z on the 6th, analysis of satellite imagery gave the first indications that a low-level circulation center was developing. Sparse synoptic data up to this time had only indicated that a very broad 10 to 15 kt (5 to 8 m/s) cyclonic circulation was present. The persistence and improved organization of the convection resulted in the disturbance being mentioned in the 060600Z Significant Tropical Weather Advisory (ABEH PGIW). The disturbance was assessed as having a "fair" potential for further development (meaning that it was considered likely that a TCFA would be issued during the next 24 hours). Indeed, this was the case.

Analysis of satellite imagery during the next ten hours showed continued development, with Dvorak intensity analysis of the 061600Z imagery estimating surface winds of 25 kt (13 m/s). This was confirmed by a late 061200Z ship report near the Mortlock Islands (Satawan Atoll WMO 91338) which observed northwest winds of 30 kt (15 m/s). As a

result, a TCFA was issued at 061700Z.

Just prior to 070000Z, the first aircraft reconnaissance mission was conducted into the disturbance. It located a 25 kt (13 m/s) circulation center at 062238Z approximately 60 nm (111 km) northeast of the Mortlock Islands near 5.8N 154.4E. As the WC-130 exited to the southwest a short time later, a small area of 30 kt (15 m/s) surface winds was observed. This prompted the first warning on Elsie, as a 30 kt (15 m/s) tropical depression, valid at 070000Z.

Elsie was upgraded to a 35 kt (18 m/s) tropical storm at 070600Z based on synoptic data received from the Mortlock Islands. The tropical cyclone briefly attained an intensity of 40 kt at 071200Z.

From the time Elsie was detected until the time JTWC went to warning status, the disturbance had moved to the northwest at about 7 kts (13 km/hr). After 070000Z, however, Elsie accelerated to the northwest as it moved around the western periphery of the subtropical ridge, passing east of Truk (WMO 91334) at about 071000Z. As Elsie moved further north (Figure 3-01-1) it encountered strong southerly winds aloft from an upper-level anticyclone south of Wake Island (WMO 91245). These winds sheared off the central convection. As a result, Elsie quickly lost all organization and rapidly weakened. Its low-level circulation could not be located on satellite imagery or by aircraft reconnaissance after 082100Z. The final warning was issued at 090000Z.

As Elsie passed east of Guam it did enhance the tradewinds, with gusts to 31 kt (16 m/s) observed at the U. S. Naval Oceanography Command Center/Joint Typhoon Warning Center building on Nimitz Hill. After Elsie dissipated, a secondary circulation formed in its wake near Guam and persisted for two days until it also moved to the northeast and dissipated.

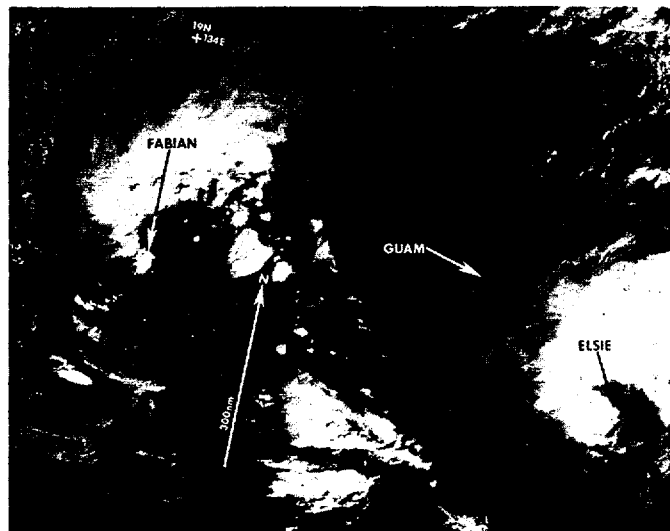
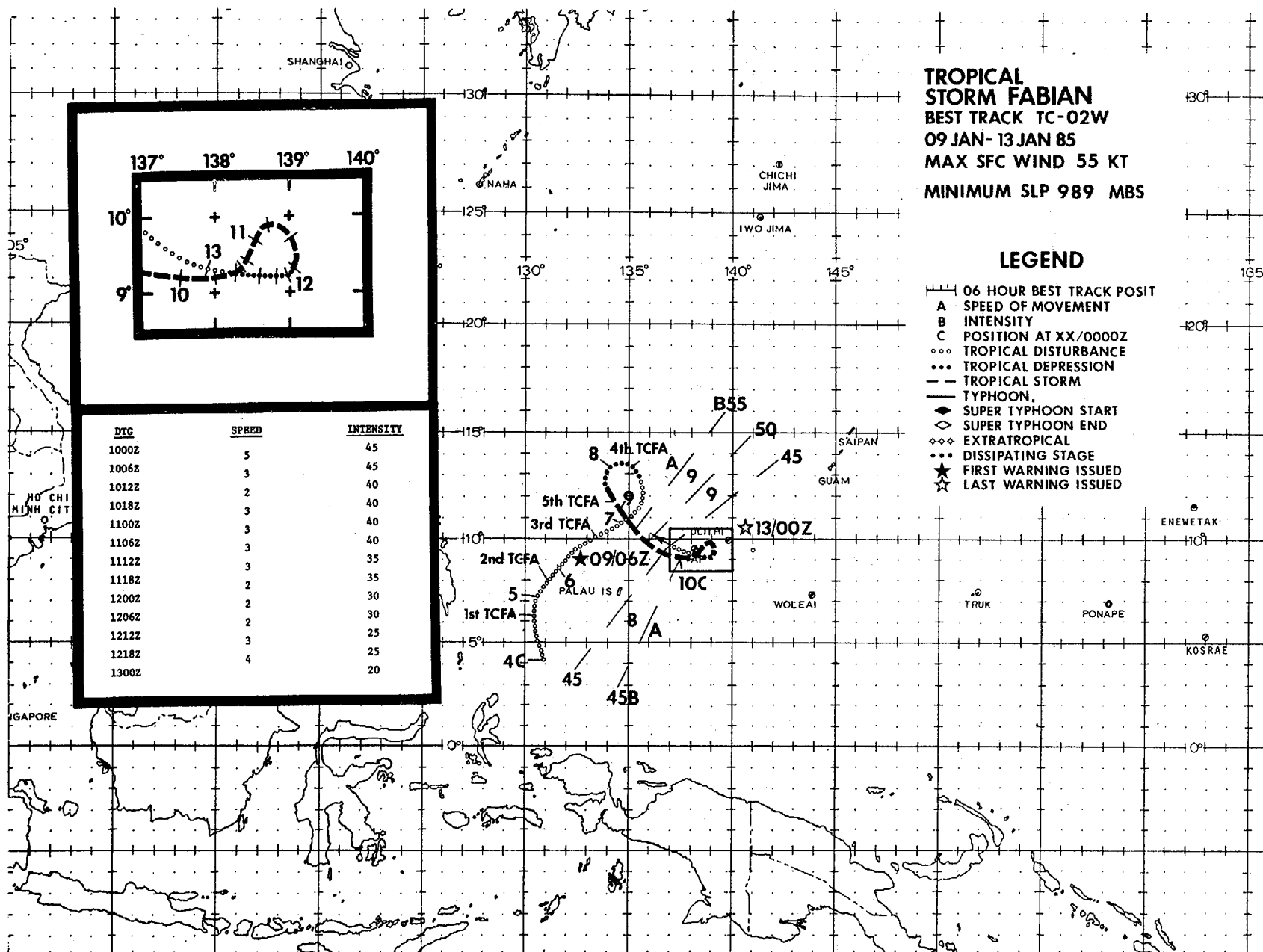


Figure 3-01-1. Tropical Storm Elsie weakening southeast of Guam. Later, strong upper-level winds north of Elsie sheared away the central convection. Rapid weakening and dissipation quickly followed. (The disturbance that would soon develop into Tropical Storm Fabian is located to the northwest of Elsie) (080047Z January DMSP visual imagery).





TROPICAL STORM FABIAN (02W)

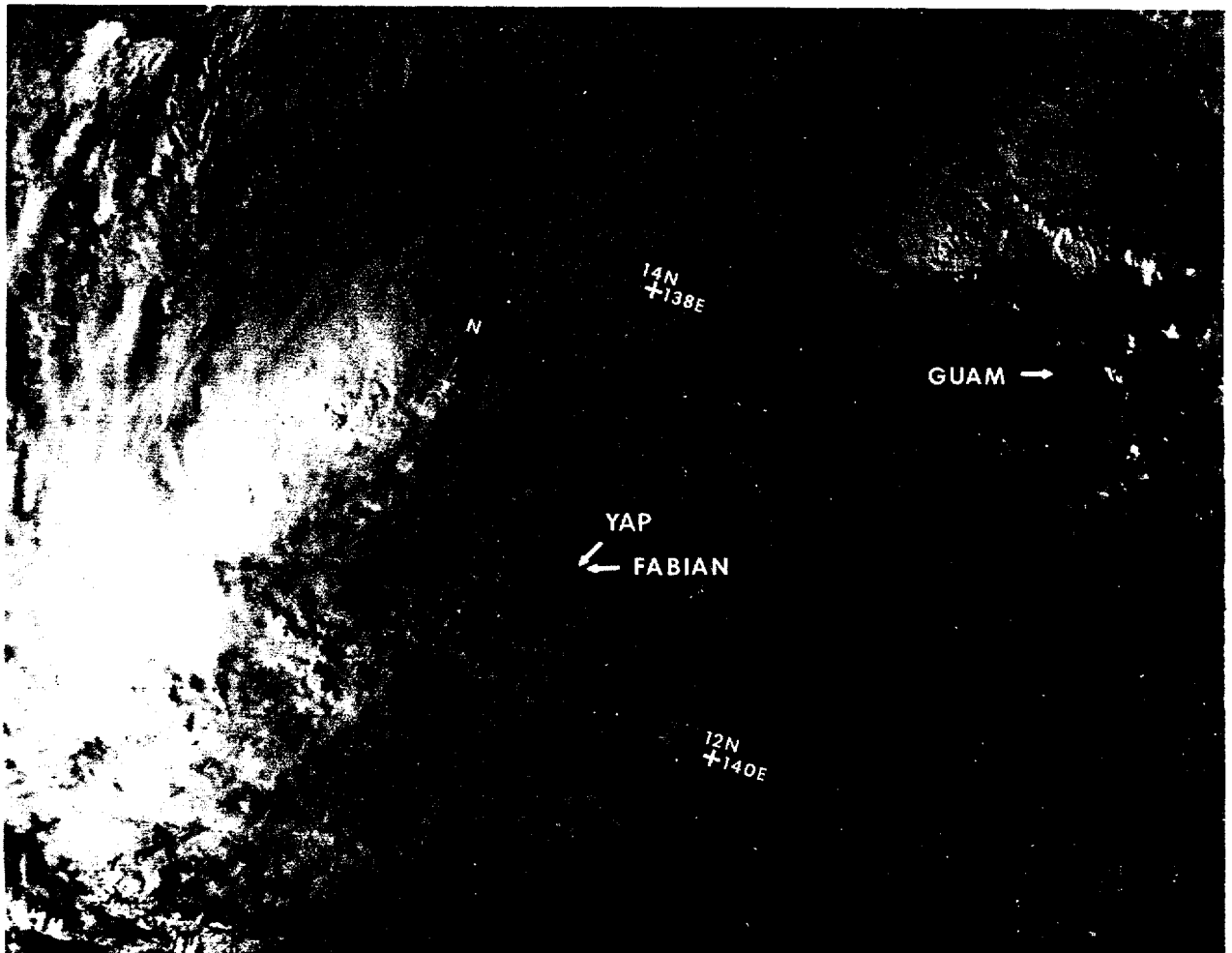


Figure 3-02-1. The development of Tropical Storm Fabian marked the first time in twenty years that two tropical storms formed in WESTPAC during January. Fabian developed at the western end of the near-equatorial trough, and as a result had major interactions with the northeast monsoon. Not surprisingly, the strongest winds were consistently observed in the tropical cyclone's western semi-circle, where the gradient between the low central pressure of Fabian and the higher pressures of the Siberian anticyclone was the greatest. The [above] satellite imagery shows Fabian, as a weakening Tropical Storm, with a well-defined low-level circulation. Fabian's low-level circulation was exposed for much of its lifetime due to strong upper-level winds from the south which sheared the convection to the north. The Tropical Storm passed very close to Yap (WMO 91413) and caused considerable crop damage on some of the outer islands (100630Z January NOAA visual imagery).

# TYPHOON

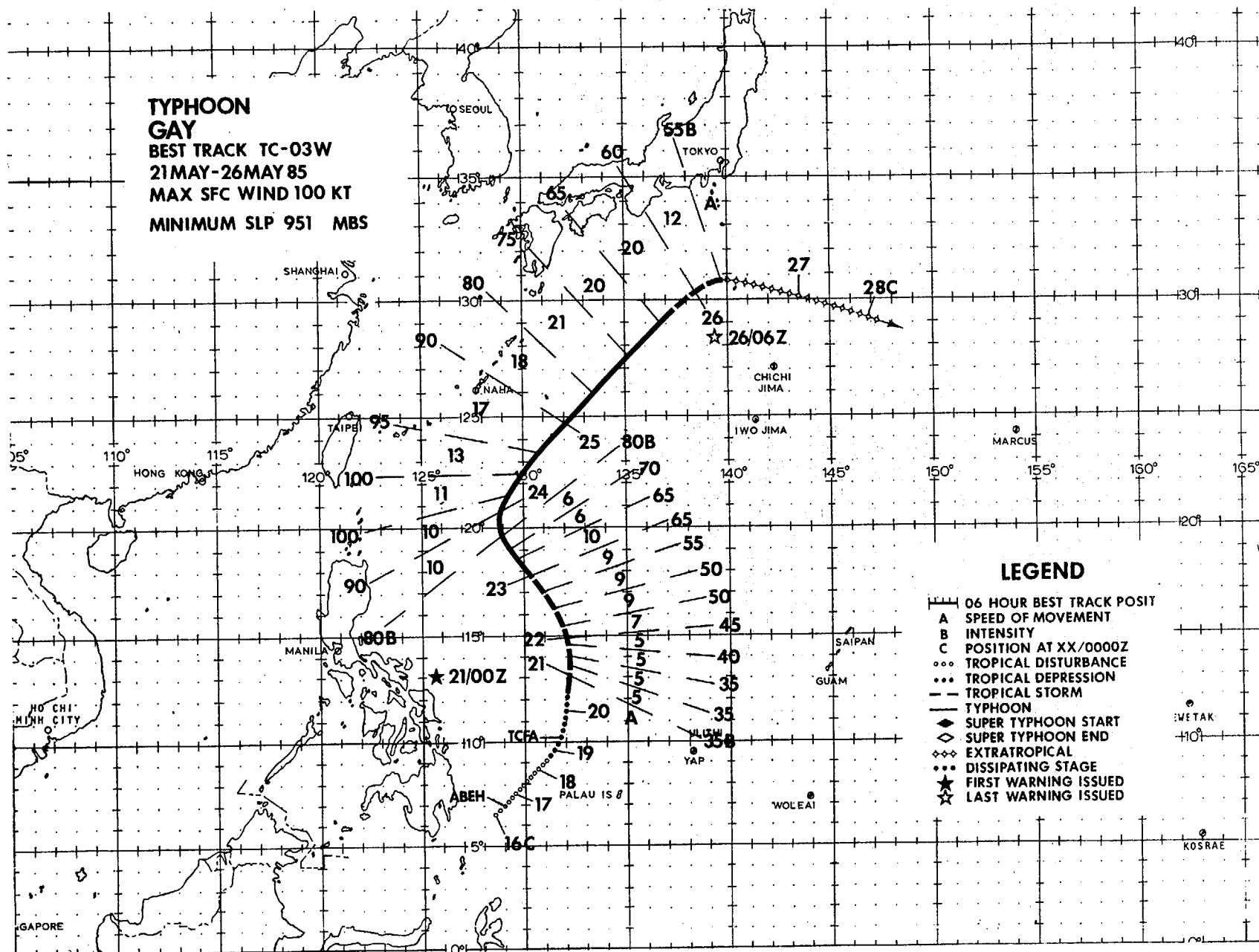
## GAY

BEST TRACK TC-03W

21 MAY-26 MAY 85

MAX SFC WIND 100 KT

MINIMUM SLP 951 MBS



### LEGEND

- 06 HOUR BEST TRACK POSIT
- A SPEED OF MOVEMENT
- B INTENSITY
- C POSITION AT XX/0000Z
- ... TROPICAL DISTURBANCE
- ... TROPICAL DEPRESSION
- ... TROPICAL STORM
- ... TYPHOON
- ◆ SUPER TYPHOON START
- ◇ SUPER TYPHOON END
- ◇◇ EXTRATROPICAL
- ... DISSIPATING STAGE
- ★ FIRST WARNING ISSUED
- ☆ LAST WARNING ISSUED

Typhoon Gay was the first tropical cyclone to reach typhoon intensity in 1985. It was also the season's first to enter the mid-latitude westerlies and recurve. The formation of Gay followed more than four months of inactivity in WESTPAC and marked the start of the 1985 summer tropical cyclone season.

The tropical disturbance that eventually intensified into Typhoon Gay was first detected by synoptic data on 16 May as a weak surface circulation 380 nm (704 km) west-southwest of Koror (WMO 91408). The convection in this area appeared to be random. Another area of disorganized convection was developing further east along 139E under an area of upper-level diffluence associated with a westward moving upper-level anticyclone. To the north, a tropical upper-tropospheric trough (TUTT) extended from the Volcano Islands southwest to just east of the Philippines. Figure 3-03-1 shows the movements and locations of the upper-level anticyclonic and low-level cyclonic circulations over a five day period as Gay went through its formative stages. Although the upper-level and low-level circulations became nearly vertically aligned on 19 May, the disturbance still struggled for two more days before reaching tropical storm intensity. The most probable cause for this slow intensification was the close proximity of the TUTT to the north, which restricted the upper-level outflow to the northwest (Figure 3-03-2).

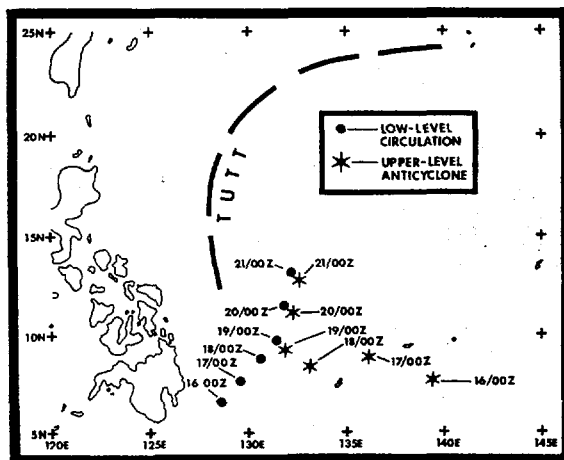


Figure 3-03-1. These plots show the positions and movements of the upper-level anticyclonic and low-level cyclonic circulations during Gay's formative period. The juxtaposition of these upper- and low-level circulations on 19 May usually indicates the tropical cyclone is reaching maturity. However, the presence of the TUTT to the north and northwest is thought to have impeded development through the 21st.

Between 0000Z and 0600Z on the 19th two different tactical DMSP sites, based upon Dvorak intensity analyses of satellite imagery, estimated that the disturbance had 30 kt (15 m/s) surface winds. These increased intensity estimates were founded on the more organized intense convection associated with the upper-level circulation center, which was then displaced approximately 50 nm (93 km) southeast of the surface center. These satellite reconnaissance inputs prompted a TCFA to be issued at 190800Z. At the time of the TCFA, sparse synoptic data near the disturbance center could not confirm the satellite derived intensities. However, synoptic data on the periphery of the disturbance implied that at least a 15 kt (8 m/s) circulation was present. Until this time, the only reported stronger wind was the gradient-level wind at Koror (WMO 91408) which increased from 9 kt (5 m/s) at 171200Z to 27 kt (14 m/s) at 180000Z as the disturbance passed west of the island late on the 17th. For the remainder of the 19th and into the 20th, with the TUTT continuing to exert influence on the disturbance, there was no significant improvement in the tropical cyclone's organization. As a result, the TCFA was reissued at 200700Z.

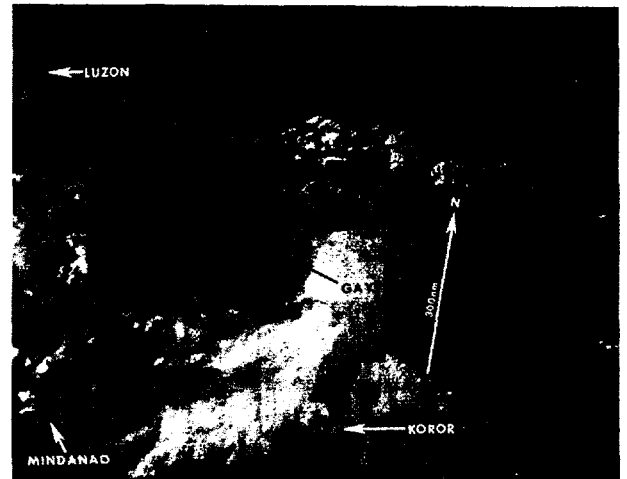


Figure 3-03-2. The tropical disturbance, which would later develop into Typhoon Gay, is interacting with the upper-level trough to the northwest. The outflow is restricted on the northwest side of the tropical cyclone (200518Z May NOAA visual imagery).

The first warning on Gay was issued at 210000Z after visual satellite imagery showed the convection was developing over the low-level circulation and Dvorak intensity analysis estimated that 35 kt (18 m/s) surface winds were present. The presence of the upper-level trough and its restrictive influence on outflow aloft strongly influenced the intensity forecasts on the first nine JTWC warnings. Gay was expected to strengthen only slowly, then maintain

intensity or weaken slightly in the extended outlook periods. These scenarios appeared valid based on satellite derived intensity analyses and forecasts, and on expectations that the upper-level trough would persist. Post-analysis revealed these intensities were consistently low. This was primarily due to the lack of any aircraft reconnaissance or synoptic data confirming the intensity, and partially due to the TUTT weakening faster than expected.

Gay attained typhoon intensity at about 230000Z just prior to the first aircraft reconnaissance penetration at 230830Z. The Aerial Reconnaissance Weather Officer (ARWO) reported Gay as very compact, with 65 kt (33 m/s) surface winds surrounding a 15 nm (28 km) diameter eye, and a 971 mb minimum sea-level pressure (MSLP). Gay's intensification to typhoon strength can be attributed to the significant weakening of the TUTT on the 22nd and to its tight circulation. In this case, the Typhoon's small size allowed it to mature in an area where a larger circulation would have interacted unfavorably with the surrounding atmosphere. Consequently, Gay became vertically stacked and developed a ragged eye while moving northwest with the mid-level steering flow around the western periphery of the subtropical ridge. This set the stage for Typhoon Gay's final phase.

By 230000Z, with a frontal boundary and associated mid-latitude trough quasi-stationary across the Ryukyu Islands, a recurvature scenario seemed most probable. JTWC incorporated this into the warnings and called for recurvature along the subtropical ridge axis near 22N in 48 hours. This scenario was ahead of all forecast aids (Figure 3-03-3), especially the OTCM (One-way Interactive Tropical Cyclone Model), JTWC's best forecast aid. With Gay continuing to intensify and move northwest, Kadena AB (WMO 47931) set Condition of Readiness III at 232230Z. Fortunately, Gay came under the influence of the mid-latitude westerlies and recurved earlier than forecast passing well south of Okinawa. Just prior to Gay's recurvature, another mid-lati-

tude mid-level trough began to dig unseasonably southward across eastern China northwest of Gay. This apparently increased the upper-level outflow ahead of the trough and may be the reason why Gay continued to intensify for 6 to 12 hours after recurvature. Gay reached a peak intensity of 100 kt (51 m/s) between 240600Z and 241200Z (Figure 3-03-4). This intensification correlates well with the studies by Riehl (1972) and Guard (1983) on the intensification of recurving tropical cyclones in WESTPAC.

After recurvature, Gay started a gradual acceleration to the northeast with satellite imagery indicating interaction with the frontal boundary beginning at 241200Z. By 0600Z on the 25th, Gay was entraining modified polar air into the low-level circulation and the eyewall was disintegrating. Extratropical transition had begun and the intense central convection started displacing outward. A steady decrease in convective organization and intensity continued as the mid-latitude trough moved rapidly eastward from the Yellow Sea over Japan. Gay was downgraded to a Tropical Storm at 260000Z.

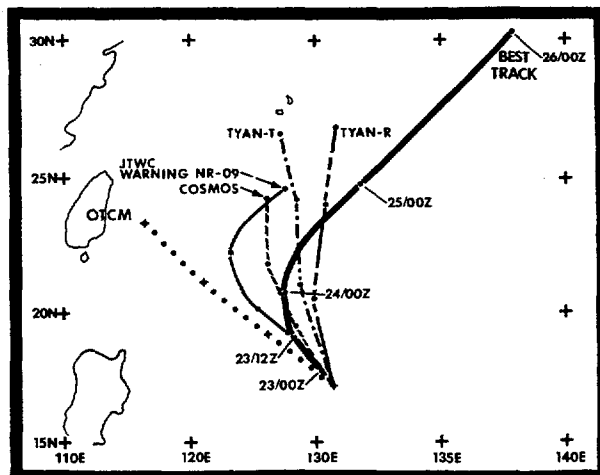


Figure 3-03-3. These plotted forecast aids were available to the Typhoon Duty Officer (TDO) at the time the first recurvature forecast was issued. OTCM, JTWC's best aid, failed to predict the recurvature. OTCM guidance repeatedly failed to forecast recurvature, in this case, until after it had actually occurred!

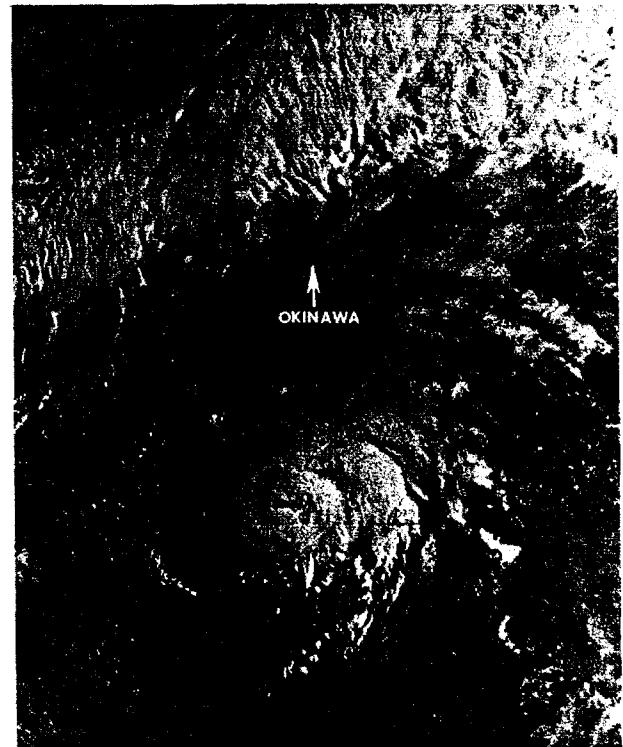


Figure 3-03-4. This early morning picture reveals Typhoon Gay near maximum intensity. (Note Gay's developing eye). The proximity of the frontal boundary to the north led to a recurvature forecast, overruling the the incorrect guidance from the forecast aids (232127Z May DMSP visual imagery).

Figure 3-03-5 shows the effect of the strong vertical wind shear on the remaining convection from the storm's circulation. Gay completed extratropical transition at 260600Z when the final warning was issued.

After completing extratropical transition, the nearly convection free low-level circulation drifted eastward and eventually dissipated. There were no reports of lives lost or damage to shipping from Typhoon Gay.

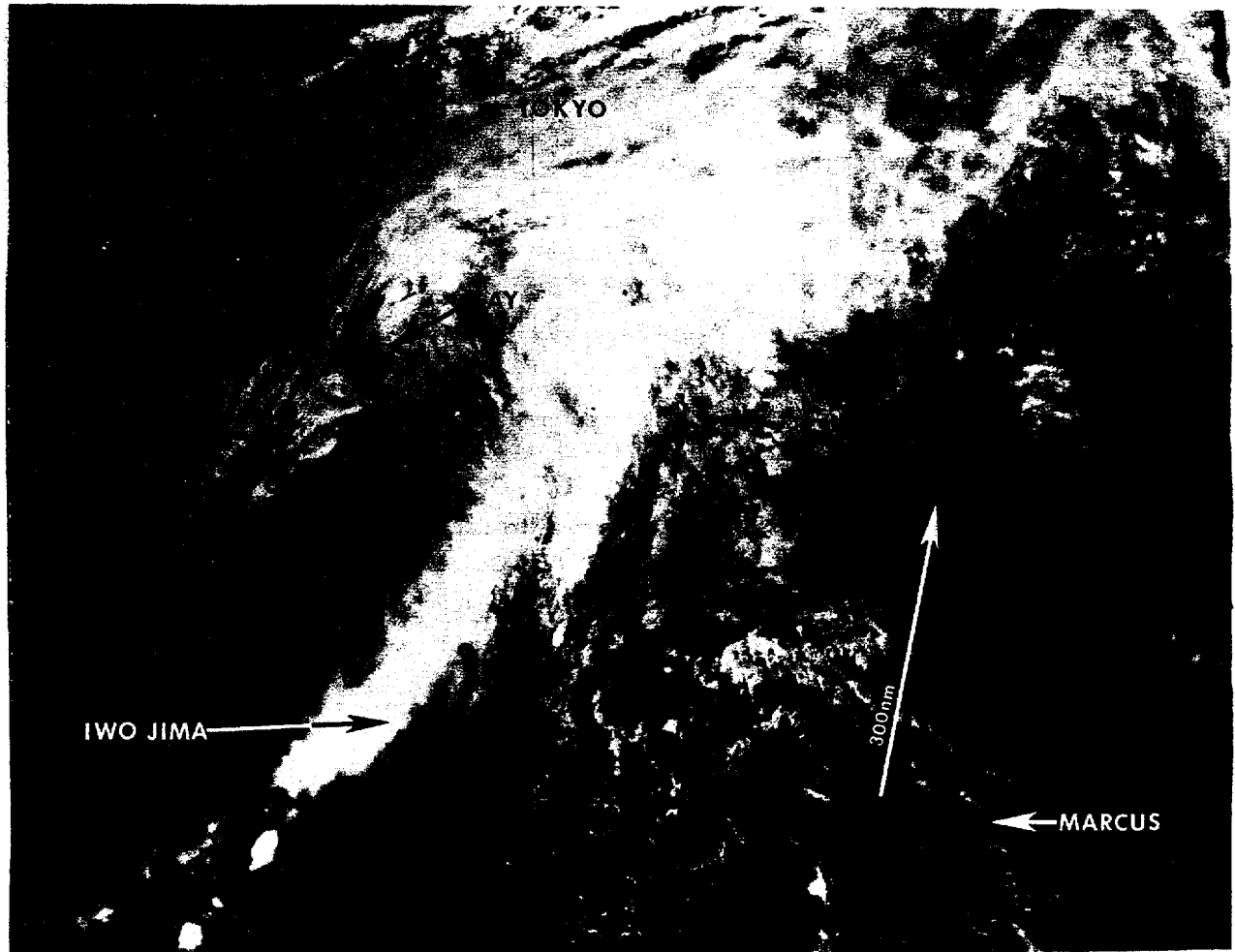
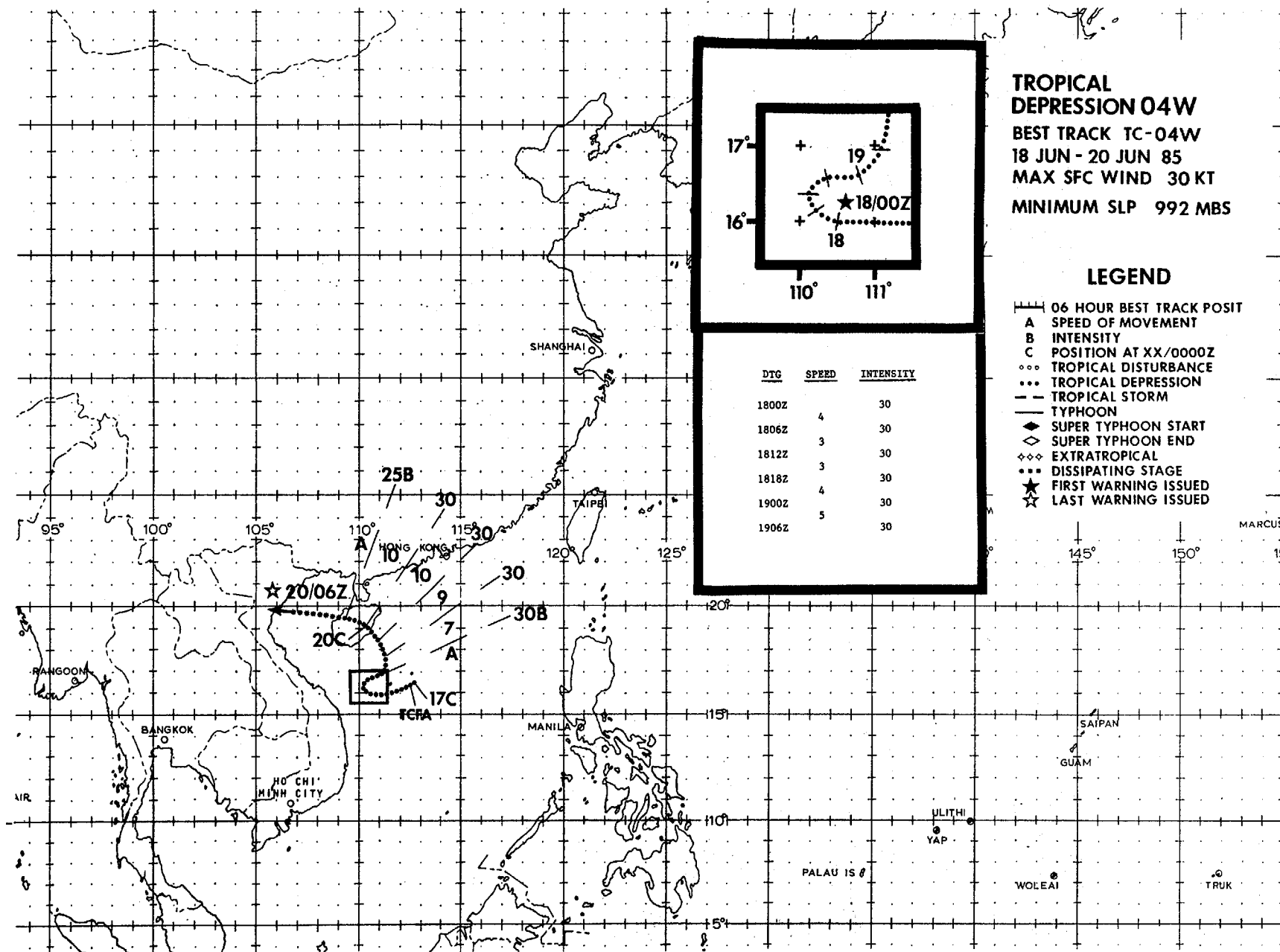


Figure 3-03-5. As Gay completes extratropical transition, the upper-level westerlies are shearing the convection away to the northeast of the low-level circulation center (260413Z May NOAA visual imagery).



TROPICAL DEPRESSION 04W

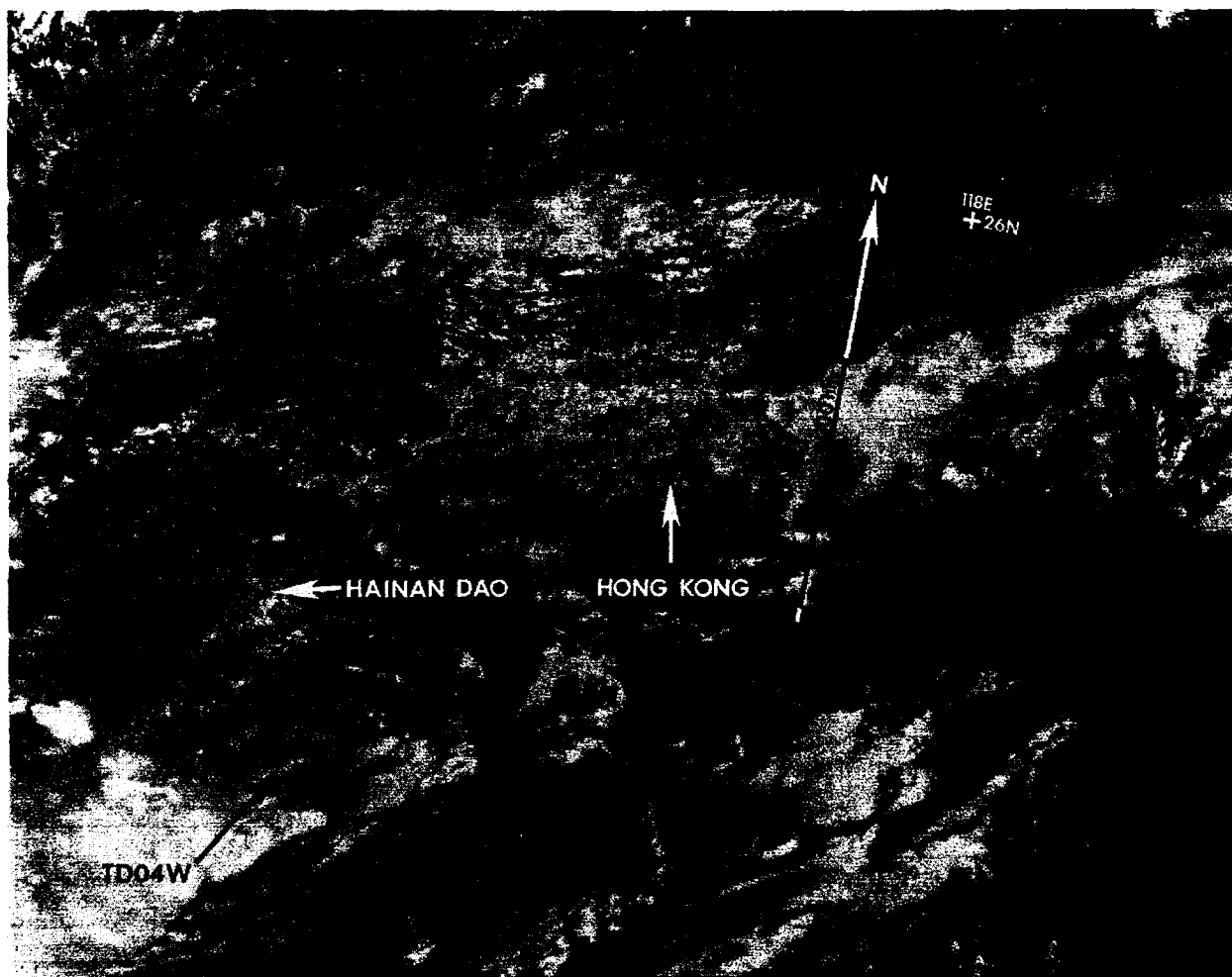
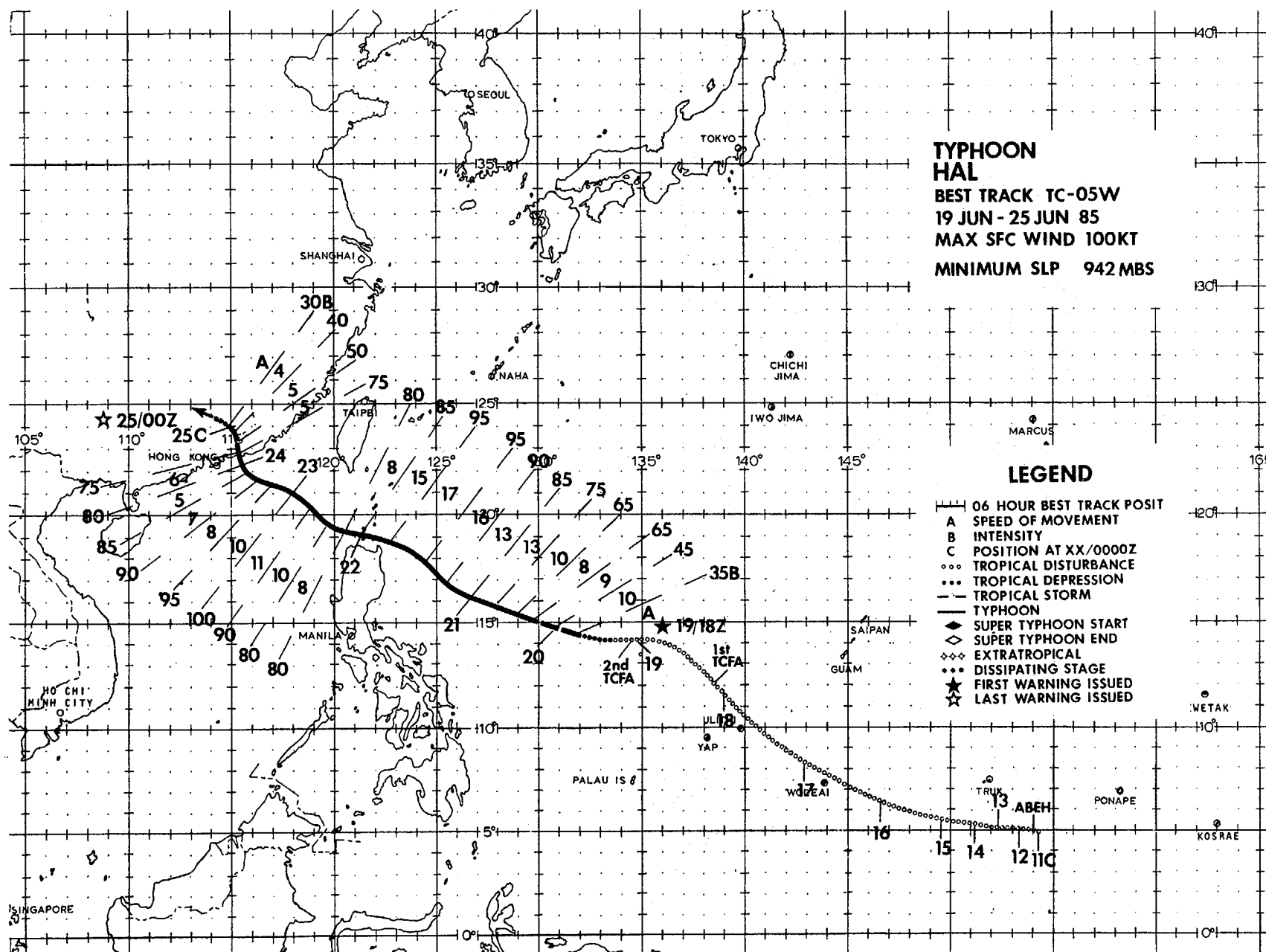


Figure 3-04-1. Tropical Depression 04W developed in the northern end of the monsoon trough in late June and remained embedded in the trough throughout its lifetime. Due to strong vertical wind shear aloft from the northeast, the low-level circulation center was often observed near the northeast edge of the convection (see the above imagery). This strong shearing environment prevented Tropical Depression 04W from intensifying above 30 kt (15 m/s) (190153Z June DMSP visual imagery).





# TYPHOON HAL (05W)

Typhoon Hal, the fifth tropical cyclone of the 1985 WESTPAC season, developed from a southwest monsoon trough disturbance. Hal caused considerable forecast difficulties because JTWC's primary forecast aid, OTCM, was unable to resolve a narrow mid-level subtropical ridge due to its relatively coarse grid spacing.

After Typhoon Gay completed extratropical transition on 26 May, a springtime weather pattern returned to the tropical western North Pacific. A strong tropical upper-tropospheric trough (TUTT) became established over most of the area, resulting in strong surface ridging from the Dateline westward to the Malay Peninsula and a large-scale suppression of convective activity. Transient mid-latitude short wave troughs passed north of a quasi-stationary Polar front that extended from near Hainan Island to about 300 nm (556 km) north of Minami-Torishima (WMO 47991). By 1 June, a weak low-level southwest monsoon flow had returned to the South China Sea.

There was a significant surge in the southwest monsoon commencing on 8 June, and by 12 June the low-level southwest monsoon flow extended as far eastward as Guam (WMO 91212).

Typhoon Hal was first detected as a weak tropical disturbance in the near-equatorial trough at 05N 154E on 11 June. The disturbance showed poor organization as it moved slowly westward during the next three days. Most of the intense convection was located west of the low-level circulation center and showed signs of cross-equatorial outflow after 14 June. On the 15th, the disturbance began moving west-northwest and showed signs of increasing organization. By 18 June, the disturbance had merged with the strong low-level southwest monsoon flow and had taken on the characteristics of a monsoon trough disturbance. As shown in Figure 3-05-1, the disturbance was sheared from the north by upper-level flow which left a broad, weak low-level circulation in

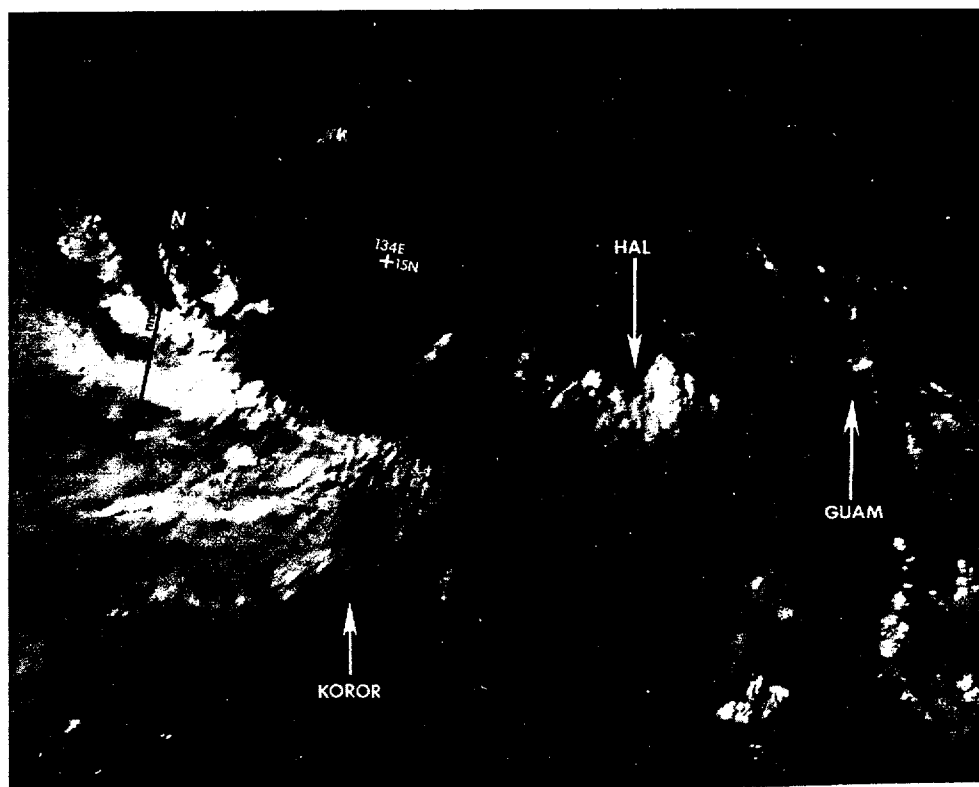


Figure 3-05-1. The tropical disturbance that developed into Typhoon Hal with strong upper-level shear from the north confining the intense convection to the south semicircle. Only scattered cumulus are evident in the north semicircle. The low-level circulation is in the form of a broad trough at this time (180511Z June NOAA visual imagery).

the north semicircle with scattered cumulus clouds. The intense convection was located in the south semicircle where the upper-level flow was divergent toward the southwest. By 1800Z on the 19th, satellite imagery indicated that the upper-level shear from the north had decreased and that a tropical cyclone scale low-level circulation had formed. The system had been the subject of a TCFA for 40-hours when the first warning was issued at 191800Z. Once convection started to appear in the north semicircle and the system showed signs of cirrus outflow toward the north, intensification proceeded quickly. By 200600Z, only 12-hours after

the first warning, the cyclone had reached typhoon intensity. Figure 3-05-2 shows a plot of the aircraft reconnaissance mission flown at that time. Notice the location of the maximum surface winds. In this case, the maximum surface winds are located approximately 90 nm (167 km) from the center of the cyclone. This large separation is a characteristic of many cyclones that evolve from strong monsoon troughs. Typhoon Hal continued intensifying during the next 24-hours and developed a large, ragged eye as shown in Figure 3-05-3. This feature is also a characteristic of this type of cyclone. The satellite picture also shows a TUTT cell located east of

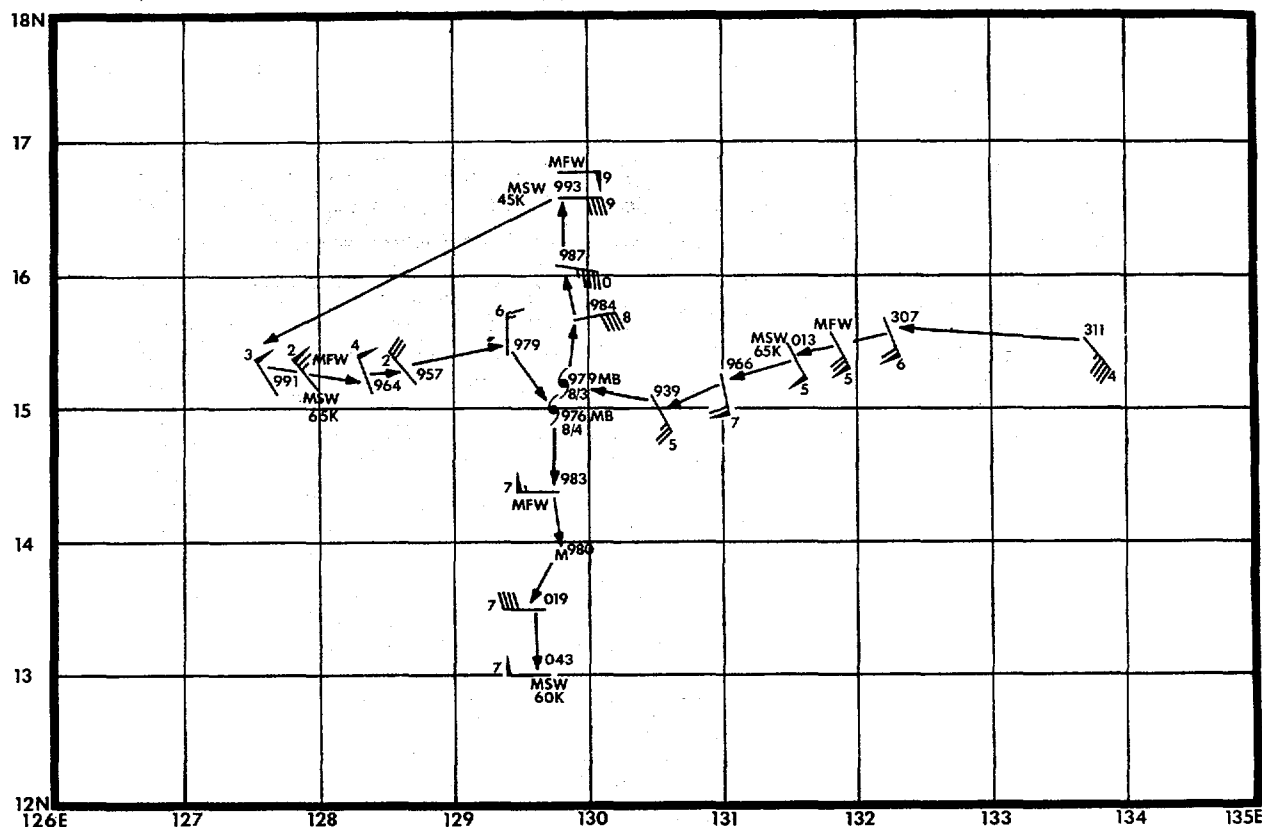


Figure 3-05-2. Plot of aircraft reconnaissance data from 200500Z to 201000Z June showing the maximum surface winds located approximately 90 nm (167 km) from the cyclone center. "MFW" represents the maximum observed flight level winds and "MSW" represents the maximum surface winds observed.



Figure 3-05-3. Typhoon Hal with a large, ragged eye. Most of the intense convection is in the south semicircle. (210109Z June DMSP visual imagery).

Hal that enhanced the upper-level outflow pattern in that direction. Figure 3-05-4 shows Typhoon Hal near the time of its maximum intensity.

Except for a few short-term variations, Hal moved in a west-northwestward direction during its five-day lifetime as a tropical storm and typhoon. This is interpreted in post-analysis as a normal south-of-the-subtropical ridge track movement. Figure 3-05-5 shows the 500 mb wind pattern at

201200Z, 18-hours after the first warning was issued, but still representative of the environment present throughout Hal's lifetime. Note the narrow subtropical ridge north of Hal that extends westward towards China. Based on just this pattern and assuming that it would persist, a forecast track of west-northwest would have been a good choice. However, JTWC's primary forecast guidance, the OTCM (One-way Interactive Tropical Cyclone Model)

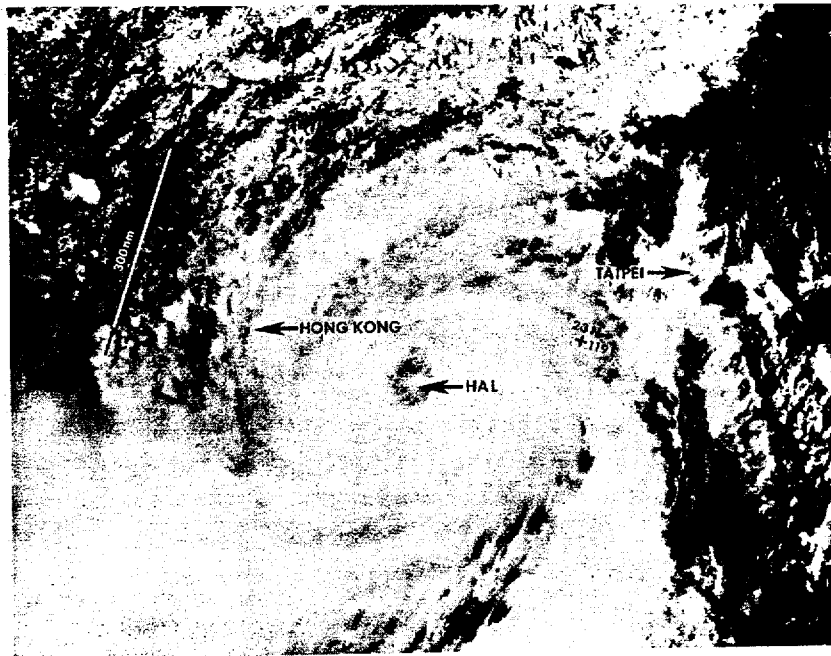


Figure 3-05-4. Typhoon Hal near the time of maximum intensity (230559Z June NOAA visual imagery).

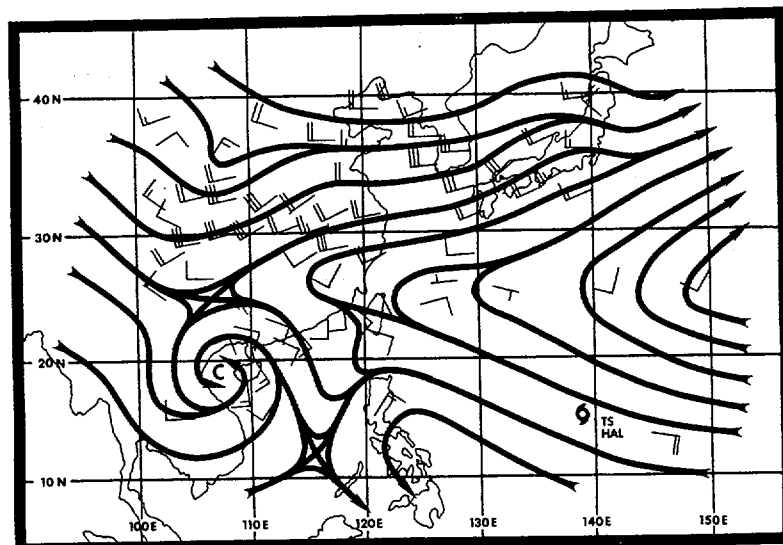


Figure 3-05-5. The 201200Z June 500 mb analysis showing the narrow mid-level subtropical ridge north of Hal. This ridge kept Hal from taking a more northerly course and entering the westerlies, contrary to the guidance provided by OTCM.

consistently indicated a more northward, and even a recurving northeastward, track. Figure 3-05-6 is a plot of the OTCM forecast tracks starting with the one on which the first warning was based. JTWC followed the guidance offered by the OTCM, and as a result, the forecast tracks were consistently north of Hal's actual track. In post-analysis it is apparent that OTCM was unable to resolve the narrow mid-level ridge because of the relatively coarse grid size (205 km) that the model uses. The flow that OTCM "saw" influencing the movement of Hal was the westerlies on the north side of the ridge. This resulted in the northward and recurving component in the OTCM forecasts. This situation will likely arise again in the future years, and will be closely watched for by the forecasters at JTWC as a result of this experience.

The Philippine island of Luzon experienced the strongest effects as the center of Typhoon Hal passed just 30 nm (56 km) off the north coast and westward through the Luzon Straits. The death toll was 23 persons with nine others reported as missing. There was widespread flooding and crop damage. Total damage was estimated at more than \$10 million. Eight crewmen of the US Navy frigate Kirk (FF-1087) were injured when a large wave crashed over the bow. The ship was operating in the South China Sea about 5 nm (9 km) southwest of Subic Bay. High winds caused superficial damage to the hull of the destroyer USS Oldendorf (DD-972) when a drifting, unmanned barge struck the ship while it was moored at Subic Bay. Strong winds tore the barge from its mooring in mid-harbor shortly before the incident occurred. As

Typhoon Irma approached from the east, Subic Bay received 30 in (762 mm) of rainfall during the period 26-28 June as a result of the strong low-level southwest monsoon flow that continued over the area after Hal had moved into China and dissipated as a significant tropical cyclone.

Taiwan was also affected by Typhoon Hal as it caused strong winds and heavy rains. Two people died, 18 injured, and five people listed as missing as a result of the typhoon. Eastern Taiwan experienced the heaviest rainfall, with almost 9 inches (229 mm) being reported. The heavy rainfall caused flooding that was responsible for most of the death, injury, and damage.

Typhoon Hal made landfall approximately 75 nm (139 km) east-northeast of Hong Kong (WMO 45005) at 240500Z. Maximum mean hourly wind speed reported at the Royal Observatory was 22 kt (11 m/s) from the west-northwest, with a peak gust to 49 kt (25 m/s). A gust to 50 kt (26 m/s) was recorded at the Hong Kong International Airport (WMO 45007). Some minor injuries were reported and the property damage was slight. All modes of transportation were disrupted on 23 and 24 June. Heavy rain on 25 and 26 June, after Hal had moved inland, caused numerous landslides in the Hong Kong area with only a few minor injuries.

Over mainland China, 13 more people died with some 40,000 homes and 321,000 acres (130,000 hectares) of crops damaged.

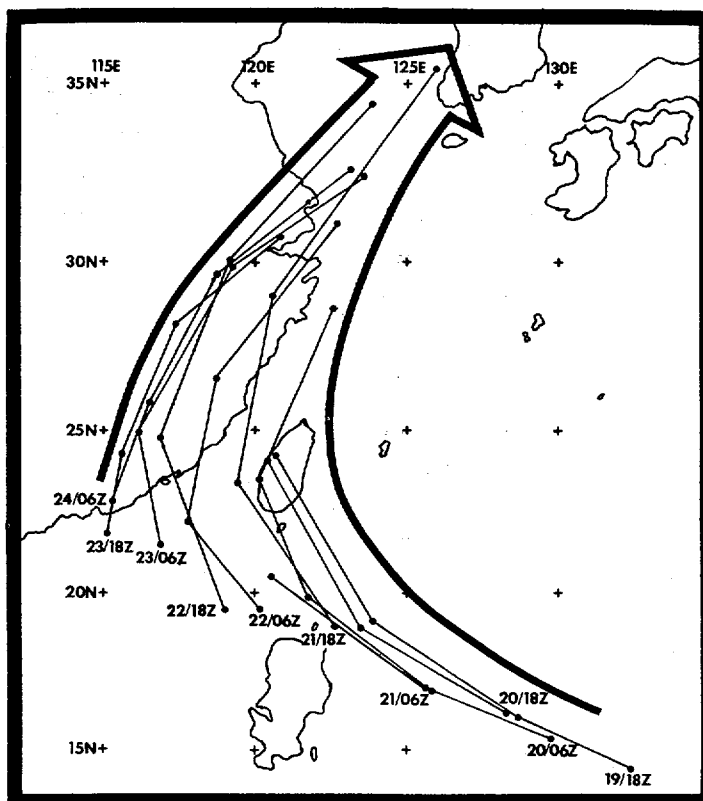
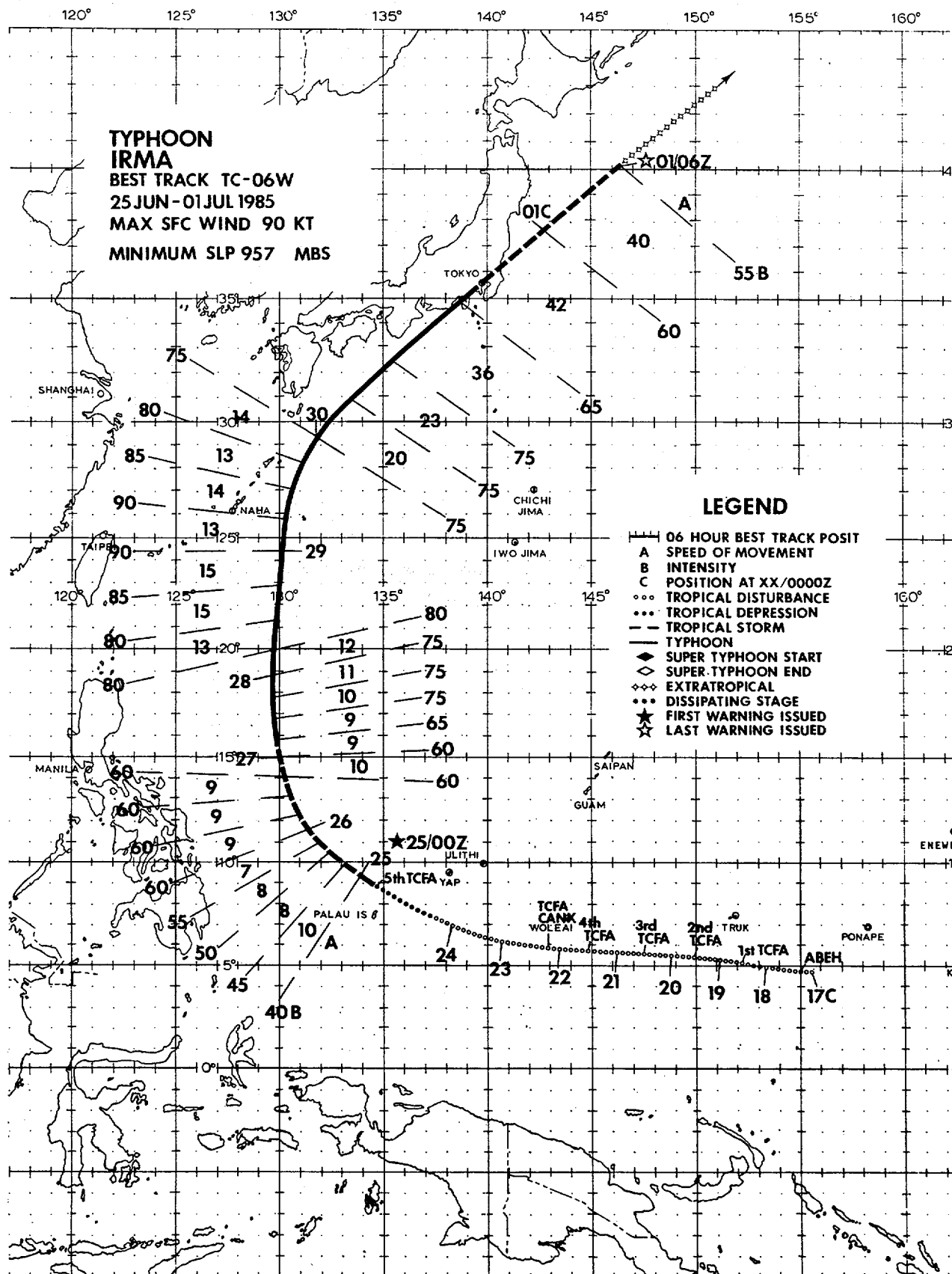


Figure 3-05-6. Plot of the OTCM (One-Way Interactive Tropical Cyclone Model) forecast guidance at 12-hourly intervals starting when the first warning was issued.



Although Typhoon Irma was not one of the more intense systems of the year, it became noteworthy due to the magnitude of property damage and loss of life it caused in the Philippines; and later, by passing directly over the Tokyo metropolitan area. It was the third significant tropical cyclone to develop in June within the monsoon trough and the first (in June) to recurve into the mid-latitude westerlies.

Typhoon Irma originated in the eastern extension of the monsoon trough in mid-June. It was slow to develop, taking eight days to become a tropical storm. At 0000Z on the 17th, the disturbance which later developed into Irma was located approximately 220 nm (407 km) southwest of Ponape (WMO 91348). Synoptic data showed a broad weak surface circulation with winds of 5 to 10 kt (3 to 5 m/s). Another disturbance, which would shortly develop into Typhoon Hal, was located to the northwest in the same trough 270 nm (500 km) east-southeast of Yap (WMO 91413). A broad surface ridge north of both disturbances dominated the northwest Pacific.

When the disturbance was initially mentioned on the 170600Z Significant Tropical Cyclone Advisory (ABEH PGTW), satellite imagery indicated that an upper-level cold low in the tropical upper-tropospheric trough (TUTT) was present northeast of Guam. This upper-level low, which was positioned 7 to 10 degrees of latitude north-northwest of Irma, was contributing to the upper-level diffluence and enhancing the convective activity in the vicinity of the disturbance. The potential for significant tropical cyclone development was evaluated as "fair" (meaning that issuing a TCFA during the advisory period was likely). By 0900Z on the 18th, the disturbance had moved west-northwest and was 150 nm (278 km) south-southeast of Truk (WMO 91334). Satellite imagery indicated the amount of convection was increasing and had more organization. Consequently, a TCFA on the system was issued at 181200Z and aircraft reconnaissance requested for the following day.

Over the next three days satellite imagery showed vigorous, but poorly organized, convection. The aircraft reconnaissance flight on the 19th of June at the 1500 ft (457 m) level was unable to locate a circulation center and reported a MSLP of 1006 mb. On the following day, aircraft reconnaissance found a surface circulation with a 5 nm (9 km) diameter area of light and variable surface winds, a drop in the MSLP of 4 millibars from the previous day and surface winds of 10 to 20 kt (5 to 10 m/s). The flow aloft over the disturbance was hampered by in-

creased outflow from Hal to the west. During this period TCFAs were re-issued at 1200Z on the 19th through the 21st of June. Early on the 22nd, the convection within the disturbance became so suppressed that the TCFA was cancelled at 220500Z.

Unfavorable vertical shear from Hal hindered development of the disturbance until the 24th. The 241200Z synoptic data showed increasing southwesterly low-level flow entering the disturbance. This coincided with Typhoon Hal making landfall over southern China. Subsequent satellite imagery at 241600Z revealed a significant increase in the size of the central cloud mass. The fifth, and final, TCFA on this system followed at 241730Z.

With Hal weakening overland in mainland China, Irma now began to intensify in earnest. The first warning on the system was issued at 250143Z, after the Dvorak intensity analysis of the 250000Z satellite imagery showed the disturbance had increased to tropical storm intensity. Aircraft reconnaissance later in the day (250516Z) located a 994 mb circulation center with 45 kt (23 m/s) maximum surface winds 90 nm (167 km) east-northeast of the center.

The initial forecasts called for Irma to follow in Hal's footsteps up the monsoon trough into the South China Sea and around the subtropical ridge. Due to the uncertainty about the analysis over the data sparse Philippine Sea, 400 mb synoptic track aircraft missions were flown on 25 and 26 June to help define the mid-level flow to the north of Irma. These flights confirmed the presence of lower 400 mb heights in the ridge along 130E, which indicated the ridge would not steer Irma into the South China Seas as it had done with Hal. JTWC now forecast a more northward movement with eventual recurvature to the northeast. This forecast scenario proved correct.

Irma slowed slightly as it approached the end of the ridge at 130E longitude and continued to intensify. Early on the 27th, Irma attained typhoon intensity as verified by synoptic ship observations of 65 kt (33 m/s) north-northeast of the center and the Dvorak intensity analysis. For the next two days (Figure 3-06-1) Irma moved northward and reached a maximum intensity of 90 kt (46 m/s) with a MSLP of 957 mb at 290000Z.

Along with reaching maximum intensity, Irma also came under the influence of the mid-latitude westerlies. Within 24-hours, Irma was accelerating rapidly to the northeast headed for Tokyo and the



Kanto Plain area of Japan's Honshu Island. Simultaneously, the system began weakening and undergoing extratropical transition. Aircraft reconnaissance on the 30th indicated entrainment of the cooler, drier air into the system. The Aerial Reconnaissance Weather Officer (ARWO), at 300817Z, reported a 30 nm (56 km) elliptical eye with a slight tilt to the north-northeast.

By 010600Z, Irma had completed extratropical transition and the last warning was issued. The remains of Irma continued to move northeast toward the Kuril Islands where it merged with a complex low pressure area just south of the Kamchatka Peninsula.

In summary, as the Typhoon passed east of the Philippines on 28 and 29 June, heavy rains associated

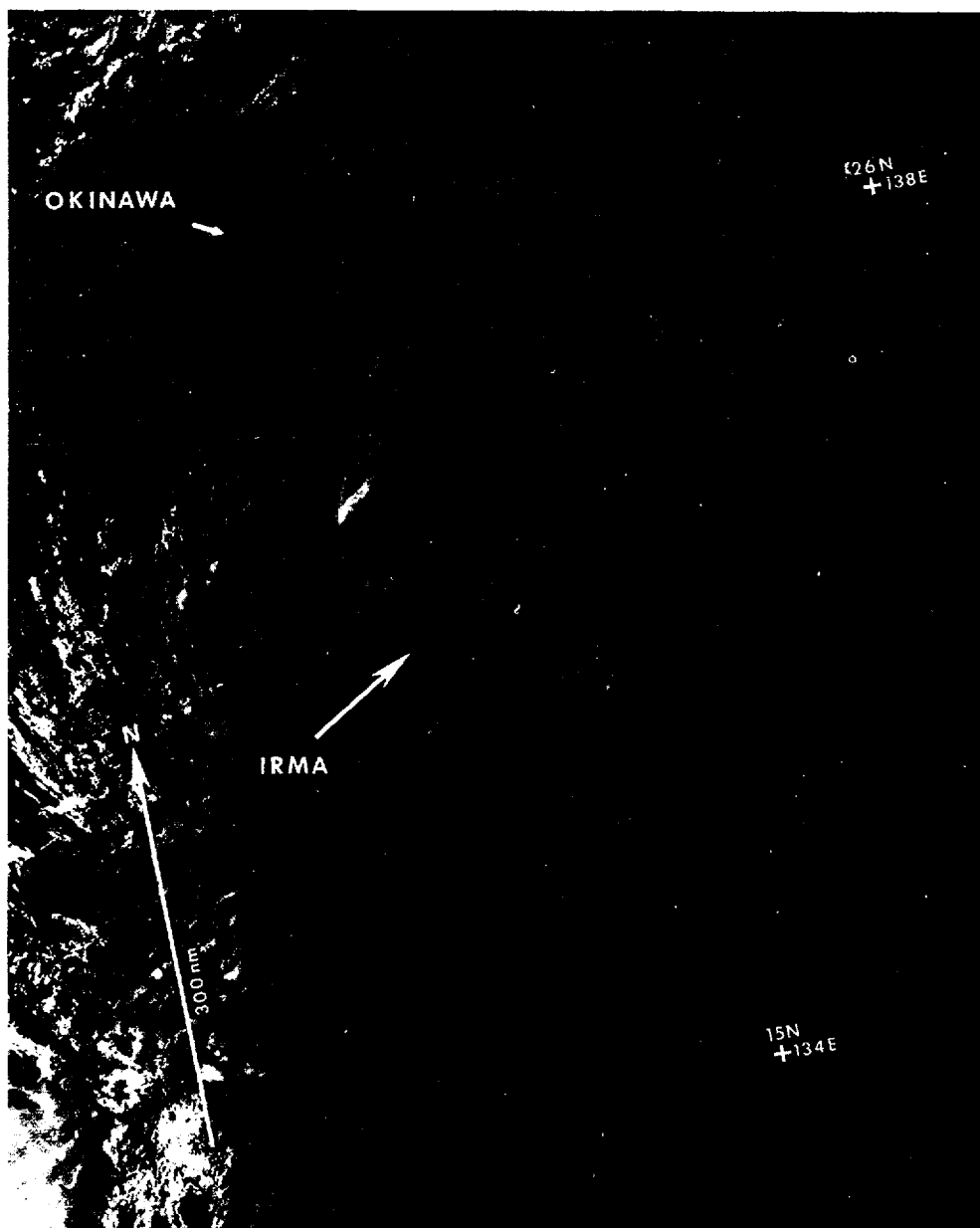


Figure 3-06-1. Irma, with maximum winds of 80 kt (41 m/s), nearing peak intensity south of Okinawa, Japan. (With the sun low in the west the cloud top topography is striking) (280931Z June DMSP visual imagery).

with the strong south westerly monsoon flow from the South China Sea across the island of Luzon produced more than 28 inches (711 mm) of rain. Flooding was widespread across areas of Manila and other sections of Luzon. At least 46 people perished in these floods; additionally, over 1,500 lost their homes. Later, when Irma made landfall on the southeastern tip of Honshu at 301800Z, maximum winds were estimated at 65 kt (33 m/s). The Naval Oceanography Command Facility at Yokosuka reported maximum winds

of 51 kt (26 m/s) with a peak gust to 83 kt (43 m/s). The associated barograph trace is shown in Figure 3-06-2. Various military activities at Yokosuka reported minor damage and flooding, but no significant personal injuries. However, Japan police reported three deaths and five people were missing as a result of Irma. Twelve bridges were reported out, flood damage occurred to over 20,000 homes and power outages affected about 440,000 households.

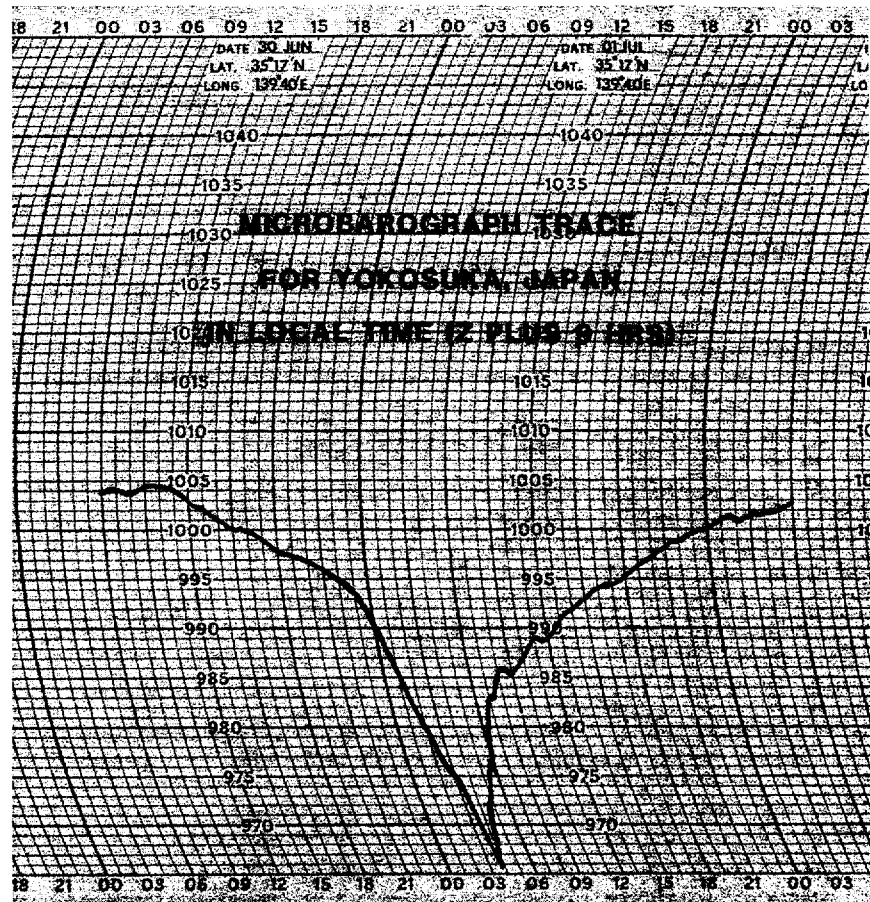
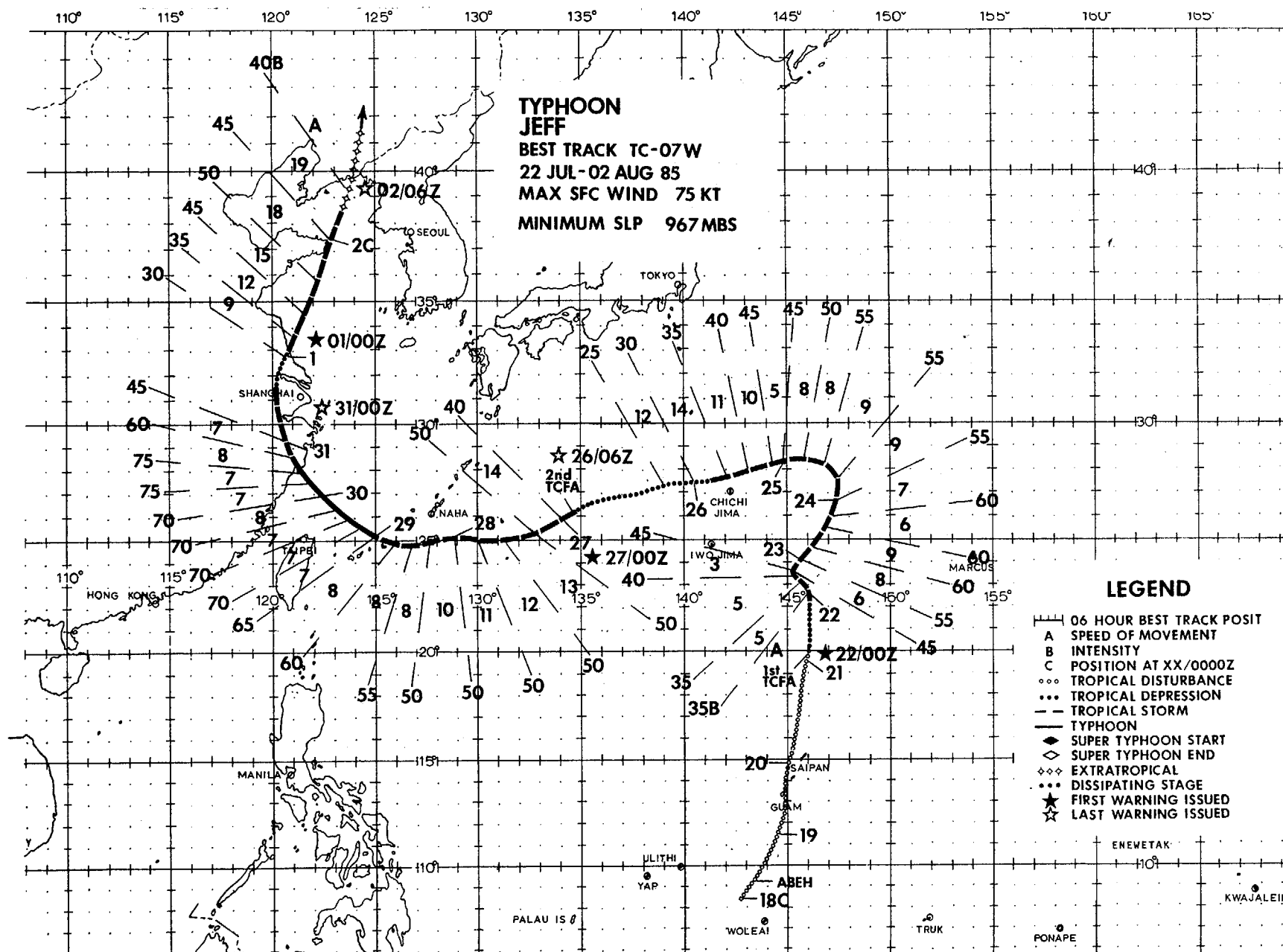


Figure 3-06-2. Barograph trace from the Naval Oceanography Command Facility in Yokosuka documenting Irma's passage over the Kanto Plain. The minimum sea-level pressure recorded was 963.3 mb at 301930Z.



# TYPHOON JEFF (07W)

Typhoon Jeff was the longest-lived tropical cyclone of the 1985 season. It required a total of forty-one warnings and was finalled by JTWC on three separate occasions. During its twelve day life span, Jeff peaked in intensity three times: once east of the island of Iwo Jima; once west of Okinawa, Japan; and the third time over the Yellow Sea. Jeff, as it turned out, would be the only tropical cyclone to develop during July, a month that normally produces five cyclones.

After Typhoon Irma became extratropical on 1 July, tropical activity in the western North Pacific decreased. One significant tropical disturbance developed east of the Philippines on 4 July and moved into the South China Sea on the 6th before dissipating east of Hong Kong (WMO 45005) on 8 July. This disturbance was the subject of a TCFA from the 4th through the 7th. After this disturbance dissipated, the tropics stayed inactive until Typhoon Jeff developed a week later.

The low-level circulation which was to mature into Typhoon Jeff, was spawned in the monsoon trough south of Guam on 18 July in a broad area of disorganized cloudiness that stretched along ten degrees north latitude. Consolidating slowly, the system drifted northward across the island of Guam and through the northern Marianas, bringing little more than increased rainshower activity. Three days after genesis, the development of persistent central convection and better cloud organization prompted a TCFA, valid at 210200Z. Aircraft reconnaissance into the disturbance a few hours later was unable to locate a surface circulation, but instead found a broad trough with 10 to 15 kt (5 to 8 m/s) surface winds and a MSLP of 1006 mb. Early the next morning, a second aircraft reconnaissance mission found a tropical depression with a 1002 mb central pressure. As a result, the first warning was issued at 220000Z. For the next two days Jeff continued to intensify, reaching a peak of 60 kt (31 m/s) on the 23rd.

Up to this point, the steering flow had remained weak. Initially, Jeff's movement had been to the northwest, but then changed to the northeast in response to the approach of a mid-latitude trough from the northwest. Forecasting recurvature into the mid-latitude westerlies ahead of the trough was the most attractive possibility, especially since the tropical cyclone was already at 25N latitude and had been steadily tracking northeastward for nearly 24-hours. In contrast to the persistent northeasterly movement, both numerical forecast aids (NTCM and OTCM) consistently indicated a northwesterly track. Because of the major difference between what was actually happening and the guidance provided by the aids, the possibility of a return to a westerly or northwesterly track was still considered. The "less" likely alternative forecast scenario, i.e. northwestward movement, was repeatedly

mentioned in the Prognostic Reasoning Messages (WDPAL PGTW), but the official forecast was for recurvature. Unfortunately, the "more" likely recurvature scenario to the northeast did not last long.

Late on the 23rd as the trough approached, vertical wind shear from the west increased over the system. It soon became apparent that Jeff was weakening and the persistent central convection was shearing away to the east (Figure 3-07-1). The mid-latitude trough passed to the east on the 24th, leaving behind Jeff's exposed low-level circulation.

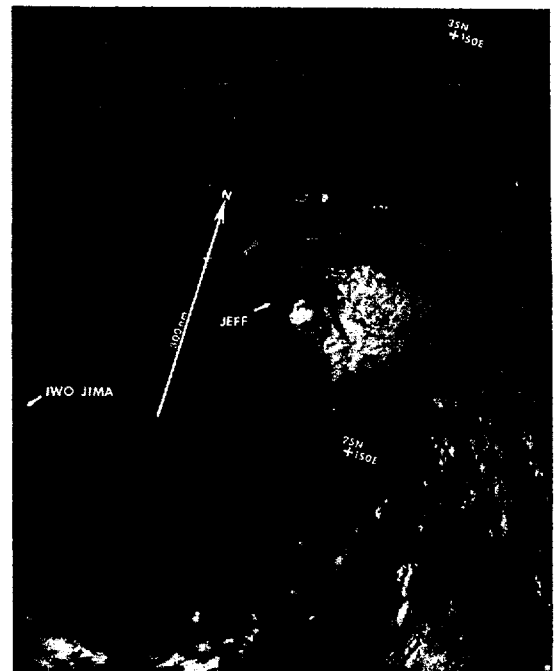


Figure 3-07-1. The low-level center of Tropical Storm Jeff located near the western edge of the central dense overcast. Strong upper-level westerly winds are shearing away the central convection to the east and will soon expose the low-level circulation center (240318Z July NOAA visual imagery).

The residual low-level vortex then began to move westward, embedded in the southeastern portion of the low- to mid-level anticyclone which was centered over northern Honshu. Without any regeneration of the central convection on the 25th or the 26th, Jeff

continued to weaken. By 260600Z the maximum surface winds had dropped below 30 kt (15 m/s). Despite the fact that a well-defined low-level circulation was still present, the lack of persistent central convection and the systems rapid movement to the west-southwest made further development seem unlikely (Figure 3-07-2). As a consequence, the final warning was issued at 260600Z, with the caveat that "the system will be closely monitored for indications of possible regeneration." That was precisely what happened! Almost immediately after Jeff was finalled, convection began to redevelop about the low-level center since the shearing influence of the trough was absent.

Throughout the night of the 26th Jeff regenerated, and JWC immediately alerted Kadena AB (WMO 47931) and other customers on Okinawa of the change. Weather satellite reconnaissance revealed a dramatic increase in central convection when warnings were again issued on Jeff, as a 35 kt (18 m/s) Tropical Storm, at 270000Z (Figure 3-07-3). Because Jeff was less than 24-hours from affecting Okinawa, Kadena AB went to Condition of Readiness III as a precaution. As Jeff neared Okinawa it slowed, passing about 75 nm south of Okinawa at 280530Z. The warnings verified well. Maximum sustained winds at Kadena AB were 25 kt (13 m/s), with a peak gust to

39 kt (20 m/s) at 280208Z. Naha (WMO 47930) had a peak gust of 47 kt (24 m/s) at 280355Z. Eighteen hours after passing south of Okinawa, Jeff attained typhoon intensity. By that time, the Typhoon had turned to the west-northwest as it started to move around the western side of the subtropical ridge. Further intensification to a peak of 75 kt (39 m/s) occurred as Typhoon Jeff approached, and made land-fall on, the coast of mainland China approximately 180 nm (333 km) south of Shanghai (WMO 58367) (Figure 3-07-4). Once onshore, surface frictional effects caused a rapid decrease in maximum winds. The persistent central convection began to fall apart and, once again, the system was finalled, although "movement back off the coast and regeneration in the Yellow Sea" remained a distinct possibility (Figure 3-07-5).

Indeed, Jeff was not finished yet. Warning number 36 was issued at 0000Z on 1 August as meteorological satellite reconnaissance reported significantly increased convection over water. The track was now to the north-northeast around the western edge of the subtropical ridge. Acceleration was gradual as Jeff redeveloped maximum surface winds of 50 kt (26 m/s) by 1800Z on 1 August. Strong south-westerly winds aloft hindered the system's attempt to further intensify and achieve vertical alignment

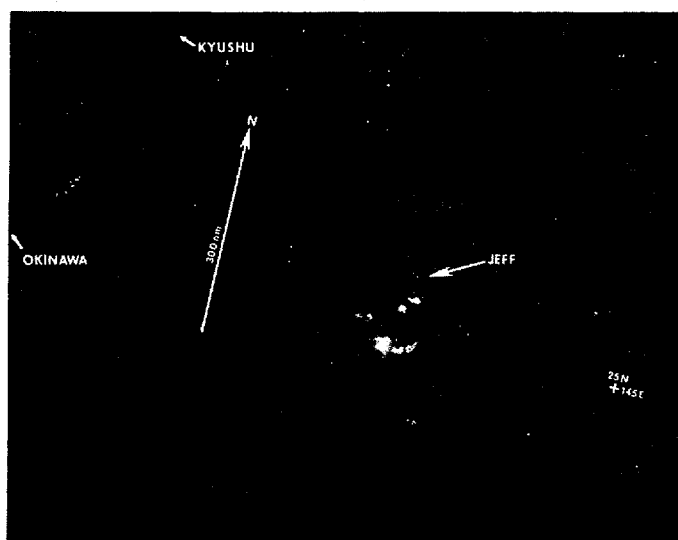
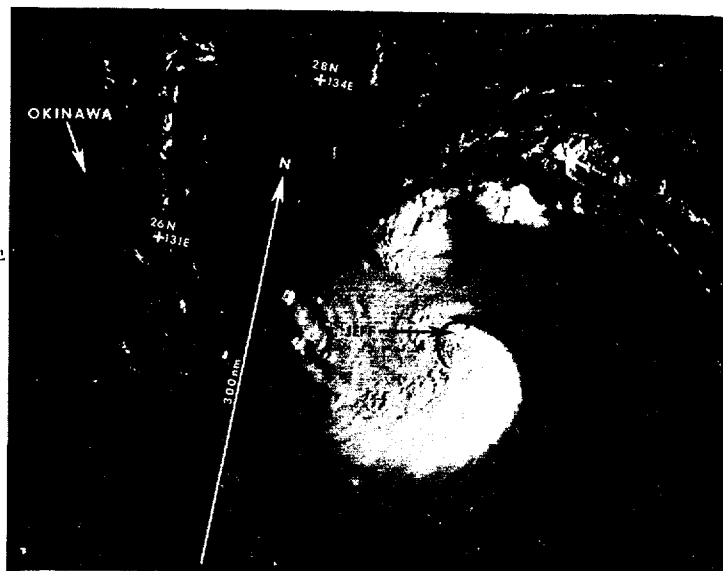


Figure 3-07-2. The nearly convection free low-level circulation of Jeff as it was finalled for the first time (260508Z July NOAA visual imagery).

Figure 3-07-3. Typhoon Jeff just after its dramatic regeneration during the night (270048Z July DMSP visual imagery).



between the low-level cyclone and anticyclone aloft. Then, at 0600Z on 2 August Jeff was finalled for the third and last time after completing extratropical transition in the northern Yellow Sea.

In retrospect, eastern China bore the brunt of Typhoon Jeff. The provinces of Shanghai and coastal Zhejiang were battered. News reports indi-

cated at least 180 people were killed, 1400 injured and tens of thousands left homeless. In addition, 1400 watercraft, mostly fishing boats, were lost or badly damaged. Some 75,000 acres (30,352 hectares) of crops were destroyed and another 400,000 acres (161,878 hectares) badly damaged, by the typhoon. China's irrigation network was severely disrupted by flooding.

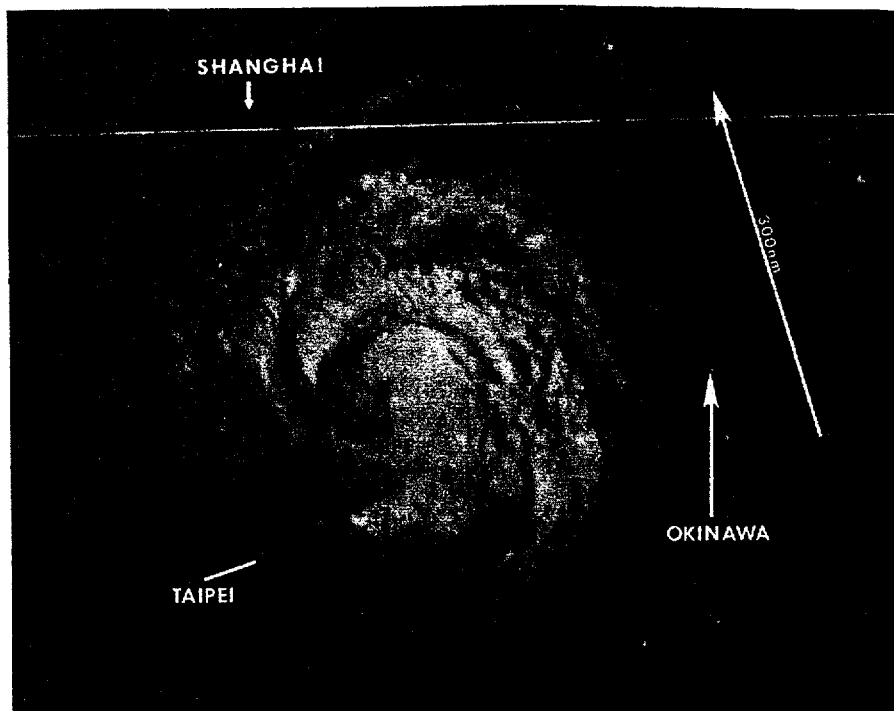


Figure 3-07-4. Typhoon Jeff near maximum intensity less than 18-hours from making landfall over eastern mainland China. During the hours immediately preceding landfall, a small banding eye formed (292303Z July NOAA visual imagery).

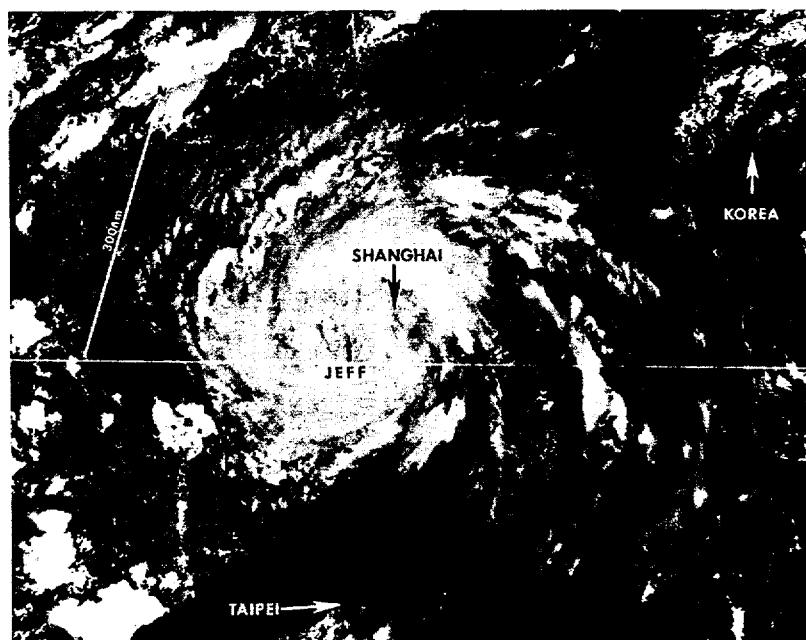
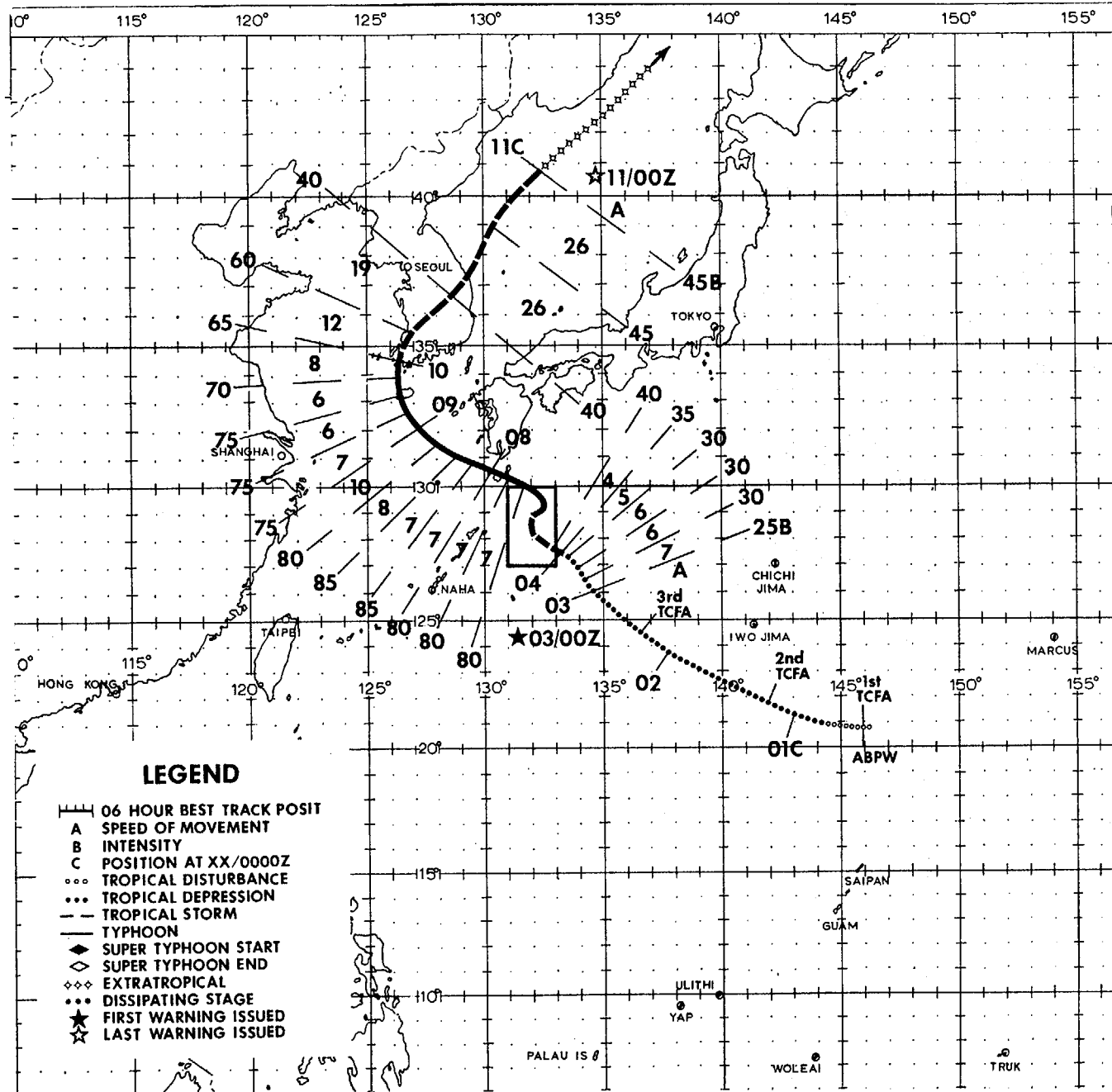
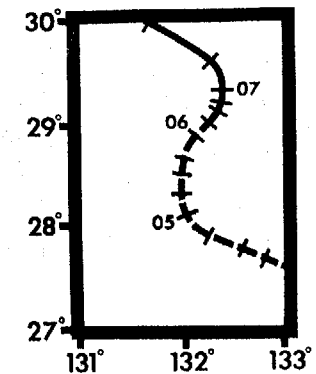


Figure 3-07-5. Jeff over mainland China after being finalled for the second time. Jeff spent nearly 36 hours over mainland China before moving back over open water and reintensifying (310556Z July NOAA visual imagery).



## TYPHOON KIT

BEST TRACK TC-08W  
03 AUG-11 AUG 1985  
MAX SFC WIND 85 KT  
MINIMUM SLP 959 MBS



DTG	SPEED	INTENSITY
0406Z	4	40
0412Z	3	45
0418Z	3	45
0500Z	2	50
0506Z	2	55
0512Z	2	55
0518Z	2	55
0600Z	2	60
0606Z	2	65
0612Z	2	70
0618Z	1	75
0700Z	1	80
0706Z	3	80
0712Z	7	80

Typhoon Kit was the first of seven tropical cyclones to reach warning status during August 1985. As was the case with its predecessor, Typhoon Jeff, Kit's recurvature posed considerable forecast problems. Like many WESTPAC tropical cyclones, Kit developed from an area of increased convection in the eastern portion of the monsoon trough.

As the remnants of Typhoon Jeff transited eastern China, satellite imagery early on 31 July showed that a possible circulation with good convective organization was rapidly forming north of Guam. This area of disturbed weather was developing at the northeast end of the monsoon trough, which at the time was linked to the trailing end of an old frontal boundary. The presence of this frontal boundary may have provided some initial low-level cyclonic shear to account for the system's rapid formation. Synoptic data indicated that a low-level circulation was present in the disturbed area with winds of 10 to 20 kt (5 to 10 m/s) and a MSLP of 1004 mb. The disturbance was mentioned on the Significant Tropical Advisory (ABEH PGTW) at 310451Z, but development was so rapid and the satellite signature so impressive, that a TCFA was issued by 310600Z. No significant additional development occurred overnight, however, as the system moved to the west-northwest. The first aircraft reconnaissance mission into the disturbance the following day found winds of only 20 kt (10 m/s) on the west side of a 1004 mb surface trough. The TCFA was reissued on the 1st as development still appeared likely. Follow-on aircraft reconnaissance was requested for the 2nd. This time the investigative mission located a 30 nm (56 km) wide surface circulation center with better organized winds of 10 to 20 kt (5 to 10 m/s) and a MSLP of 1005 mb, one millibar higher than on the previous day. A third TCFA followed at 020600Z as the disturbance tracked to the northwest. Aircraft reconnaissance was again requested.

The next aircraft reconnaissance mission flew into the system late on the 2nd, closed a circulation at 022204Z and reported that the MSLP had decreased to 1000 mb. Both aircraft and synoptic data now indicated 25 kt (13 m/s) surface winds near the center. JTWC responded by issuing the first warning on Tropical Depression 08W valid at 030000Z. During the next 24-hours the tropical depression slowly intensified while moving to the northwest along the southern periphery of a high pressure ridge located over Japan.

Tropical Depression 08W was upgraded to Tropical Storm Kit at 040000Z after aircraft reconnaissance

reported 35 kt (18 m/s) winds in all quadrants. Once upgraded, Kit continued to intensify and move slowly west-northwestward for the next 24 hours. Extended forecasts, based on FNOC's NOGAPS prognoses, indicated that Kit would move northwestward around the ridge which was expected to be displaced southeastward in advance of an approaching trough. This would result in Kit recurving to the northeast after 36 hours and eventually make landfall on Japan (Figure 3-08-1). However, the trough was weaker than forecast so instead of eroding the ridge and allowing Kit to recurve into the westerlies, the trough only temporarily weakened the ridge as it passed to the north. Kit responded to the trough passage by slowing and turning to the north on the 5th. Typhoon Kit then moved slowly northward through the 6th and into the 7th while continuing to intensify. By the 7th the trough had passed to the east and the tropical cyclone was left in the weakness between the subtropical ridge to the east and a weaker anticyclone over mainland China. With the passage of the mid-latitude trough over the subtropical ridge, the ridge began to build westward on the 7th. Kit responded by resuming a course to the west-northwest and intensifying (Figure 3-08-2). Kit attained its maximum intensity of 85 kt (44 m/s) at 080600Z southwest of Kyushu as it moved into the East China Sea. With FNOC's NOGAPS progs indicating another mid-latitude trough approaching from the west, and Kit definitely nearing the western end of the subtropical ridge axis, recurvature over South Korea, with extratropical transition in the Sea of Japan, appeared likely. After 081200Z, Kit began to weaken as relatively cooler and drier low-level air was entrained into the vortex's southwest quadrant.

Kit recurved south of the Korean peninsula and was barely at typhoon strength when landfall occurred on the southwest tip of South Korea early on the 10th. Kit still packed quite a punch, however. Torrential rains on the island of Cheju and southern coastal Korea caused extensive property and crop damage. At least ten people were reported missing or killed. Additionally a Department of Defense communications site in the area received an estimated 1.5 million dollars damage. With extratropical transition in progress, Kit rapidly lost strength while accelerating northeastward into the Sea of Japan. Extratropical transition was completed and JTWC issued the final warning on Kit at 110000Z. Subsequent warnings on the extratropical remnants of Kit were contained in the NAVOCEANCOMCEN GUAM Northwest Pacific Extratropical Wind Warning bulletins.



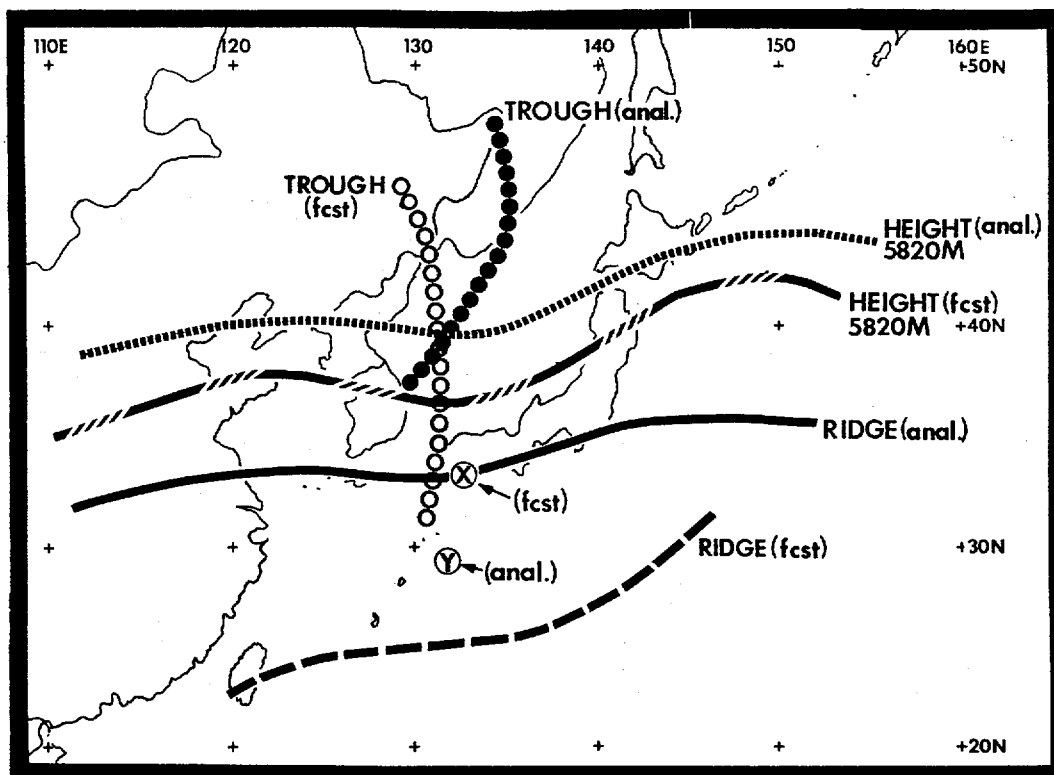


Figure 3-08-1. Comparison of 500mb 48-hour prognosis with verifying 500mb analysis. This chart depicts the major 500mb features available from the 48-hour prognosis valid 060000Z August: ridge axis (dashed line), trough line (open dots), 5280 meter height isopleth ( - - - - - ), and forecast warning point (X). The verifying 500mb analysis is shown for 060000Z August: ridge axis (solid line), trough line (solid dots), 5280 meter height isopleth ( ..... ), and Best Track position (Y) for Kit. In retrospect, with the 48-hour prognosis and the location of the forecast warning position (X) - north of the ridge (forecast) and east of the trough (forecast) - a recurvature scenario looks valid. The tropical cyclone is an immediate threat to Japan. However, with the verifying analysis, Kit's position (Y) remains south of the ridge (analysis) and the trough (analysis). This is not favorable for recurvature. This pattern suggests weakened steering flow, with slow and erratic tropical cyclone movement - which is what occurred on the 6th.

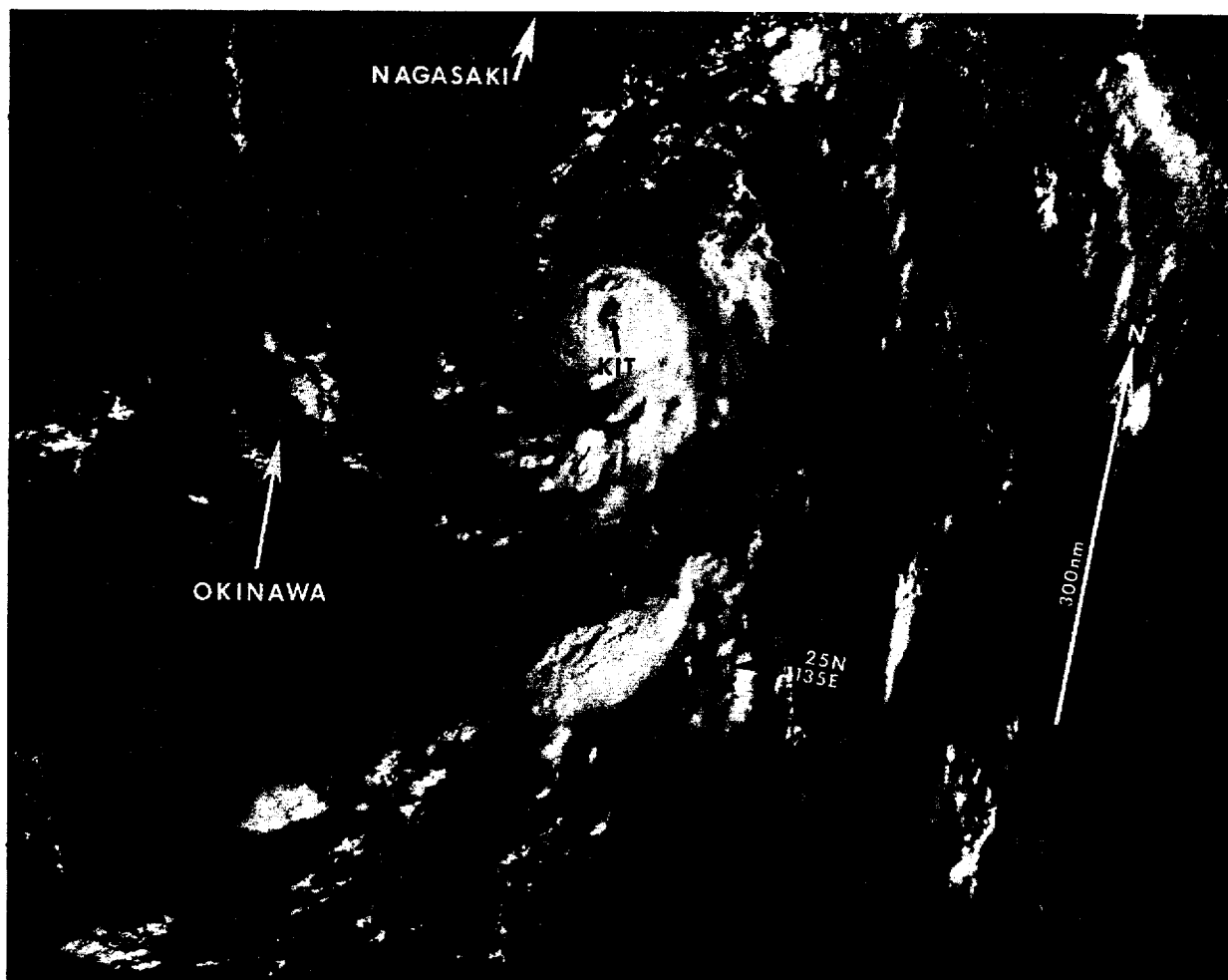
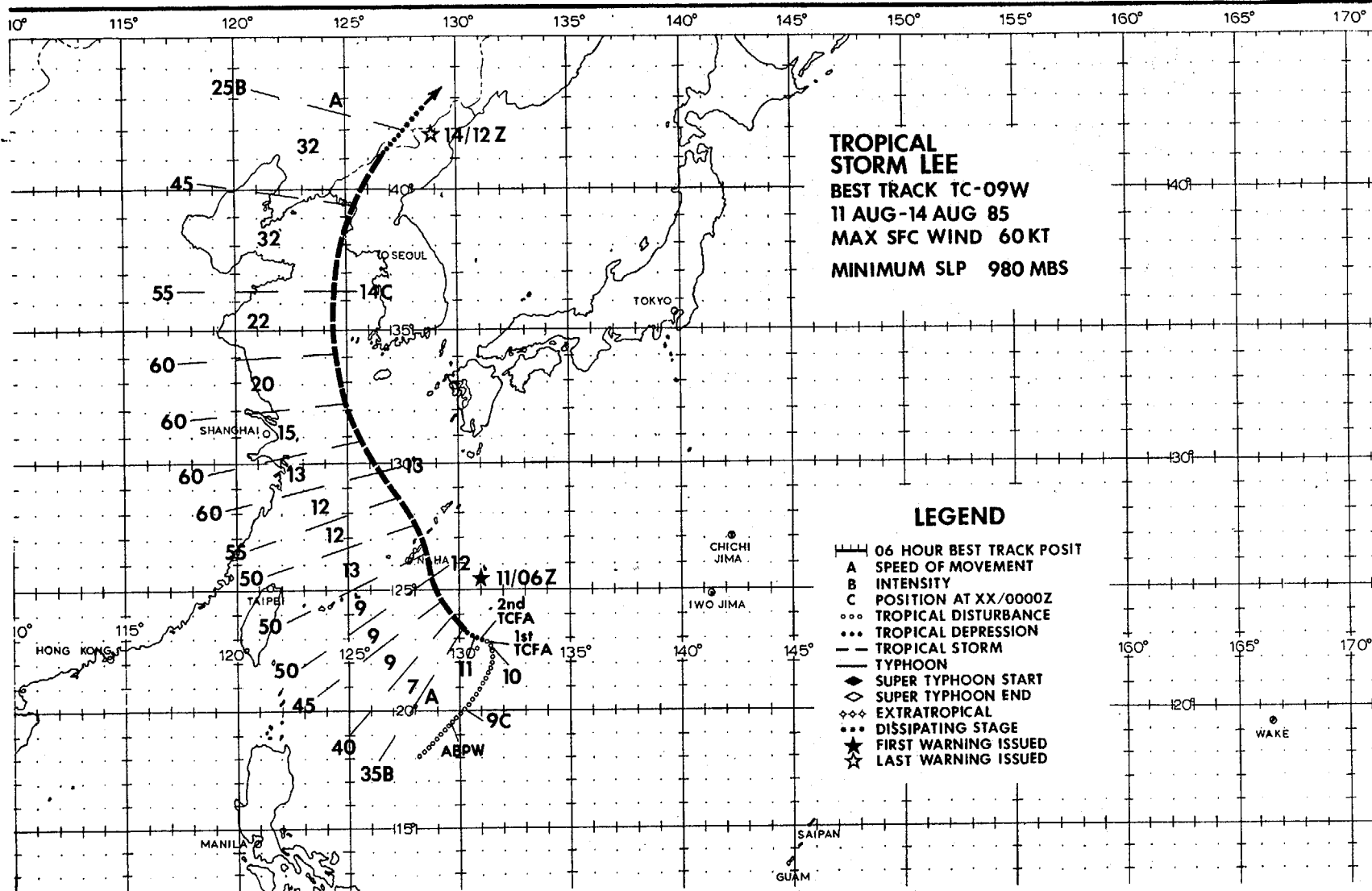


Figure 3-08-2. Typhoon Kit near maximum intensity south of the island of Kyushu, Japan. Kit remained a very compact storm for much of its lifetime, with the over-30 kt (15 m/s) and over-50 kt (26 m/s) wind radii remaining smaller than normal (070028Z August DMSP visual imagery).



Unlike its predecessors, Typhoons Irma, Jeff, and Kit, that developed on the northeast periphery of the southwest monsoon trough, Lee formed in the trough in the central Philippine Sea. Lee's initial development and movement within the monsoon trough was influenced by Typhoon Kit, which was located further to the north.

On the 31st of July, the monsoon trough was oriented southwest to northeast, extending from the central Philippine Sea eastward across the northern Mariana Islands. To set the stage, Typhoon Kit, which developed on the northeastern end of the trough, moved northwestward and intensified. As Kit's low pressure area migrated northwestward, the axis of the monsoon trough repositioned along with it until finally, on the 8th of August the monsoon trough was oriented almost north to south.

Ship reports at 081200Z indicated a broad circulation in the trough 480 nm (889 km) south of the island of Okinawa with a minimum sea-level pressure (MSLP) of 1002 mb. Satellite imagery also showed that the convection associated with this

disturbance had some curvature. Since good outflow channels were present aloft to the south and southwest, the Significant Tropical Weather Advisory (ABPW PGTW) was reissued at 082000Z to include this system.

During the following 24-hours, as the disturbance moved to the north-northeast, the convection remained on the equatorward side of the circulation center, associated with the 15-25 kt (8-13 m/s) convergent low-level wind flow. Synoptic data showed only 5 kt (3 m/s) winds on the northwest side of the circulation. This area of lighter winds underwent a change on the 10th of August. The low-level subtropical ridge built back to the north of the disturbance and across the Ryukyu Islands in the wake of Kit and the pressure gradient increased over the north side of the disturbance. In response, the broad low-level circulation consolidated with increased winds of 10-15 kt (5-8 m/s) over the northwest quadrant (Figure 3-09-1). Simultaneously, the upper-level wind reports showed an anticyclonic circulation was developing over an area of comma-shaped convection. The cloudiness increased in

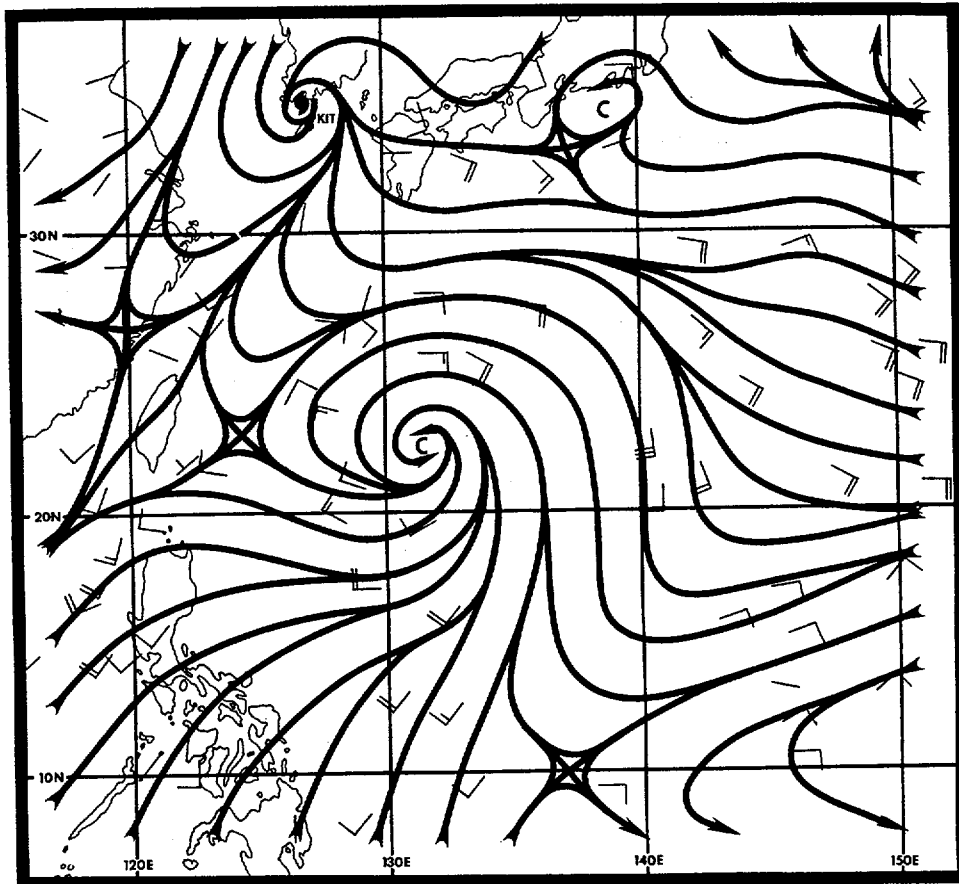


Figure 3-09-1. Surface analysis at 100000Z August showing the subtropical ridge which built across to the north of the disturbance in the wake of typhoon Kit. The monsoon depression is beginning to consolidate. The convergent flow is only on the south and east sides of the broad circulation center.

amount and was near the surface center. These events prompted the issuance of the first TCFA at 100230Z.

The initial aircraft reconnaissance mission, at 100650Z, into the disturbance reported a broad surface circulation with dimensions of 60 nm (111 km) north to south by 90 nm (167 km) east to west and a 997 mb MSLP. The new location of the circulation center, as determined by the aircraft, required the issuance of a second TCFA at 100800Z. The circulation center was relocated 115 nm (213 km) further to

the east-southeast and outside of the original TCFA area which was based on an earlier position derived from visual satellite data.

During the following twenty-four hours, Lee turned towards the northwest, moved very slowly, and showed little intensification. This slow intensification could be related to the persistent strong flow aloft from the north over the disturbance (Figure 3-09-2). Satellite imagery for the same period is shown in Figure 3-09-3).

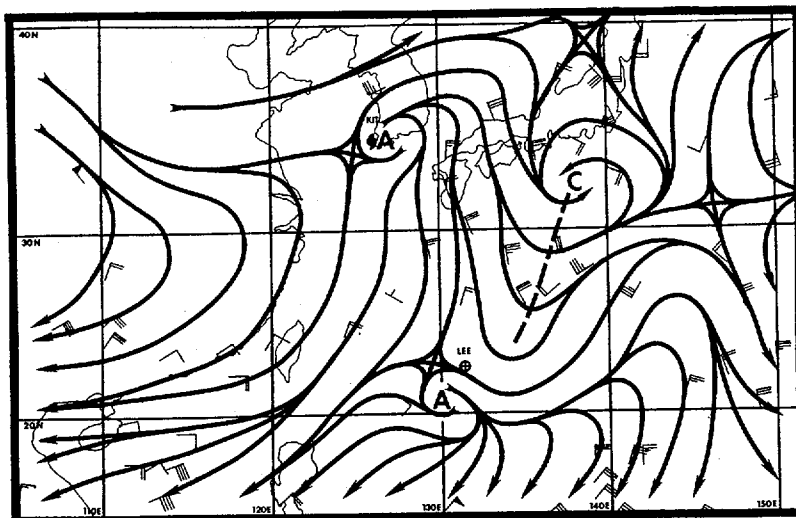
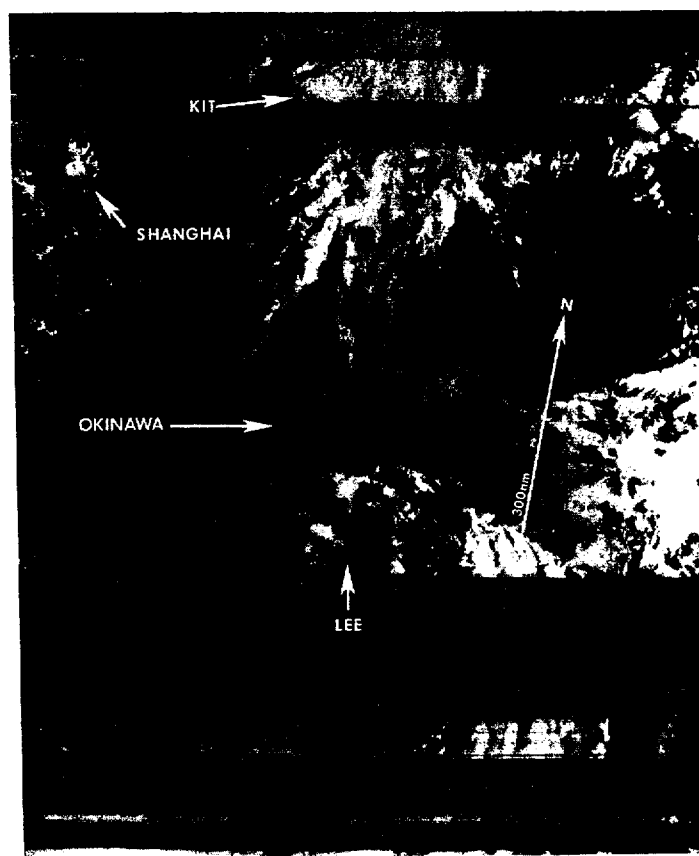


Figure 3-09-2. The 100000Z August 200 mb analysis showing the northerly flow aloft across the disturbance.

Figure 3-09-3. With the northerly flow aloft there is little convection on the poleward side of the disturbance's circulation center. The cloudiness persists over the low-level southwesterly flow (100108Z August DMSP visual imagery).



An aircraft reconnaissance flight into the disturbance at 110656Z found a 25 nm (46 km) diameter light and variable wind center with only 15 kt (8 m/s) maximum surface winds around it. However, the MSLP had dropped another 5 mb during the previous twenty-four hours to 992 mb. This supported maximum winds of 40-45 kt (21-23 m/s) based on the Atkinson/Holliday wind/pressure relationship. Aircraft, synoptic and satellite data indicated that stronger winds of 25-35 kt (15-18 m/s) were located in a band displaced 60-180 nm (111-333 km) to the east of the center. These data led to the issuance of the first warning at 110600Z. As a result, Kadena AB, Japan (WMO 47931) immediately set a Condition of Readiness III.

Fortunately, Lee continued to exhibit typical characteristics of a monsoon depression where the maximum surface winds and intense convection never consolidate at the surface center. Instead, the maximum surface winds remained in the eastern semi-circle. As a consequence, when Lee passed within 15 nm (28 km) northeast of Okinawa at 120430Z, the maximum sustained winds stayed well to the east of the island. In fact, the strongest winds experienced at Kadena AB were from the west-southwest at 22 kt (11 m/s) with 32 kt (16 m/s) approximately twelve hours later. Naha (WMO 47936) located on an elevated and exposed part of the island of Okinawa reported highest winds (in association with the southwest

monsoon flow) of 27 kt (14 m/s) with gusts to 40 kt (21 m/s) at 121948Z. At that time Lee was 170 nm (315 km) to the north-northwest of the station. Overall, Lee's track and asymmetrical wind distribution spared Okinawa, but the western coast of South Korea appeared to be the next target and preparations had begun for the tropical cyclone's approach.

On the synoptic scale, lower standard pressure-level heights prevailed over the East China Sea between the two ridges. As the mid-latitude trough (Figure 3-09-4) approached the Yellow Sea on the 13th of August, it came into phase with the short wave trough extending south-southwestward from a deepening Siberian low near 52N 116E. By 131200Z the trough was oriented along 118E longitude and the ridge over Japan continued to build northward across the Seas of Japan and Okhotsk. This caused the mid-level steering flow from the south to increase over Lee. In response, Lee steadily accelerated across the East China Sea and passed 240 nm (444 km) west of the island of Kyushu, Japan. Coastal stations on Kyushu reported 10-25 kt (5-13 m/s) sustained winds. Aircraft reconnaissance reported the band of 40-60 kt (21-31 m/s) maximum winds remained about 120 nm (222 km) west of the coast.

As Lee began to break free of the monsoon trough, it reached its peak intensity of 60 kt

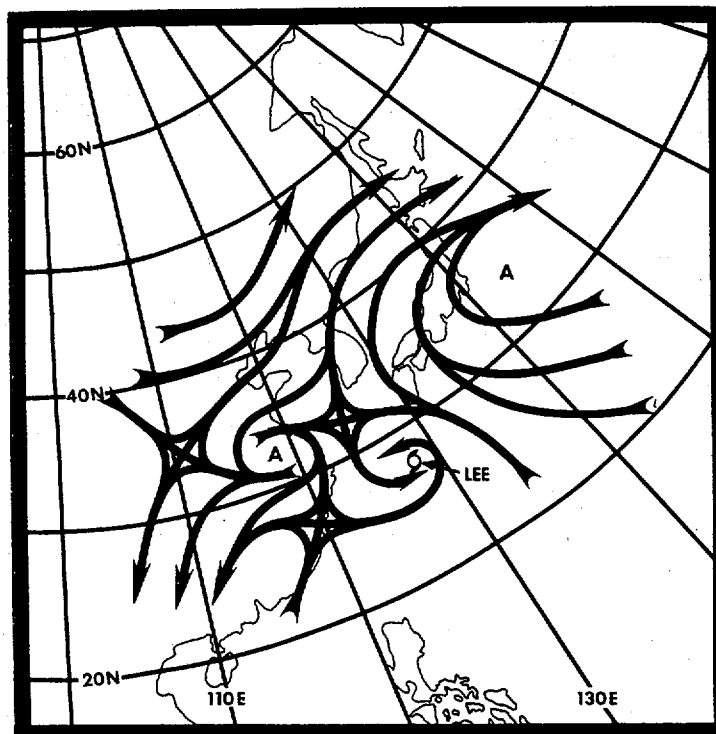


Figure 3-09-4. The 121200Z August 500 mb analysis with troughing in the subtropical ridge over the East China Sea.

(31 m/s) (Figure 3-09-5). Satellite imagery showed orientation of the supporting convection was changing, too. The strong upper-level westerlies were already pushing Lee's outflow to the northeast towards the southwest coast of South Korea.

Lee continued to accelerate and followed a northerly track across the Yellow Sea on 14 August, staying approximately 120 nm (222 km) offshore. This spared the coastline from any significant damage. A few reports of 35 kt (18 m/s) sustained winds were recorded at the southwest portion of the Korean peninsula. Later, Lee transited the North Korean coastline 60 nm (111 km) southeast of Sinuiju (WMO 54498) at 140600Z, and dissipated rapidly inland over the mountainous terrain. No reports of damage were available.

Of note, the tracks of Jeff, Kit, Lee, and later, Mamie in the Yellow Sea came under the

influence of the same synoptic scale pattern during the first three weeks of August with ridging over Japan and troughing over northeast mainland China. This pattern maintained semi-persistent south-to-north mid-level steering flow over the Yellow Sea. Each tropical system in its own time recurved around the western periphery of the subtropical ridge and accelerated. Figures 3-09-6 and 3-09-7 show the approximate location and orientation of the synoptic scale trough with respect to the point of recurvature of each tropical system. The pattern shifted eastward from Jeff to Kit, then retrograded westward with Lee, and later, Mamie's track. The points of recurvature also indicate the western extent of the subtropical ridge in each case plus the northward displacement of the ridge axis which was well north of its climatological position.

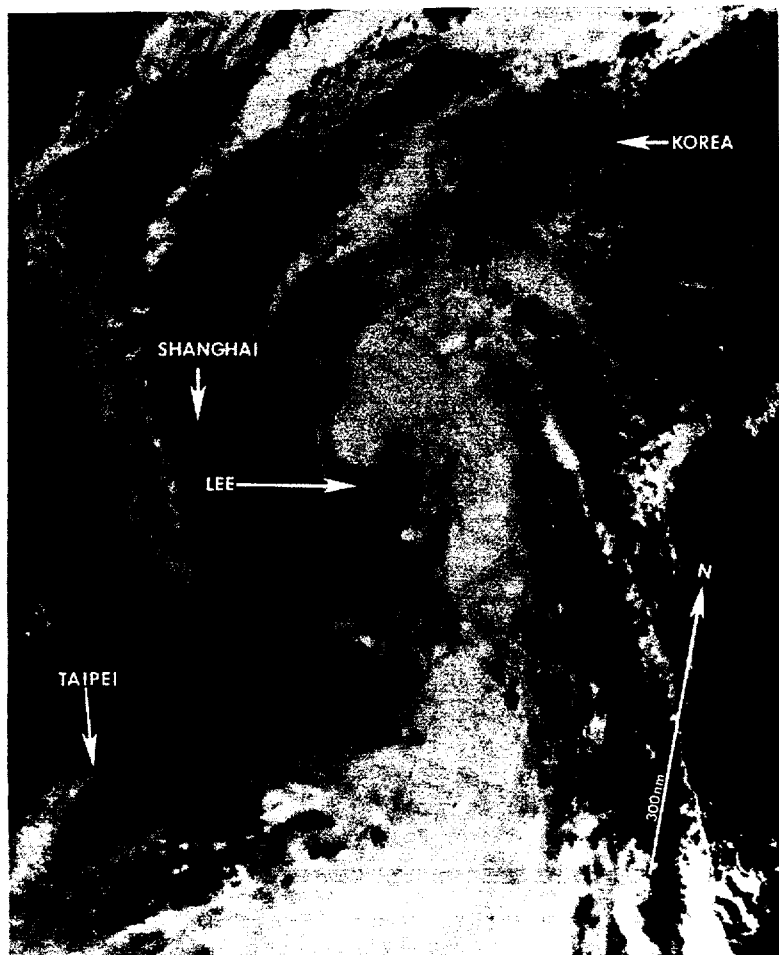


Figure 3-09-5. Tropical Storm Lee at its maximum intensity of 60 kt (31 m/s). The upper-level anticyclonic circulation displaced slightly to the northeast of the exposed low-level circulation center (130518Z August NOAA visual imagery).

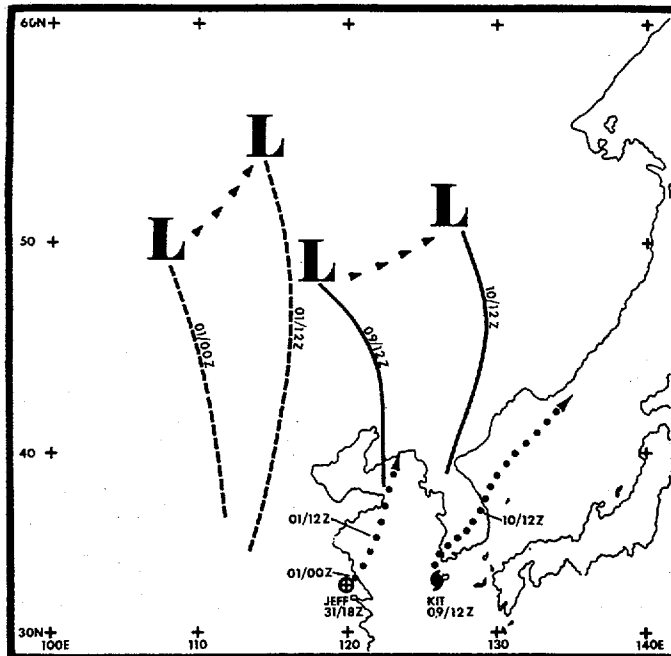


Figure 3-09-6. The best tracks (dotted line) of Jeff and Kit from the point of recurvature through the final warning are depicted. The times along the dotted lines at, or after, the recurvature point correspond with the respective positions of the mid-latitude troughs (dashed and solid lines). The arrows show the movement of the Siberian mid-level lows. Notice the Siberian low track is displaced further southeast during Kit.

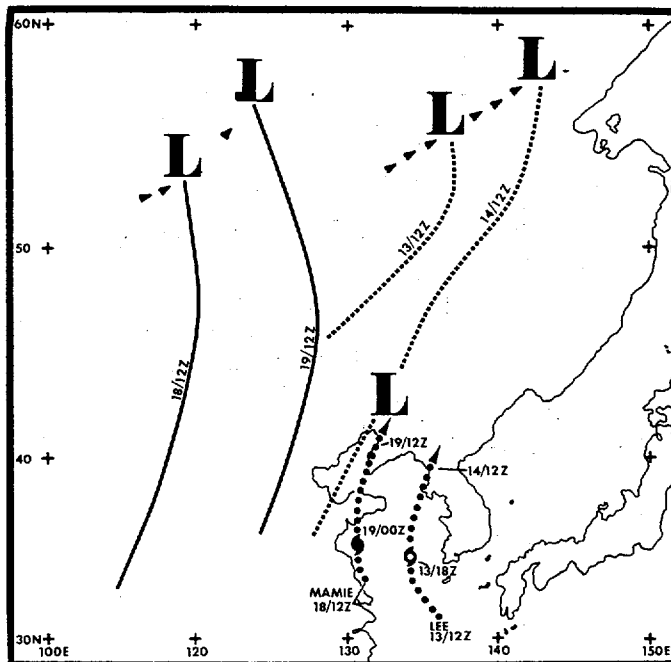
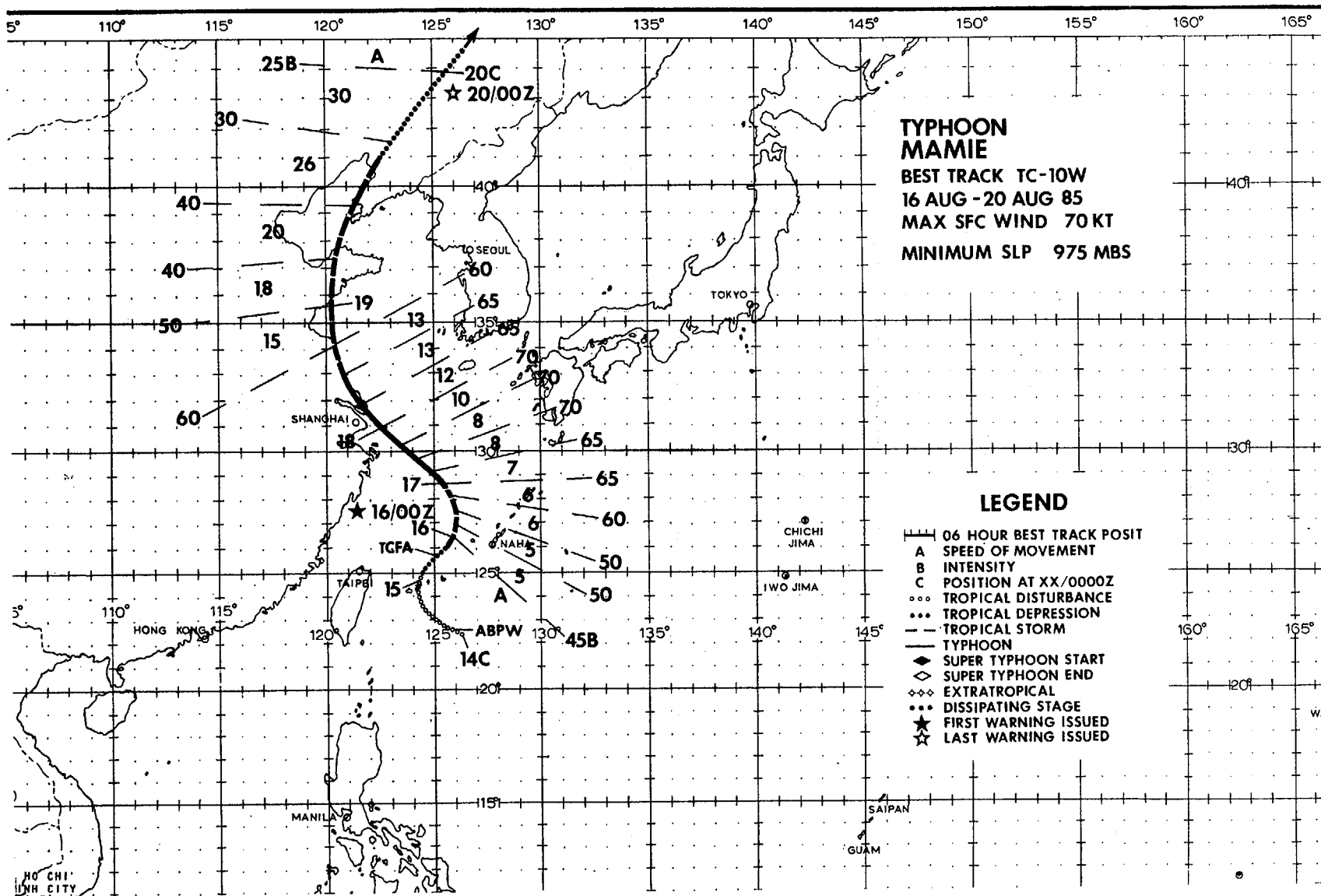


Figure 3-09-7. The best tracks (dotted line) of Lee and Mamie from the point of recurvature through the final warning are shown. The times along the dotted lines at, or after, the recurvature point correspond with the respective positions of the mid-latitude troughs (dashed and solid lines). Notice that the track of the Siberian lows retrogrades between the second and third week of August.





Despite reaching a maximum intensity of only 70 kt (36 m/s), Typhoon Mamie was one of the more destructive tropical cyclones of the 1985 western North Pacific season. Following a path similar to its predecessor, Tropical Storm Lee, Mamie was responsible for at least 35 deaths and caused heavy damage to crops, homes, and shipping. For two days, Mamie skirted a 400 nm (740 km) stretch of the eastern Chinese coast from Shanghai (WMO 58367) to the Shantung Peninsula, inundating farmland and washing away many dikes and dams with its torrential rains. More than 800,000 civilians and soldiers were mobilized to combat the flooding and repair damage. Estimates of the destruction caused by Mamie were staggering: over 6.5 million trees uprooted, 2.9 million metric tons of high stalk farm crops ruined, more than 120,000 houses destroyed or damaged, over 200 watercraft of various types sunk or driven aground, and over 122,000 domestic livestock drowned.

Mamie formed from an area of convection that was originally part of the southwest monsoon flow into Tropical Storm Lee. At 0129Z on 14 August, visual satellite imagery indicated slight curvature in an area of convection due east of Taiwan that had separated from Lee's inflow. Figure 3-10-1 shows this area and its relationship to Lee. Subsequently, the area was included as a "poor" on the 140600Z Significant Tropical Weather Advisory (ABPW PGIW). Satellite imagery through the remainder of the 14th showed the disturbance was turning to the north and becoming more organized as the separation from Lee's wind field increased. The 150600Z ABPW PGIW bulletin reflected this development by upgrading the potential for development to "fair" and aircraft reconnaissance of the disturbance was requested for the following morning.

At 151200Z, a TCFA was issued, based on increased curvature of the convective bands and anticyclonic cirrus outflow indicated by satellite imagery. At this point, the area was beginning to intensify more rapidly than before, due partly to Lee's waning influence on the new circulation. At 152340Z, aircraft reconnaissance closed-off a circulation of tropical storm intensity 90 nm (167 km) due west of Okinawa, prompting the issuance of the first warning on Mamie at 160000Z. Less than three hours later Kadena AB on Okinawa reported its strongest winds from Mamie - south at 20 kt (10 m/s) with a peak gust to 35 kt (18 m/s).

On 16 August Mamie began to turn to the northwest. This turn was due to the low-level ridge north of Mamie strengthening slightly as the mid-latitude trough that had interacted with the remnants of Tropical Storm Lee began to move rapidly to the east in the mid-latitude westerlies. However, the ridge never became strong enough to stop Mamie from heading north-northwest, then north through a weak area in the ridge that persisted throughout Mamie's lifetime. Mamie continued to intensify, reaching typhoon intensity at about 170000Z as it moved northwest at 7 kt (13 km/hr) toward Shanghai (WMO 58367).

The Typhoon reached a peak intensity of 70 kt (36 m/s) 12-hours later at 171200Z, just prior to affecting the Chinese coast near Shanghai (Figure 3-10-2). Mamie traversed the Chinese coastline, hitting Tsingtao, with decreased winds of 50 kt (26 m/s) at about 190200Z. Mamie then turned north around the western periphery of the subtropical ridge and crossed the Shantung Peninsula, striking Yantai, China (near Fushan WMO 54764) at about 190600Z.

Mamie accelerated to 20 kt (37 km/hr) and weakened to a 40 kt (21 m/s) tropical storm just prior to crossing the Yellow Sea and moving toward Dairen, China (WMO 54662). After making landfall just west of Dairen at 191200Z, Mamie began to dissipate over land. Because Mamie's intensity decreased to an estimated 25 kt (13 m/s) and due to its location over the mountains of northeast China, the last warning was issued at 200000Z.

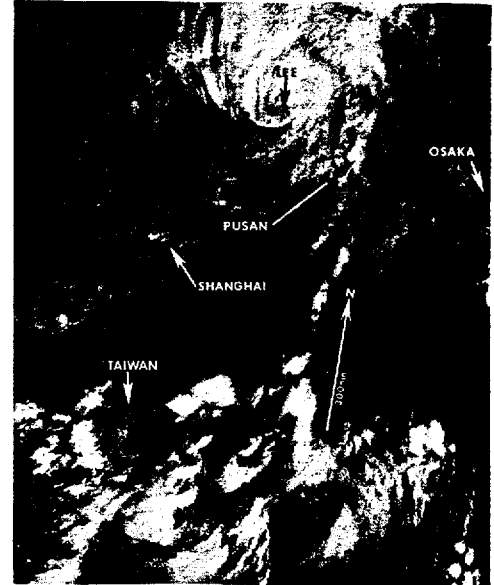


Figure 3-10-1. The tropical disturbance that became Typhoon Mamie is located east of the island of Taiwan. The slightly curved convective band and separation from the cloudiness associated with Tropical Storm Lee to the north were the first signs of organization (140129Z August DMSP visual imagery).

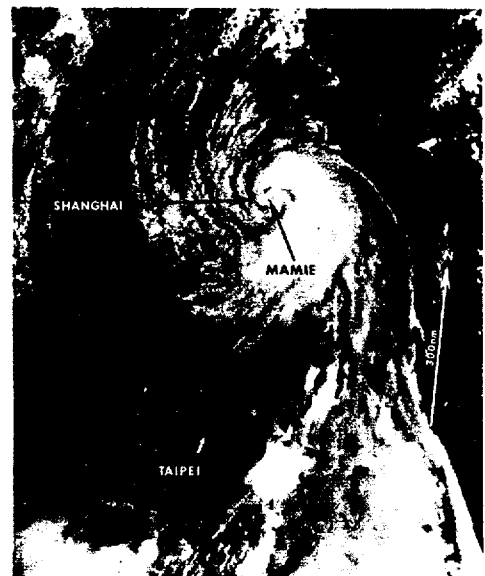
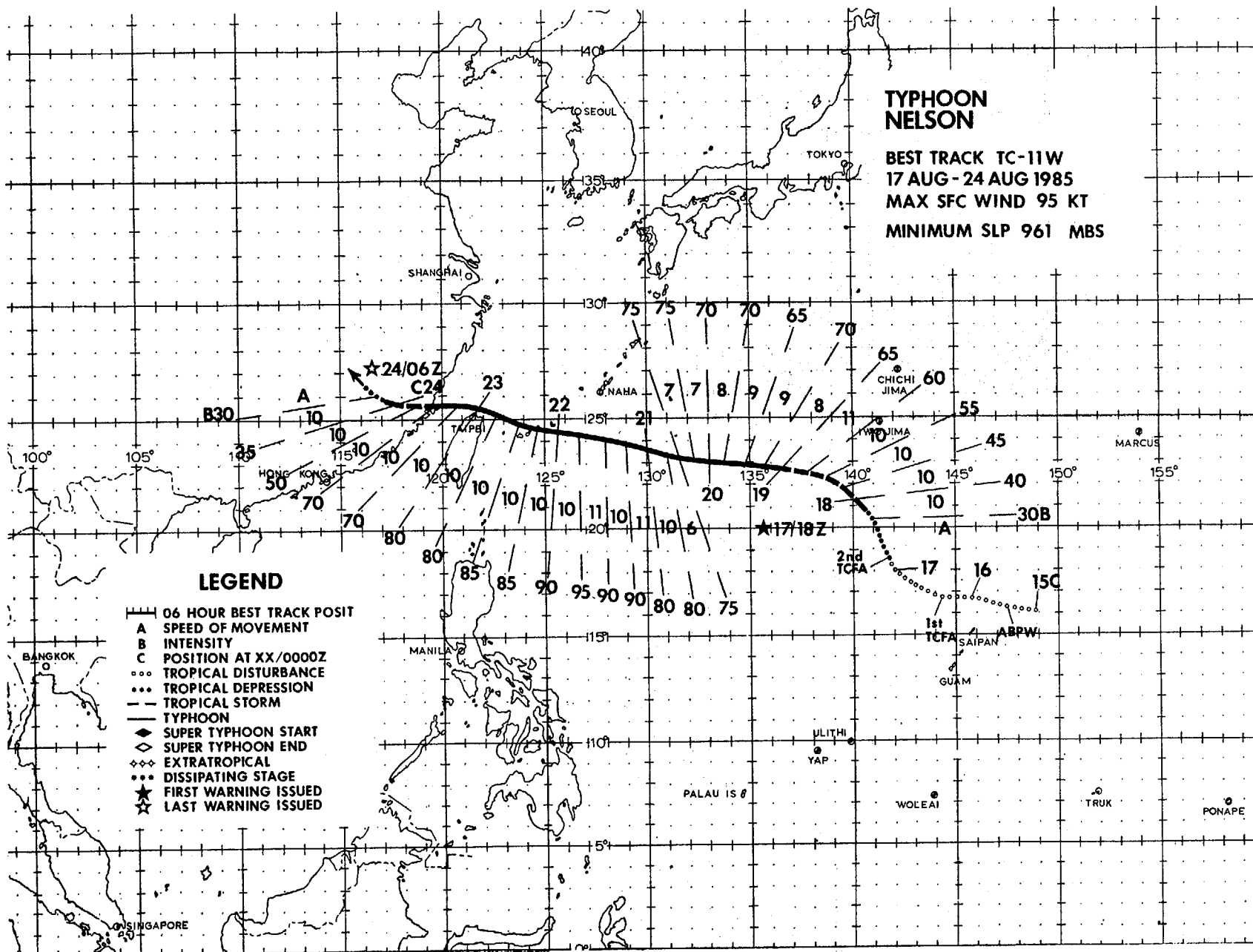


Figure 3-10-2. Mamie with typhoon force winds passing just east of Shanghai, China (180149Z August DMSP visual imagery).

# TYPHOON NELSON

BEST TRACK TC-11W  
17 AUG - 24 AUG 1985  
MAX SFC WIND 95 KT  
MINIMUM SLP 961 MBS



#### TYPHOON NELSON (11W)

Typhoon Nelson was the fourth of seven tropical cyclones that developed over the Northwest Pacific in August. It caused substantial damage and loss of life as it passed through the southern Ryukyu Islands, brushed by northern Taiwan and crossed into mainland China.

On 14 August Tropical Storm Lee was dissipating as it moved across North Korea and Typhoon Mamie was building near the southern Ryukyu Islands just east of Taiwan. The following day the disturbance that developed into Typhoon Nelson was first noticed as a small, but persistent, area of poorly organized convection 150 nm (278 km) east-northeast of the island of Saipan in the Marianas. The area was located in the near-equatorial trough where the convective cloudiness was enhanced by the divergent upper-level flow associated with an upper cold low in the tropical upper-tropospheric trough (TUTT). Synoptic data at 150000Z indicated that southwesterly gradient-level flow from the Philippine Sea was near the disturbance. These factors, plus the satellite imagery at 150300Z which showed a slight cyclonic curvature in the convection, prompted mention of the area on the 150600Z Significant Tropical Weather Advisory (ABPW PGIW).

During the next 24-four hours, satellite imagery revealed a marked increase in the amount of convection over the northeastern portion of the disturbance with another larger area of unorganized convection moving toward the disturbance from the west-southwest. By 160000Z, synoptic data indicated that the southwesterly gradient flow had propagated eastward to the disturbance and an associated upper-level anticyclone had formed over the disturbance. A Tropical Cyclone Formation Alert (TCFA) followed at 160625Z.

Aircraft reconnaissance late on the sixteenth was unable to locate a surface circulation. However, the aircraft reconnaissance weather officer

(ARWO) did report: a narrow low-level trough that was 200 nm (370 km) in extent and elongated northeast-southwest; three possible 1002 mb pressure centers; and maximum winds of 10-20 kt (5-10 m/s) to the north of the trough. The TCFA was reissued at 170555Z.

A dramatic increase in both the cyclonic curvature and amount of central convection occurred at 171600Z. The Dvorak intensity estimate of the system was 35 kt (18 m/s). This intensity estimate together with the continuing development of the system led to the first warning on Nelson at 171800Z. Aircraft reconnaissance at 172131Z confirmed this development, and more, when gale force surface winds were located north of a 989 mb low pressure center. Specifically, the flight revealed the 700 mb center was displaced 31 nm (57 km) to the northwest of the surface center and a band of 45 kt (23 m/s) low-level winds was located 90 nm (167 km) to the north-northwest.

Due to the uncertainty in the Fleet Numerical Oceanography Center (FNOC) mid-level wind fields in the data sparse region south of Japan, a 400 mb synoptic track mission was flown early on the 18th to better define the mid-level steering flow north of Nelson. Data from this flight confirmed that the ridge extended westward over Nelson and indicated forecasts for an "under the ridge" scenario were appropriate. This forecast scenario proved to be correct.

Further intensification occurred as Nelson assumed a more west-northwesterly track. At 190000Z, Nelson was upgraded to a typhoon after aircraft reconnaissance indicated the system had a 5 nm (9 km) diameter light/variable wind center with a 979 mb MSLP and 65 kt (33 m/s) maximum surface winds displaced 40-120 nm (74-220 km) northwest of the center. Almost three days later, at 211800Z, Nelson reached a peak intensity of 95 kt (49 m/s) with a MSLP of 961 mb (see Figure 3-11-1).

Nelson passed between the Ryukyu Islands of Yaeyama and Miyako early on 22 August and continued moving west-northwestward under the ridge. Early on 23 August (Figure 3-11-2), the typhoon skirted northern Taiwan passing within 25 nm (46 km) of Taipei (WMO 58968). The tropical cyclone quickly transited the Formosa Straits and made landfall 40 nm (74 km) southwest of Fuchou (WMO 58847) in China's Fuchien province at 241400Z.

In retrospect Nelson's passage between Yaeyama and Miyako Islands resulted in more than 1.5 million dollars in damage to banana and sugar cane crops. As Nelson skirted northern Taiwan, four people were reported killed from the associated winds and tor-

rential rains. At landfall in China's Fuchien province, another forty-eight people perished, with an additional 329 reported injured, more than 5,000 homes destroyed, 969 fishing boats sunk and about 178,500 acres of crops lost.

After Nelson dissipated, an additional three days of heavy rains associated with the remains of the system affected many areas of eastern China. At least 147 people were killed and more than 30,000 persons were driven from their homes by flooding in Hunan province further inland. Later, Shanghai reported 50,000 homes with flood damage resulting from these heavy rains inland.

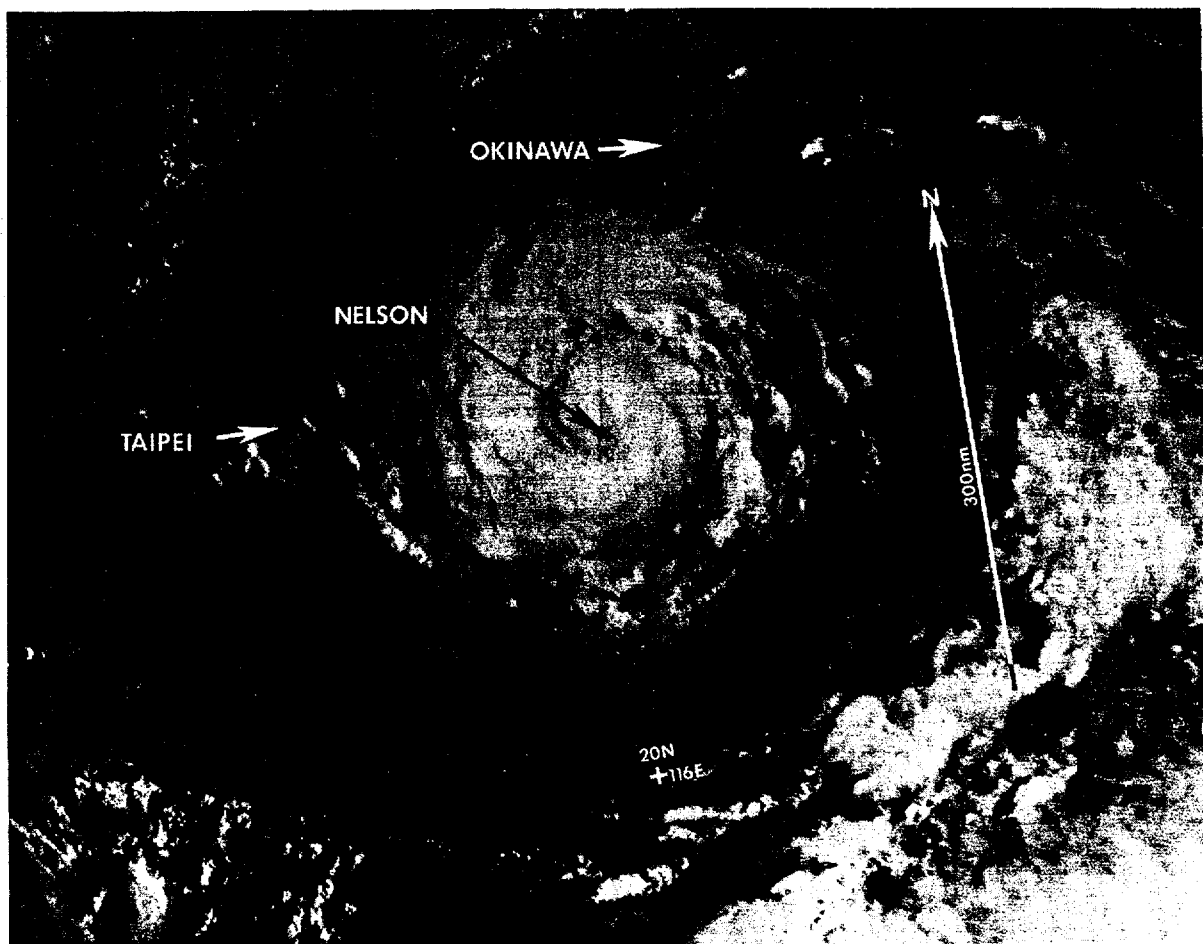


Figure 3-11-1. Typhoon Nelson near maximum intensity (212352Z August NOAA visual imagery).

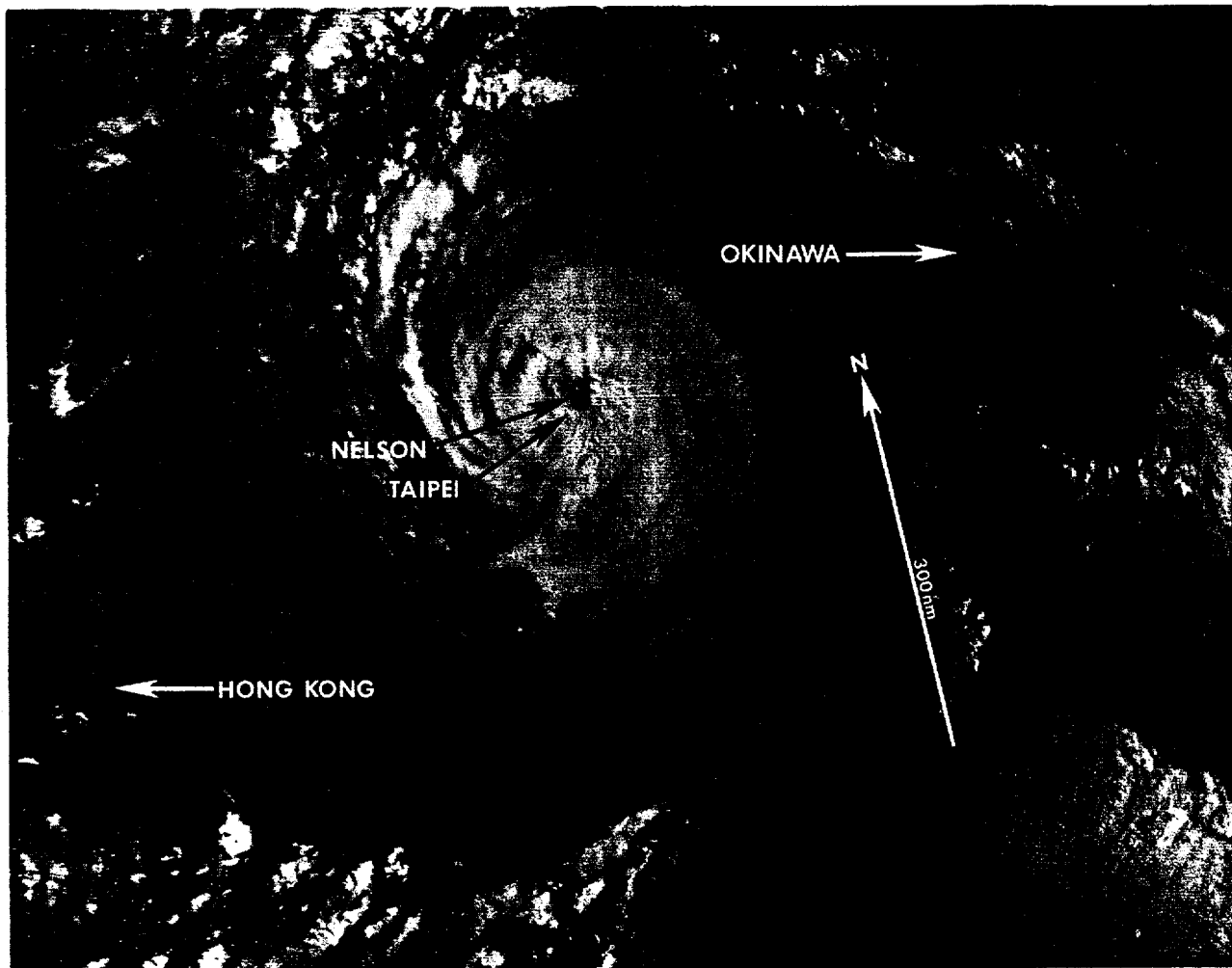
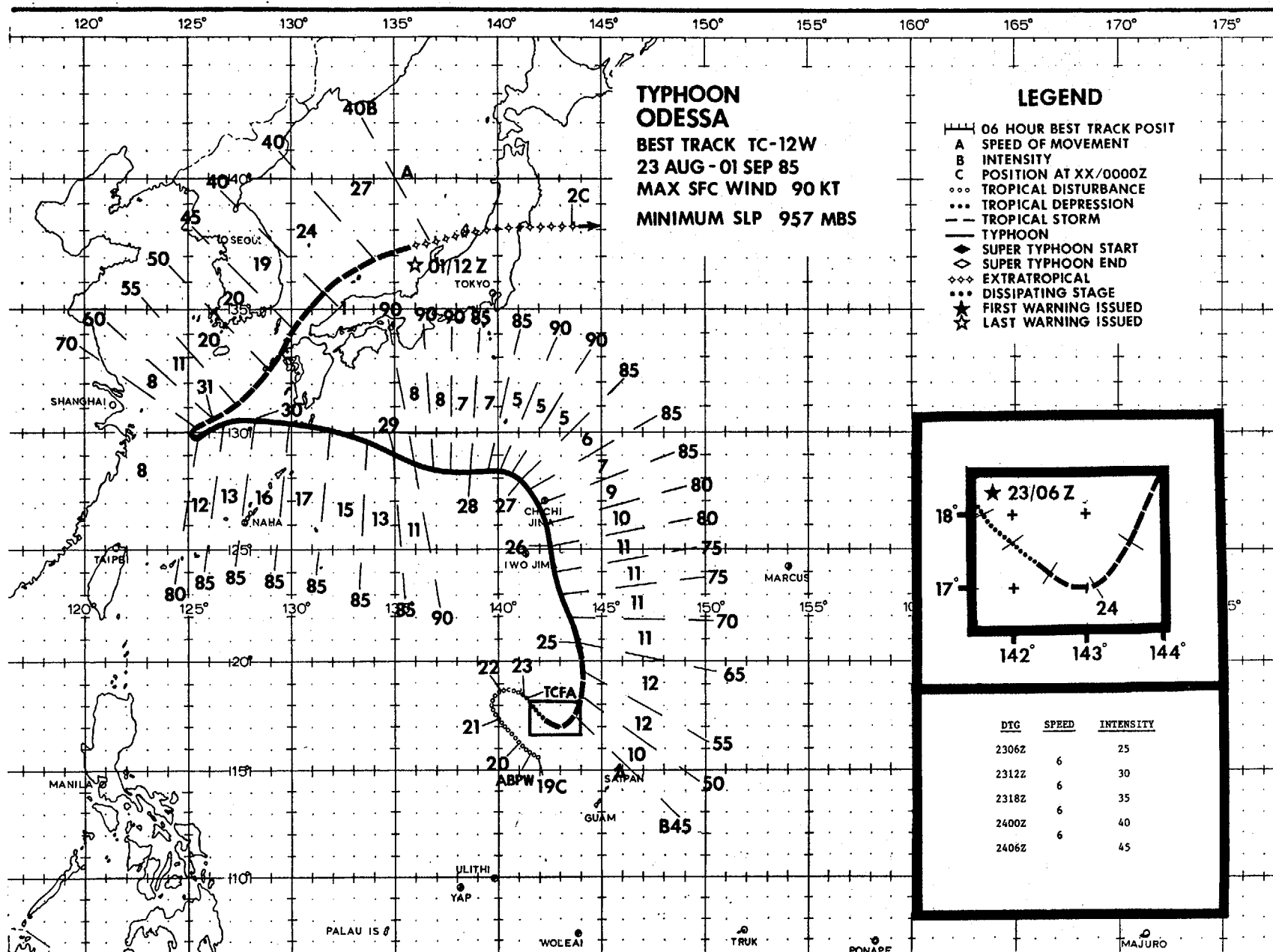


Figure 3-11-2. Nelson skirting the island of Taiwan  
(222334Z August NOAA visual imagery).



Odessa persisted for almost two weeks and required a total of thirty-eight warnings - in this regard, only Typhoon Jeff with forty-one exceeded Odessa's total during 1985 season. The system became part of a multiple tropical cyclone outbreak along with Typhoon Pat and Tropical Storm Ruby. At one time five tropical cyclones were in warning status. Ultimately, Odessa underwent a complex binary interaction with Typhoon Pat south of Japan before completing extratropical transition over the Sea of Japan.

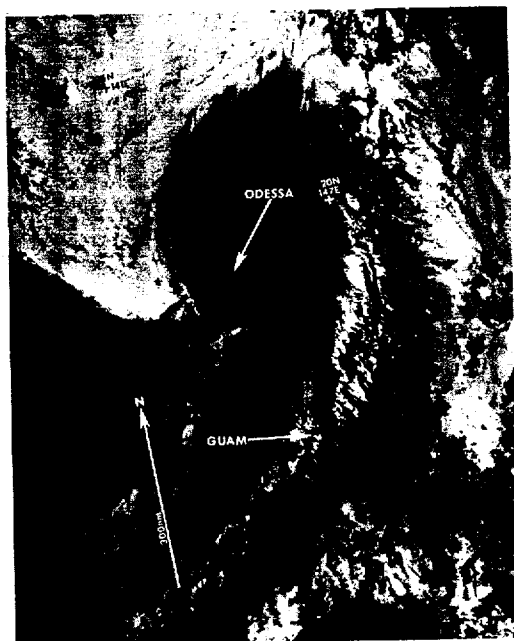


Figure 3-12-1. Nighttime imagery of Odessa with a single outflow channel that is directed equatorward (241227Z August DMSP infrared imagery).

By the third week of August, Typhoon Nelson had moved westward across the northern Philippine Sea. At that time, the eastern end of the monsoon trough extended across the Philippine Sea to the vicinity of Guam. The eastern end of the low latitude westerly monsoonal flow, where it interacted with the easterly tradewinds, became the preferred location for maximum cloudiness. Initially, on 19 August, the deep convection in this area appeared random with little, or no, curvature, but its persistence was sufficient reason for its inclusion on the Significant Tropical Weather Advisory (ABPW PGTW). With maximum surface winds in the monsoonal flow of 15 to 20 kt (8 to 10 m/s) and a minimum surface pressure of 1006 mb, the potential for development was rated as poor.

This potential for intensification changed to fair at 220600Z as the convective mass began to increase in size over a low-level circulation which began to separate from the surrounding cloudiness. A TCFA followed at 230230Z based on meteorological satellite imagery which showed a Central Dense Overcast (CDO). Aircraft reconnaissance was scheduled for the next day. The persistent CDO, a favorable outflow channel aloft to the south, and a pre-existing low-level circulation center, prompted the first warning for Tropical Depression 12W a short time later at 230600Z. The Depression was upgraded at 240000Z when aircraft reconnaissance observed sustained surface winds of 30 kt (15 m/s) that were gusting to 55 kt (28 m/s) southeast of the center - the MSLP was estimated to be 1000 mb (Post analyses revealed that Odessa reached tropical storm intensity shortly before 231800Z). The aircraft also discovered that the low-level center had drifted south-eastward during the night, when interpretation of infrared satellite imagery was restricted to positioning the poorly defined upper-level circulation center.

Erratic movement became less of a concern as Odessa matured and assumed a north-northwestly track. Aircraft reconnaissance at 242340Z reported typhoon

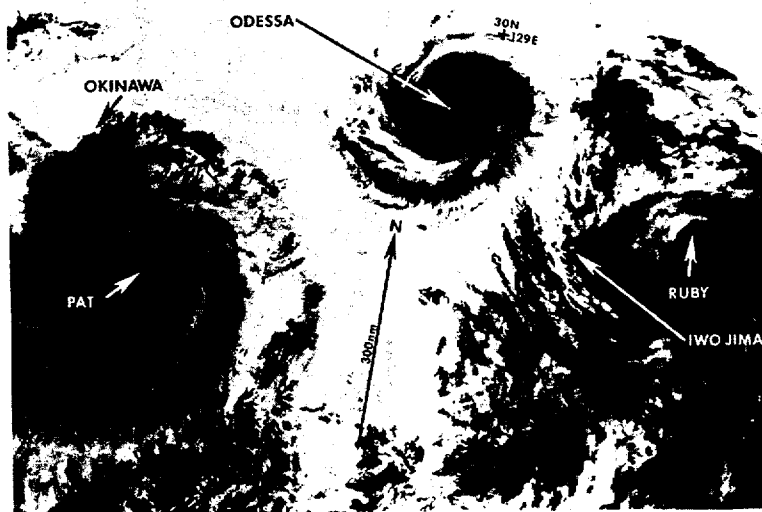


Figure 3-12-2. Odessa with channel-less or no-channel outflow (281024Z August NOAA infrared imagery).



intensity winds and a circular eye 15 nm (28 km) in diameter. The warning valid at 250000Z, upgraded Odessa to a Typhoon. Odessa remained a compact typhoon for the following six days. Of interest in this regard was the change in the outflow channel from equatorward, during the maturation process, to the absence of the channel, during the small, but intense, typhoon stage. Compare Figures 3-12-1 and 3-12-2 to appreciate the shift of outflow.

Odessa's north-northwesterly movement slowed

as it approached the subtropical ridge axis. The critical forecast - whether to go through the ridge or westward under the ridge - was handled well. The primary aids, the One-way Interactive Tropical Cyclone Model (OTCM) and Nested Tropical Cyclone Model (NTCM), (Figure 3-12-3) were at odds apparently due to their respective sensitivities to the narrow ridge to the north. NTCM provided the better guidance in this case. Odessa tracked, as forecast, and turned westward under the influence of the narrow subtropical ridge over Japan.

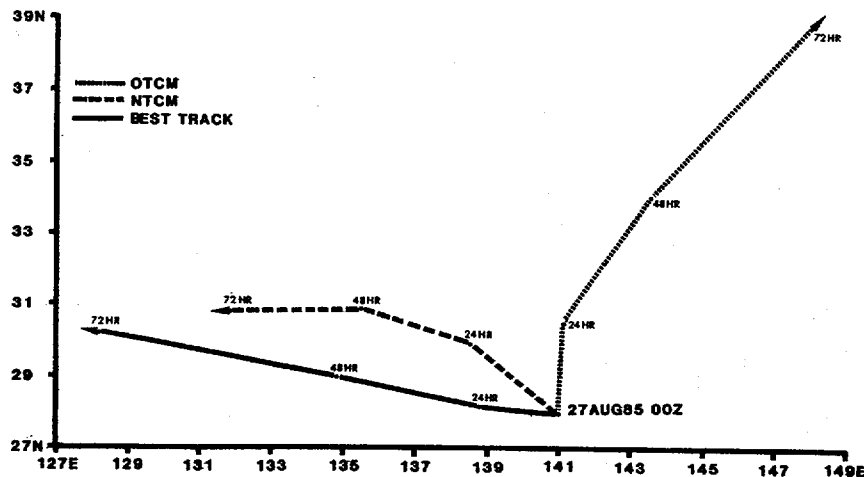
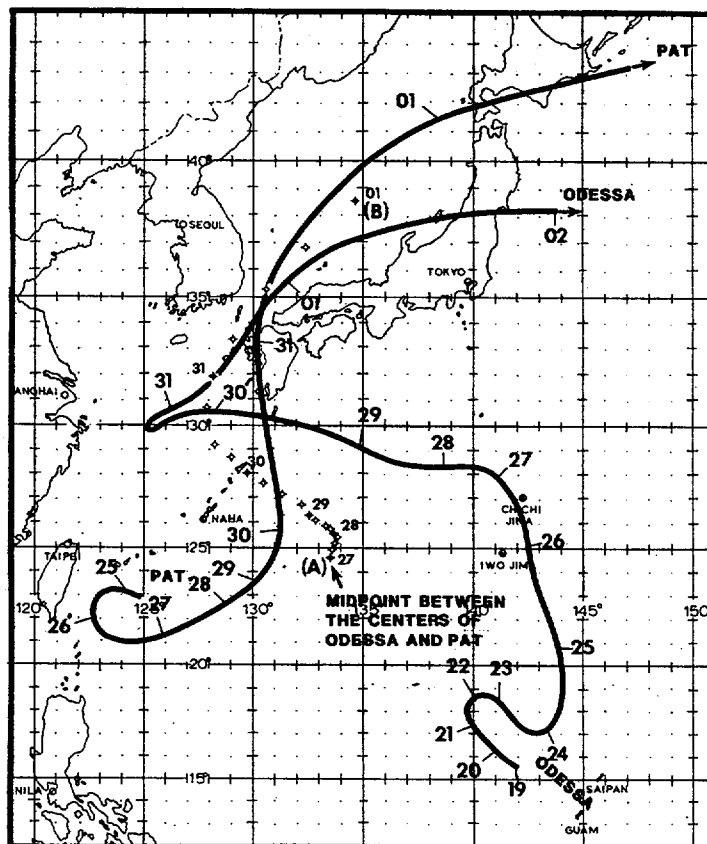


Figure 3-12-3. Primary aids, NTCM and OTCM, provide conflicting guidance. NTCM correctly senses the track to the West. The best track position is a solid line.

Figure 3-12-4. Best track positions for Pat and Odessa. The small symbols from (A) to (B) are the midpoints between the respective centers of Pat and Odessa at each six hourly interval.



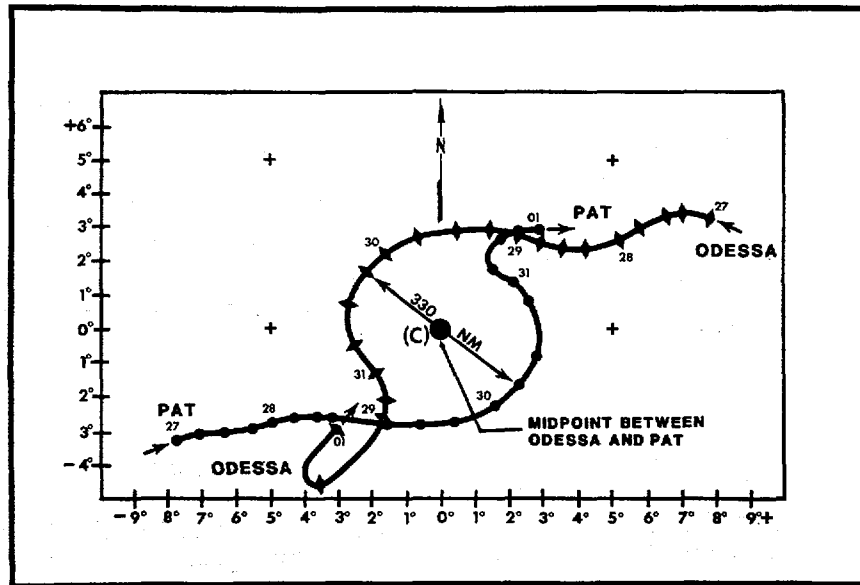
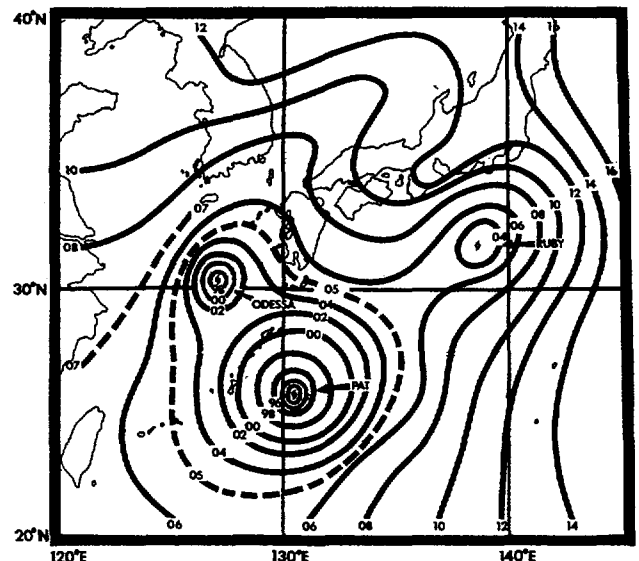


Figure 3-12-5. The singular point at (C) contains all the midpoints taken from the (A) to (B) in the previous Figure 3-12-4. The positions of both Pat and Odessa relative to the midpoint reflect the inward, spiralling interaction between the two systems with time.

As the tropical cyclone pressed ahead on its new track, it began to accelerate in response to the approach of Typhoon Pat from the south. The complex interaction between the spatially proximate cyclones, or binarys, is not readily apparent from Figure 3-12-4, which depicts the superimposed tracks. If the midpoint is determined for each six hourly time period, the locus of midpoints from A to B results (see Figure 3-12-4). When this locus becomes a singular point (C) in Figure 3-12-5 and the respective positions of the two typhoons are replotted

relative to (C), the subtle attraction and cyclonic rotation into a circle of 330 nm (611 km) becomes apparent. It is interesting to compare the relative sizes of Pat, which is average, and Odessa, which is small and compact (reference the surface isobaric analysis in Figure 3-12-6). Returning to Figure 3-12-5, it is important (next) to note the departure of both typhoons from the 330 nm (611 km) circle at 310000Z. This was the beginning of extratropical transition and separation. Satellite imagery is provided in Figure 3-12-7.

Figure 3-12-6. Isobaric analysis for 300000Z August indicates the size difference between Pat and the small compact Odessa. The weaker system to the northeast is Tropical Storm Ruby, which remained solitary and apparently didn't enter into the interaction.



The movement of Odessa under the ridge had served the prognostic reasoning well since the 27th. The forecast remained conservative and held to persistence as Odessa began to display erratic behavior, but the ridge to the north had changed. Both aids, OTCM and NTCM, indicated north to north-easterly movement (see Figure 3-12-8). When Pat started accelerating northeastward across Japan, Odessa executed an abrupt turn to the northeast and followed on its heels. Forecasts for Odessa's forward motion proved too slow as it accelerated into

the Sea of Japan and began extratropical transition. Fortunately the system was compact and weakening or damage might have been more widespread. In Kyushu and other southern islands of Japan strong rains and winds from Odessa knocked out power and caused fishing vessels to capsize. Ships remained in port at Sasebo, Japan (WMO 47812) as Odessa passed sixty miles to the north. The final warning was issued at 011200Z September as the extratropical remains of Odessa approached northern Honshu.

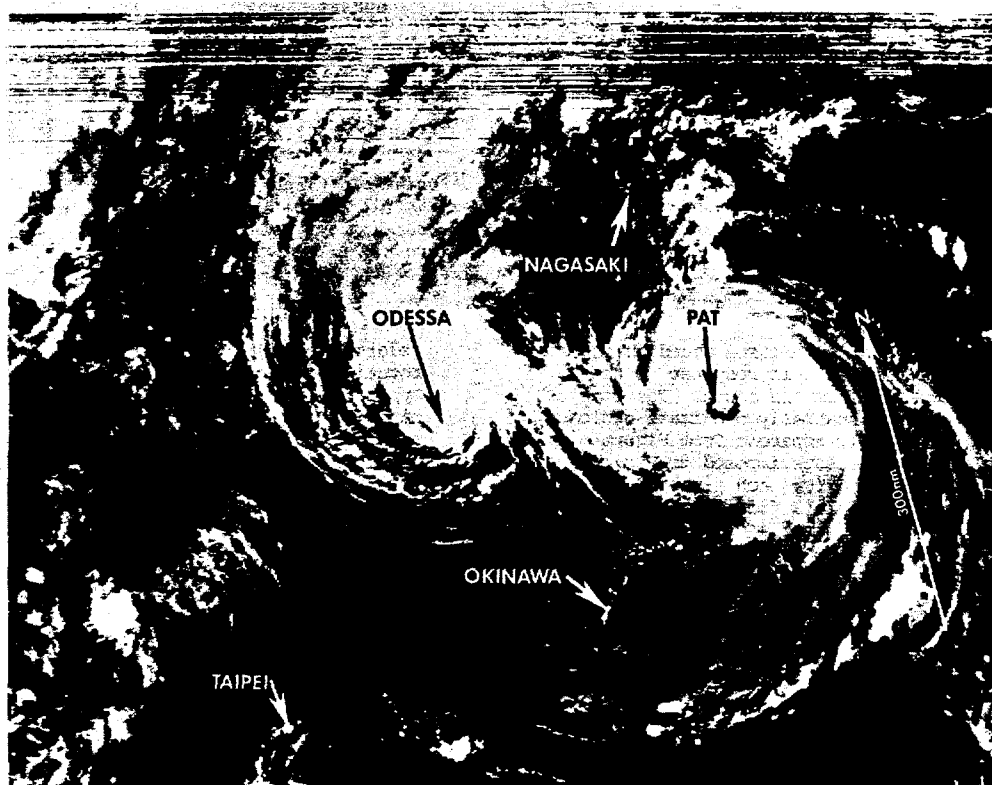


Figure 3-12-7. In this moonlight photo Pat's ragged eye and large surrounding cloud mass dwarf Odessa, which is also at typhoon intensity (301348Z August DMSP visual imagery).

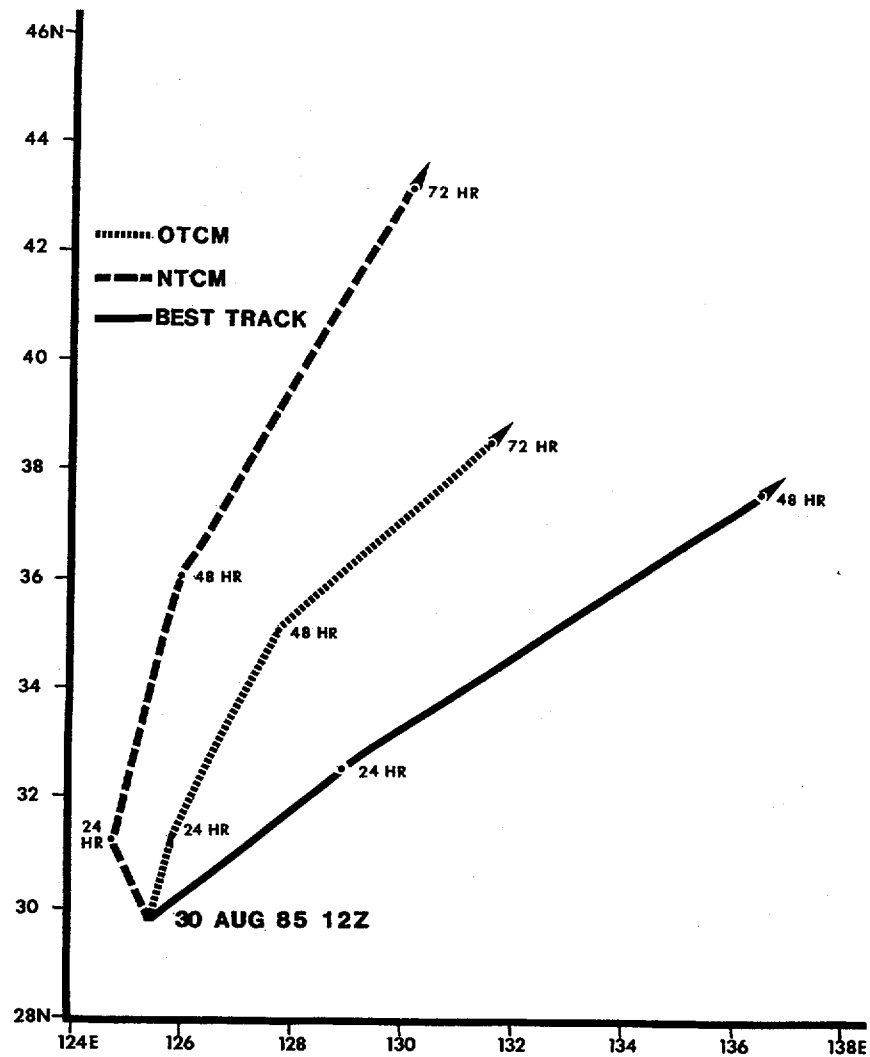
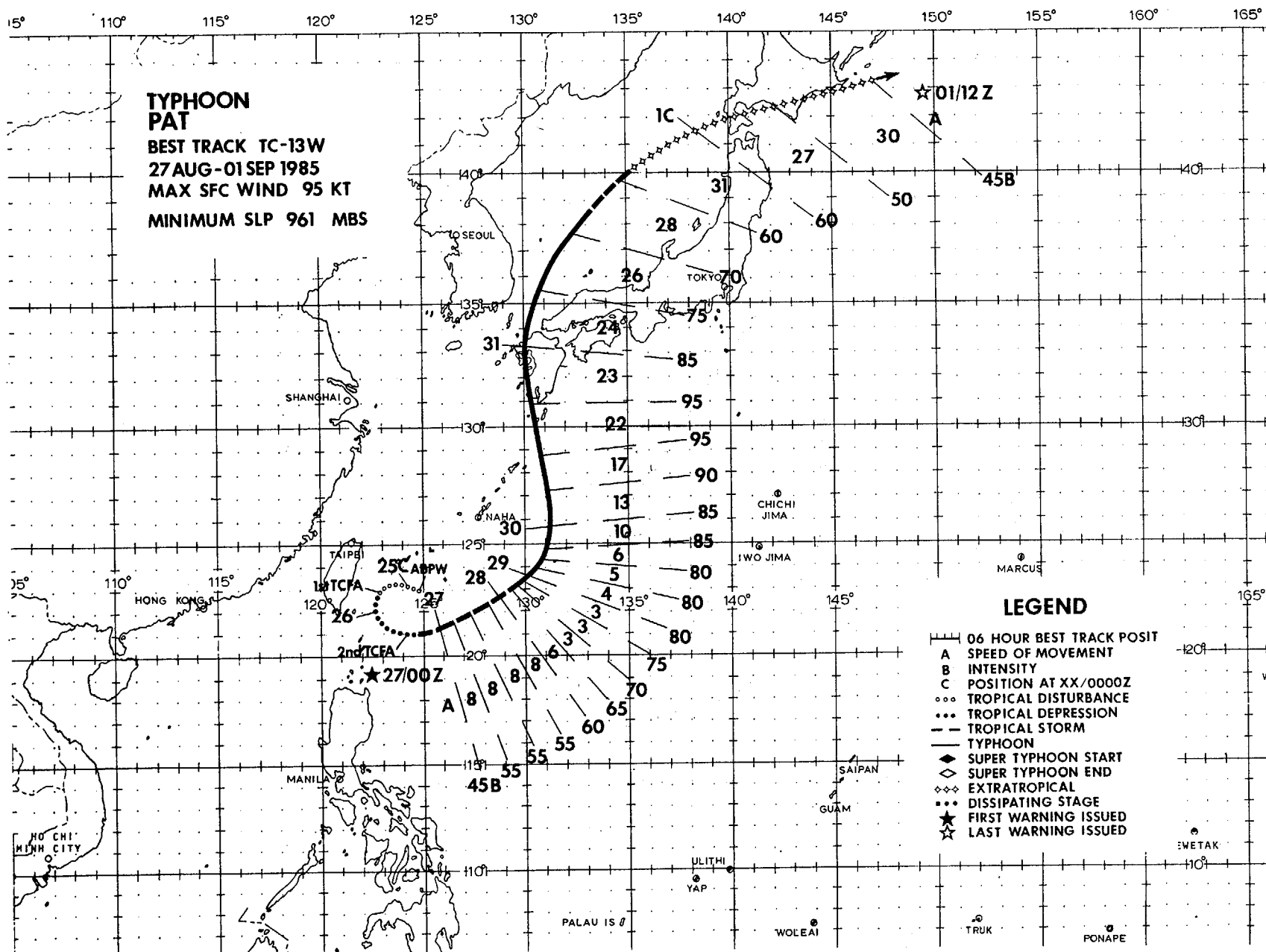


Figure 3-12-8. Primary aids, NTCM and OTCM, at 301200Z August reflect a north to northeasterly track. The best track positions (solid line) indicate the guidance was basically correct.

**BEST TRACK TC-13W  
27 AUG-01 SEP 1985  
MAX SFC WIND 95 KT  
MINIMUM SLP 961 MBS**



64

# TYPHOON PAT (13W)

Typhoon Pat developed east of Taiwan in the monsoon trough a few days after Typhoon Odessa and one day before Tropical Storm Ruby. Pat was significant due to the complex forecasting problems it caused and the damage it inflicted in Japan. The presence of two other storms (Odessa and Ruby) presented a variety of possible forecast interactions. The movement of each cyclone had to be considered in combination with the changing synoptic pattern.

The monsoon trough remained quite active the last two weeks of August. The disturbance which eventually evolved into Pat, originated in the wake of Typhoon Nelson as it moved into eastern China. The 241900Z Significant Tropical Weather Advisory (ABPW PGTW) first identified this disturbance as an area of enhanced convection in the monsoon trough. The convergence in the southwest monsoon flow combined with upper-level divergence provided an environment favorable for continued development.

The first Tropical Cyclone Formation Alert (TCFA) was issued at 251530Z when synoptic data indicated the minimum sea-level pressure (MSLP) had dropped to 1002 mb and winds of 25 kt (13 m/s) were present. An aircraft reconnaissance mission flew to investigate the region on the 26th. Although it was unable to locate a circulation, the data collected indicated the disturbance was developing - the MSLP had fallen to 999 mb and 40 kt (21 m/s) winds were observed on the south side of the monsoon trough. As a result, the TCFA was renewed at 261530Z. Figure 3-13-1 shows the active monsoon trough at this time. The disturbance is visible on the western side of the imagery with Typhoon Odessa further to the east.

Aircraft reconnaissance early on the 27th located the circulation center, prompting issuance of the first warning, valid at 270000Z. By this time

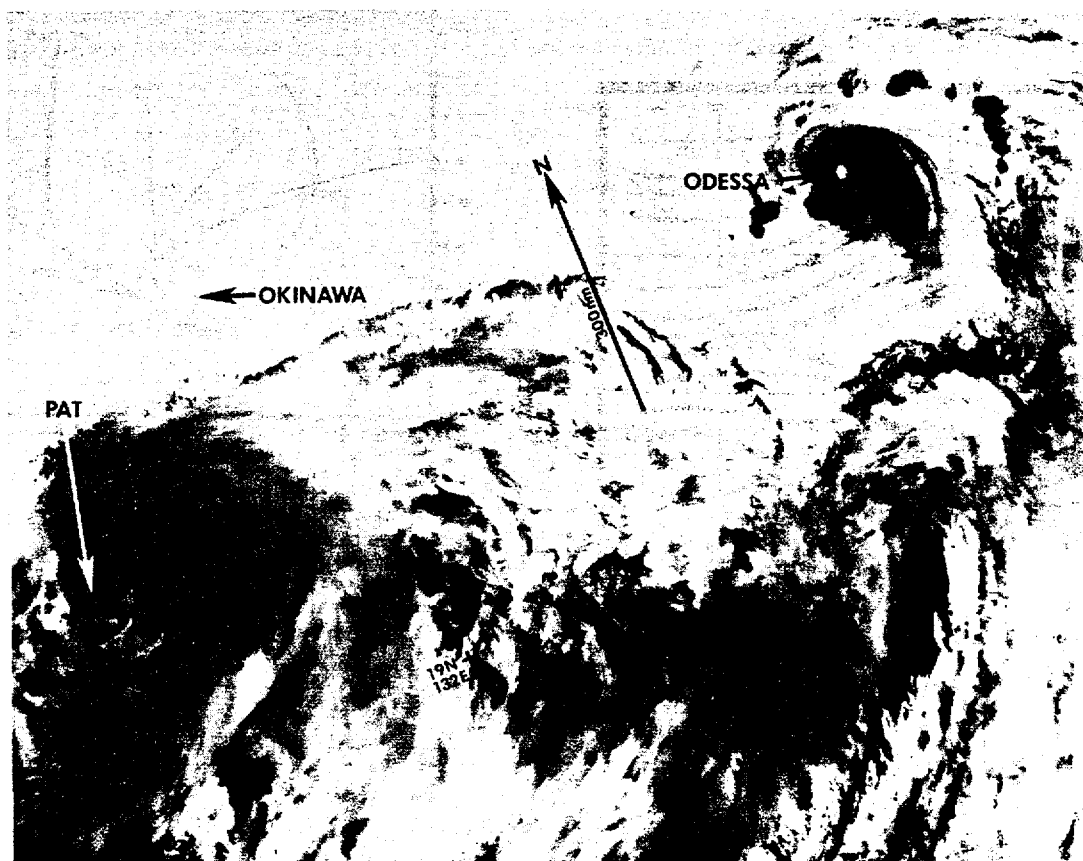
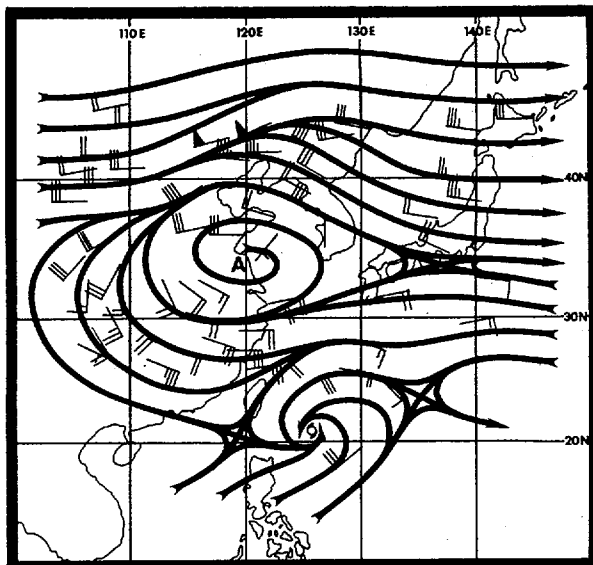


Figure 3-13-1. The tropical disturbance which became Typhoon Pat is visible as an organized area of convection in the monsoon trough. (Typhoon Odessa can also be seen) (261328Z August DMSP infrared imagery).

Pat, due to the enhanced southwesterly monsoon flow, already was at tropical storm intensity. As mentioned earlier, a large number of different factors needed to be taken into account in Pat's forecast.

Determining the direction of the track was the first problem. Because the cyclone was poorly defined on satellite imagery and as a consequence difficult to position, Pat was believed to be moving west-northwest for the first two warnings, when it was actually moving east-northeast. This was critical since persistence from past movement is often a major forecast consideration, especially in the short term forecasts. Figures 3-13-2 and 3-13-3 show some of the data available to the forecasters. A streamline analysis of the 270000Z August 500 mb data has been completed in Figure 3-13-2 to show the location of the subtropical ridge north of Pat. Figure 3-13-3 depicts the first set of forecast aids, using the east-northeast persistence track as a basis, along with the forecast and best track. The most striking feature is, that despite a lot of different options provided by the aids, none really hit the mark at seventy-two hours.

Figure 3-13-2. Mid-tropospheric (500 mb) wind flow at 270000Z August. The dominant synoptic feature is the subtropical ridge extending across China and Japan to the north of Pat.



hit the mark at seventy-two hours.

The forecast called for Pat to move along the monsoon trough to the east-northeast; separate from the trough, and turn back to the west-northwest under the subtropical ridge. This was in reasonable agreement with the One-way Interactive Tropical Cyclone Model (OTCM) model which is usually the best performing forecast aid. The Fleet Numerical Oceanography Center (FNOC) 72-hour 500 mb Navy Operational Global Atmospheric Prediction System (NOGAPS) prognosis called for the ridge to weaken as a trough moved eastward across Mongolia. It appeared, however, that the ridge would remain strong enough to keep Pat south and west of Japan. As it turned out, the prognosis was slow on the movement of the trough, which resulted in the ridge weakening over western Japan.

For the rest of the 27th and all of the 28th, Pat remained in the monsoon trough and continued drifting to the northeast. The forecast situation was further complicated by the presence of Typhoon

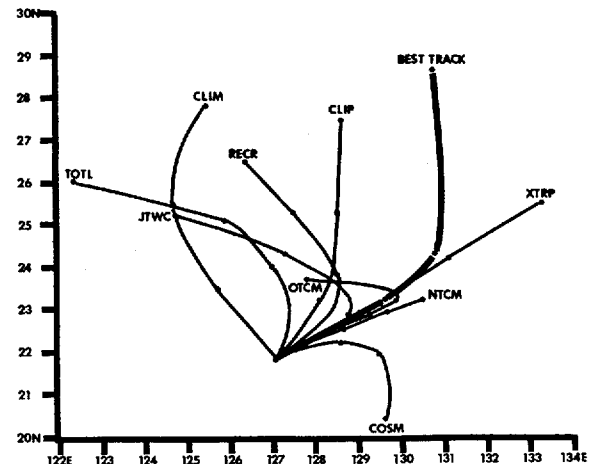


Figure 3-13-3. The primary forecast aids at 271200Z, along with the forecast and post analysis best track; all valid for 72-hours. None of the aids are able to provide correct guidance at seventy-two hours.

Odessa and Tropical Storm Ruby. Figure 3-13-4 shows Pat on the 28th - Odessa and Ruby are also visible. Despite the three cyclones being so close, each was moving a different direction. Pat was moving north-eastward, Odessa west, and Ruby north-northwest. According to the OTCM, Pat should stay under the ridge. The forecast reflected this guidance and continued to show a turn to the northwest.

The 290600Z OTCM was the first to suggest a track change for Pat, taking it around the ridge and into the Sea of Japan. In analyzing this change, the presence of Odessa was closely examined. Odessa

was moving west and located only 380 nm (704 km) north-northeast of Pat. The OTCM, however, had Odessa moving north into the Sea of Japan, despite the fact Odessa was continuing to move westward under the ridge.

On the 29th, the OTCM guidance was rejected and Pat was forecast to turn to the northwest. It was believed that the ridge over Japan was too narrow for the OTCM to pick up with its relatively large grid spacing. The fact that the OTCM was consistently wrong with Odessa reinforced this belief. In post analysis, however, it is believed Odessa kept moving

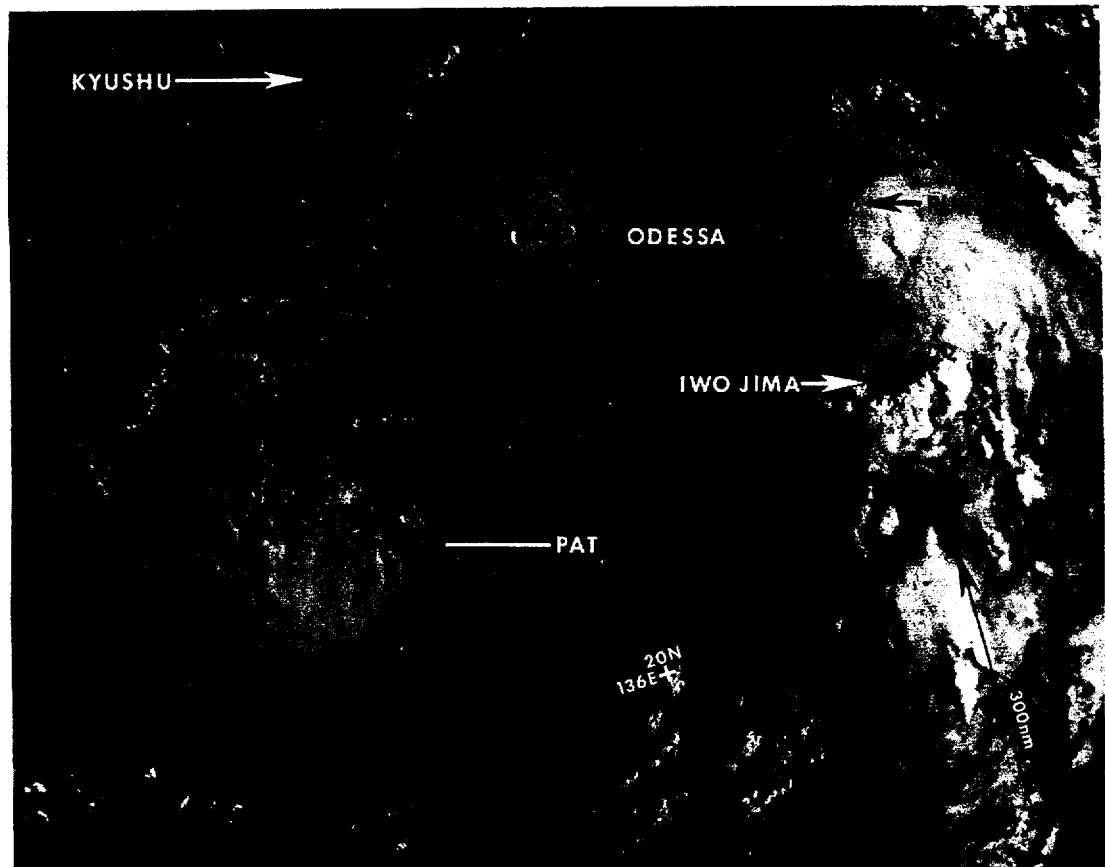


Figure 3-13-4. Three active tropical cyclones south of Japan and all moving different directions. Typhoon Pat is heading northeast, Typhoon Odessa is heading west, and Tropical Storm Ruby is heading north-northwest (282303Z August NOAA visual imagery).



westward at this stage due to binary interaction with Pat rather than from a response to the ridge. Visual satellite imagery early on the 30th (Figure 3-13-5) shows the two were spatially proximate. It is reasonable to believe that if Pat had been the only tropical cyclone in the region at this time, the forecast probably would have been changed on the 29th rather than on the 30th; providing Japan an additional 24 hours of warning time.

With the additional data received on the 30th, it became evident that Pat was not responding to the steering flow of the ridge and was going to hit the Japanese island of Kyushu. The 301200Z forecast was the first to reflect this change. Figure 3-13-6 shows the 500 mb data available at that time. When comparing it with Figure 3-13-2, it is evident that major synoptic changes took place in seventy-two hours. The anticyclone over the China coast was gone and a trough was located just northwest of the Korean Peninsula.

An in-depth look at the interaction between Pat and Odessa, revealed the two typhoons rotated cyclonically around each other. The affect on Odessa's track was greater, however, since Pat was the larger system. Odessa kept moving westward, aided by interaction with Pat. It was interesting to note that Pat did not turn to the north and accelerate until Odessa rotated across to the north-northwest. Then, as soon

as Pat was east-northeast of Odessa, Odessa turned to the northeast and both cyclones accelerated into the Sea of Japan. The closest point of approach between the two was 270 nm (500 km).

At that point, the forecast was straightforward with extratropical transition taking place in the Sea of Japan. Figure 3-13-7 shows Pat during its transition with stable stratocumulus clouds present around a large open center and convection limited to the northeast quadrant. Pat completed extratropical transition at approximately 312100Z. The warnings continued warning on the system until it moved across the island of Hokkaido in northeastern Japan. The final warning was issued at 011200Z.

Typhoon Pat caused significant damage in southwestern and northeastern Japan; primarily on the islands of Kyushu and Hokkaido. Kyushu was hit the hardest with wind gusts of 107 kt (55 m/s) reported at 301940Z in Kagoshima (WMO 47851). Misawa AB (WMO 47580) recorded sustained winds of 33 kt (17 m/s) with a peak gust to 52 kt (27 m/s) at 010710Z when extratropical remnants of Pat crossed the northern Japanese islands. A total of 23 people were reported killed with over 180 people injured. An estimated 3,000 homes were damaged and 148 watercraft of varying sizes lost. Pat also severely disrupted transportation by land, sea and air.

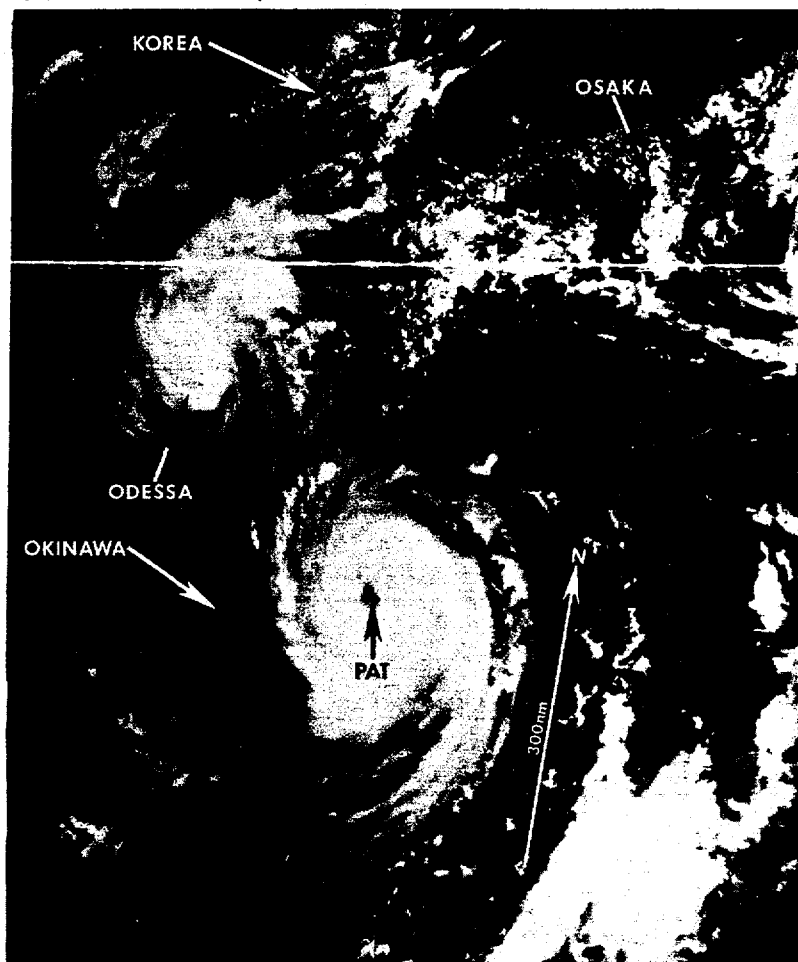


Figure 3-13-5. Typhoon Pat moving northward towards Kyushu and interacting with Typhoon Odessa. Pat is the larger of the two typhoons (300538Z August NOAA visual imagery).

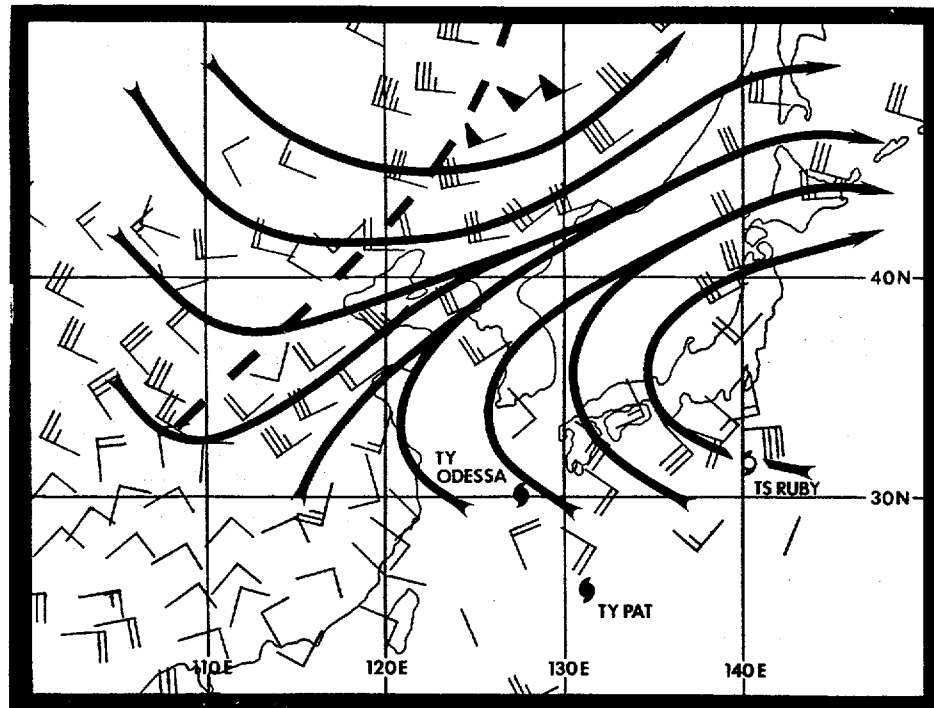


Figure 3-13-6. Mid-tropospheric (500 mb) wind flow at 300000Z August seventy-two hours after Figure 3-13-2. The anticyclone over the coast of China is gone and a trough is moving into the region from the northwest.

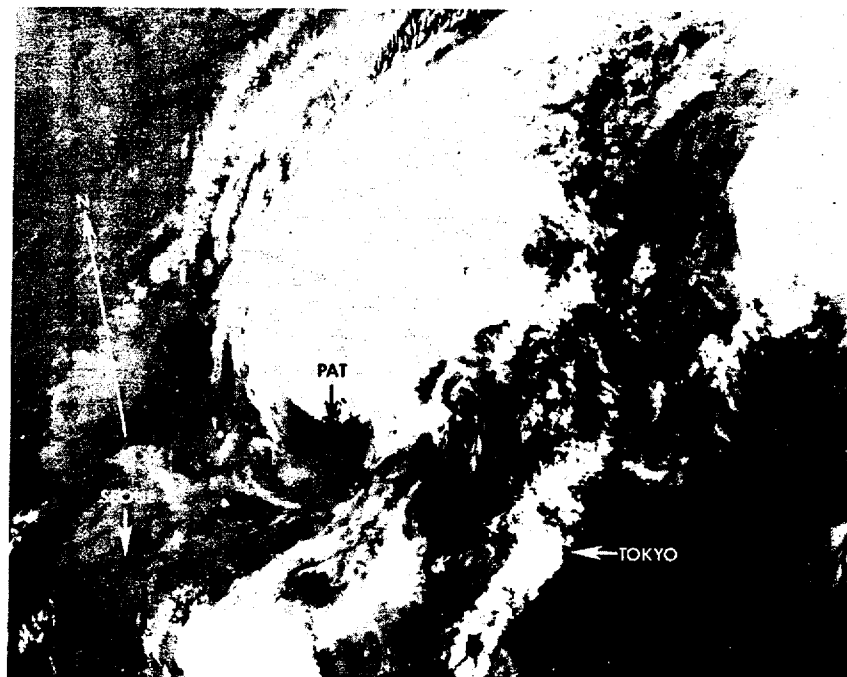
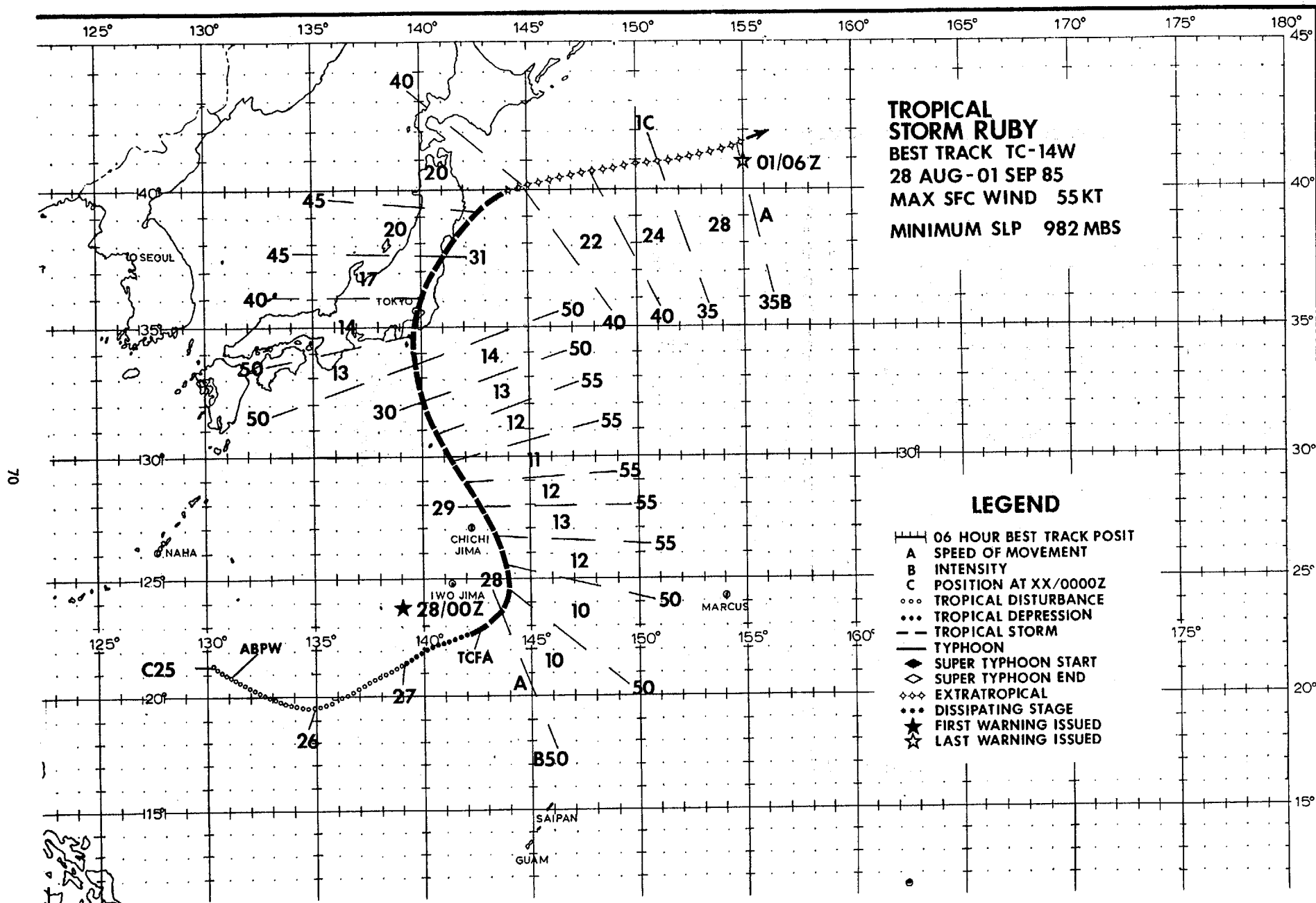


Figure 3-13-7. Pat has nearly completed its transition to an extratropical low in the Sea of Japan. The convection is moving to the northeast leaving behind a broad, exposed low-level circulation center (311813Z August NOAA infrared imagery).



# TROPICAL STORM RUBY (14W)

Ruby was the last of three disturbances to develop in the active southwest monsoon trough near 20N latitude during late August. Unlike its predecessors, Typhoons Odessa and Pat, Ruby did not engage in any complex binary interaction, but appeared to remain a solitary system. Ruby was noteworthy in that it tracked directly over the Tokyo metropolitan area.

On 24 August the well-developed monsoon trough was displaced north of its climatological position and provided large scale low-level converging flow. This flow was the combination of the southwest monsoon and the southeast trades around the southwest periphery of the strong subtropical ridge located east of Japan. The low-level monsoon trough had a narrow, but active, tropical upper-tropospheric trough (TUTT) located aloft and to the north, and the upper-level near-equatorial ridge to the south.

Synoptic data on the 25th of August revealed a small (60 nm (111 km) diameter) circulation with a minimum sea level pressure (MSLP) of 1006 mb 330 nm (611 km) south-southeast of the island of Okinawa. Initial mention of this area appeared on the 250600Z Significant Tropical Weather Advisory (ABPW PGTW). The disturbance weakened a day later. Post-analysis showed the circulation tracked eastward and the convection associated with the disturbance exhibited typical monsoon depression characteristics - some curvature, but the enhanced convection only on the equatorward side of the trough. Increased surface winds of 25 kt (13 m/s) on the eastern side of the

circulation and a steady drop of sea-level pressure to 1002 mb, prompted new mention of the disturbance on the Significant Tropical Weather Advisory (ABPW PGTW) at 270600Z. A Tropical Cyclone Formation Alert (TCFA) followed at 271800Z based on a 25 kt (13 m/s) satellite intensity estimate based on convection that had consolidated into a ragged central dense overcast (CDO) feature. Aircraft reconnaissance was subsequently scheduled for the daylight hours of the 28th of August. At that time the typhoon forecaster was faced with a dilemma: was the flare-up of convection at the end of the monsoon trough just another clash of the low-level southeasterlies, or was the signature that of a maturing tropical cyclone? Ruby's relatively close proximity to Typhoon Odessa (to the northwest) and the apparent weak surface inflow in the northwest quadrant, as depicted by the sparse synoptic data, deepened the uncertainty concerning the intensity of the system.

The question was answered when the initial aircraft reconnaissance mission at 280020Z reported an elliptical eye forming and a minimum sea-level pressure of 982 mb. Based on this information, the first warning on Tropical Storm Ruby was issued immediately. Satellite imagery showed the cloudiness was comma shaped with a large band of convection coming into the center from the southeast. This convective band was positioned over the strong zone of convergence between the monsoon and the southeast trades. The data sparse analysis at 280000Z, shown in Figure 3-14-1, depicts this convergent area. Additionally, aircraft reconnaissance reported that

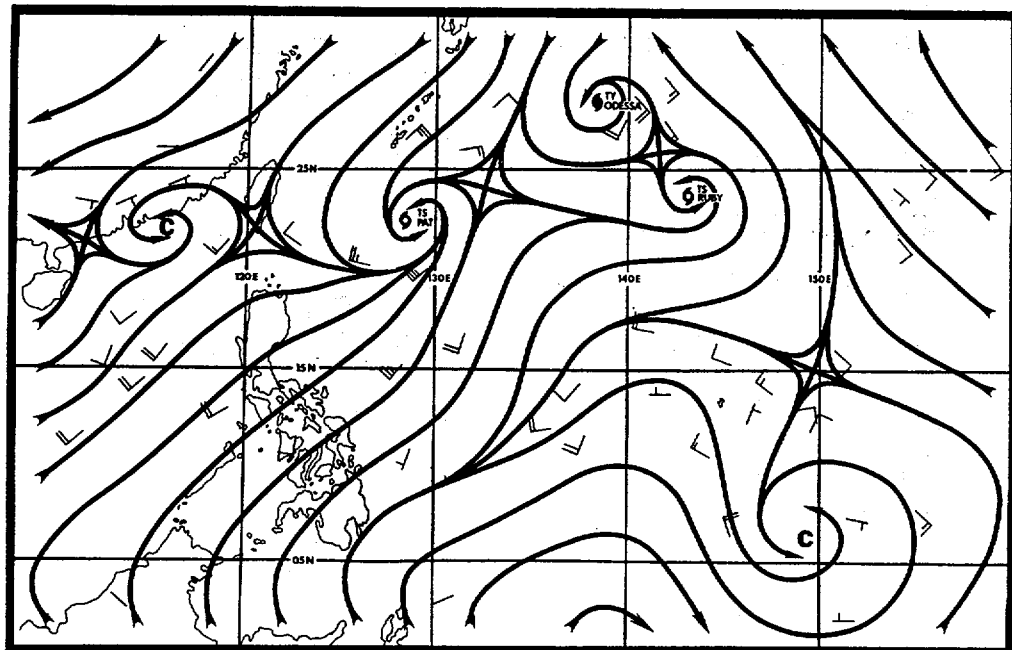


Figure 3-14-1. Surface/gradient analysis at 280000Z showing Tropical Storm Ruby located at the eastern end of the southwest monsoon flow where it converges with the southeast trades.

maximum sustained winds of 50 kt (26 m/s) with gusts to 65 kt (33 m/s) were restricted to the area of the low-level convergence and cloud band. Elsewhere, to the west and southwest, the aircraft found only 15-30 kt (8-15 m/s) surface winds. Figure 3-14-2 shows the proximity of Odessa to Ruby. The continuous vertical shear from the outflow of Odessa to the northwest appears to have hampered Ruby's further development.

During the following twenty-four hours, Ruby turned northwestward and gradually increased speed. Finally, late on the 29th, Ruby appeared to be breaking free of the monsoon trough. The forecast philosophy throughout the 28th and 29th of August was for Ruby, like Odessa, to turn more westward, stay equa-

torward of the narrow subtropical ridge and pass south of Honshu, Japan. This forecast scenario was based on Ruby's interaction with Typhoon Pat. Ruby was forecast to be pulled around the northern periphery of Pat's much larger circulation, which was centered southeast of Okinawa, Japan. Initially, the synoptic situation and, as a result, the meteorological reasoning appeared to be similar to that for Odessa and contrary to guidance provided by the best forecast aid, the One-way Tropical Cyclone Model (OTCM). OTCM moved Ruby northward into the subtropical ridge and towards Honshu, Japan, but at a slower speed than it had previously with Odessa. OTCM apparently was responding to the approach of a mid-latitude short wave trough. Figure 3-14-3 compares



Figure 3-14-2. Nighttime moonlight satellite imagery of Ruby. The close proximity of Odessa to Ruby appears to have hampered Ruby's further development. Ruby is near maximum intensity of 55 kt (28 m/s) (281248Z August DMSP visual imagery).

OTCM guidance with the forecasts for warnings 04 through 08. By following the forecast philosophy that OTCM still could not resolve the narrow subtropical ridge (due to its larger internal grid spacing), the warnings failed to reflect Ruby's gradual recurvature and subsequent landfall until approximately six hours before the event.

Over a thirty-six hour period, between 281200Z and 300000Z, the Tropical Storm maintained a maximum intensity of 55 kt (28 m/s). Ruby packed 55 kt (28 m/s) winds as it moved south of Tokyo, Japan, but began to weaken just prior to moving into Tokyo Bay

and the Kanto Plain. Satellite imagery showed Ruby lost most of its central convection before making landfall due to interaction with the mid-latitude westerlies. Yokosuka received maximum sustained winds of 33 kt (17 m/s) with gusts to 47 kt (24 m/s) at 301420Z, as Ruby passed 5-10 nm (9-19 km) to the east. During this period Tokyo received three inches (76 mm) of rain and minor damage - trees down, windows broken and power outages for thousands of homes. After twelve hours over land, Ruby moved back into the Pacific and completed extratropical transition at 311000Z.

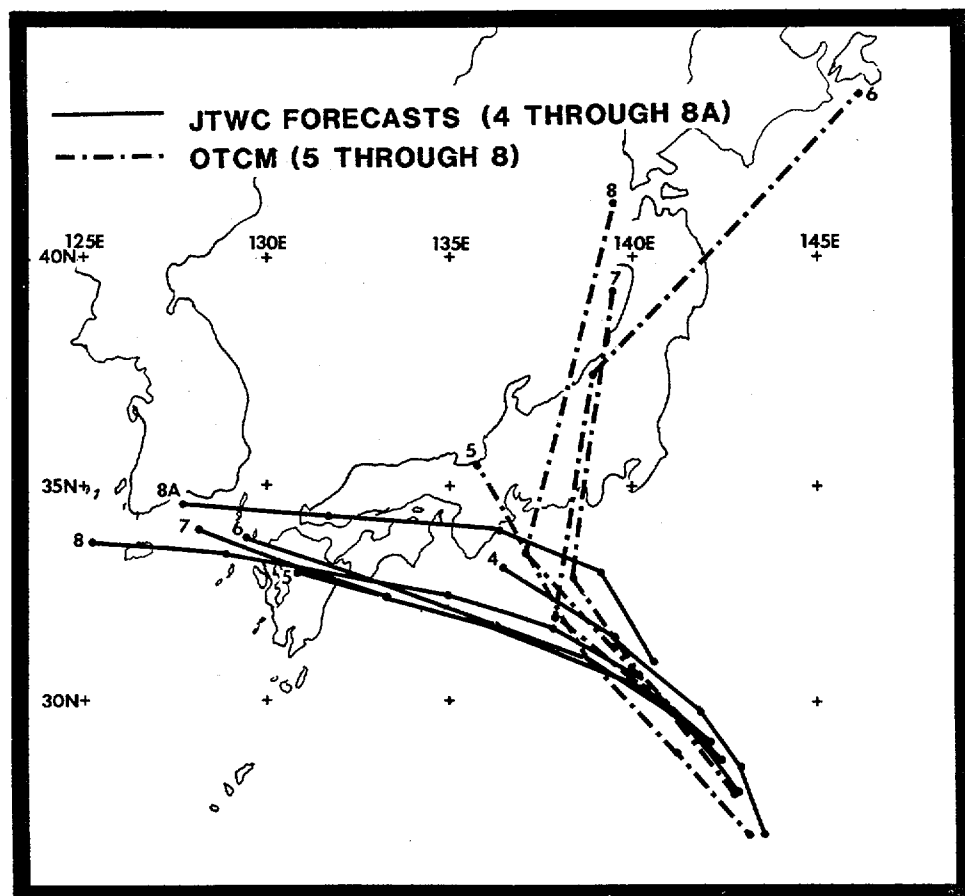
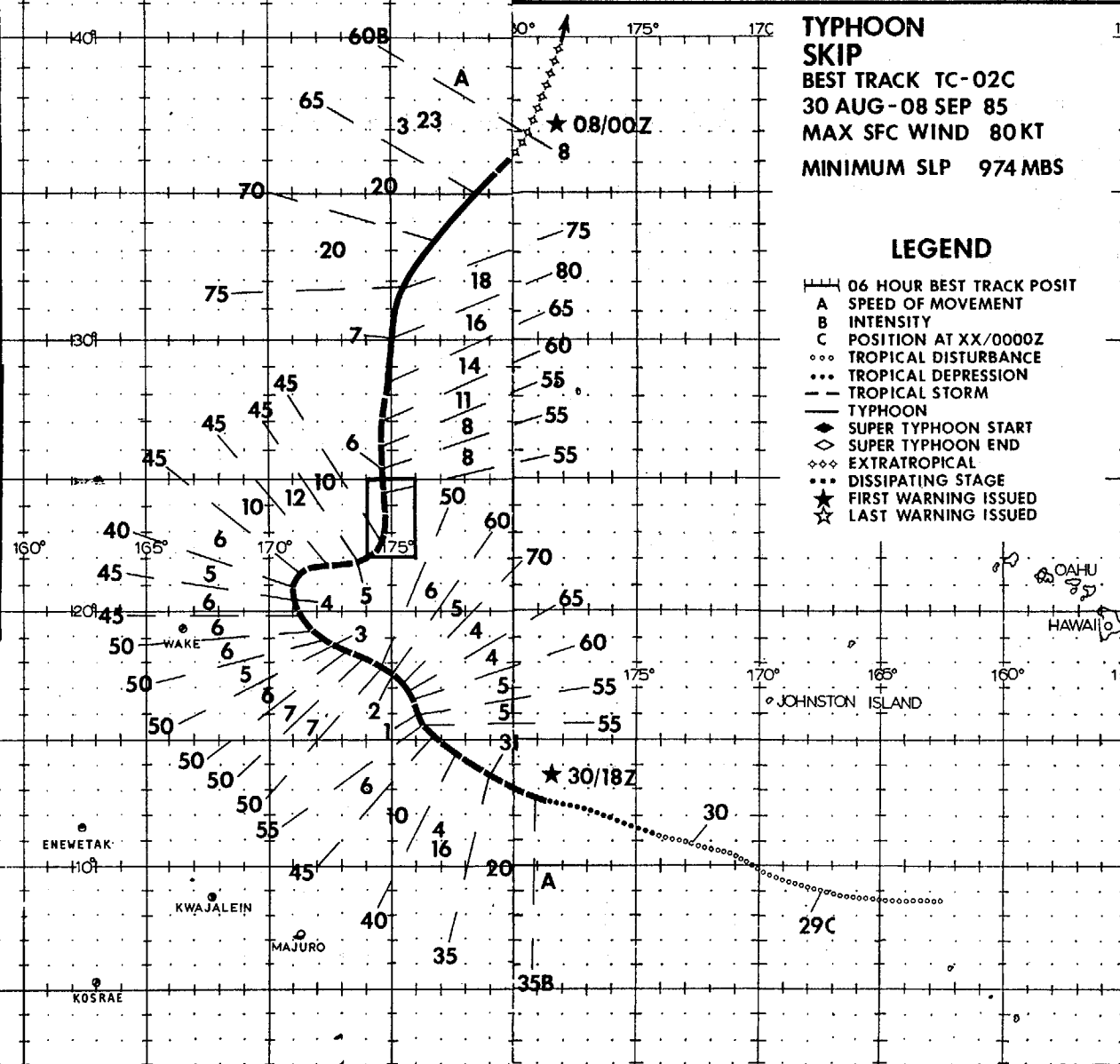
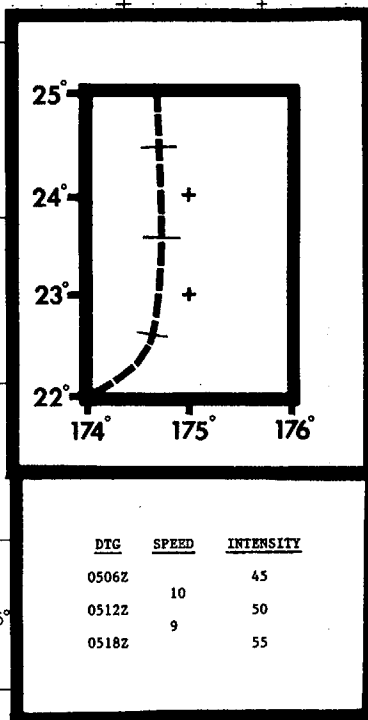


Figure 3-14-3. A comparison of OTCM guidance and the forecasts for five warnings (04 through 08).



Typhoon Skip was the first system in the North Pacific to be warned on by both the Naval Western Oceanography Center (NWOC), Pearl Harbor, Hawaii and the Joint Typhoon Warning Center (JTWC), since Tropical Storm Carmen (02) in early April, 1980. (Note: Tropical cyclones east of the dateline are the responsibility of the Central Pacific Hurricane Center (CPHC), Honolulu, Hawaii, but all warnings and alerts are issued in coordination with NWOC.) Skip developed in the central North Pacific and transited the dateline twice. Additionally, the system achieved typhoon intensity twice: once east-southeast, and then later northeast, of Wake Island.

Satellite imagery detected an area of organized convection along the near-equatorial trough on the 28th of August. This disturbance raced west-northwestward for the next forty-eight hours under pressure from the strong mid-Pacific subtropical ridge. On 30 August, despite the 20 kt (10 m/s) plus movement, satellite images showed the cloud system's organization had increased significantly. This prompted the issuance of a Tropical Cyclone Formation Alert (TCFA) at 301730Z by NWOC. Almost immediately the TCFA was followed by the first warning at 301800Z on Tropical Depression 02C. As Skip transited the dateline from east to west, it became the fourth of what would be a five tropical cyclone scenario in the same ocean basin. The other systems that were part of this unusual event were Odessa, Pat, Ruby near Japan and Tess southwest of Guam.

Responsibility was transferred at the dateline from NWOC to JTWC for the second warning. The following warning upgraded Skip to a tropical storm at 310600Z based on satellite intensity estimates (post analysis later showed that Skip had reached tropical storm intensity six hours earlier, at 310000Z). Coincident with intensification Skip also began to slow its forward motion. The system obtained typhoon intensity at 011200Z. A weakening trend set in on 02 September as a mid-level trough approached from the northwest, but Wake Island was still threatened by Skip's approach. Finally, late on the 3rd, Skip turned away from Wake Island and moved towards the north. The Tropical Cyclone then executed an abrupt turn to the east and moved eastward for eighteen hours. During this period the central convection was displaced, by stronger winds aloft, to the east and northeast of the low-level circulation center.

On 05 September, after the passage of a mid-level trough, Skip resumed a northward track through the subtropical ridge and began to intensify and accelerate. A distinct eye developed (see Figure 3-02C-1) as the peak intensity of 80 kt (41 m/s) was reached on 07 September. But this peak was short lived, as increased wind shear aloft from mid-latitude westerlies and interaction with a trailing cold front came into play. Extratropical transition was rapidly completed near the dateline at 072100Z. The warning responsibility was transferred from JTWC to NWOC once again as Skip transited the dateline, this time from west to east, and the last warning followed at 080000Z.

In retrospect, Skip provided its share of forecasting difficulties due to its location in the data sparse central North Pacific and the complex interaction between mid-latitude troughing and the subtropical ridge. Skip also proved to be a challenge for the 54th Weather Reconnaissance Squadron to fly primarily for two reasons: its remote location, which required staging at the islands of Kwajalein and Wake; and the simultaneous occurrence of the multiple tropical cyclone outbreak in the western North Pacific, that stretched aircraft reconnaissance assets to their limit. Once it became apparent that Wake Island was no longer threatened by Skip, aircraft reconnaissance tasking was cancelled.

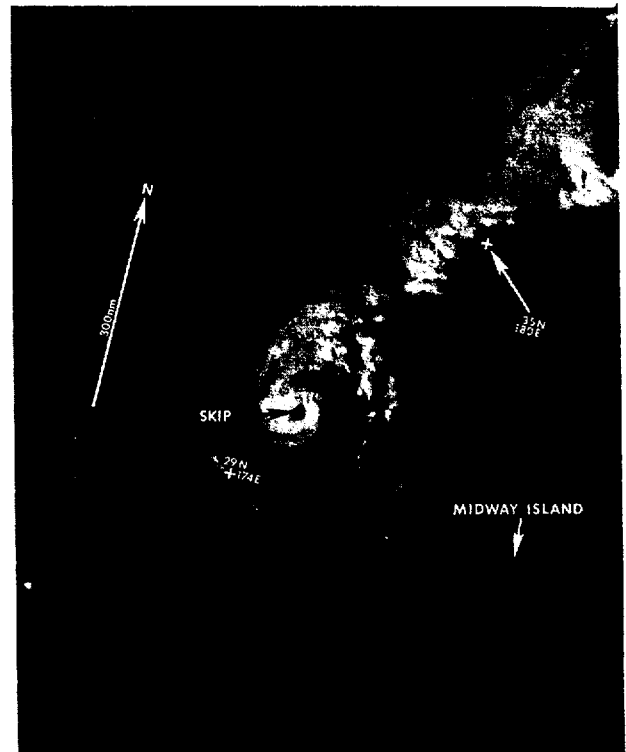


Figure 3-02C-1. Typhoon Skip at maximum intensity with a well defined eye. Skip trails at the end of a cold frontal cloud band that extends to the northeast (070229Z September NOAA imagery).



# TYPHOON TESS

BEST TRACK TC-15W

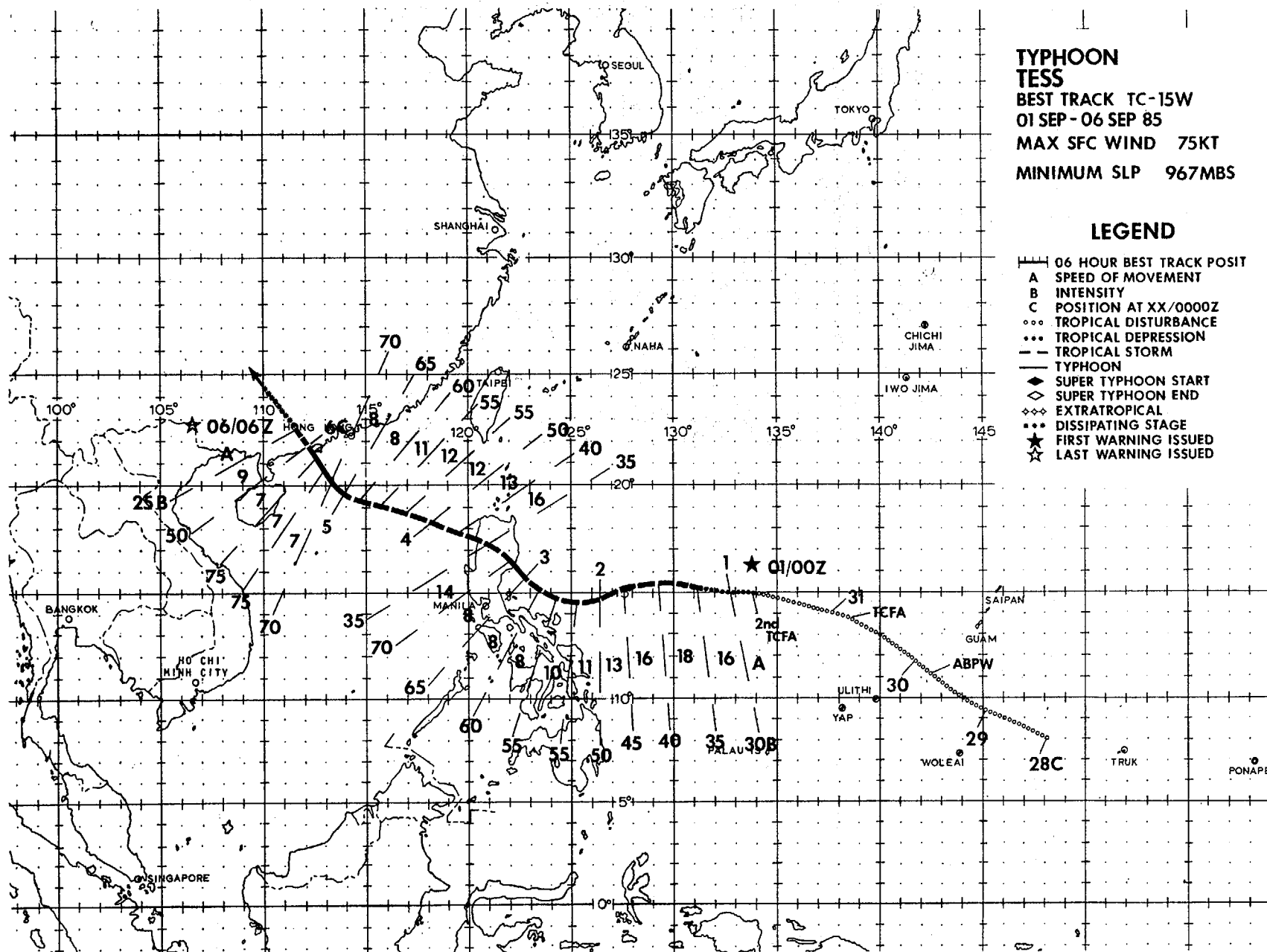
01 SEP-06 SEP 85

MAX SFC WIND 75KT

MINIMUM SLP 967MBS

## LEGEND

- 06 HOUR BEST TRACK POSIT
- A SPEED OF MOVEMENT
- B INTENSITY
- C POSITION AT XX/0000Z
- ... TROPICAL DISTURBANCE
- ... TROPICAL DEPRESSION
- TROPICAL STORM
- TYPHOON
- ◆ SUPER TYPHOON START
- ◇ SUPER TYPHOON END
- ◆◆ EXTRATROPICAL
- ... DISSIPATING STAGE
- ★ FIRST WARNING ISSUED
- ☆ LAST WARNING ISSUED



Typhoon Tess, the first of five significant tropical cyclones to develop in September, originated as a low latitude disturbance southeast of Guam (WMO 91217). Although bringing needed rain to the Philippines during a spell of drier than normal weather, Tess also brought unwanted death and destruction. Four people perished, several were missing and at least 300 were left homeless as this tropical cyclone crossed northern Luzon and disrupted air, ground and sea transportation. In addition, a tornado spawned by Tess, ravaged the coastal town of Lemery, 50 nm (93 km) south of Manila (WMO 98425).

During the last days of August, the monsoon trough was displaced poleward and extended from the northern South China Sea eastward encompassing Typhoons Pat and Odessa, and Tropical Storm Ruby. This left a broad zone of low-level southwesterly flow across the Philippine Sea. The surface/gradient level streamline analysis for 280000Z (Figure 3-15-1) indicated anticyclonic flow over Guam and a cyclonic circulation to the southeast. This cyclonic circulation center, which was moving northwestward, remained at the western end of a band of maximum cloudiness that showed no organization. Initial conditions for development of this low latitude disturbance were unfavorable because of the strong vertical shear from the equatorward outflow channel of the multiple tropical cyclones to the north.

At 1200Z on 30 August satellite data indicated that the area of cloudiness, then located 300 nm (556 km) west of Guam, had shown a marked increase in organization and amount of convection over the previous 12-hours. Synoptic data at that time confirmed the existence of a low-level circulation, a gradual decrease in sea-level pressure and winds estimated at 10 to 20 kt (5 to 10 m/s). These data prompted issuance of the first of two TCFA's at 301930Z. Aircraft reconnaissance was requested for the next day.

On 010126Z September, the first aircraft reconnaissance flight into the system verified the location of the surface circulation, and found

surface winds of 30 to 35 kt (15 to 18 m/s) and a MSLP of 1003 mb. The first warning on Tropical Depression 15W followed at 010400Z. The center of the depression was located 600 nm (1111 km) east of Manila. The tropical cyclone was moving rapidly westward under the steering influence of the subtropical ridge which lay to the north. As the system matured, satellite imagery detected the formation of a ragged Central Dense Overcast (CDO). Based on the persistent CDO and associated intensification trend, Tropical Depression 15W was upgraded to Tropical Storm Tess at 011200Z (Post analyses showed that Tess actually had reached tropical storm intensity six hours earlier). Aircraft reconnaissance 36 hours later at 022351Z found 65 kt (33 m/s) maximum surface winds and a MSLP of 983 mb. As a result, Tess was further upgraded to typhoon status. At that time, Typhoon Tess was located by a combination of aircraft, satellite and radar information approximately 130 nm (241 km) east-northeast of Manila. Tess was destined to make landfall over Luzon within six hours. As Tess neared Luzon, it took a jog to the northwest sparing the Manila area from the strongest effects of the typhoon.

Landfall over northern Luzon resulted in the temporary downgrading of Tess to a tropical storm at 031200Z. However, within eleven hours Tess had cleared Luzon and was again over water in the South China Sea. Redevelopment to typhoon intensity was forecast and did occur at 050000Z when the Typhoon was located 170 nm (315 km) south of Hong Kong (WMO 45005) (Figure 3-15-2). Tess continued northwestward under the influence of the subtropical ridge and within 24 hours moved inland over the southern coast of mainland China near Yangjiang (WMO 59663), 120 nm (222 km) west-southwest of Hong Kong. The final warning was issued at 060600Z.

Despite passing well south of Hong Kong, Tess generated a peak gust to 60 kt (31 m/s) at the Royal Observatory, and 65 kt (33 m/s) at the Hong Kong International Airport (WMO 45007). Although considerable flooding and crop damage occurred over southern China as Tess moved inland, there were no reports of death or injuries.

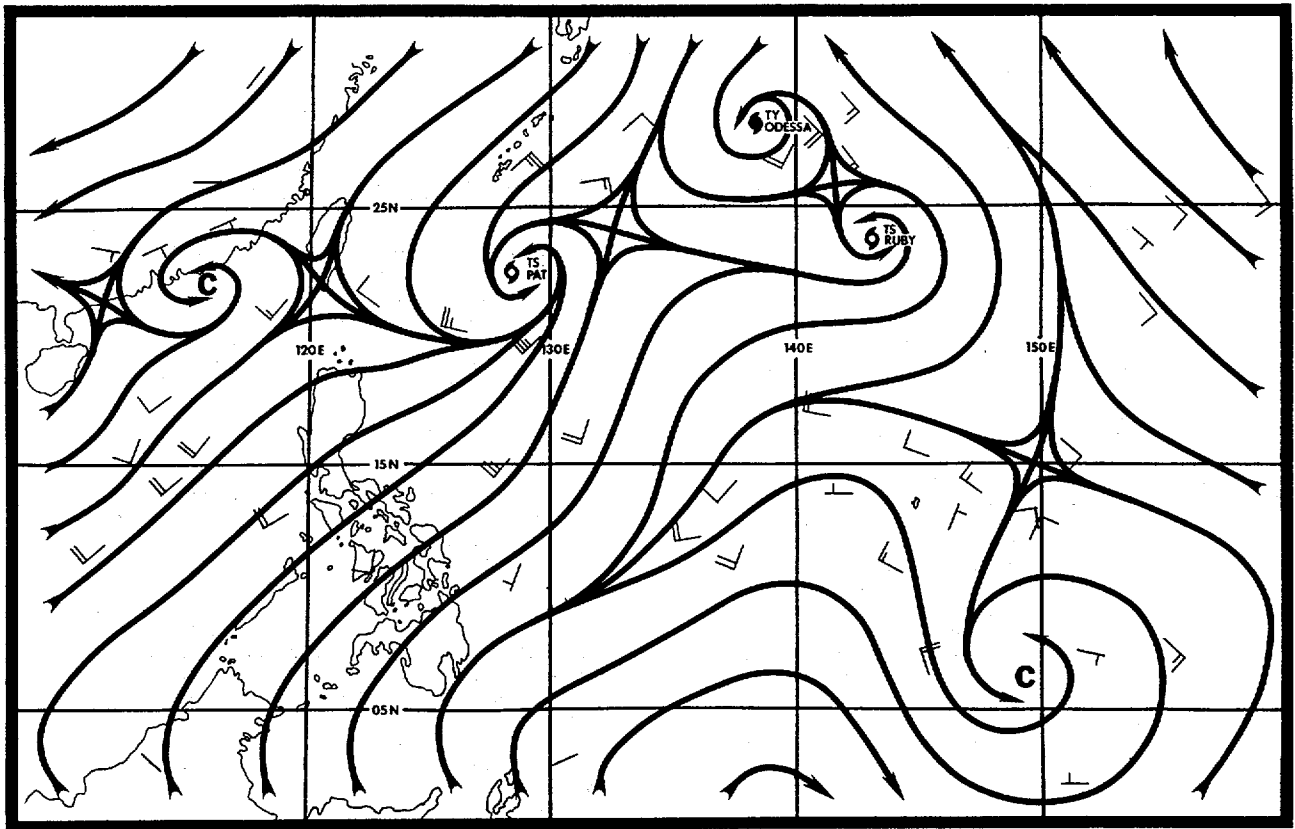


Figure 3-15-1. The 280000Z August surface/gradient level streamline analysis of the southwest monsoonal flow across the Philippine Sea. The low-latitude disturbance southeast of Guam was the precursor of Tess.

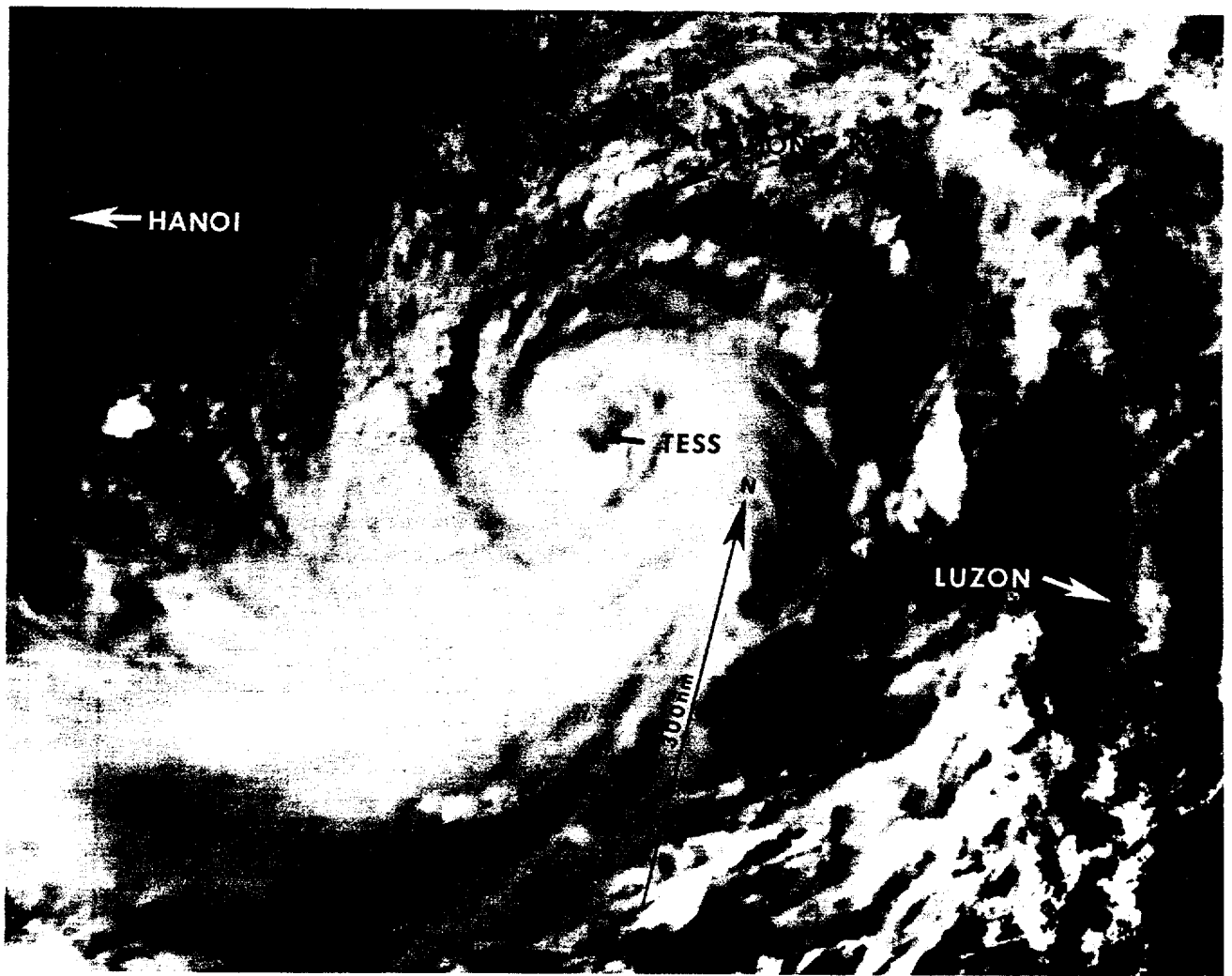
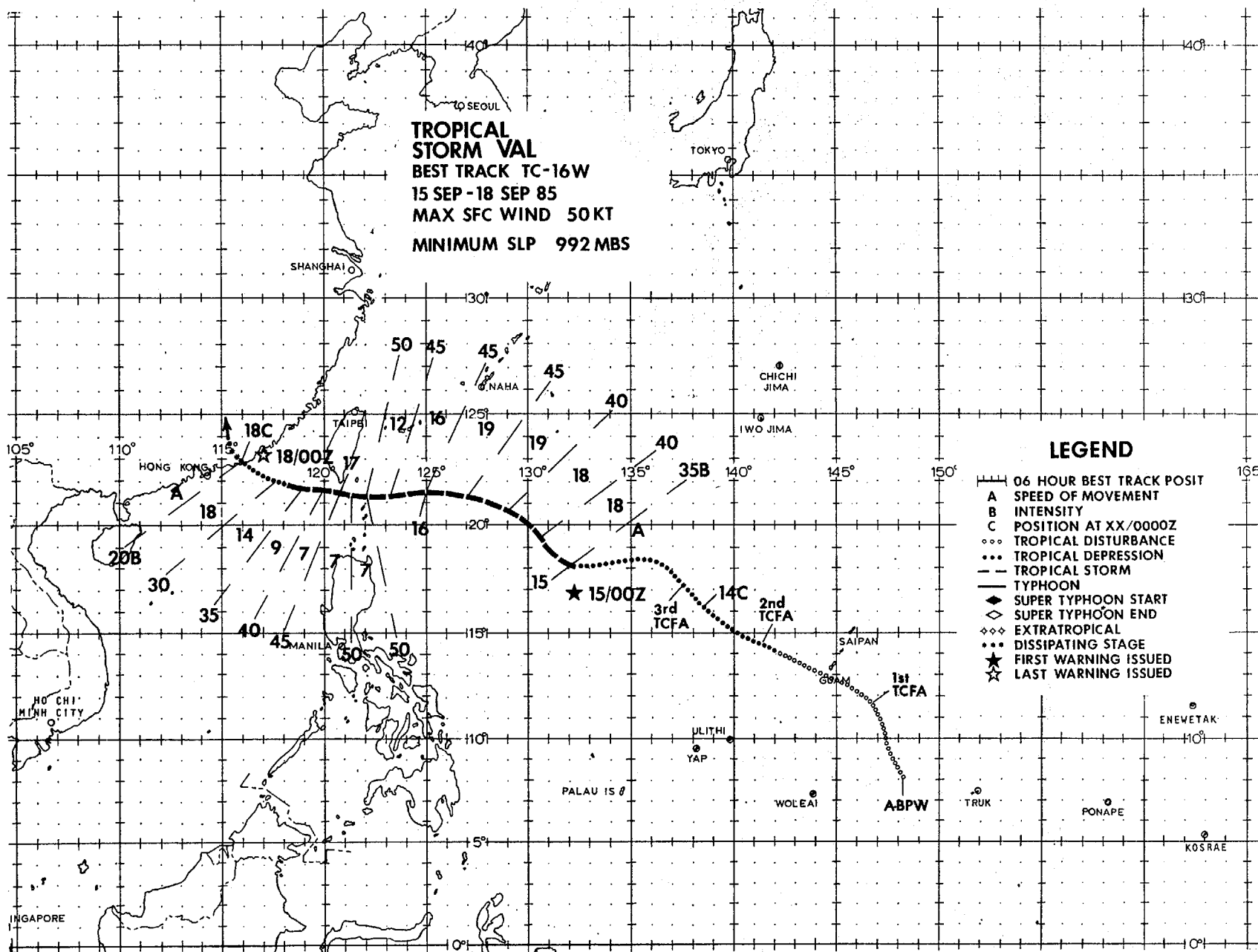


Figure 3-15-2. Typhoon Tess, with a ragged eye, near peak intensity. The coastline along the northern Gulf of Tonkin is to the west of Tess' cirrus outflow (050229Z September DMSP visual imagery).



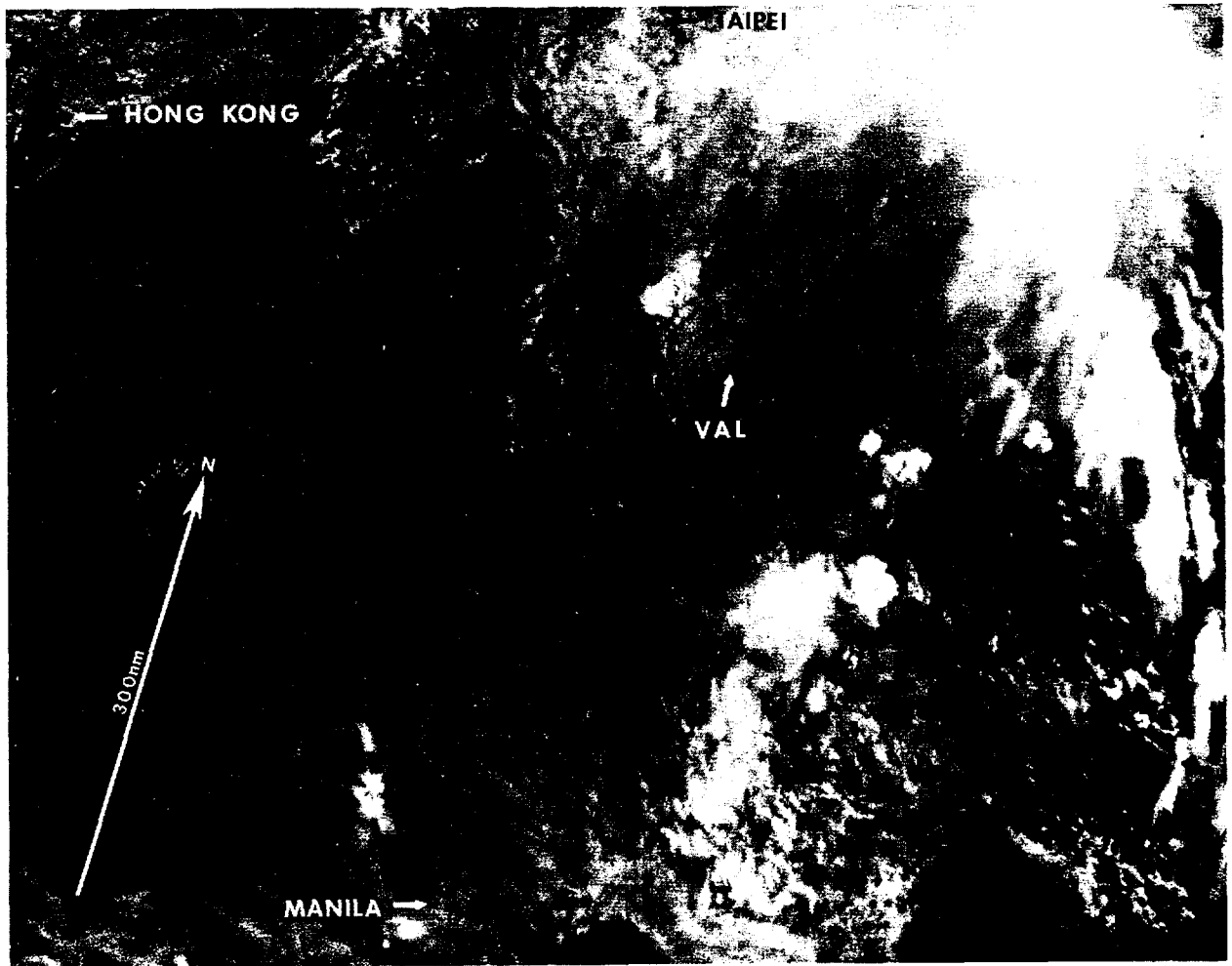
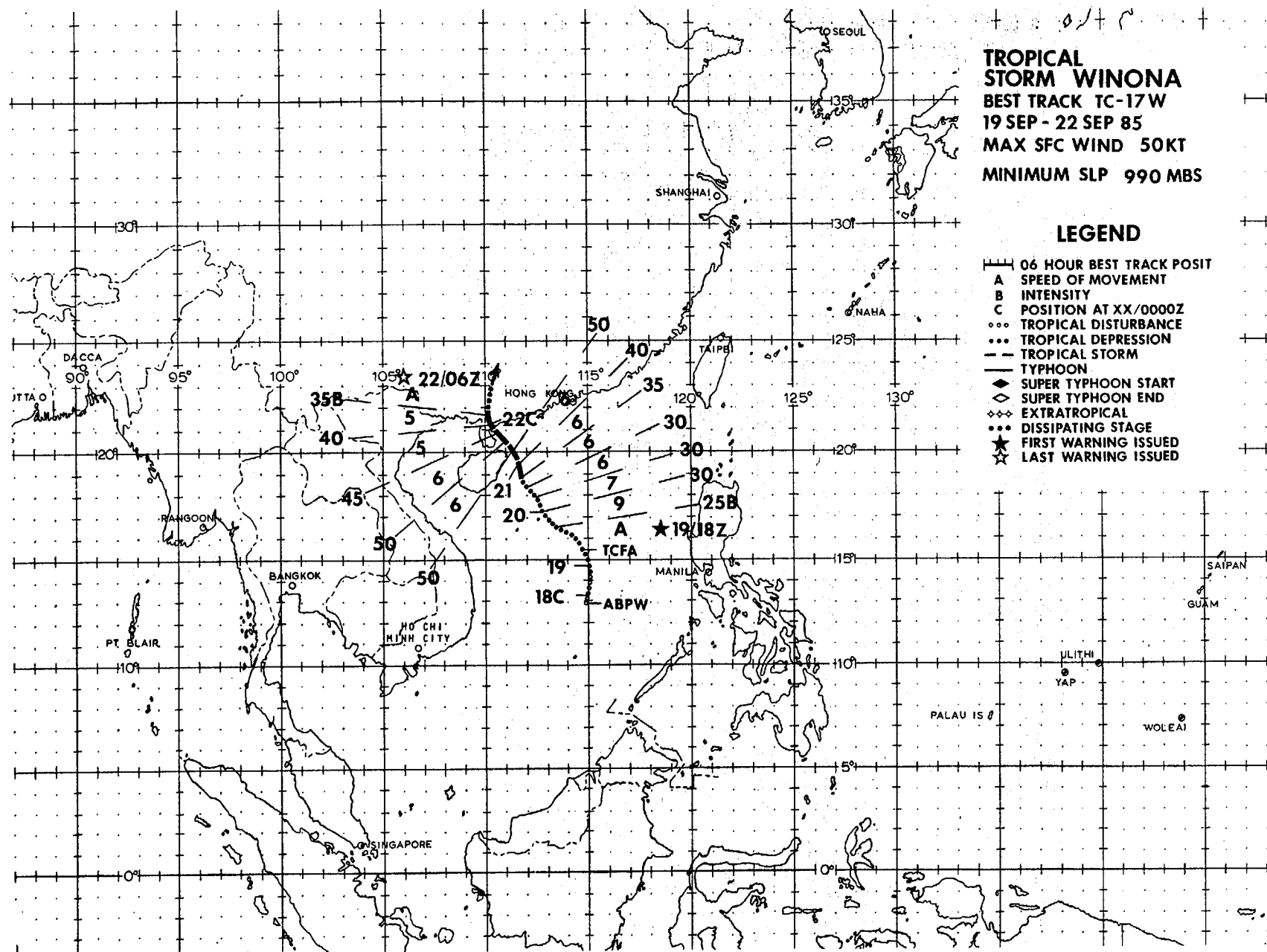


Figure 3-16-1. Tropical Storm Val was the first of two successive storms to reach a peak intensity of 50 kt (26 m/s). Originating in the monsoon trough southeast of Guam, it slowly developed as it moved northwest out of the trough. After moving into the central Philippine Sea, Val took a more westerly heading, paralleling the subtropical ridge axis to the north. Val remained poorly organized much of its lifetime, with the low-level center often difficult to locate from both satellite imagery and aircraft reconnaissance data. The above imagery shows one of the few times the low-level center could be identified. As Val approached Taiwan, its circulation became further disrupted. The low-level circulation center tracked west while most of the convection became displaced to the northwest and enhanced by Taiwan's mountainous terrain. The convection attempted to redevelop over the low-level wind center as Val transited the Luzon Straits, but without success. As a result, Val weakened prior to making landfall on mainland China and was not identifiable as a tropical cyclone after 180000Z. Due to the threat posed by Val, Hong Kong (WMO 45005) did go to Condition of Readiness II at 161500Z. However, Val dissipated earlier than anticipated and no significant weather was reported (160558Z September NOAA visual imagery).

**TROPICAL  
STORM WINONA**  
BEST TRACK TC-17W  
19 SEP - 22 SEP 85  
MAX SFC WIND 50KT  
MINIMUM SLP 990 MBS

# **LEGEND**

- 06 HOUR BEST TRACK POSIT
- A SPEED OF MOVEMENT
- B INTENSITY
- C POSITION AT XX/0000Z
- ... TROPICAL DISTURBANCE
- ... TROPICAL DEPRESSION
- TROPICAL STORM
- TYPHOON
- ◆ SUPER TYPHOON START
- ◇ SUPER TYPHOON END
- ◇◇◇ EXTRATROPICAL
- ... DISSIPATING STAGE
- ★ FIRST WARNING ISSUED
- ★ LAST WARNING ISSUED



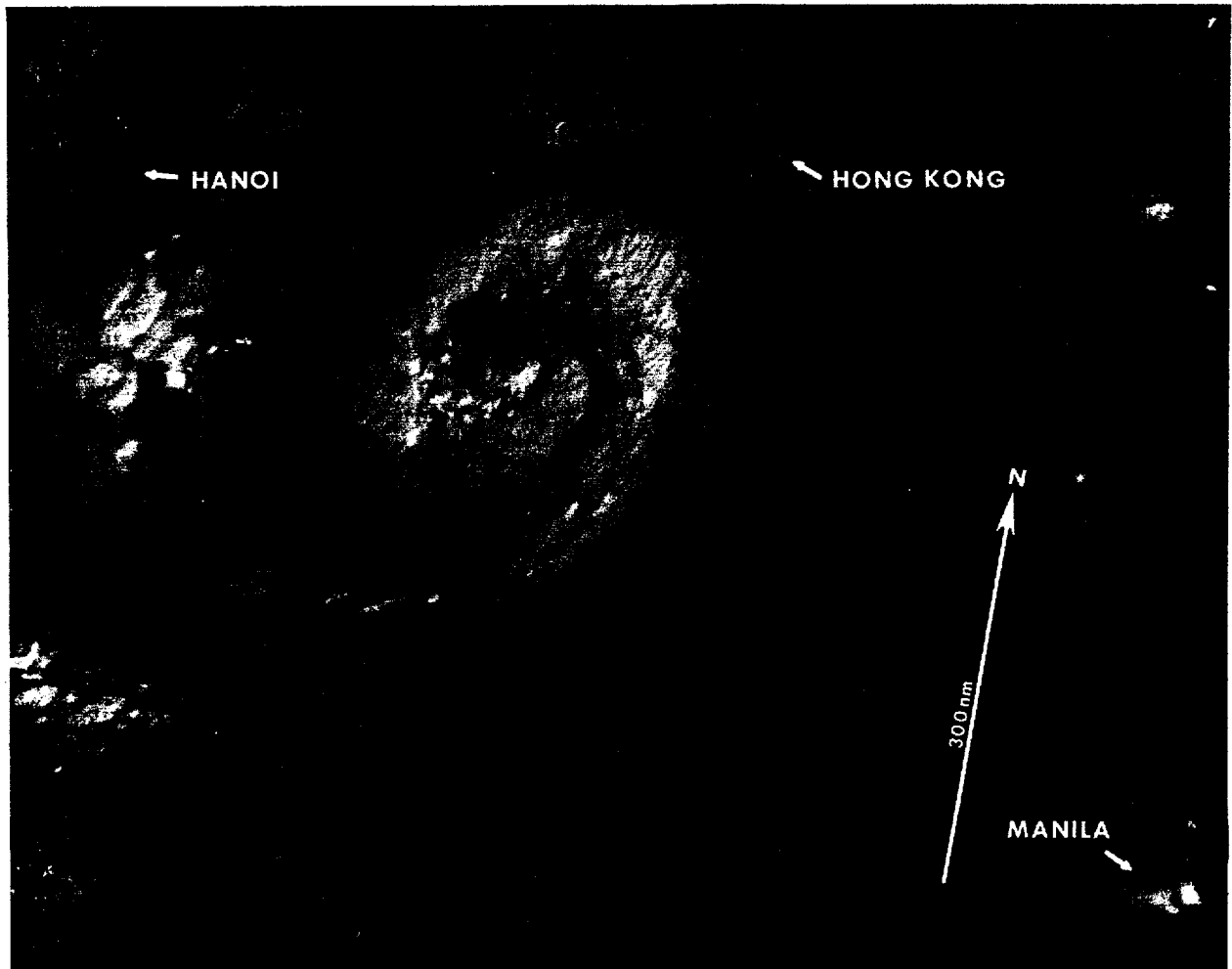


Figure 3-17-1. After the remnants of Tropical Storm Val dissipated over eastern China, excess vorticity at the base of the monsoon trough formed a surface circulation in the central South China Sea. Two days later this circulation intensified into Tropical Storm Winona. Winona tracked to the north-northwest as it intensified, moving around the western periphery of the subtropical ridge which was extending westward across the Philippine Sea. Winona made landfall as a 50 kt (26 m/s) tropical storm just west of Zhanjiang, China (WMO 59658) at about 212000Z. There were no reports of damage as it moved inland and dissipated. The satellite imagery above shows Winona just prior to reaching maximum intensity. Note the well-defined convective banding surrounding the center of the storm (210208Z September DMSF visual imagery).



# TYPHOON ANDY

BEST TRACK TC-18W

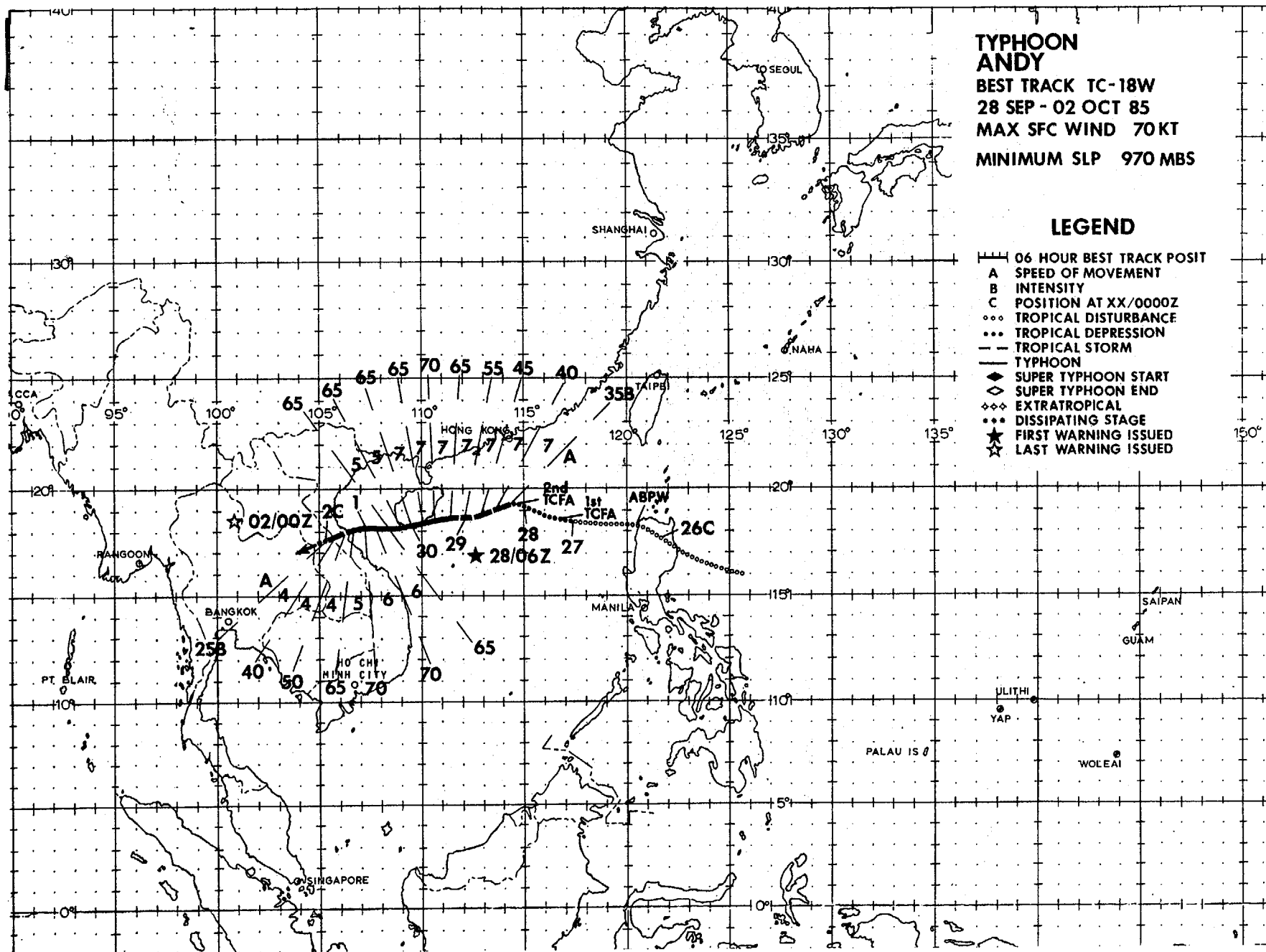
28 SEP - 02 OCT 85

MAX SFC WIND 70 KT

MINIMUM SLP 970 MBS

## LEGEND

- 06 HOUR BEST TRACK POSIT
- A SPEED OF MOVEMENT
- B INTENSITY
- C POSITION AT XX/0000Z
- ... TROPICAL DISTURBANCE
- ... TROPICAL DEPRESSION
- TROPICAL STORM
- TYPHOON
- ◆ SUPER TYPHOON START
- ◇ SUPER TYPHOON END
- ◆◆ EXTRATROPICAL
- ... DISSIPATING STAGE
- ★ FIRST WARNING ISSUED
- ★ LAST WARNING ISSUED



# TYPHOON ANDY (18W)

Typhoon Andy was a relatively short-lived tropical cyclone. Developing in the South China Sea, Andy transited uneventfully to the west-south-west. Although the cyclone made landfall twice at or near typhoon strength, there were no reports of serious damage or injuries.

The disturbance that eventually developed into Typhoon Andy was first detected late on 25 September as a small area of intense convection in the monsoon trough east of the Philippines. This compact CDO feature was part of a larger area of disturbed weather which had persisted east of Mindanao for several days. The southern portion of this large area had been the subject of a TCFA on the 24th and 25th. When the area of convection moved northwest across northern Luzon early on the 26th and entered the South China Sea, development of Andy began in earnest.

Between 260000Z and 270000Z the tropical disturbance moved to the west-northwest and slowly consolidated. Coincidentally, an early season surge in the northeast monsoon was underway generating 25 to 40 kt (13 to 21 m/s) winds across the Taiwan Straits and the northern South China Sea. This surge most probably contributed to the excess low-level cyclonic vorticity needed to produce a lee-side circulation off the northwest coast of Luzon. The development of this low-level vortex is thought to have aided the development of Andy. At 270000Z, Dvorak intensity analysis of the cloud system estimated 30 kt (15 m/s) surface winds were present. Sparse supporting synoptic data at that time showed only 20 to 25 kt (10 to 13 m/s) surface winds near the disturbance's center. However, due to the improved organization and the expectation for further development, a TCFA was issued at 270300Z. Less than three hours later, satellite imagery revealed the presence of a partially exposed low-level circulation center.

Over the next 24 hours, the system continued to move to the west-northwest in the monsoon trough. Despite the presence of the low-level circulation center on satellite imagery on the 27th, aircraft reconnaissance early on the 28th was unable to find a surface circulation. But, because winds of 25 to 30 kt (13 to 15 m/s) and a 1001 mb MSLP were observed, the TCFA was reissued at 280300Z.

The first warning on Andy, as Tropical Depression 18W, followed several hours later at 280600Z. By that time it had become apparent the system was more than just a benign circulation in the monsoon trough. Dvorak intensity analyses by two different tactical DMSP sites estimated the intensity at 30 and 45 kt (15 m/s and 23 m/s). As Tropical Depression 18W matured, it came under the influence of low- to mid-level ridging to the north. The Tropical Cyclone responded by turning to the west-southwest. It moved in this direction for the remainder of its lifetime.

Continuing to intensify, Andy attained typhoon strength about 24 hours after the first warning, at 290600Z. At that time, the Dvorak intensity analysis was a T4.0, supporting 65 kt (33 m/s) surface winds. Andy's intensification to a typhoon coincided with the formation of a small ragged eye. Typhoon Andy first made landfall on the southern tip of Hainan Island just east of Yai-Xian (WMO 59948) at 291800Z with maximum sustained winds of 65 kt (33 m/s), gusts to 80 kt (41 m/s). After a glancing blow to Hainan (Figure 3-18-1), Andy continued west-southwestward across the southern Gulf of Tonkin and reached its maximum intensity of 70 kt (36 m/s) at 301800Z. Typhoon Andy made landfall as a minimal strength typhoon approximately 30 nm (56 km) north of Dong Hoi, Vietnam (WMO 48848) at 011000Z. The tropical cyclone rapidly weakened as it moved inland. The last warning, issued at 020000Z, downgraded Andy to a 25 kt (13 m/s) tropical depression as it dissipated over central Laos.

Although a tropical cyclone of this magnitude would normally be expected to cause widespread damage, none was reported. Extensive preparations made prior to the cyclone's arrival probably lessened the impact of Andy's passage.

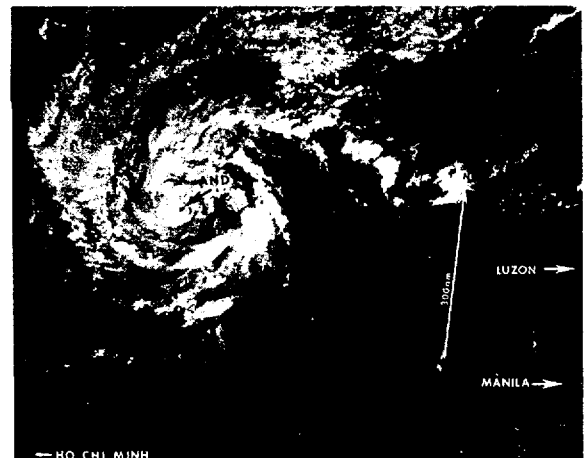
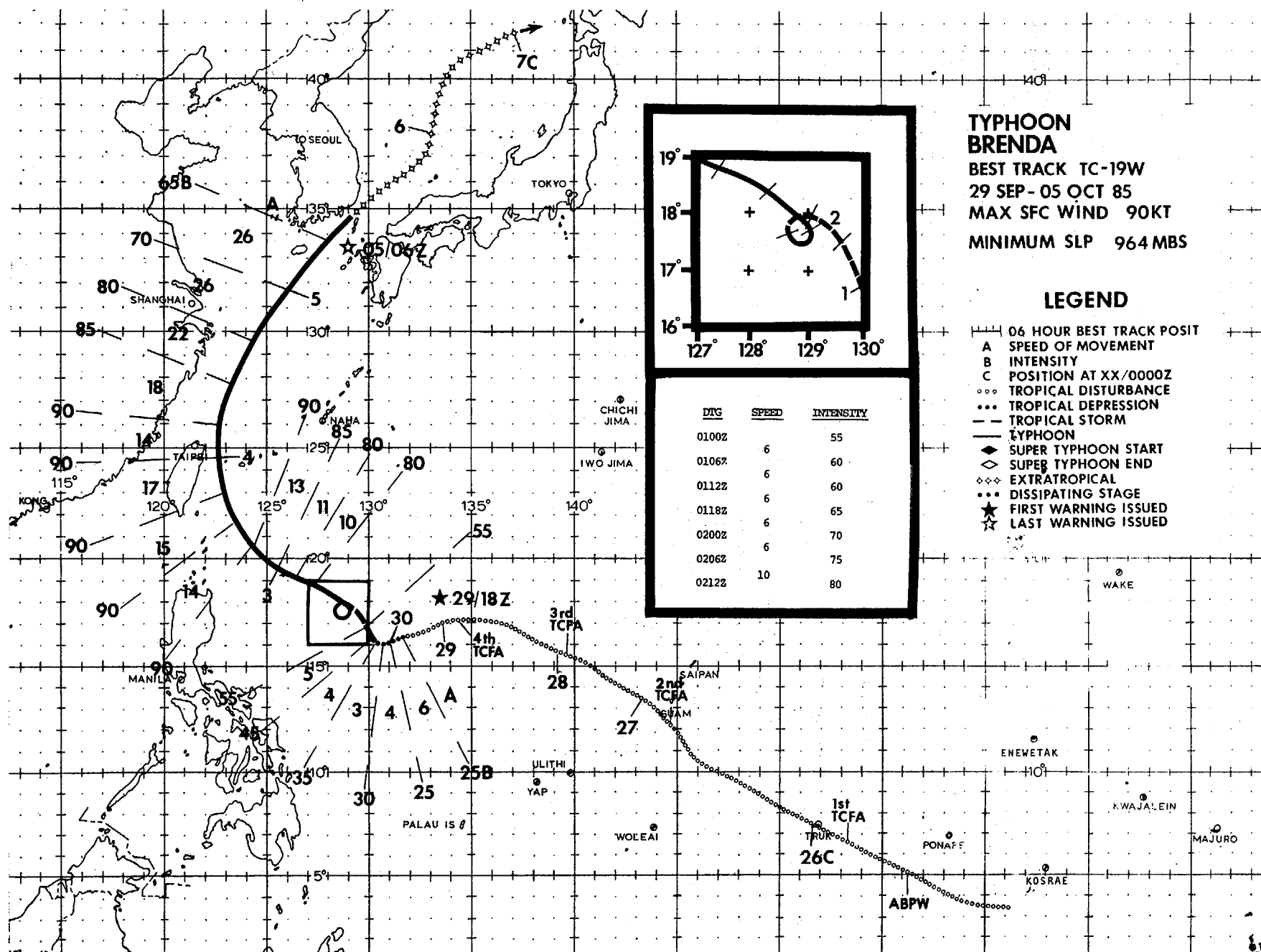


Figure 3-18-1. Typhoon Andy, with a small eye, as it entered the Gulf of Tonkin (300228Z September DMSP visual imagery).



Typhoon Brenda developed from a broad, persistent area of convection in the monsoon trough. Its life was influenced by two mid-latitude troughs. The first caused erratic early movement. The second caused Brenda to recurve into the mid-latitude westerlies, a track which was well-forecast by the Joint Typhoon Warning Center.

The disturbance that would become Brenda was first noticed on 25 September as a large area of persistent convection southeast of Truk (WMO 91334). (Further west, the early signs of Typhoon Andy were evident in the western Philippine Sea). Although the system was disorganized, good upper-level outflow was evident. The proximity of the tropical disturbance to Guam and its impressive satellite signature resulted in the issuance of the first of four TCFA's at 252230Z. Aircraft reconnaissance early on the 26th was unable to locate a surface circulation, but did find a broad area of troughing. The area tracked northwest through the 26th, with the convec-

tion covering a broad area and upper-level outflow remaining favorable. This prompted the reissuance of the TCFA, at 262230Z, but once again aircraft reconnaissance early on the 27th was unable to locate a circulation. This scenario repeated itself the next day. Finally, late on 28 September, the deep convection began to show an increase in amount and organization. A few hours later, after the fourth TCFA was issued, aircraft reconnaissance found a closed 15 kt (8 m/s) circulation at 290329Z. The slow development of the disturbance was surprising, since it appeared that all the necessary ingredients for development were present. It is thought that the extremely broad size of the disturbance may have prevented a faster development, which is more typical of WESTPAC tropical cyclones (Figure 3-19-1).

The first warning on Brenda was issued at 292347Z, valid at 291800Z, based upon aircraft reconnaissance which located a 20 kt (10 m/s) circulation and a MSLP of 1000 mb - a drop of three

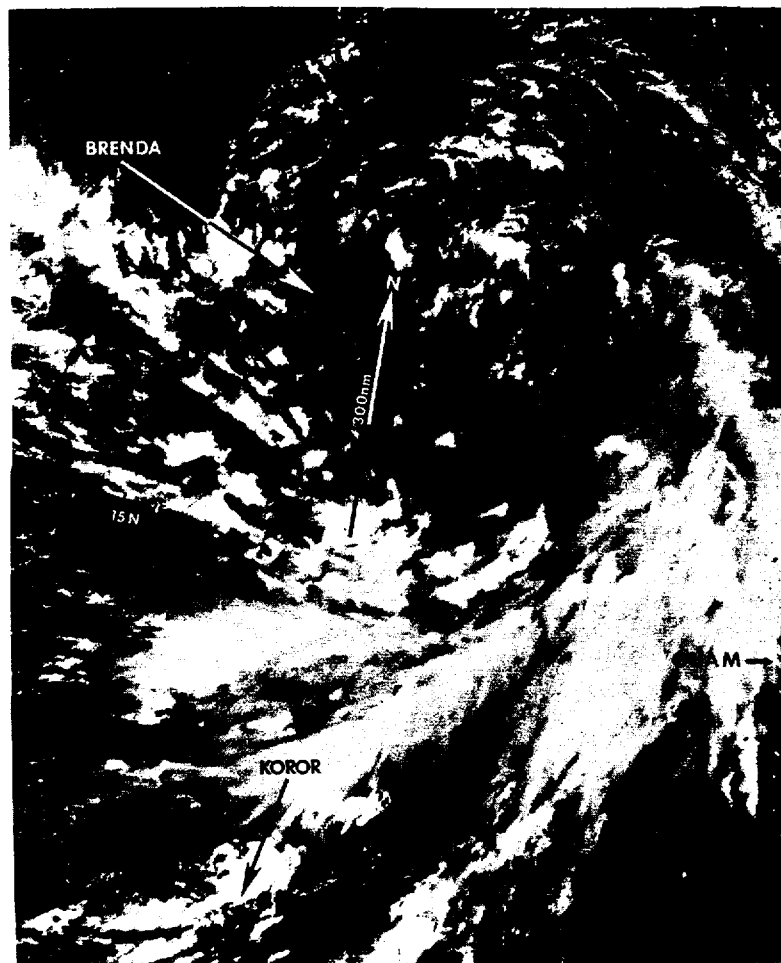


Figure 3-19-1. Visual imagery of the Tropical Disturbance at the time aircraft reconnaissance first located a surface circulation center. This extremely broad area of convection showed little change from the 25th through the 28th. Most of the curvature due to an upper-level anticyclone. The abnormally large size of the disturbance may have slowed development (290107Z September DMSP visual imagery).

millibars in less than 24-hours. Initial forecasts called for the system to gradually increase in intensity, move west-northwest and cross northern Luzon. This was based on the expectation that the subtropical ridge would maintain itself north of Brenda. But, Brenda moved west-southwest followed by a brief turn to the northwest before apparently completing a small cyclonic loop on 1 October. These movements were related to the passage of a mid-latitude trough to the north. Although the trough did not completely weaken the ridge, it eroded the ridge enough to affect the steering flow. As a result, Brenda moved slowly and erratically. By the 2nd, the trough had passed to the northeast and the subtropical ridge began to rebuild. Brenda responded by turning back to the west-northwest while continuing to intensify,

eventually reaching typhoon force at 011800Z. At that point it appeared that Brenda would miss northern Luzon and track just south of the island of Taiwan.

On 2 October, aircraft reconnaissance determined that the Typhoon had increased in strength and was more circular. With another mid-latitude trough approaching from mainland China, it appeared that Brenda's track would again be affected in 24- to 36-hours. Using this information and the belief that the subtropical ridge was not going to build far enough west to drive Brenda through the Luzon Straits, the forecast track was revised to recurve Brenda around the end of the ridge just east of Taiwan. Figure 3-19-2 shows the forecast aids

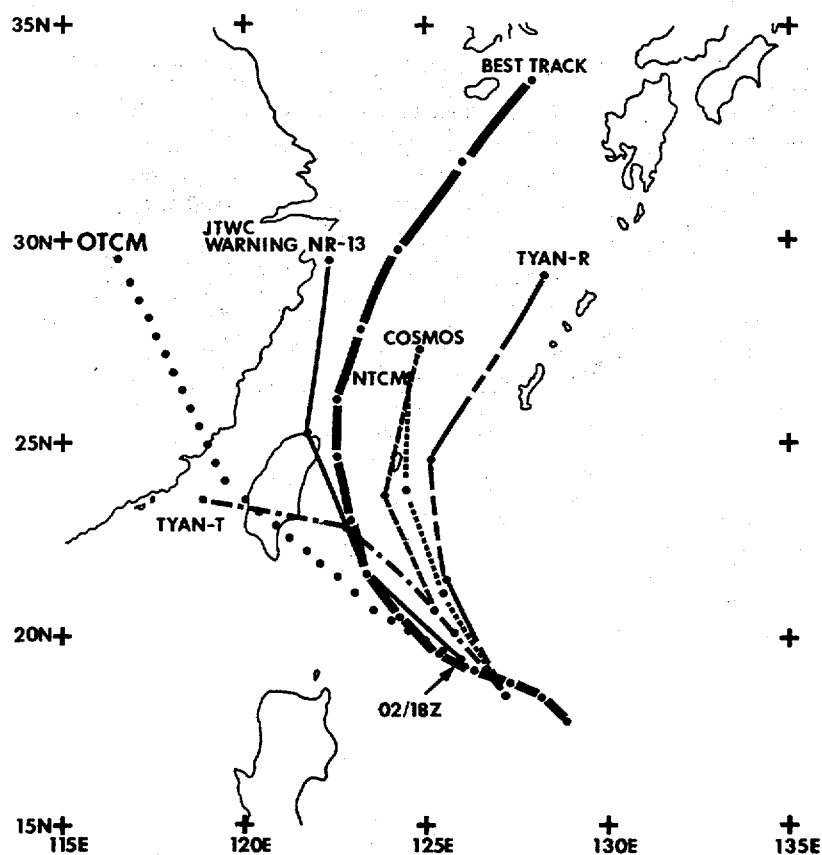


Figure 3-19-2. Forecast aids at 24-hour intervals, when the first recurvature forecast was issued, are compared to the warning and Brenda's best track. While some aids (NTCM, COSMOS and TYAN RECURVER) forecast recurvature; OTCM, JTCW's best aid during the past few years fails to indicate recurvature. All aids are slow in forecasting the speeds of movement during recurvature.

available to the TDO when the first recurvature forecast was issued. This forecast differed considerably from those of other warning agencies, but proved to be quite accurate, although the speed of movement was slow.

Brenda had a unique signature on satellite imagery because of its extremely large eye. Aircraft reconnaissance confirmed the existence of a large banding eye on 3 October. Satellite imagery showed a ragged eye, often larger than 60 nm (111 km) in diameter (Figure 3-19-3). The large eye lasted from 030000Z until Brenda moved around the ridge and began to accelerate into the westerlies on 4 October.

During recurvature, Brenda performed as forecast. It reached a maximum intensity of 90 kt (46 m/s) at 030600Z, and maintained that intensity for 24-hours, as it turned to the north and passed east of Taiwan. Under the influence of the mid-

latitude westerlies north of the ridge axis, Brenda turned to the northeast and accelerated, passing just south of Korea on the 5th. Extratropical transition was underway by 050000Z and the final warning was issued at 050600Z. The extratropical remains of Brenda passed through the Korea (Tsushima) Strait and entered the Sea of Japan at 051200Z before slowing down and weakening.

Known damage from Brenda was limited to the southern Korean Peninsula and adjacent islands. Nearly 12 inches (30 cm) of rain was reported over a large area. The Korean National Disaster Relief Center reported 14 dead, 43 missing, and damage to 167 houses, 630 watercraft, and 34,600 acres (14,000 hectares) of rice paddies as a result of the storm's passage. Damage was greatest on the island province of Cheju and the two provinces near the coastal city of Pusan (WMO 47153) in the southeast corner of the peninsula.

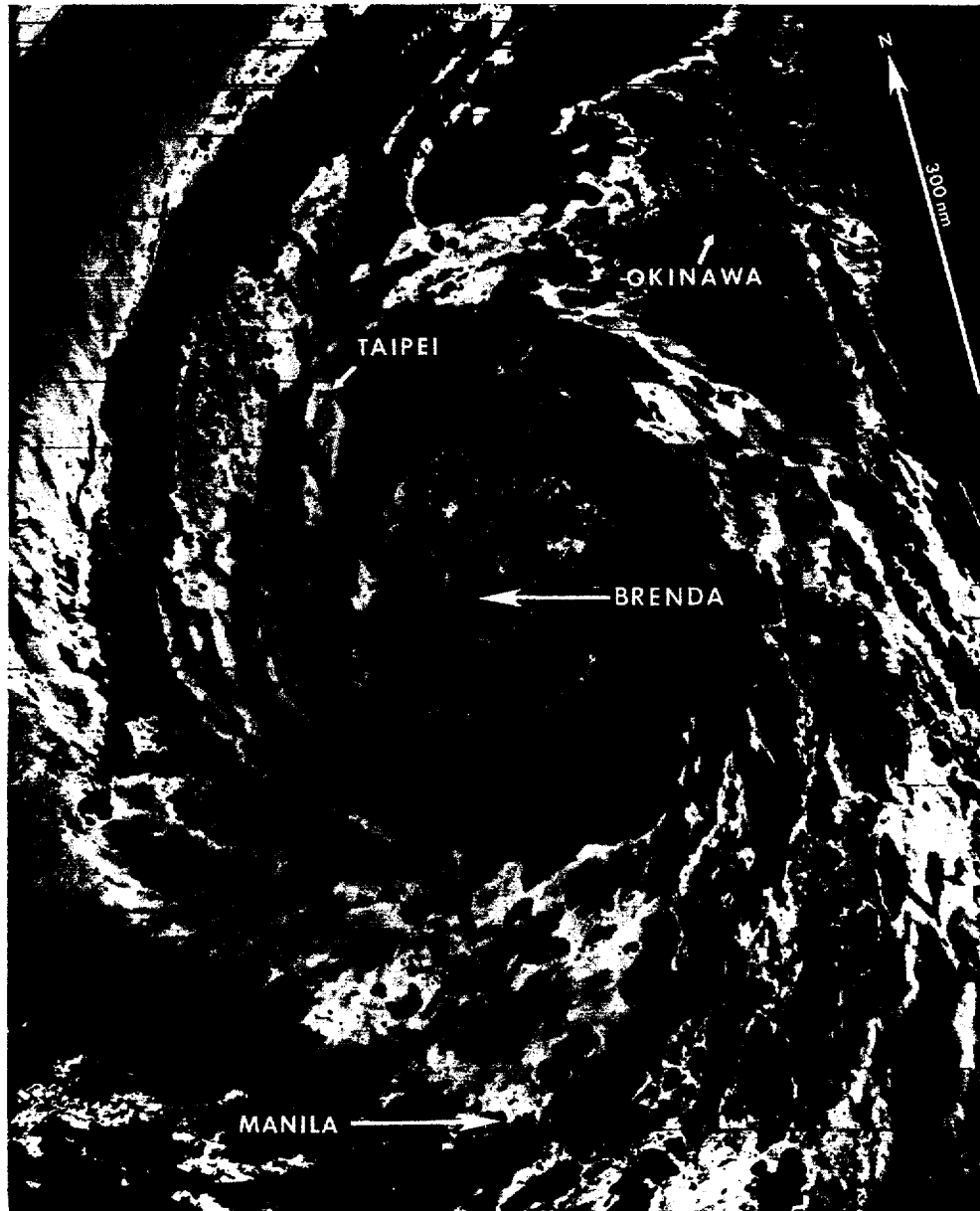


Figure 3-19-3. Nighttime enhanced infrared imagery of Brenda's large eye. The eye is 75 nm (139 km) in diameter (031407Z October DMSP enhanced infrared imagery).

# TYPHOON CECIL

BEST TRACK TC-20W

12-16 OCT 1985

MAX SFC WIND 100 KT

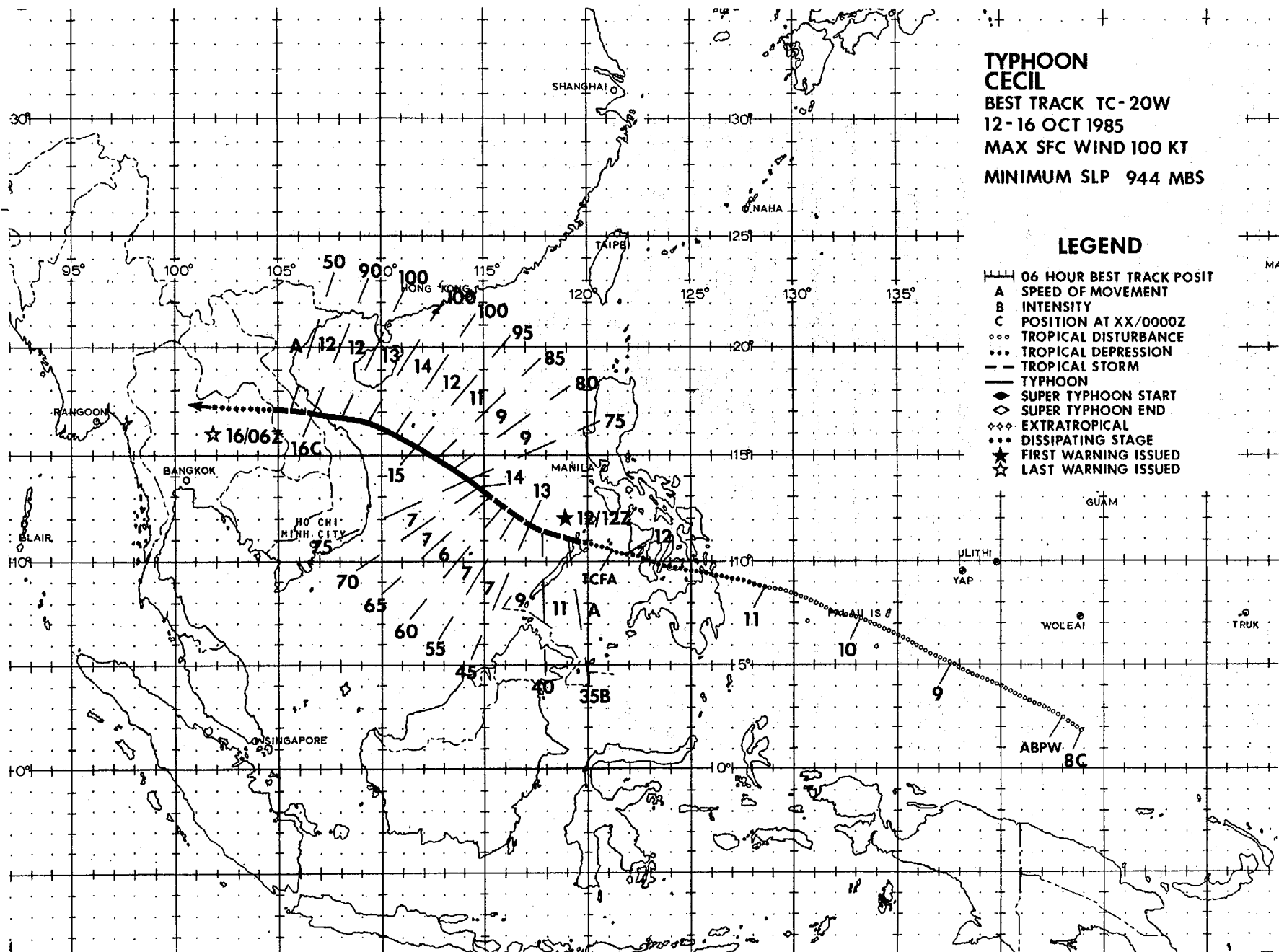
MINIMUM SLP 944 MBS

## LEGEND

- 06 HOUR BEST TRACK POSIT
- A SPEED OF MOVEMENT
- B INTENSITY
- C POSITION AT XX/0000Z
- ... TROPICAL DISTURBANCE
- ... TROPICAL DEPRESSION
- TROPICAL STORM
- TYPHOON
- ◆ SUPER TYPHOON START
- ◇ SUPER TYPHOON END
- ◇◇◇ EXTRATROPICAL
- ... DISSIPATING STAGE
- ★ FIRST WARNING ISSUED
- ☆ LAST WARNING ISSUED

MA

06



Typhoon Cecil was one of several tropical cyclones to hit Vietnam during the autumn of 1985. In its wake, more than 700 were left dead and half-a-million homeless. The dollar value of the damage caused by Cecil has been estimated to be in excess of 65 million dollars.

Typhoon Cecil began innocently enough as an area of increased convective activity south of the Caroline Islands on the 8th of October. Satellite imagery at 080600Z showed a large area of strong, slightly curved convection extending along 04N from 136E to 145E. Supporting synoptic data showed convergent cross-equatorial flow. Over the next 72-hours, the tropical disturbance tracked to the west-northwest towards northern Mindanao, passing just south of the Belau (Palau) Islands late on the 9th. It maintained good upper-level outflow, enhanced by upper-level troughing to the north, and became more organized at the lower levels. Aircraft reconnaissance first located a surface circulation east of Mindanao at 110222Z. Maximum sustained winds at that time were 15 to 20 kt (8 to 10 m/s) and the MSLP was estimated to be 1006 mb.

Further organization of the low-level center was slowed as the disturbance passed through the islands of the southern Philippines. With continued development considered likely once the disturbance crossed the Philippines, a TCFA was issued at 120330Z for the northern Sulu Sea westward into the South China Sea. By 121200Z the disturbance had moved west of Palawan Island into the South China Sea. Little damage was sustained in the southern Philippines due to its passage. By then, satellite imagery indicated that the system had begun to consolidate over water, prompting JTWC to issue the first warning on Tropical Depression 20W at 121200Z. Initially, Cecil was expected to consolidate rapidly and traverse the South China Sea making landfall within 72-hours of the first warning over southern Vietnam.

Post-analysis indicated that Cecil was already at tropical storm intensity upon emerging into the South China Sea. It then turned to a more north-westerly heading and tracked along the southern edge of a ridge over eastern China and the East China Sea. Cecil steadily intensified as it moved northwest, reaching typhoon intensity by 131800Z. By that time satellite imagery showed that Cecil was slowing to 7 kt (13 km/hr) and developing an eye. The slower movement and a slightly more northward track meant that Cecil would not make landfall as early as previously expected. Aircraft reconnaissance at 130824Z confirmed the presence of a 20 nm (37 km) diameter eye and a minimum sea-level pressure of 984 mb.

Cecil took three days to cross the South China Sea. During the latter half of this transit, Cecil maintained an eye and continued to intensify at a steady rate. The low- to mid-level ridge was not as strong as forecast, so Cecil maintained a track to the northwest. As Cecil passed south of Hainan Island on the 15th (Figure 3-20-1), it was at its maximum intensity of 100 kt (51 m/s). By 151200Z, interaction with the topography of Vietnam and Hainan was preventing further intensification by hampering low-level inflow. The mid-level subtropical ridge remained across the island of Taiwan and mainland China. This turned Cecil on a more westerly track, resulting in landfall about 40 nm (74 km) north of Hue (WMO 48852) at 152200Z. Cecil continued to move west and weaken, dissipating over the Laos/Thailand border on the 16th. The final warning was issued at 160600Z.

Officials in Binh Tri Thien Province in central Vietnam described Typhoon Cecil as "the worst natural disaster yet in central Vietnam ...causing... damage worth more than 65 million dollars". At least 702 people were confirmed dead with 128 still missing and 560,000 left homeless. In addition to destroying or damaging 200,000 or more homes, Cecil also destroyed about 850 fishing boats and other small vessels. Winds of up to 90 kt (46 m/s) combined with flooding to ruin 70,000 hectares (172,900 acres) of rice and other crops. A 200 bed hospital was destroyed, five other hospitals damaged, and 250 dispensaries swept away, along with almost 9,000 classrooms with accompanying school equipment and textbooks. Dikes, canals, and pumping stations sustained almost one million dollars in damage. Telephone lines, electricity service, and roadways were cut, bringing business to a halt and hampering relief efforts. It will be many years before this province, one of Vietnam's poorest, recovers from the accumulated affects of this and the other tropical cyclones which affected Vietnam in 1985.

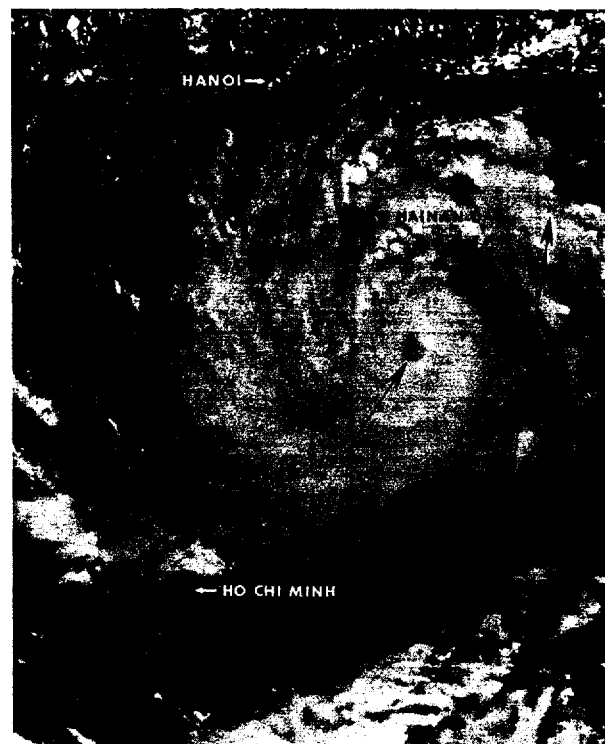
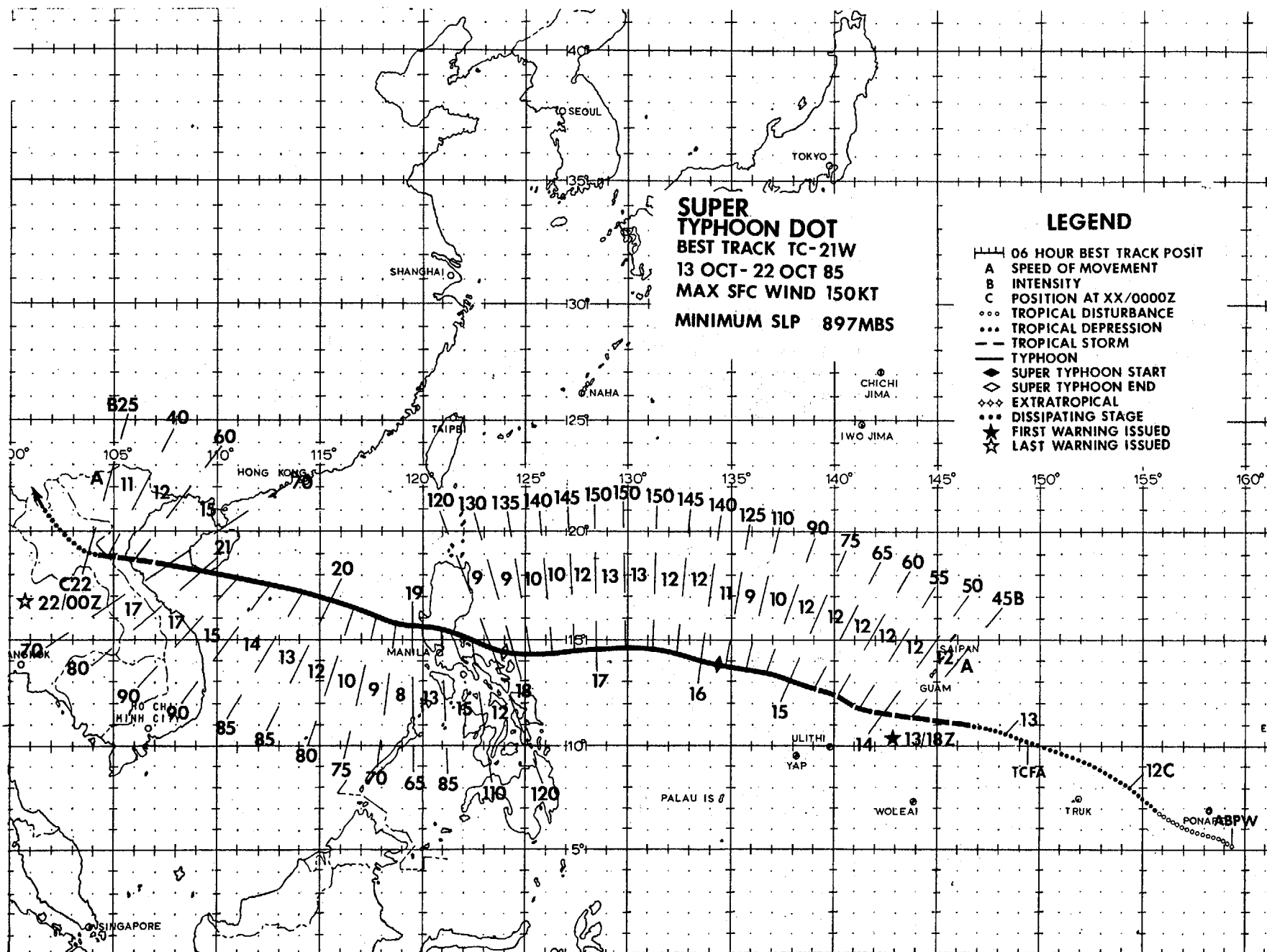


Figure 3-20-1. Typhoon Cecil at maximum intensity passing south of Hainan Island (150733Z October NOAA visual imagery).





After Typhoon Brenda, which had developed in the low-level southwest monsoon trough, completed extra-tropical transition on the 5th of October, the mid-level subtropical ridge became well-established over the Northwest Pacific. This synoptic feature would confine the development of tropical cyclones to low latitudes near 10N in the near-equatorial trough. Also coincident with Brenda's movement to the north was the replacement of the low-level southwest monsoon flow over the South China Sea with north-to-northeasterly flow off of the Asian continent.

Typhoon Dot was the only super typhoon (intensity equal to or greater than 130 kt (67 m/s)) of the 1985 WESTPAC season. It intensified (deepened) explosively causing intensity forecast difficulties. Other distinguishing characteristics were the small

size of the area of intense convection, the small radius of maximum wind, and the absence of low-level southwest monsoon inflow. Also of interest was the large wind radius in the northwest semicircle (when it was located southeast of Luzon) where surface winds were enhanced by a strong pressure gradient between the tropical cyclone and a polar high pressure cell located near 40N 110E.

Dot was first detected as a tropical disturbance in the near-equatorial trough, 150 nm (278 km) south-east of Ponape (WMO 91348) on the 11th of October. Figure 3-21-1 shows the disturbance on the 12th of October exhibiting signs of organization in its upper-level outflow. The system moved west-northwest and reached tropical storm intensity on the 13th south of Guam.

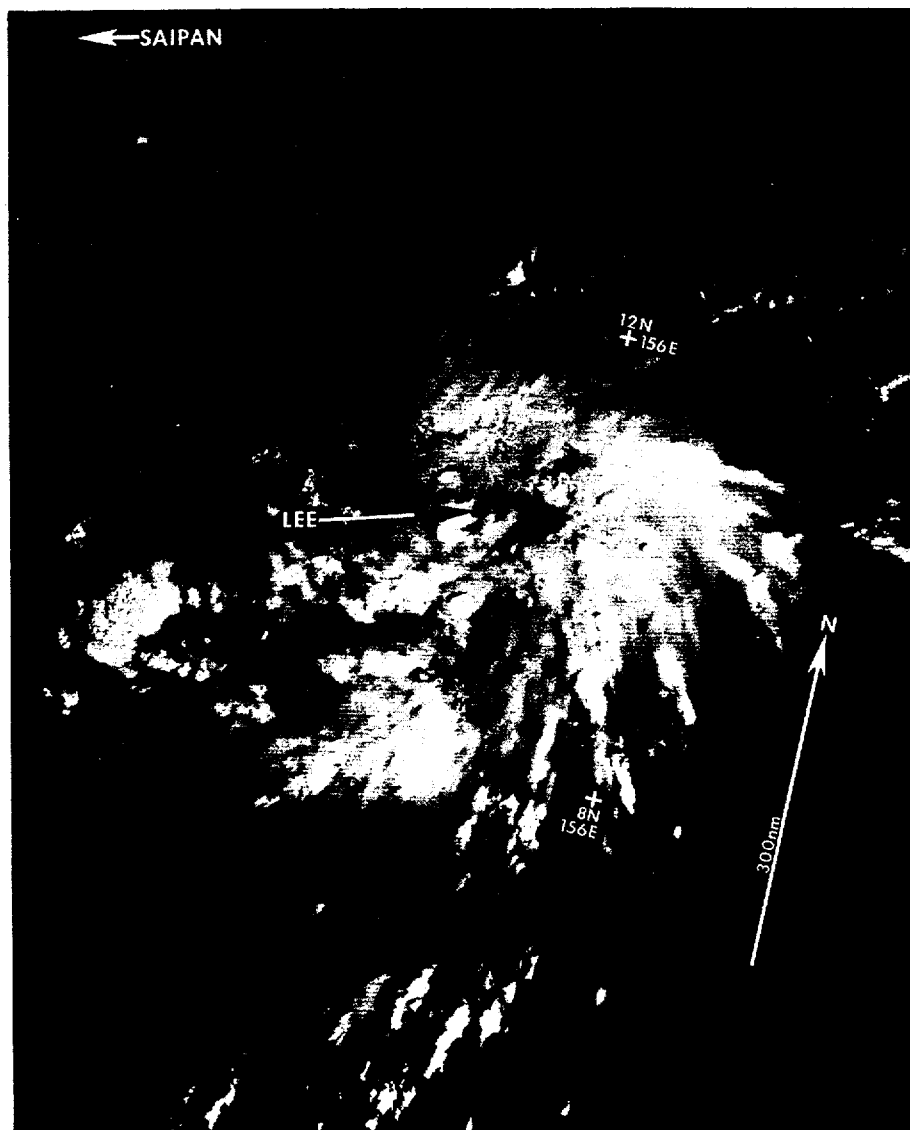


Figure 3-21-1. Super Typhoon Dot as a disturbance in the near-equatorial trough with signs of organized upper-level outflow (120006Z October DMSP visual imagery).

The track forecasts for Typhoon Dot did not present any significant difficulty for the forecasters at JTWC. Figure 3-21-2 shows that the mid-level easterlies dominate the Trust Territories westward through the Philippine Islands and into Southeast Asia at 120000Z. With no change expected in the orientation or strength of the ridge, a west-northwest track at 10 to 20 kt (19 to 37 km/hr) under this ridge was considered to be the best forecast. This was in agreement with climatological and analog forecast guidance. The two numerical models, OTCM (One-way interactive Tropical Cyclone

Model) and NTCM (Nested Tropical Cyclone Model), were of little help during the crucial first four days of forecasts (when Dot was approaching the Philippines). Due to computer problems at Fleet Numerical Oceanography Center (FNOCC) the older Primitive Equation (PE) model was run in place of the Navy Operational Global Atmospheric Prediction System (NOGAPS). Later, it was determined that OTCM, when running with data from the PE model, didn't have access to the necessary data fields. Subsequently, OTCM was modified to accept the needed data.

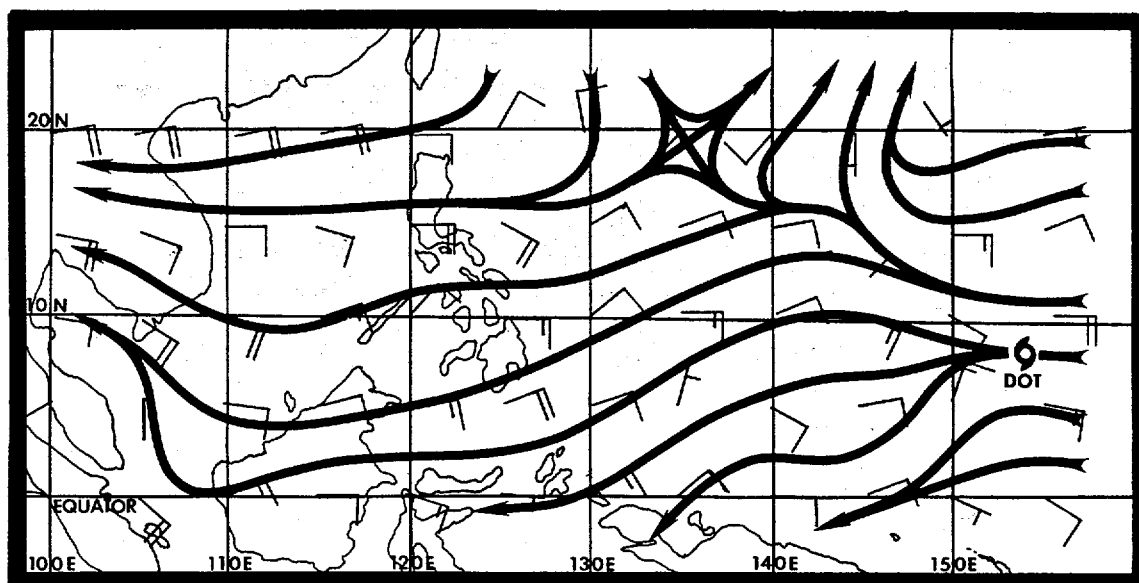
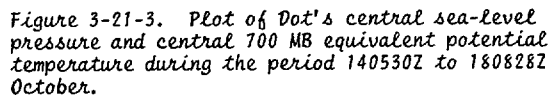


Figure 3-21-2. 400 mb Numerical Variational Analysis (NVA) at 120000Z October showing easterlies over Dot's future track to the west-northwest.

tion. The technique calls for intensification to below 925 mb (how far below can be estimated from the technique also) whenever the plots of central sea-level pressure and Theta-E intersect near the critical values of 950 mb and 360 degrees Kelvin (both values being statistical means derived from past intense storms). Figure 3-21-3 is a plot of Dot's central sea-level pressure and Theta-E during the period 140530Z to 180828Z. At Point A (142130Z), the two lines show a tendency to intersect (notice extrapolation to Point A'). However, Point B (150022Z) reflects a decrease in Theta-E. Then, at Point C (150615Z), this trend reverses and again extrapolation to Point C' would indicate intersection. Point D (150853Z) shows a slight



decrease in Theta-E and no intersection. The next available aircraft reconnaissance data was not received until 152102Z, and by that time Dot's central sea-level pressure had plummeted to 906 mb and the central 700 mb temperature had soared from 20 Celsius to 30 Celsius (yielding a Theta-E of 372 K when paired with the dewpoint temperature of 11 Celsius). This forecast method is a reliable one in most instances. However, Typhoon Dot demonstrates a situation when the lack of timely aircraft data prevented the effective use of the technique. In post-analysis, if pressure, temperature, and dewpoint data had been available around 151200Z it is a distinct possibility that the intersection of the central sea-level pressure line and the Theta-E line would have been observed.

The reliability of this forecast technique was mentioned earlier. However, in addition to the timing problem already mentioned, a couple of factors

should be pointed out. First, the computation of Theta-E is very sensitive to dewpoint temperature (and to a lesser degree ambient temperature). The dewpoint measurement is also sensitive to a sometimes non-homogeneous distribution of moisture in the storm's center. Second, a rarer but sometimes complicating factor is the complexity and delicacy of the dewpoint hygrometer which is an alternately cooled/heated mirror coupled with a thermistor. The dewpoint temperature is recorded when a thin film of dew forms on the mirror. Malfunctions of the instrument occasionally occur.

To give the reader an indication of what impact not knowing that Dot was going to explosively deepen had on the intensity forecasts can be seen in Figure 3-21-4. The graph depicts the best track intensities (at six hour intervals) for the period 131800Z to 181200Z compared to the corresponding 12-, 24-, 48-, and 72-hour intensity forecasts. Twelve-hour fore-

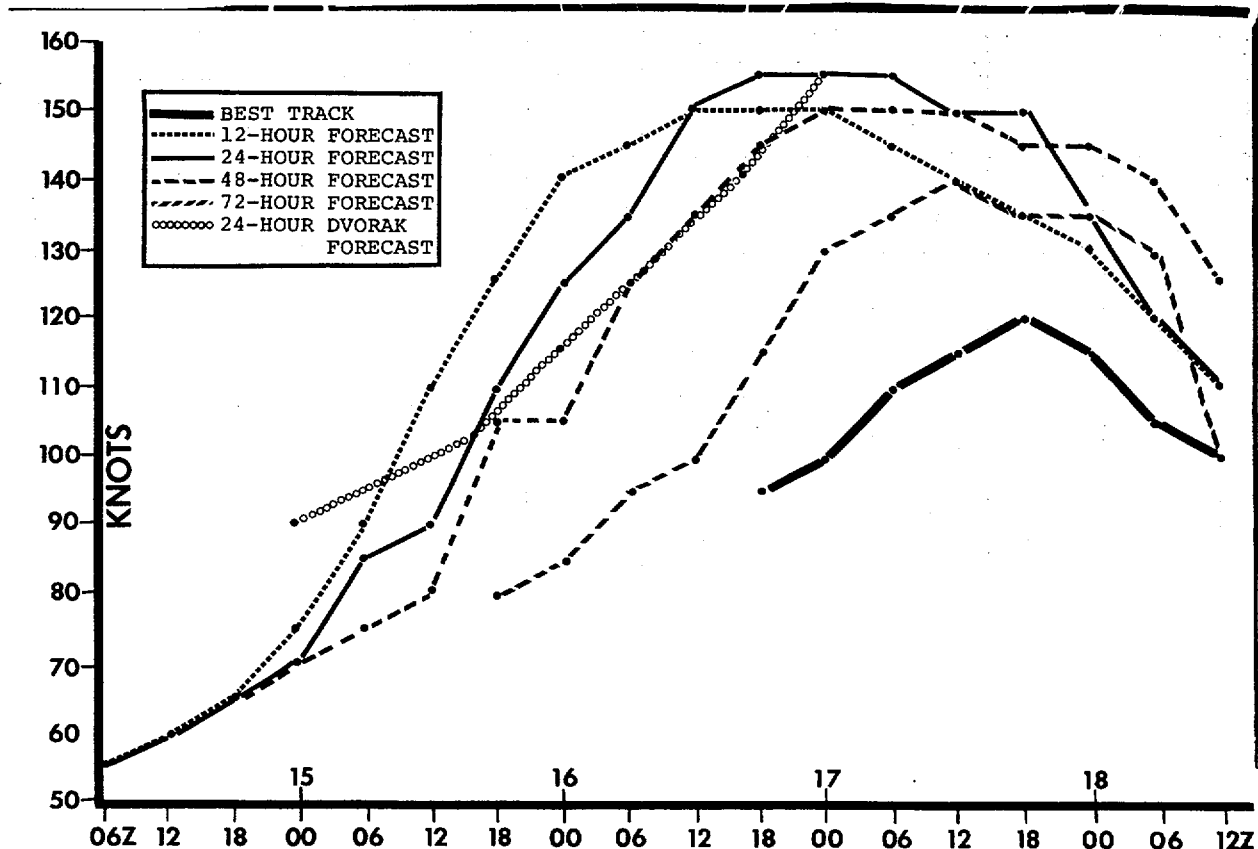


Figure 3-21-4. Plot of Dot's best track intensities at six-hour intervals and corresponding 12-, 24-, 48-, and 72-hour forecast intensities for the period 131800Z to 181200Z October 85.

casts for the period 151200Z through 160600Z were 20, 15, 15, and 10 kt (10, 8, 8, and 5 m/s) low. For the same period twenty-four hour forecasts were 30, 20, 35, and 20 kt (15, 10, 18, and 10 m/s) below the best track intensities. From the graph one can see that the 24-hour forecast intensity curve is very close to the Dvorak forecast intensity curve. This is usually the case since the Dvorak model is the main JTWC 24-hour intensity forecast tool. The problem with explosive intensification really starts showing up at the 48-hour forecast period. The 48-hour intensity forecasts during the period 151800Z through 161800Z October were 45, 55, 50, 50, and 35 kt (23, 28, 26, 26, and 18 m/s) too low. The three 72-hour forecasts that were effected by the explosive deepening were for the period 161800Z through 170600Z Oct and were 55, 50, and 35 kt (28, 26, and 18 m/s) too low. After Dot had explosively deepened, the intensity forecasts reflected the storm's high initial intensity and the forecast errors decreased signi-

ficantly with the average 12-hour intensity forecast error for the period 140600Z through 181200Z (18 cases) being 5 kt (3 m/s), the average 24-hour error for the period 141800Z through 181200Z (16 cases) being 14 kt (7 m/s), the average 48-hour error for the period 151800Z through 181200Z (12 cases) being 24 kt (12 m/s), and the average 72-hour error for the period 161800Z through 181200Z (8 cases) being 28 kt (14 m/s). The point being made is that a forecaster doesn't necessarily have to know 72 hours ahead of time that a system is going to explosively deepen, but if he knows 12 or 24 hours ahead of time then the longer range forecasts made during that period will reflect the higher storm intensity and be more accurate.

Figure 3-21-5 shows Super Typhoon Dot at maximum intensity with a well-defined eye and intense convection confined to a small area around the system. Aircraft reconnaissance on the 16th and 17th of



Figure 3-21-5. Super Typhoon Dot at maximum intensity with a well-defined eye and small surrounding ring of intense convection (170147Z October DMSP visual imagery).

October consistently located the maximum surface winds 5 to 10 nm (3 to 5 km) from the center and radar eye diameters of 10 to 15 nm (5 to 8 km).

Figure 3-21-6 shows the surface wind circulation pattern around Dot (while it was southeast of Luzon) at 181200Z October. Strong winds extended out much further in the northwest semicircle where the surface winds were from the north to northeast. This increased flow resulted from a strong pressure gradient that existed between Dot and a polar high-pressure cell located near 40N 110E. The figure also shows the absence of any enhanced low-level southwest monsoon flow over the South China Sea.

The threat posed by Super Typhoon Dot caused all U.S. military installations in the Philippines to be placed in Tropical Cyclone Condition of Readiness I and resulted in the evacuation of aircraft from Cubi Point NAS and Clark AB, and the movement of several ships from Subic Bay. Seventy-four peoples were reported killed, more than 50,000 left homeless, and damage to buildings and crops estimated at 1.3 million dollars. NAVOCEANCOMFAC Cubi Point reported a peak gust of 19 kt (10 m/s) and Det 5, 20WS at

Clark AB reported maximum sustained winds of 27 kt (14 m/s) with a peak gust of 44 knots (23 m/s). Dot was a very intense typhoon but the damage done in the Philippines was certainly limited by the storm's small diameter of maximum wind, its small area of intense convection, its path of approach to Luzon (this kept most of the low-level flow parallel to the mountainous terrain, reducing orographically-enhanced rainfall), and the absence of enhanced low-level southwest monsoon flow.

After entering the South China Sea late on the 18th of October with minimal typhoon intensity, Dot began regaining organization overwater and continued on a west-northwesterly track. By 201200Z, the Typhoon's intensity peaked at 90 kt (46 m/s) 300 nm (556 km) south-southwest of Hong Kong (WMO 45007). Dot weakened as it churned across the southern tip of Hainan Island, leaving at least two dead, 2300 houses collapsed, and flooding in its wake. Crossing the Gulf of Tonkin in less than a day, it slammed into the coast of North Vietnam 130 nm (241 km) south of Hanoi (WMO 48819). The final warning on Dot was issued at 220000Z as the system dissipated over the rugged mountains inland.

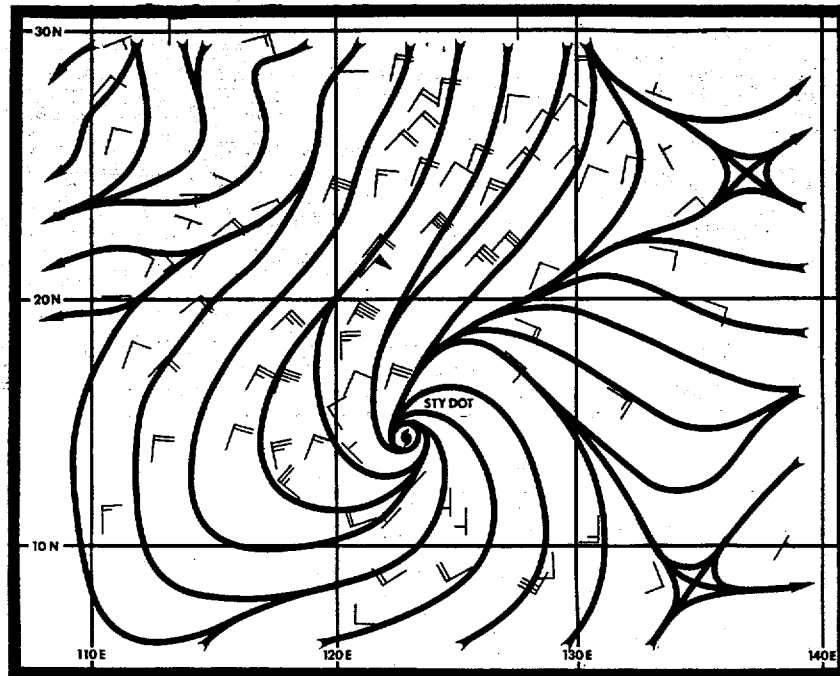


Figure 3-21-6. Surface analysis at 181200Z October showing strong winds extending out a great distance in the northwest semicircle and the absence of (convection-enhanced) low-level southwest monsoon flow.

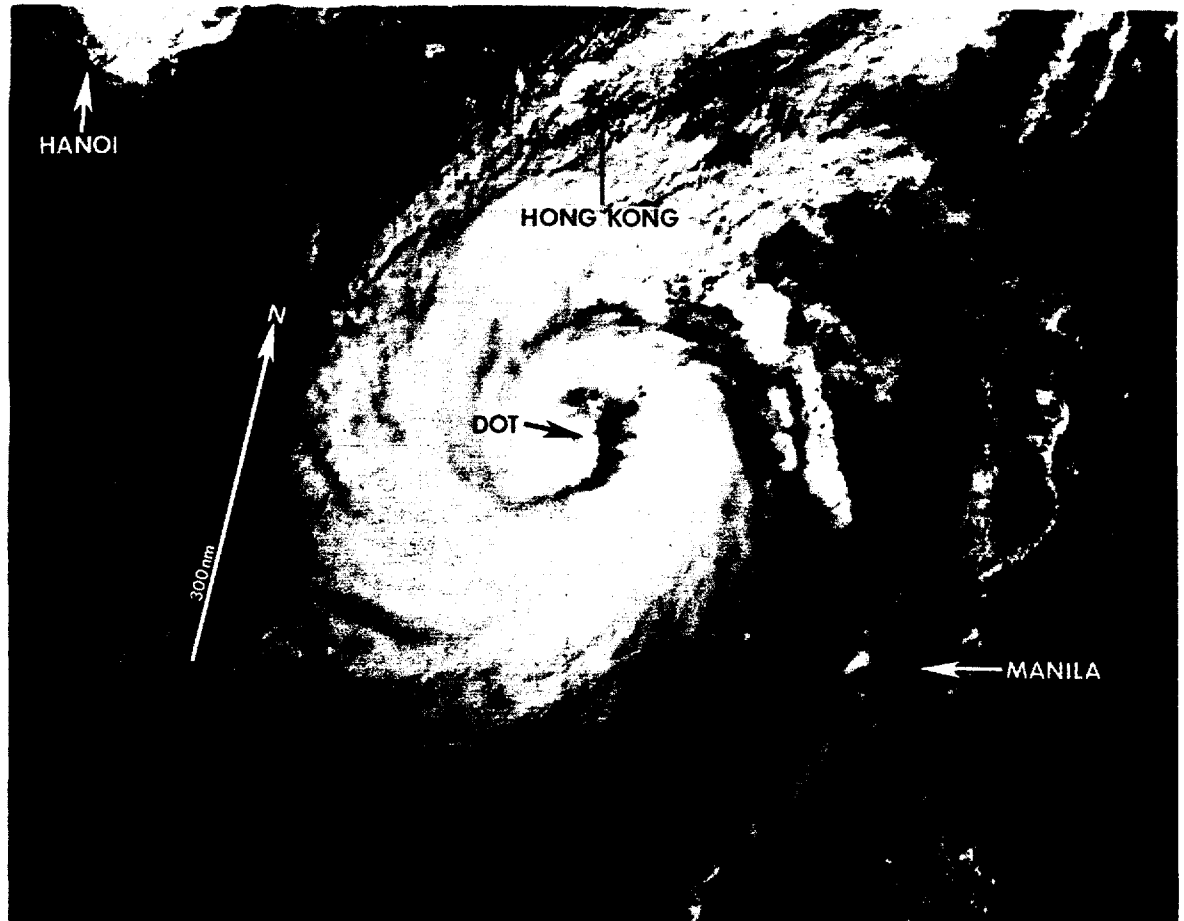


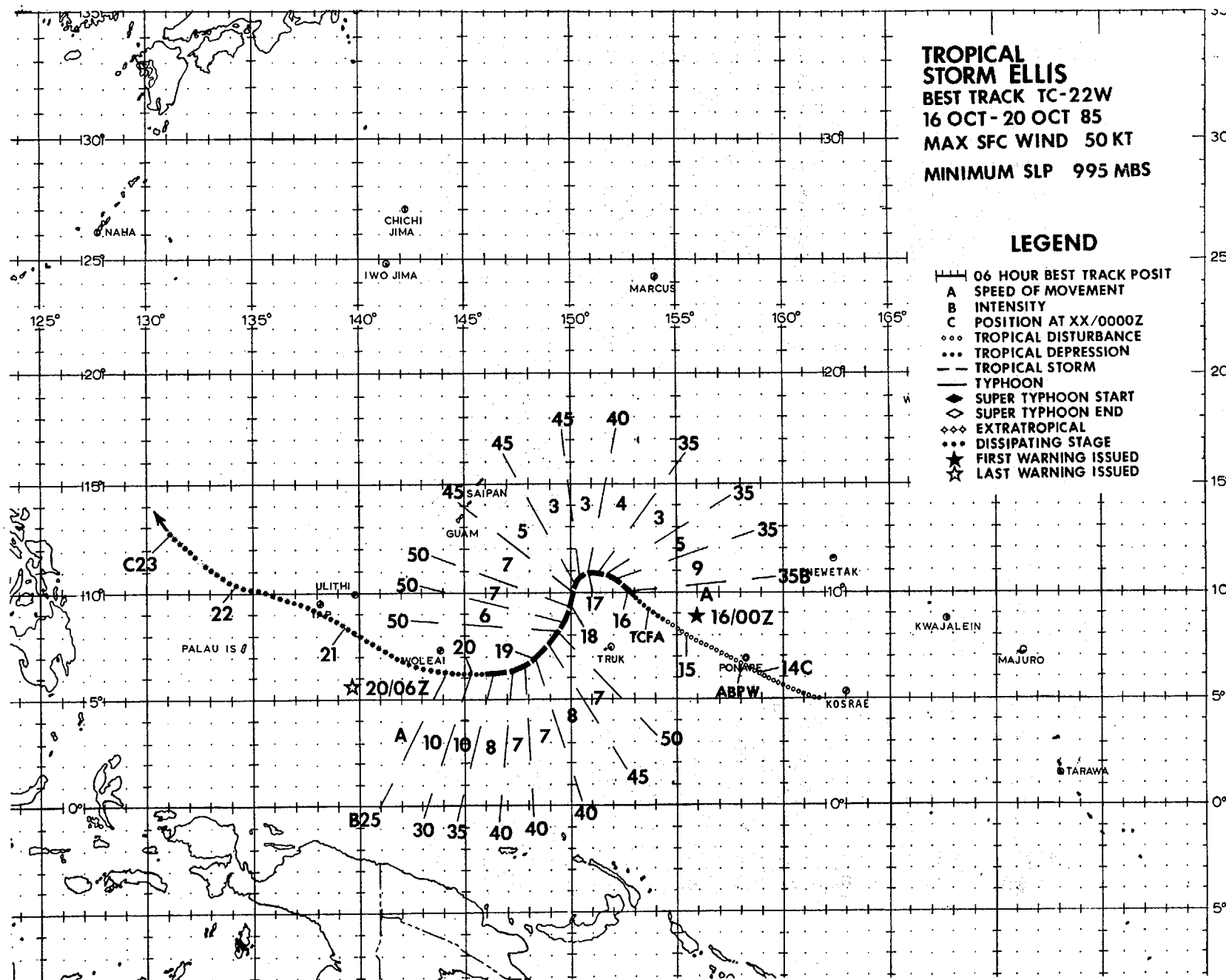
Figure 3-21-7. Super Typhoon Dot with 85 knots (44 m/s) after crossing Luzon and re-intensifying in the South China Sea (200227Z October DMSP visual imagery).



**TROPICAL  
STORM ELLIS**  
BEST TRACK TC-22W  
16 OCT-20 OCT 85  
MAX SFC WIND 50 KT  
MINIMUM SLP 995 MBS

### LEGEND

- 06 HOUR BEST TRACK POSIT
- A SPEED OF MOVEMENT
- B INTENSITY
- C POSITION AT XX/0000Z
- ... TROPICAL DISTURBANCE
- ... TROPICAL DEPRESSION
- TROPICAL STORM
- TYPHOON
- ◆ SUPER TYPHOON START
- ◇ SUPER TYPHOON END
- ◆◆ EXTRATROPICAL
- ... DISSIPATING STAGE
- ★ FIRST WARNING ISSUED
- ☆ LAST WARNING ISSUED



# TROPICAL STORM ELLIS (22W)

Tropical Storm Ellis, which formed in the wake of Super Typhoon Dot, proved to be a relatively short-lived system. Although it did not pass close enough to any populated areas to cause significant damage, Ellis was noteworthy since it presented a unique forecasting problem. Originally forecast to move west-northwest under the subtropical ridge and pass relatively close to Guam, it actually slowed just after reaching tropical storm intensity and proceeded to move southwest for almost three days before dissipating over water.

The disturbance which eventually developed into Tropical Storm Ellis was first observed as a curved band of convection near the island of Ponape (WMO 91348) on 14 October. The area was subsequently included on the Significant Tropical Weather Advisory (ABPW PGTW) at 140600Z. The system moved west-northwest and increased in organization during the next 36-hours. At 151730Z, a Tropical Cyclone Formation Alert (TCFA) was issued and aircraft reconnaissance requested for the following day.

Interpretation of the 160000Z visual satellite imagery, using the Dvorak intensity technique, yielded a surface wind estimate of 35 kt (18 m/s).

This, in combination with aircraft reconnaissance which located a surface circulation with 35 kt (18 m/s) at the 1500 ft (457 m) level at 160458Z, prompted the first warning on Tropical Storm Ellis at 160500Z. Ellis was forecast to move west-northwest under the subtropical ridge which was apparently well established to the north of the system. At 170000Z Ellis slowed to 3 kt (6 km/hr) as the steering flow south of the subtropical ridge axis weakened in response to the passage of a mid-latitude trough to the north. The forecast philosophy of continuing the west-northwest track was not changed at this point, as a resumption of that movement was expected when the mid-latitude trough moved northeastward. In addition, the synoptic guidance appeared to be in agreement with this reasoning. Figure 3-22-1 is Fleet Numerical Oceanography Center's (FNOC) 700 mb Numerical Variational Analysis (NVA) field for 170000Z, which indicates the weak easterly flow around the subtropical ridge and the mid-latitude trough north of Ellis. The 400 mb analysis for the same time (Figure 3-22-2) indicates similar features, except the north-south extent of the subtropical ridge is much smaller. Note that the flow near Ellis is generally weak and southerly, with weak easterlies to the north.

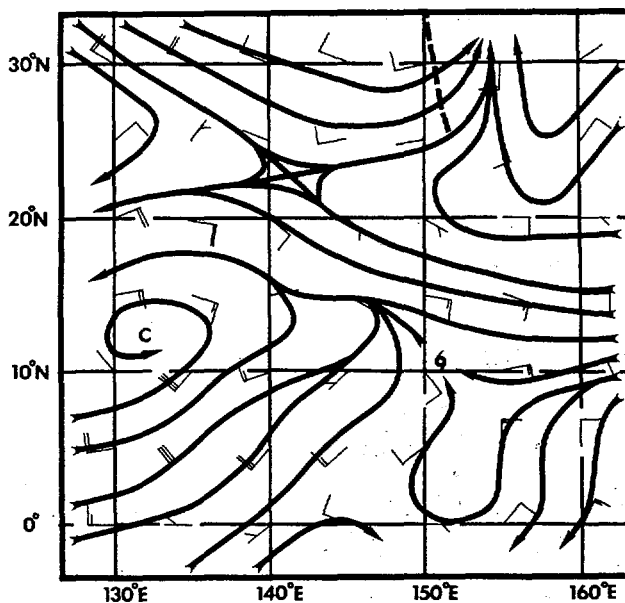


Figure 3-22-1. 170000Z 700 mb Numerical Variational Analyses (NVA) showing weak troughing and 15 kt (8 m/s) easterlies to the north of Ellis.

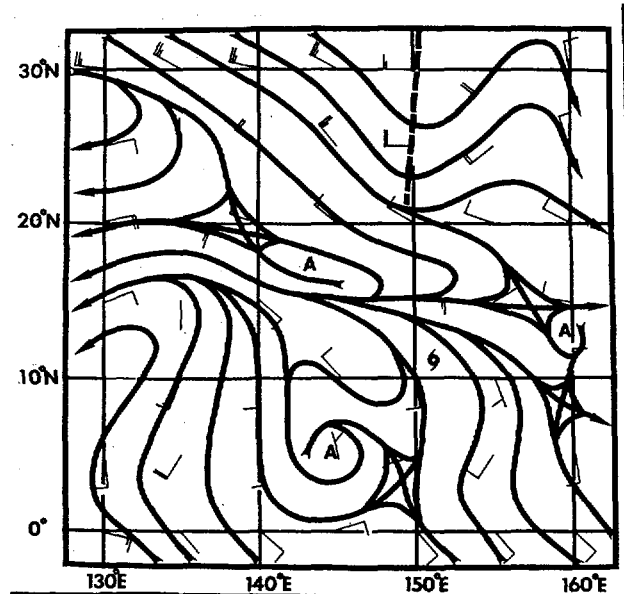


Figure 3-22-2. 170000Z 400 mb NVA depicting weak ridging north of Ellis.

Due to the uncertainty of these mid-tropospheric analyses, synoptic track aircraft missions were requested. The one flown between 0300Z and 0700Z on 17 October provided 400 mb winds in the vicinity of Ellis' forecast track. Figure 3-22-3 shows these observations. In contrast to the NVA analysis (Figure 3-22-2) for that time, the flow is generally northerly to the north and west of Ellis. The lack of data over water in the western North

Pacific was probably responsible for the disagreement between the aircraft observations and the NVA analysis at 400 mb. However, the NVA from the following day (180000Z) represented a significant change; the observations from the synoptic track were in good agreement with the new analysis at 400 mb (see Figure 3-22-4).

In the meantime aircraft reconnaissance at

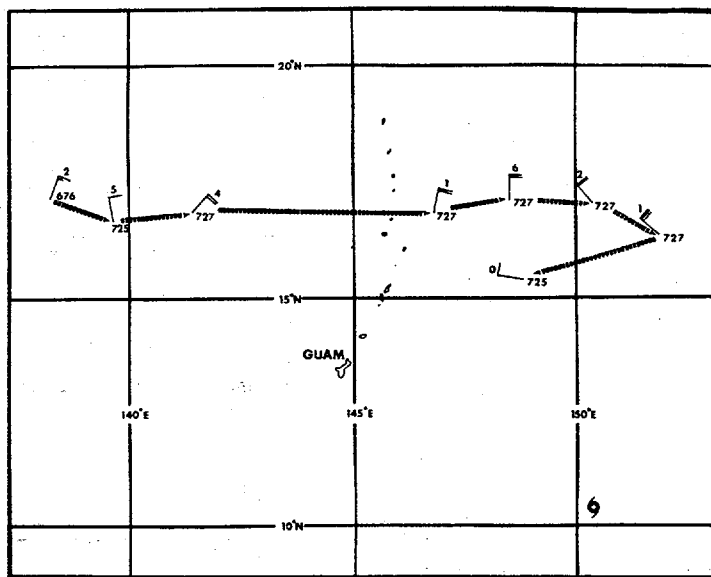


Figure 3-22-3. Observations from the aircraft reconnaissance mission synoptic track at 400 mb, indicating northerly flow vice easterly flow ahead of Ellis.

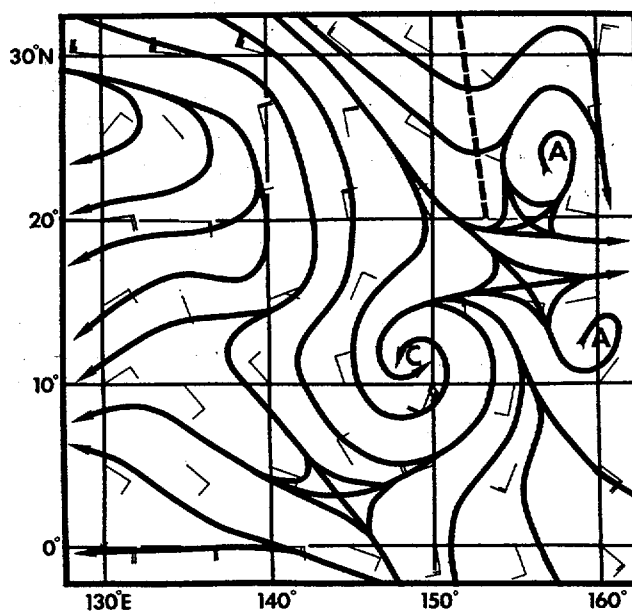


Figure 3-22-4. 180000Z October 400 mb analysis, showing northerly flow ahead of Ellis, which agrees with earlier observations from the synoptic track.

172200Z and 172345Z found the low-level circulation center well south of the forecast track, indicating Ellis had moved south-southwest during the period. At that time Ellis also reached its maximum intensity of 50 kt (26 m/s). The feature that helped to drive the low- to mid-level ridging to the west and moved Ellis to the south-southwest, was most probably an upper cold low, or cell, in the tropical upper-tropospheric trough (TUTT). The 200 mb analysis for 190000Z (see Figure 5-22-5) indicated that the TUTT cell was in close proximity to Ellis. Satellite imagery at that time indicated that upper-level outflow was suppressed in the west semicircle (see Figure 3-22-7). The low- to mid-level flow remained northerly, and Ellis continued its southwestward

track.

At 191200Z, Ellis began to weaken as it attempted to move under the TUTT cell and experienced increased vertical shear. By 200000Z the intensity had decreased to 30 kt (15 m/s) and the low-level cloud lines had lost most of their curvature. The last warning was issued at 200600Z.

In retrospect the One-way Tropical Cyclone Model (OTCM) presented a puzzle during the initial forecasts on Ellis, because of its previous performance on Super Typhoon Dot several days before. With Dot, which also formed in low latitudes, OTCM guidance repeatedly, and erroneously, drove the system equa-

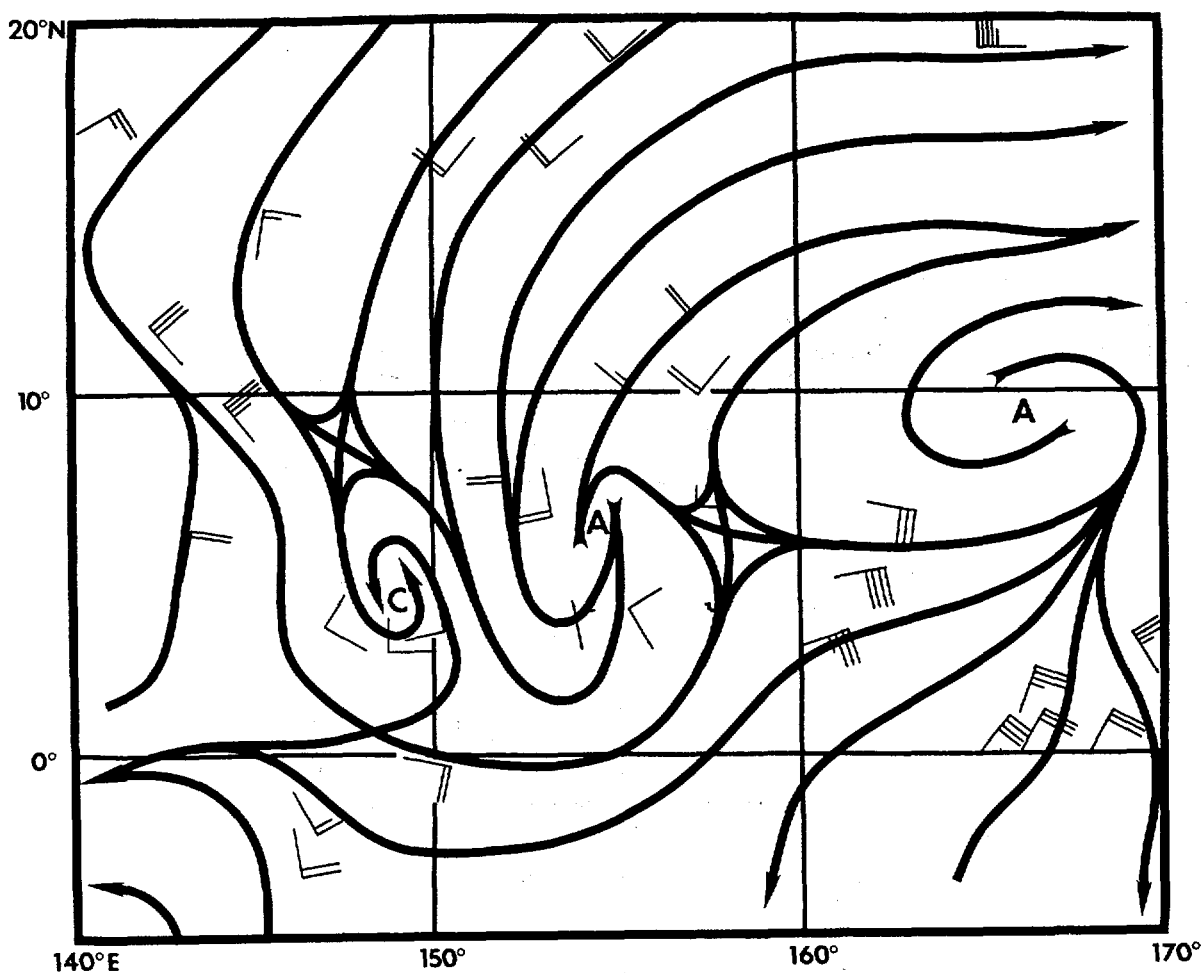


Figure 3-22-5. 190000Z October 200 mb analysis depicting the location of the TUTT and the upper-level cold low.

torward. As a consequence, the OTCM (Figure 3-22-6), which indicated southwest movement for Ellis, was highly suspect. Persistence and climatology favored a west to northwest track through the southern Mariana Islands. As it turned out, Ellis moved southwest, passing well south of the island of Guam. In this case the OTCM guidance was "right" for the "wrong" reasons. After-the-fact it was determined by the software managers at Fleet Numerical Oceanography Center that during this time the Primitive Equation (PE) model was run instead of the Navy Operational

Global Atmospheric Prediction System (NOGAPS). Since the PE model was hemispheric - not global - OTCM, when it received the data fields, only found the northern hemisphere with a boundary at the equator. Thus, for a low latitude systems like Ellis and Dot, OTCM generated a spurious vortex due to the lack of southern hemisphere fields. This caused the forecast guidance to fluctuate wildly and drive the system towards the equator. OTCM, subsequently, was modified to incorporate the latest southern hemisphere fields before running.

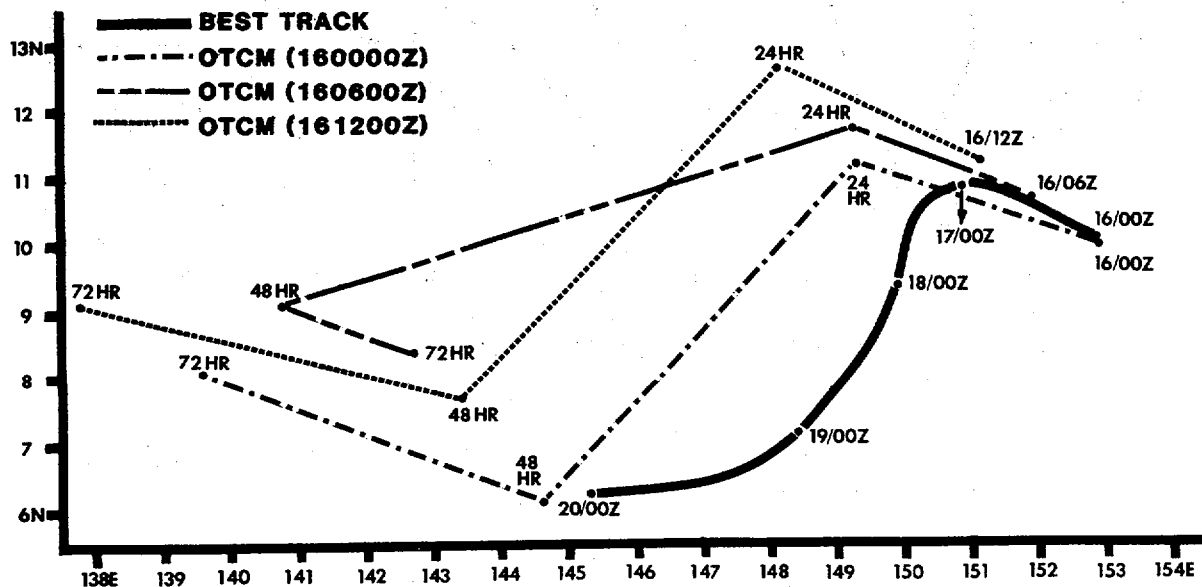


Figure 3-22-6. Comparison of the best track for Ellis with OTCM guidance for the period 160000Z through 161200Z October.

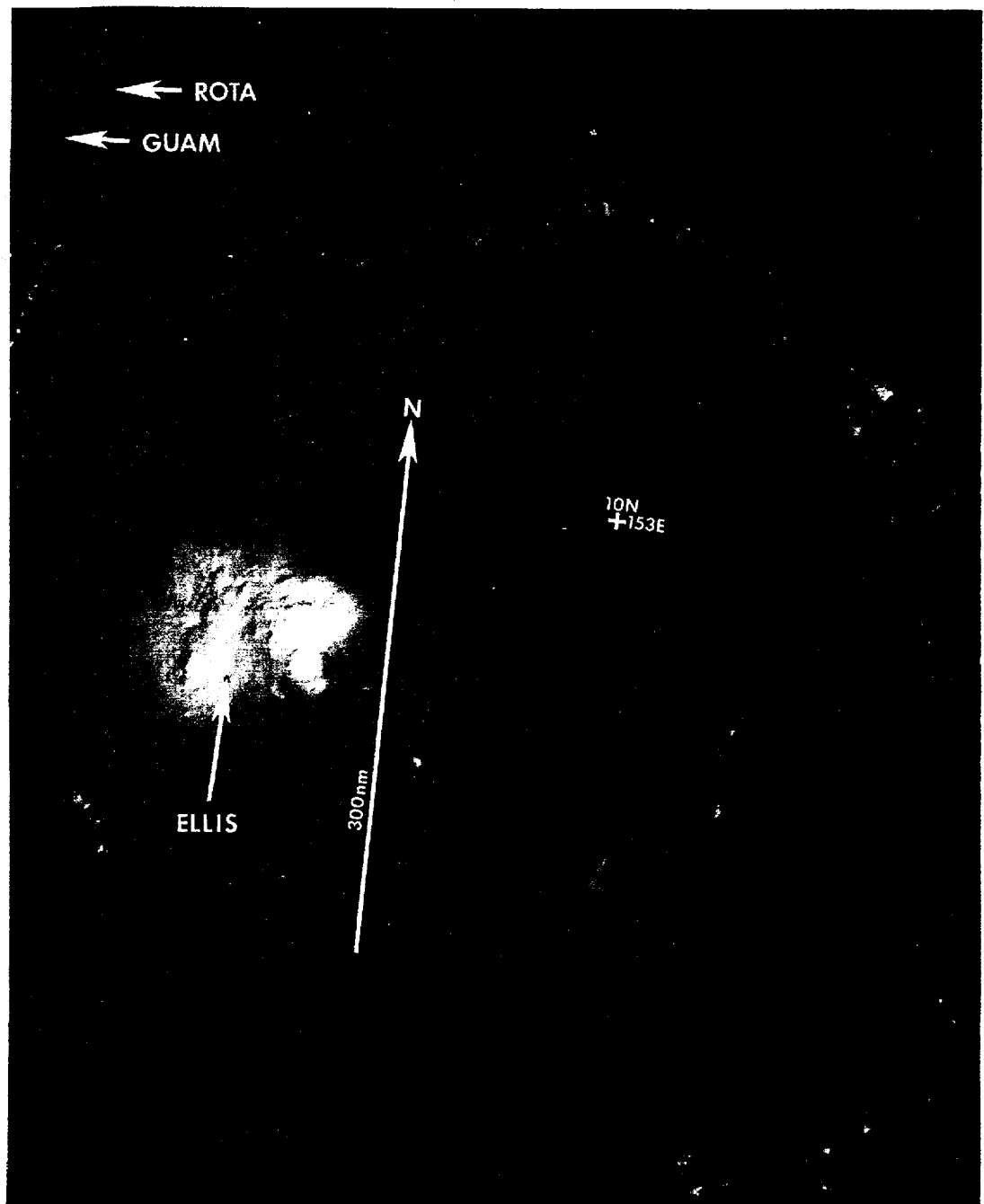


Figure 3-22-7. Tropical Storm Ellis 440 nm (815 km) south-southeast of Guam. Cirrus clouds define the outflow boundary in the eastern semicircle. Although Ellis is near the edge of the satellite imagery, the absence of cirrus in the western semicircle hints at the restricted outflow aloft due to the close proximity of the upper cold low further to the west (182325Z October DMSP visual imagery).

# TYPHOON FAYE

BEST TRACK TC-23W

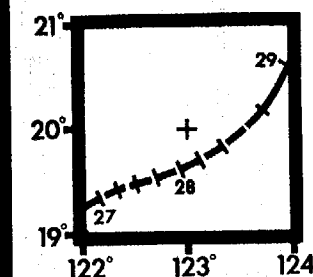
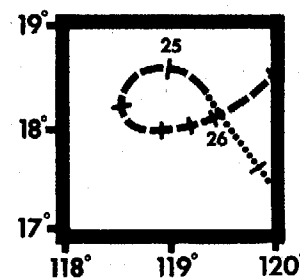
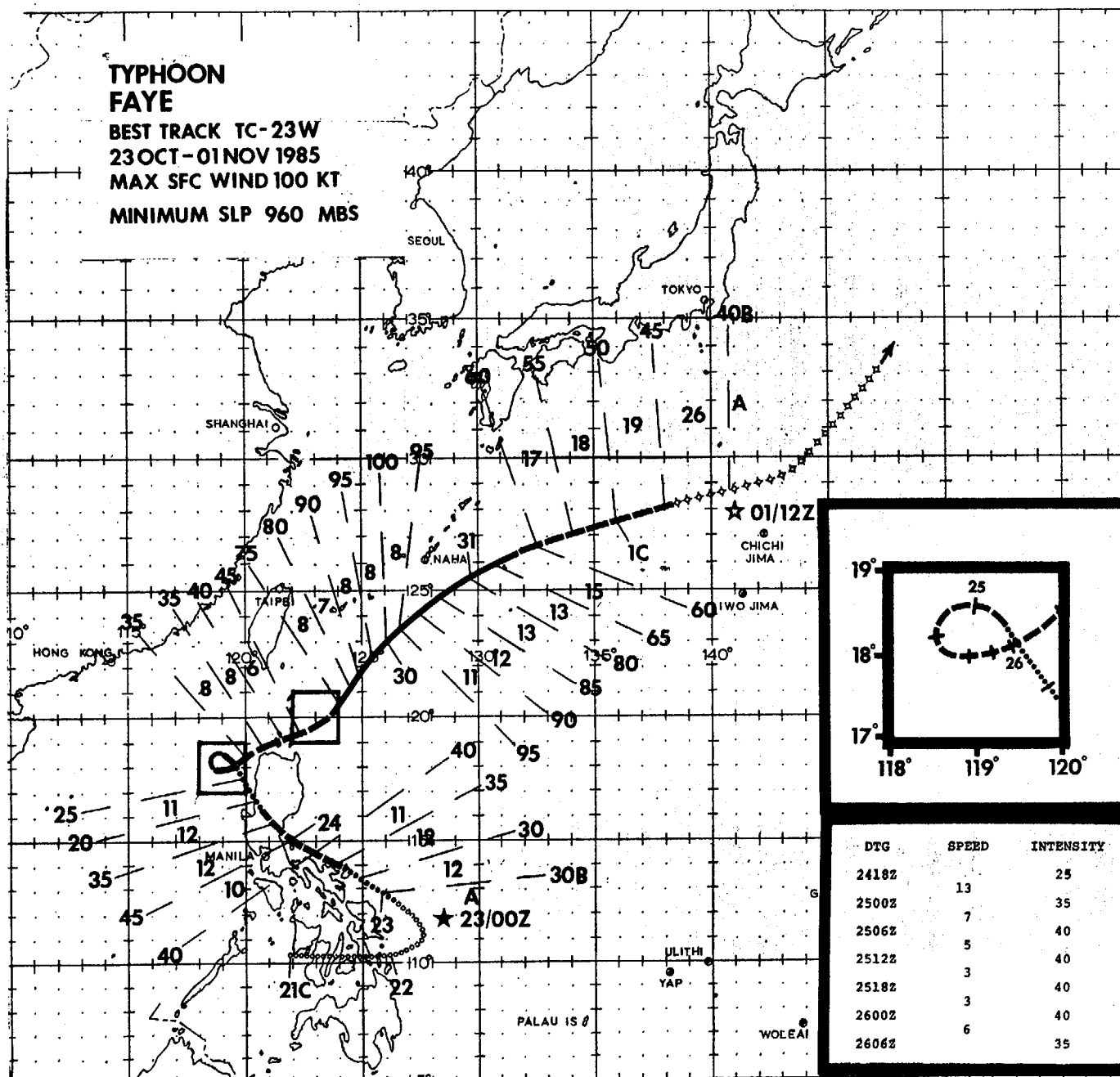
23 OCT - 01 NOV 1985

MAX SFC WIND 100 KT

MINIMUM SLP 960 MBS

## LEGEND

- 06 HOUR BEST TRACK POSIT
- A SPEED OF MOVEMENT
- B INTENSITY
- C POSITION AT XX/0000Z
- ... TROPICAL DISTURBANCE
- ... TROPICAL DEPRESSION
- TROPICAL STORM
- TYPHOON
- ◆ SUPER TYPHOON START
- ◇ SUPER TYPHOON END
- ◇◇ EXTRATROPICAL
- ... DISSIPATING STAGE
- ★ FIRST WARNING ISSUED
- ☆ LAST WARNING ISSUED



DTG	SPEED	INTENSITY
2418Z		25
2500Z	13	35
2506Z	7	40
2512Z	5	40
2518Z	3	40
2600Z	3	40
2606Z	6	35

DTG	SPEED	INTENSITY
2700Z		45
2706Z	2	50
2712Z	2	50
2718Z	2	50
2800Z	3	50
2806Z	4	55
2812Z	5	60
2818Z	5	65
2900Z		75

Faye was the last of four tropical cyclones to form in October, a month that normally accounts for five. Its formation was unusual because it was masked by two other tropical cyclones already in progress.

To set the stage, on 21 October Super Typhoon Dot was moving from the South China Sea into North Vietnam. The low-level southwesterly flow, that had been feeding into Dot, extended across the South China Sea into the Philippine Islands. A day later - with Dot over land and dissipating - a fresh outbreak of polar air from the northeast moved across the northern South China Sea and Philippines. The low-level convergence and cloudiness associated with the southwesterly monsoon flow persisted in the southern Philippine Islands - (this was the start of Faye). To the east in the Philippine Sea the remnants of Ellis were embedded in the western end of the near-equatorial trough. Ellis had been finalled at (200600Z). Although devoid of central cloudiness, it still retained some cyclonic vorticity. As the remnants of Ellis drifted west-northwestward, satellite imagery at 221200Z revealed a resurgence of its central convection. This renewed activity resulted in the issuance of two Tropical Cyclone Formation Alerts (TCFA) at 211200Z and 220300Z. The remains of Ellis, however, did not regenerate.

In conjunction with the continued interest in Ellis, an aircraft reconnaissance investigation mission was scheduled for the daylight hours on the 23rd of October. It located east-southeasterly winds at 10 kt (5 m/s) and a MSLP of 1009 mb associated with the TCFA area; however, as the flight continued to the west, it discovered 35 kt (18 m/s) winds and a MSLP of 1004 mb associated with another circulation. This prompted the first warning on Tropical Depression 23W at 230000Z. Up to this time there had been no mention of this new system in either the Significant Tropical Weather Advisory (ABPW PGTW) or the TCFA associated with Ellis. The tropical depression, once identified, moved northwestward under the subtropical ridge and slowly intensified. It reached tropical storm intensity at 231200Z. Later (240300Z), Tropical Storm Faye made landfall over central Luzon 60 nm (111 km) northeast of Manila (WMO 98429) with an intensity of 40 kt (21 m/s). Faye tracked to the northwest across Luzon in 9 hours and entered the South China Sea as a 20 kt (10 m/s) tropical depression some 130 nm (241 km) north-northwest of Manila. During the next 12-hours, Faye re-intensified over open water and moved on to the northwest. As a consequence of this northwesterly movement, Hong Kong (WMO 45005) went to Tropical Cyclone Condition of Readiness III at 250303Z.

Although, the system was forecast to move slowly to the northwest and intensify, the presence of a mid-latitude trough over mainland China changed that scenario. Faye was upgraded to tropical storm intensity late on the 24th and slowed further. Actually, satellite, radar and two aircraft reconnaissance fixes confirmed that the system completed a small cyclonic loop between 241800Z and 251800Z. Then Faye turned northeastward and accelerated through the Luzon Straits. Aircraft reconnaissance peripheral data between 262100Z and 270000Z showed the maximum surface winds to be in the northeastern semicircle. This was due to the increased pressure gradient between the low central pressure of Faye and the ridge to the northeast over Japan. For the next two days, after moving from the Straits, Faye slowed again, covering only 140 nm (259 km). The slowing trend was accompanied by intensification. Faye became a typhoon at 281800Z.

With Typhoon Faye approaching, Kadena AB on the island of Okinawa set Tropical Cyclone Condition of Readiness III (at 290900Z), and Condition II at 300310Z. During this period Typhoon Faye was at its maximum intensity of 100 kt (51 m/s) and beginning to accelerate to the northeast (see Figure 3-23-1). The closest point of approach to Kadena AB was 90 nm (167 km) to the southeast at 301900Z. Even though Faye's intensity at this time was 85 kt (44 m/s), the maximum observed winds at Kadena AB were only 18 kt (9 m/s).

After passing south of the island of Okinawa, Typhoon Faye continued to decrease in intensity due to the increased strength of the upper-level westerlies and the associated vertical wind shear. At 311200Z, 17 hours after its closest point of approach to Okinawa, Typhoon Faye was downgraded to a tropical storm. Faye continued accelerating to the east-northeast and transitioned to an extratropical low with an intensity of 45 kt (23 m/s) six hours before the final warning at 011200Z.

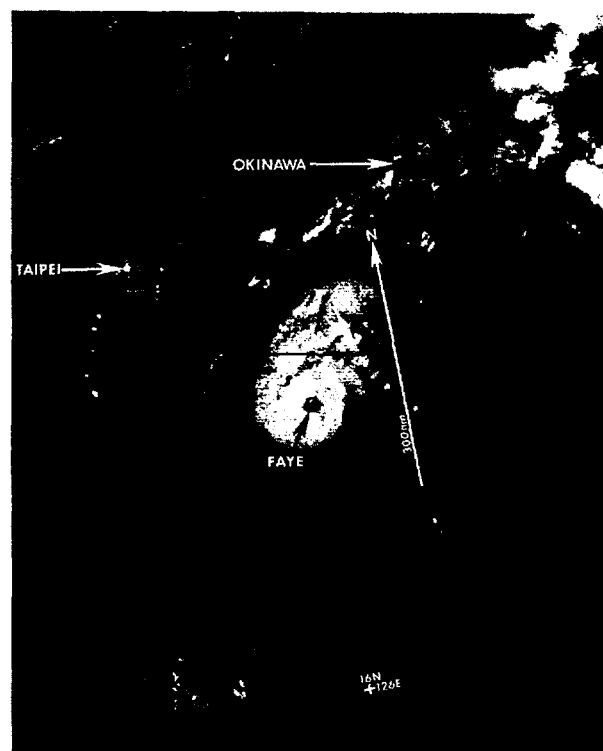


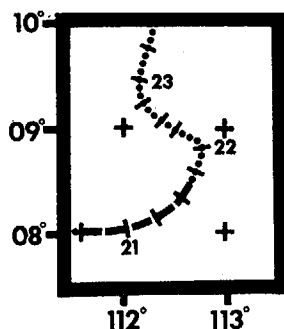
Figure 3-23-1. Nighttime moonlight imagery of Typhoon Faye one day after reaching typhoon intensity. Because this is a low-light-level image, the bright city lights along the west coast of the island of Taiwan can be seen to the west of the Tropical Cyclone [291346Z October DMSP visual imagery].



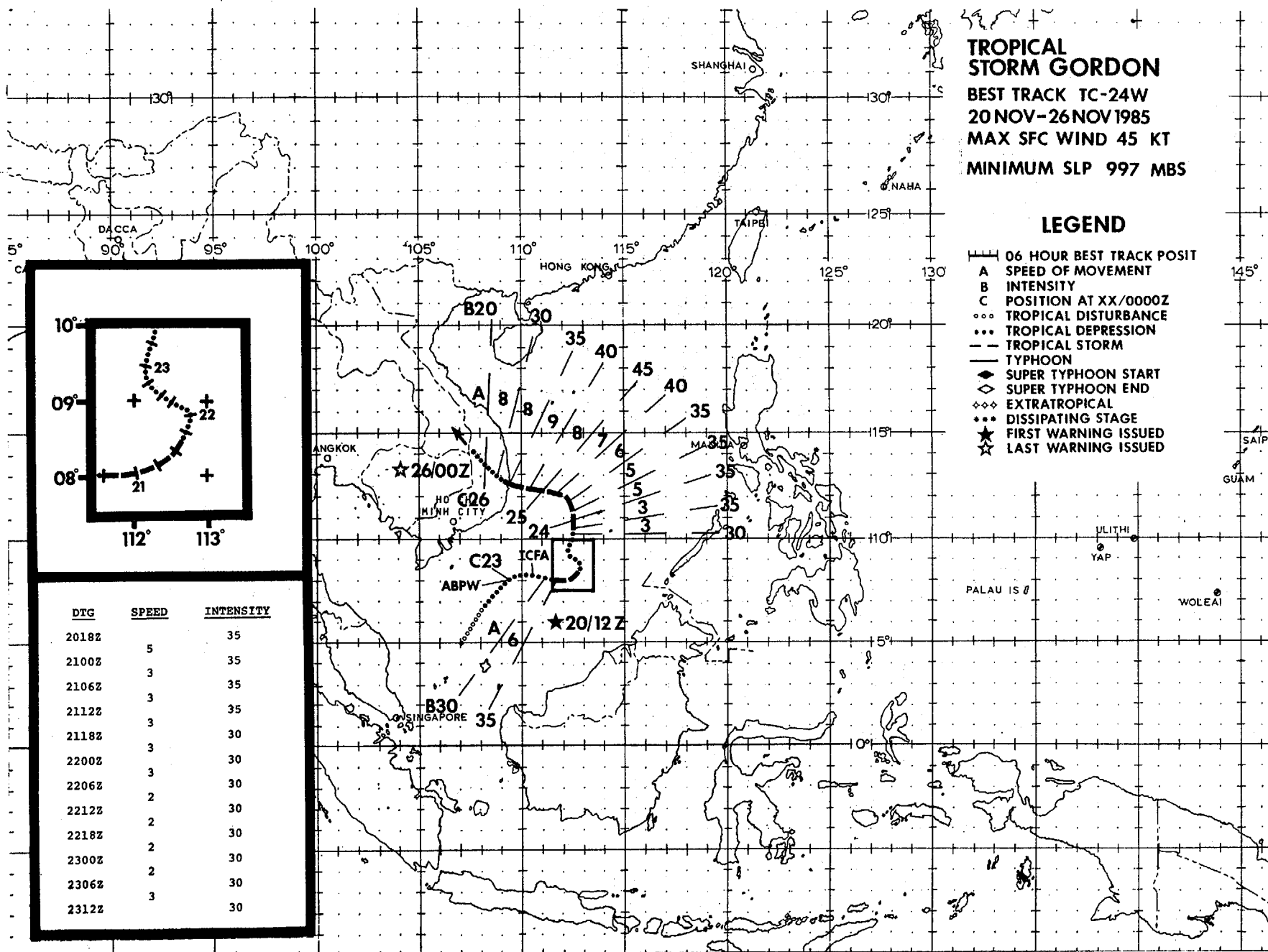
**TROPICAL  
STORM GORDON**  
BEST TRACK TC-24W  
20 NOV-26 NOV 1985  
MAX SFC WIND 45 KT  
MINIMUM SLP 997 MBS

**LEGEND**

- 06 HOUR BEST TRACK POSIT
- A SPEED OF MOVEMENT
- B INTENSITY
- C POSITION AT XX/0000Z
- ... TROPICAL DISTURBANCE
- ... TROPICAL DEPRESSION
- TROPICAL STORM
- TYPHOON
- ◆ SUPER TYPHOON START
- ◇ SUPER TYPHOON END
- ◇◇◇ EXTRATROPICAL
- ... DISSIPATING STAGE
- ★ FIRST WARNING ISSUED
- ★ LAST WARNING ISSUED



DTG	SPEED	INTENSITY
2018Z		35
2100Z	5	35
2106Z	3	35
2112Z	3	35
2118Z	3	30
2200Z	3	30
2206Z	3	30
2212Z	2	30
2218Z	2	30
2300Z	2	30
2306Z	2	30
2312Z	3	30



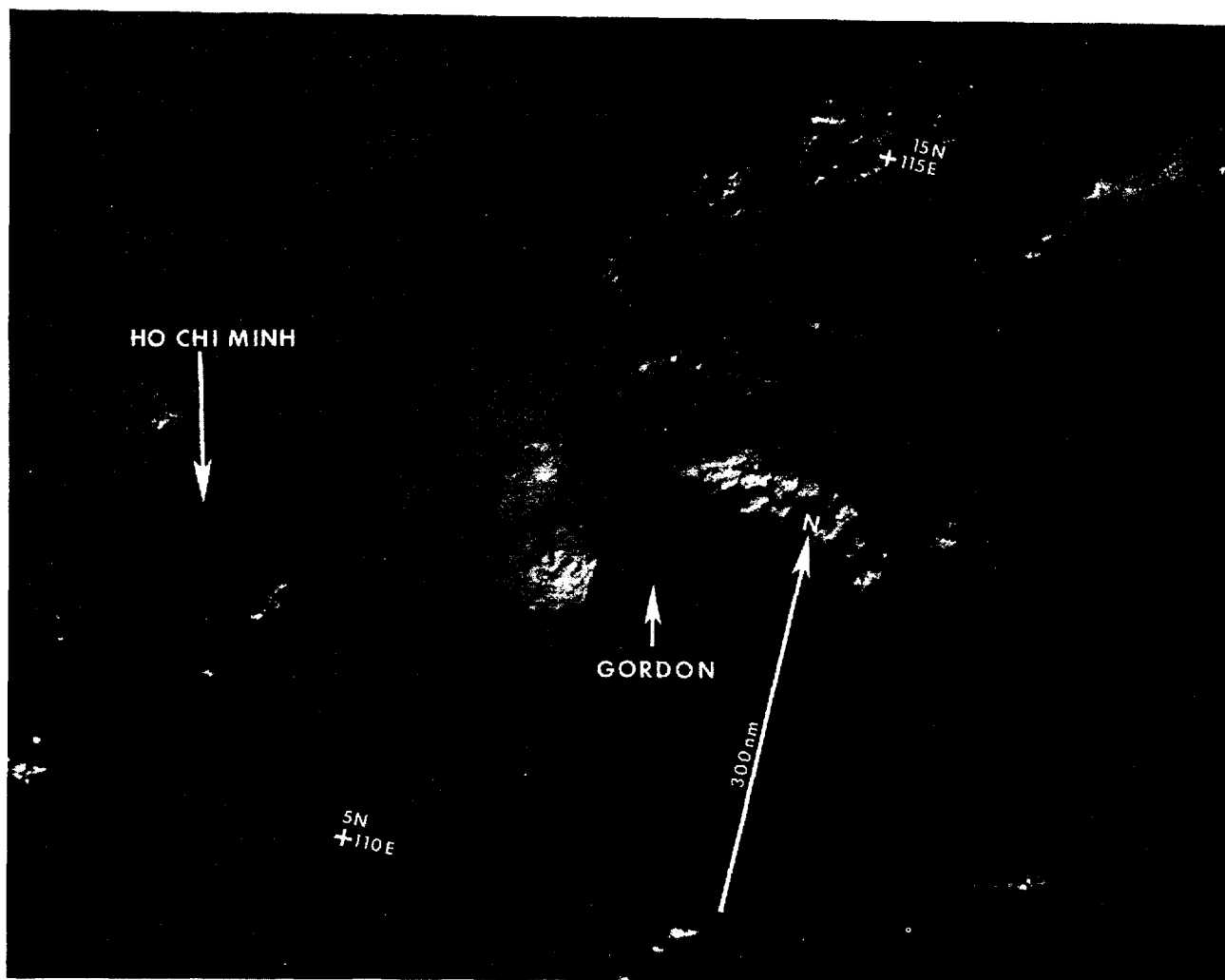



Figure 3-24-1. Tropical Storm Gordon, the only significant tropical cyclone to develop in WESTPAC during November, originated in the monsoon trough in the South China Sea. Gordon's initial intensification to a tropical storm on the 20th was coincident with a surge in the northeast monsoon which was present from late on the 19th until early on the 21st. However, by 220000Z the surge had weakened and so did Gordon. Subsequent redevelopment to tropical storm intensity on the 23rd and 24th appeared to be due to the system's development as a warm-core tropical cyclone. The USS Kitty Hawk (CV-63) Battle Group passed close to Gordon's center on the 23rd without sustaining any damage, and reported winds of 35-45 kt (18-23 m/s). Positioning the center of Tropical Storm Gordon was often difficult, particularly at night. The low-level circulation center was often several degrees away from the strongest convection, and although frequently exposed, consisted of only low-level cloudiness, which was difficult to resolve on infrared satellite imagery. The most intense convection was usually observed northwest of the low-level circulation center, as shown in the (above) imagery (230228Z November DMSP visual imagery).

BEST TRACK TC-25W  
17 DEC-24 DEC 85  
MAX SFC WIND 100 KT  
MINIMUM SLP 948 MBS

## LEGEND

-  06 HOUR BEST TRACK POSIT  
**A** SPEED OF MOVEMENT  
**B** INTENSITY  
**C** POSITION AT XX/0000Z  
 .. TROPICAL DISTURBANCE  
 ... TROPICAL DEPRESSION  
 --- TROPICAL STORM  
 ——— TYphoon  
 ◆ SUPER TYphoon START  
 ◇ SUPER TYphoon END  
 ◆◆ EXTRATROPICAL  
 ... DISSIPATING STAGE  
 ★ FIRST WARNING ISSUED  
 ☆ LAST WARNING ISSUED

# TYPHOON HOPE (25W)

Hope was a late-season typhoon that originated at low-latitude in the near-equatorial trough. It was aided in its initial development by the presence of enhanced low-level northeast monsoon flow and an associated shear zone. Typhoon Hope presented forecast problems at two different times: first at the crucial turning point from a westward to a northward track; and after recurvature when extratropical transition was imminent.

After Tropical Storm Gordon dissipated over Vietnam on the 25th of November, a winter weather pattern dominated the northwest Pacific area. Convective activity was confined to low latitudes in the near-equatorial trough. The disturbance, that was to become Typhoon Hope, was detected on the 13th of December between Truk and Pohnpei. The disturbance moved in a general westerly direction for the next three days and showed signs of slow intensification. Figure 3-25-1 shows Hope as a tropical depression located approximately 90 nm (167 km) east of Yap. By 171800Z, satellite data indicated the disturbance had further intensified while moving west-northwestward

aided by the effect of the shear zone to the north. As a result, the initial warning was issued. Between 171800Z and 191200Z December, Hope moved northwest before coming under the full steering influence of the mid-level subtropical ridge that caused the system to assume a westward track.

Tracking Hope during the period 191200Z-201200Z was facilitated by the availability of four aircraft fixes and several satellite eye fixes. Typhoon Hope reached its maximum intensity of 100 kt (52 m/s) at 200600Z (see Figure 3-25-2) just thirty hours after the initial warning. After that, Hope decreased slightly in intensity and maintained 65-75 kt (34-39 m/s) during the period 210600Z-231200Z.

After the 200300Z warning, the One-way Interactive Tropical Cyclone Model (OTCM) showed definite indications of a recurvature type track, whereas before it had indicated a generally north-westward track. The OTCM is the primary forecasting aid. The Nested Tropical Cyclone Model (NTCM) did not show signs of recurvature, but did indicate a

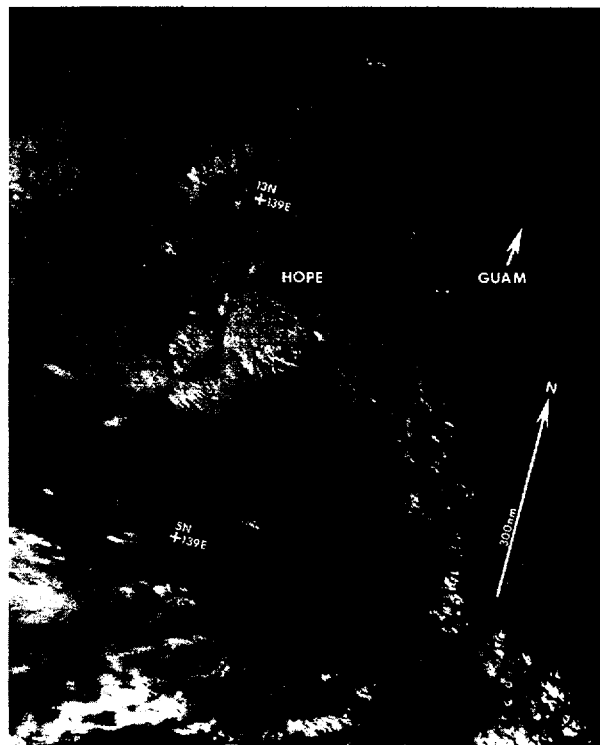


Figure 3-25-1. Hope as a tropical depression approximately 90 nm (167 km) east of Yap (WMO 91413). The shear zone to the north apparently aided Hope's development by enhancing the low-level northeast flow (170441Z December NOAA visual imagery).

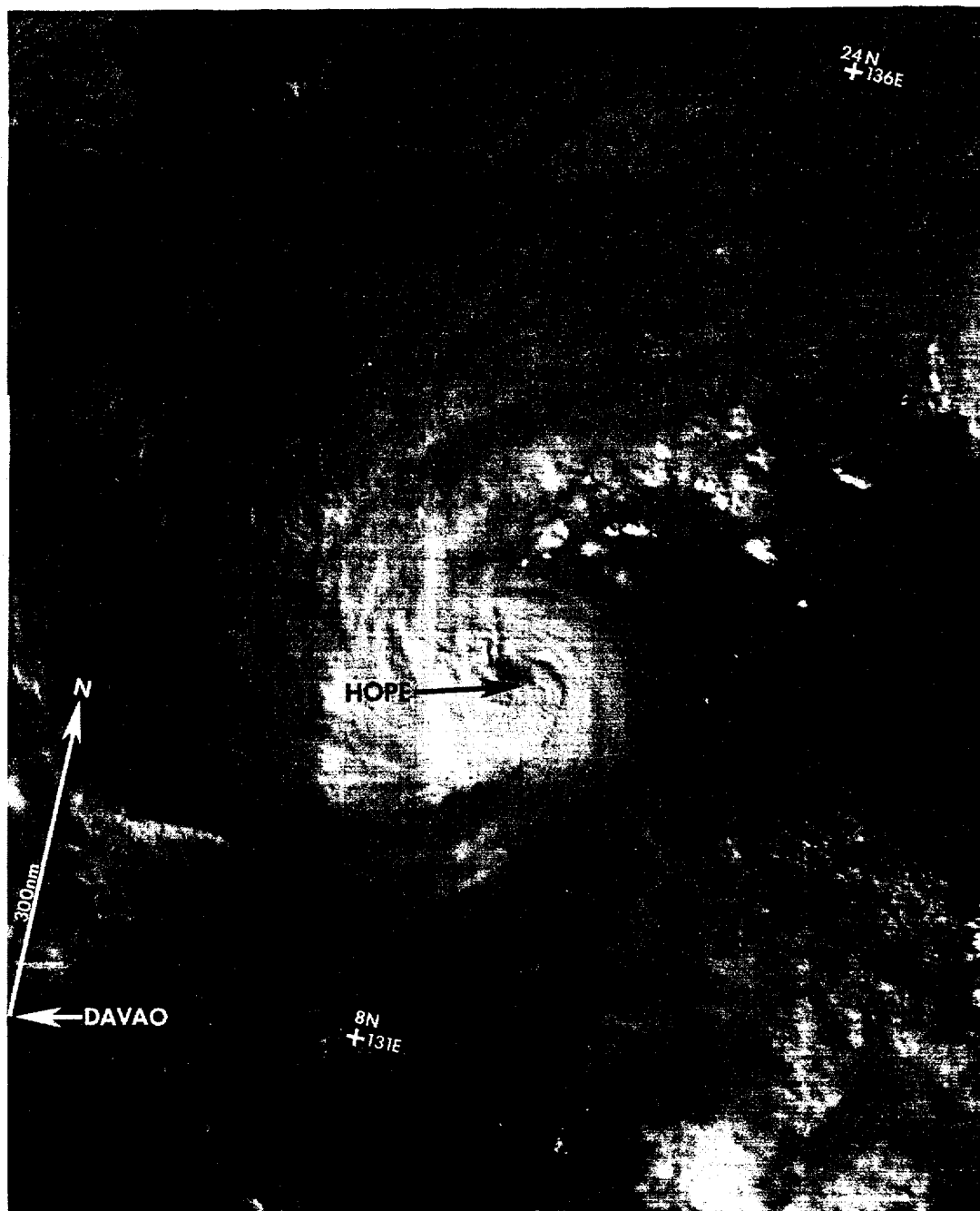


Figure 3-25-2. Typhoon Hope with a large ragged eye near time of maximum intensity (200551Z December NOAA visual imagery).

northerly track. As indicated in Figure 3-25-3, the OTCM yielded good forecast guidance during the period 191800Z-201200Z and the NTCM (Figure 3-25-4) gave fairly good guidance during the period 191800Z-210000Z. OTCM indicated a northwestward track and recurvature to the north-northeast (Figure 3-25-3) after about 48 hours. NTCM indicated a track change from northwest to northward (Figure 3-25-4). This guidance was integrated into the 201500Z warning. The track made good synoptic sense since it could be interpreted as Typhoon Hope moving around the western periphery of the mid-level subtropical ridge. The forecasts held with a curving track that started toward the west-northwest, turned north, and became northeast at about the 48 hour point.

After 201200Z December, a sequence of events started that caused major track forecast problems. As has been pointed out earlier, after 201200Z Typhoon Hope began to weaken slightly and the eye structure disappeared from satellite imagery. This resulted in doubts about the exact location of the

surface center of the typhoon. At 210842Z, a 31 hour period began during which no aircraft fixes were made on Typhoon Hope due to aircraft non-availability and maintenance problems. Under normal conditions, four aircraft fixes would have been made during that time period. Aircraft positioning of typhoons is the most accurate method available and is especially important at major track changes.

After 210000Z, the OTCM guidance stopped the recurvature scenario and started showing just a general northwest movement (Figure 3-25-5). It indicated a more westward direction with each run of the model. NTCM also indicated a northward track until 210000Z. After that time, it went to a straight westward track (Figure 3-25-6). This erroneous guidance (ie. the westward track) reflected OTCM and NTCM's inability to forecast in a winter synoptic situation. With specific reference to the model, strong middle-to-upper level westerlies apparently caused an early termination of the model run, or (as in this case) misleading guidance.

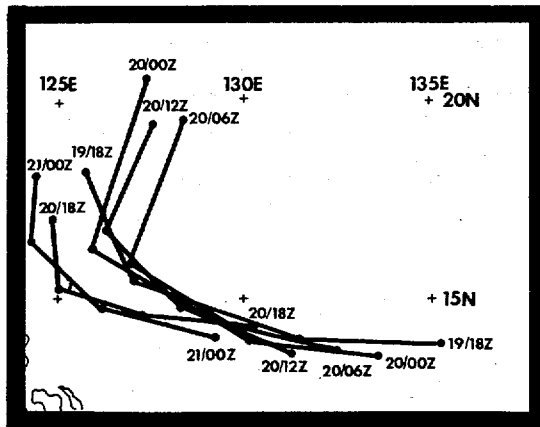


Figure 3-25-3. One-way interactive Tropical Cyclone Model (OTCM) forecast tracks for the period 191800Z-210000Z December showing a recurvature track.

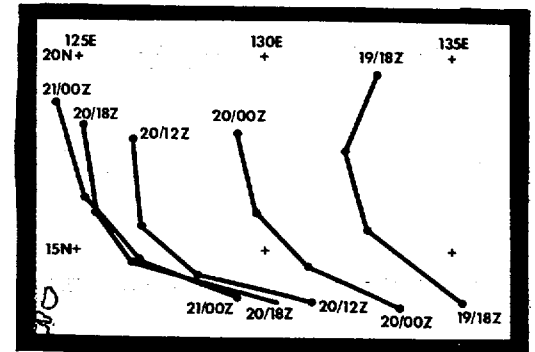


Figure 3-25-4. Nested Tropical Cyclone Model (NTCM) forecast tracks for the period 191800Z-210000Z December showing fairly good forecast track guidance in the form of tracks with northward movement.

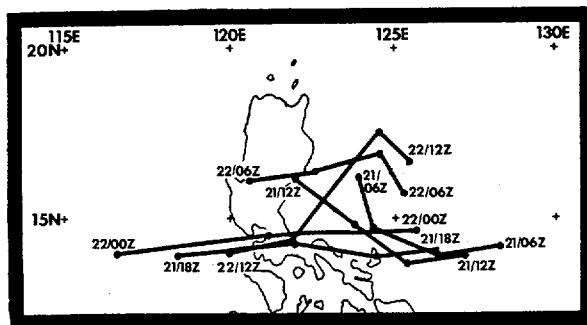
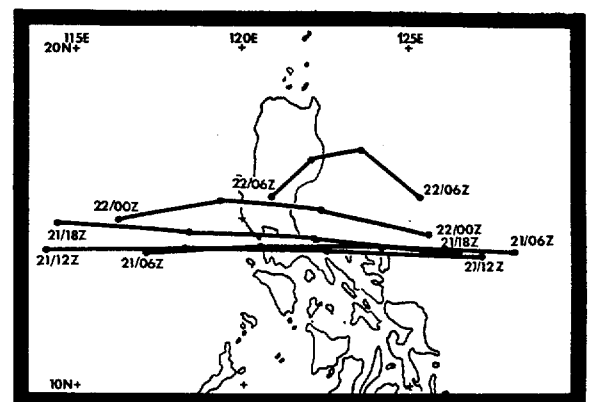


Figure 3-25-5. One-way interactive Tropical Cyclone Model (OTCM) forecast tracks for the period 210600Z-221200Z December. The forecast guidance indicates that the recurvature track is changed to westerly with time.

Figure 3-25-6. Nested Tropical Cyclone Model (NTCM) forecast guidance for the period 210600Z-220600Z December showing the swing to an almost straight westward track.



The final factor leading up to the forecast problem was Hope's continued west-northwestward movement and decreasing distance from Luzon. There was a definite need to warn of Hope's approach if there was a possibility that it was going to continue moving west-northwest and not recurve.

The combination of these events presented a dilemma for the typhoon forecaster, who had to issue the 220300Z warning. Hope was close to the critical track turning point. It was either going to continue moving west-northwest and make landfall on the east coast of Luzon, or start moving northward and recurve as had been forecast for the past 36 hours. The forecaster was presented with the following facts: (1) Hope's position was known within an estimated accuracy of 60 nm (111 km) based on poorly defined infrared satellite fixes (no satellite eye fixes or aircraft fixes being available); (2) Hope appeared to be continuing on a west-northwest track; (3) the numerical forecast models were indicating a straight westward track and had not indicated recurvature for about 24 hours; and (4) there was a definite need to warn Department of Defense interests on Luzon of Hope's approach. After carefully considering the combined effect of these factors, the forecaster decided to significantly change the forecast philosophy and forecast Typhoon Hope to track west-northwest across Luzon into the South China Sea.

During the next six hours; however, satellite fixes indicated that Typhoon Hope was moving toward

the north. A quick recovery was made on the 220900Z warning when the forecast track was switched back to one reflecting northward movement, followed by recurvature to the northeast, and decreasing intensity as extratropical transition occurred. The warnings over the next two days were accurate with a general concept of eastward movement with extratropical transition. The forecast tracks had Hope accelerating in speed and moving as far east-northeast as 27N 149E before completing extratropical transition.

In retrospect, an extratropical transition where the tropical cyclone is sheared away by upper-level westerlies and then dissipates below 20N would have been a more representative forecast for the final two days. Climatologically, this is what one would expect to happen in late December. In the case of Typhoon Hope, the 400mb trough with moderate westerlies over southern China was super-imposed over moderate-to-strong anticyclonic flow and cold air advection at the 925 mb level. These features are depicted in Figures 3-25-7 and 3-25-8. Based on these patterns, a shearing type of extratropical transition (followed by a dramatic decrease in the system's associated wind speeds) with no significant eastward acceleration is to be expected. Shearing, decreased wind speeds, and no significant eastward acceleration is exactly what happened after 240000Z. Figure 3-25-9 shows the remnants of Hope. There were no reported deaths, injuries, or property damage attributed to this late-season typhoon.

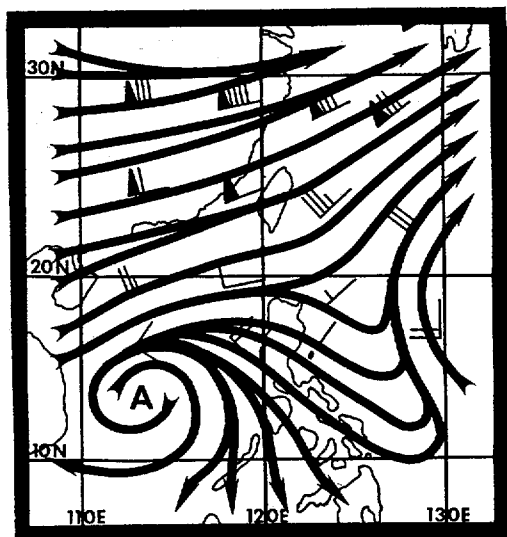


Figure 3-25-7. 400 mb Numerical Variational Analysis (NVA) at 220000Z December indicates a trough extends from near 60N 130E to 22N 107E with moderate westerlies north of Hope.

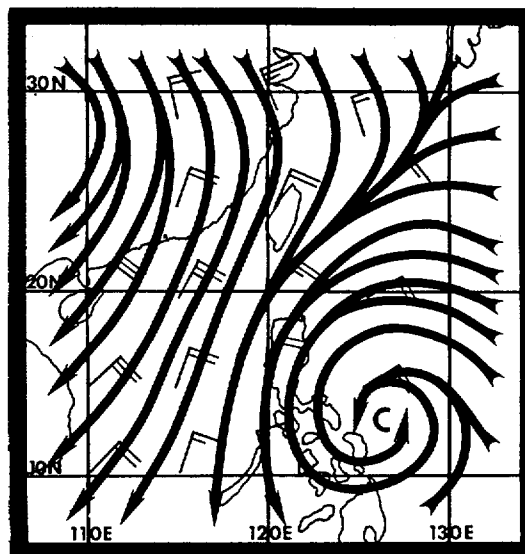


Figure 3-25-8. 925 mb NVA analysis at 220000Z showing moderate-to-strong anticyclonic flow and cold air advection over southern China.

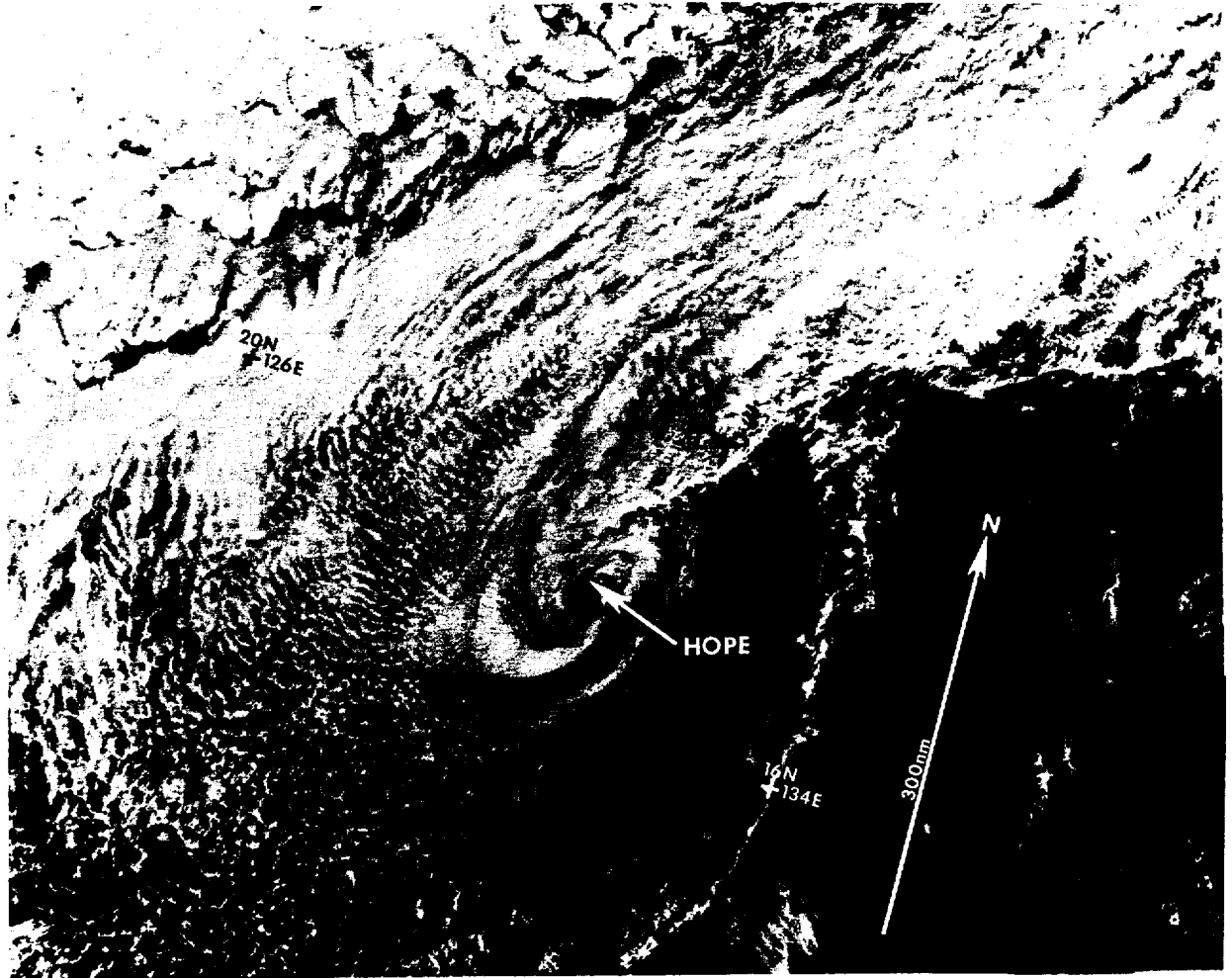


Figure 3-25-9. Typhoon Hope dissipating after having the central convection sheared away by mid- to upper level westerlies (240042Z December DMSP visual imagery).



# TROPICAL STORM IRVING

BEST TRACK TC-26W

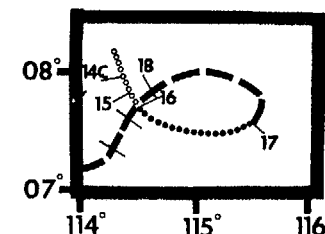
18 DEC-21 DEC 1985

MAX SFC WIND 60KT

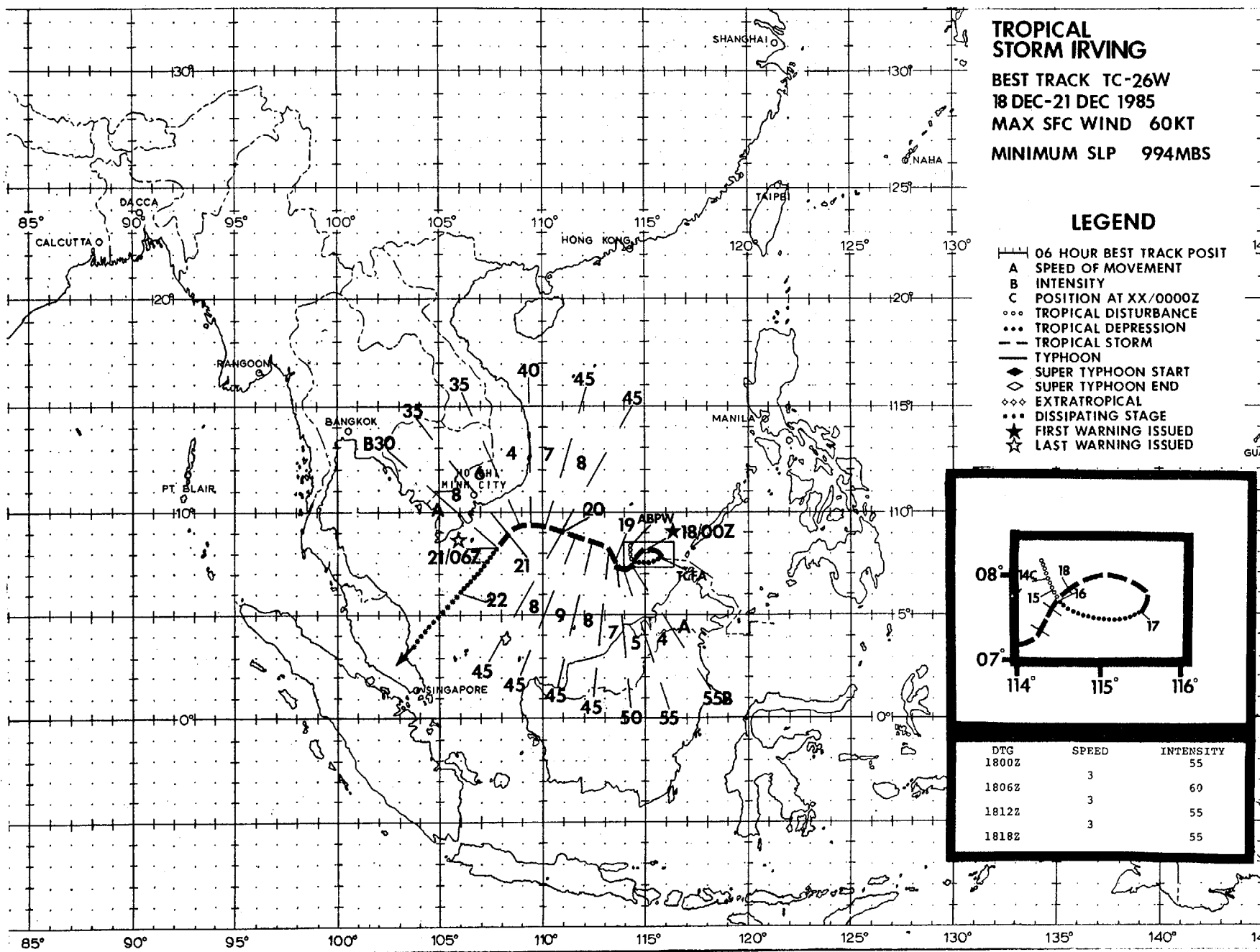
MINIMUM SLP 994MBS

## LEGEND

- 06 HOUR BEST TRACK POSIT
- A SPEED OF MOVEMENT
- B INTENSITY
- C POSITION AT XX/0000Z
- ... TROPICAL DISTURBANCE
- ... TROPICAL DEPRESSION
- TROPICAL STORM
- TYPHOON
- ◆ SUPER TYPHOON START
- ◇ SUPER TYPHOON END
- ◇◇ EXTRATROPICAL
- ... DISSIPATING STAGE
- ★ FIRST WARNING ISSUED
- ☆ LAST WARNING ISSUED



DTG	SPEED	INTENSITY
1800Z	3	55
1806Z	3	60
1812Z	3	55
1818Z	3	55



TROPICAL STORM IRVING (26W)

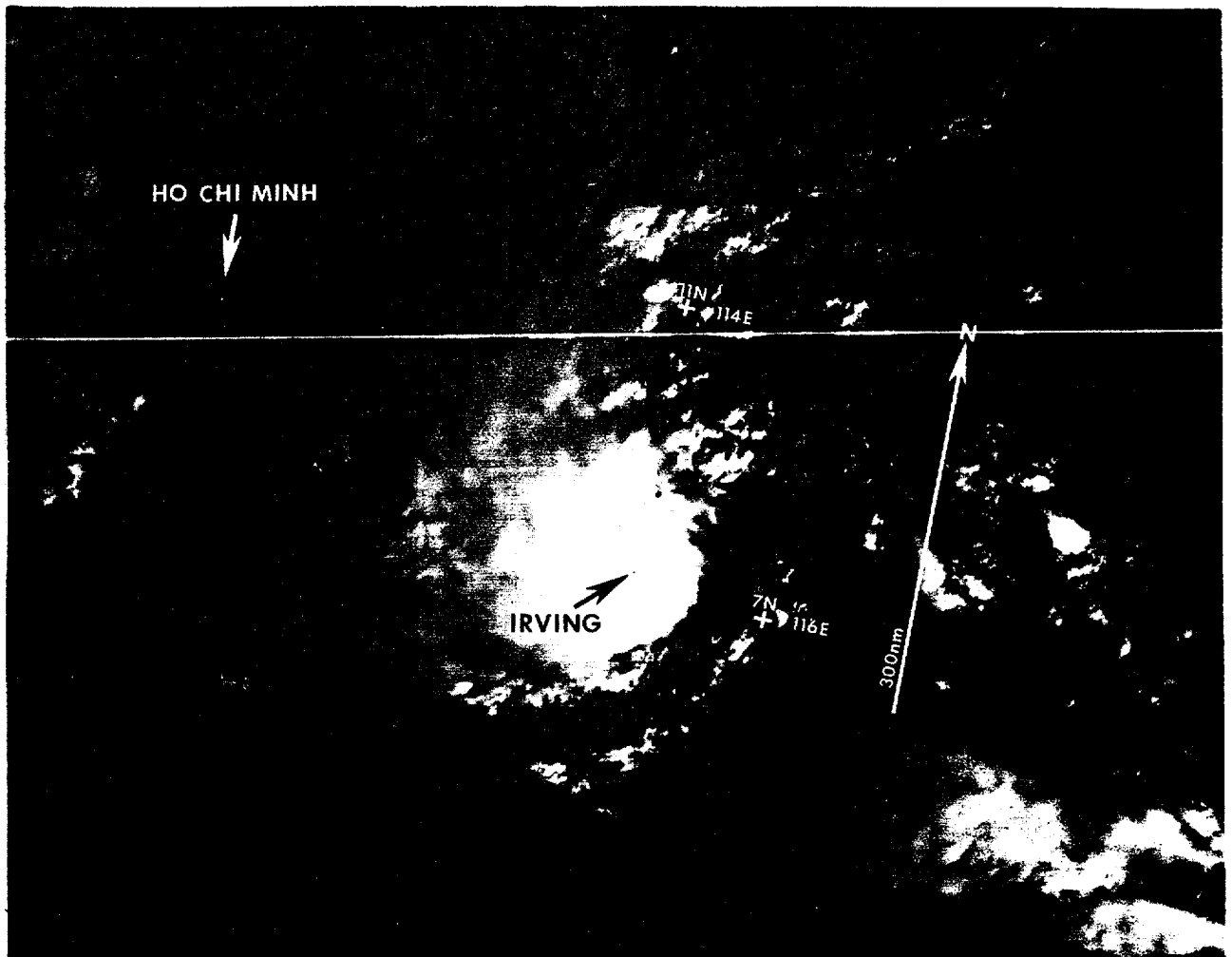


Figure 3-26-1. Tropical Storm Irving was one of two significant tropical cyclones to occur in the month of December. It formed at the western end of the low-latitude near-equatorial trough. The proximity of the low-level northeast monsoon and associated winter gales in the South China Sea masked Irving's initial development. Aircraft reconnaissance proved instrumental in locating the low-level circulation center and describing the wind field of this off-season tropical cyclone. Irving's central dense overcast and low-level cumulus spirals are visible in the (above) satellite imagery (190224Z December DMSP visual imagery).

### 3. NORTH INDIAN OCEAN TROPICAL CYCLONES

Tropical cyclone activity in the North Indian Ocean was above normal. Six significant tropical cyclones, all of tropical storm intensity, developed as compared to the climatological mean of four. These systems occurred in the spring and fall trans-

ition season, which normally encompasses the peak of the activity. Tables 3-6 through 3-8 provide a summary of information for 1985 and comparison with earlier years.

TABLE 3-6.

1985 SIGNIFICANT TROPICAL CYCLONES

TROPICAL CYCLONE	PERIOD OF WARNING	CALENDAR DAYS OF WARNING	NUMBER OF WARNINGS ISSUED	MAXIMUM SURFACE WIND KT - (M/S)	ESTIMATED MSLP MB	BEST TRACK DISTANCE TRAVELED NM - (KM)
TC 01B	23MAY - 25MAY	3	8	60 (31)	979	515 (954)
TC 02A	29MAY - 31MAY	3	12	50 (26)	987	609 (1128)
TC 03B	9OCT - 11OCT	3	7	50 (26)	988	667 (1235)
TC 04B	15OCT - 16OCT	2	4	50 (26)	987	296 (548)
TC 05B	15NOV - 18NOV	4	12	55 (28)	983	843 (1561)
TC 06B	11DEC - 14DEC	4	11	50 (26)	987	1025 (1898)
1985 TOTALS:		19	54			

TABLE 3-7.

1985 SIGNIFICANT TROPICAL CYCLONES

NORTH  
INDIAN OCEAN

	JAN	FEB	MAR	APR	MAY	JUN	JUL	AUG	SEP	OCT	NOV	DEC	TOTAL
1985 TROPICAL CYCLONES	0	0	0	0	2	0	0	0	0	2	1	1	6
1975 - 1985 AVERAGE	.1	-	-	.1	.8	.4	-	.1	.3	1.1	1.4	.4	4.5
CASES	1	-	-	1	9	4	-	1	3	12	15	4	50

FORMATION ALERTS: 5 out of 8 Formation Alerts developed into significant tropical cyclones. Tropical Cyclone Formation Alerts were issued for all significant tropical cyclones, except one, that developed during 1985.

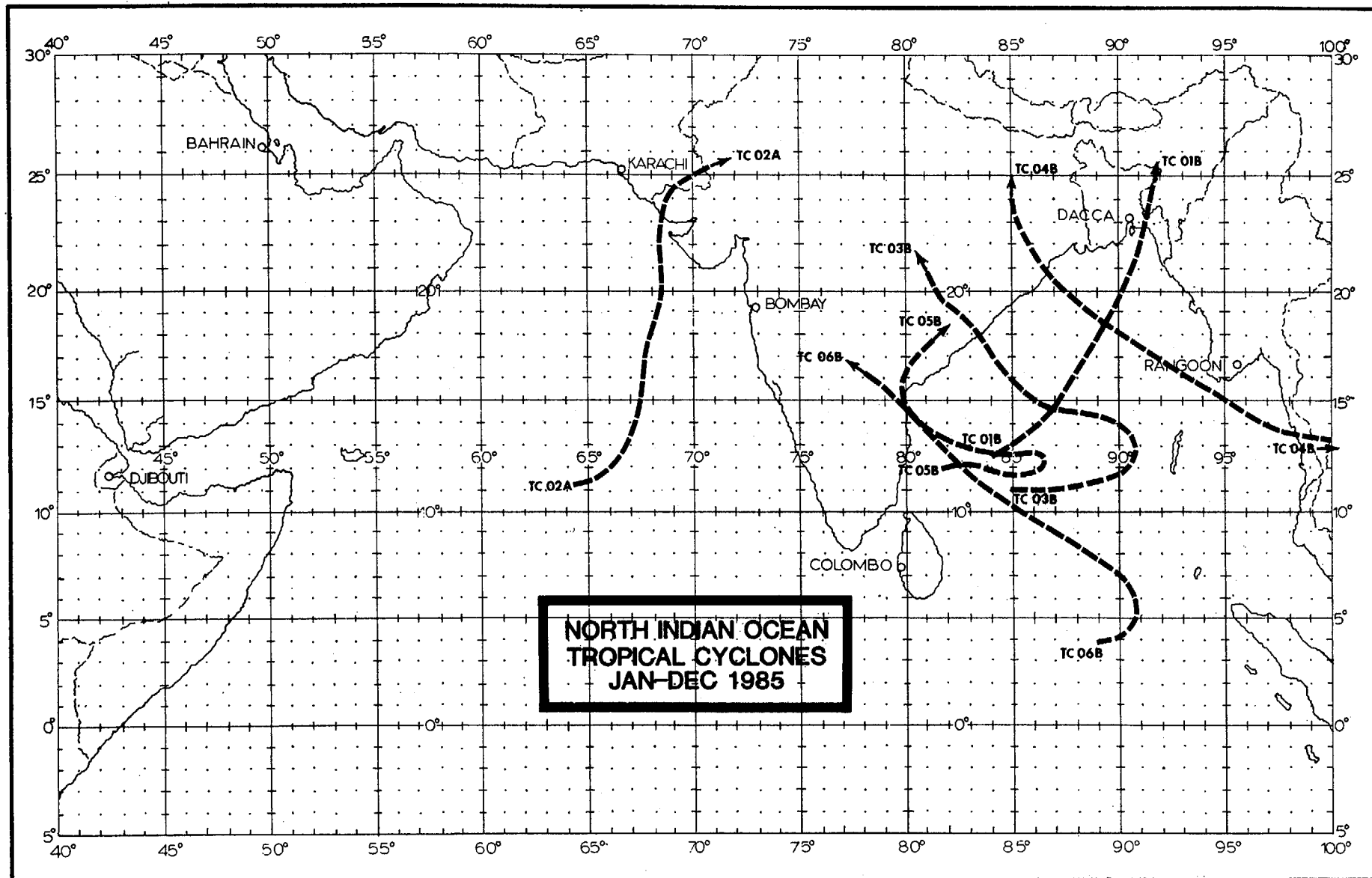
WARNINGS

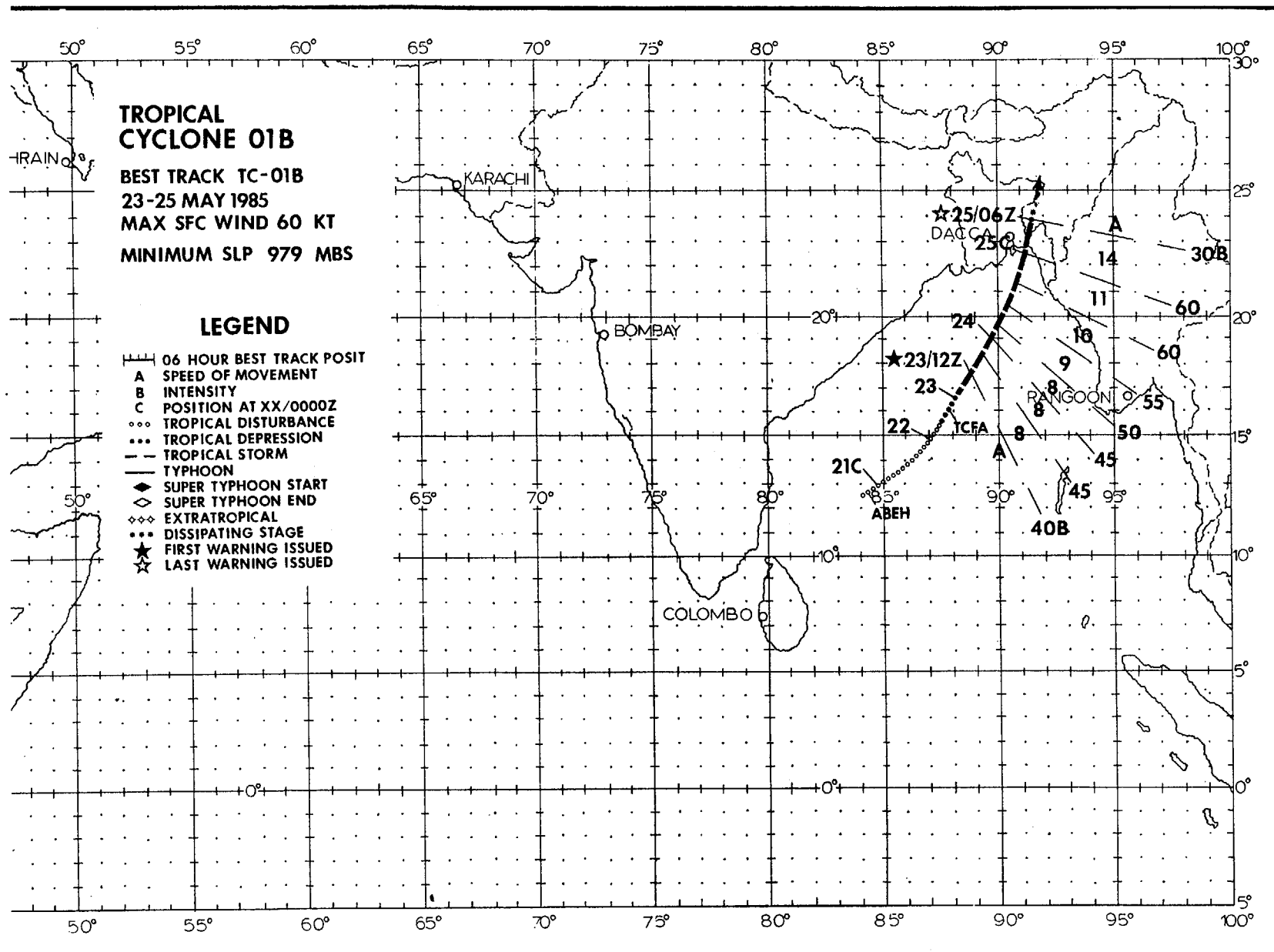
Number of warning days:	19
Number of warning days with two tropical cyclones in region:	0
Number of warning days with three or more tropical cyclones in region:	0

TABLE 3-8.

<u>YEAR</u>	<u>JAN</u>	<u>FEB</u>	<u>MAR</u>	<u>APR</u>	<u>MAY</u>	<u>JUN</u>	<u>JUL</u>	<u>AUG</u>	<u>SEP</u>	<u>OCT</u>	<u>NOV</u>	<u>DEC</u>	<u>TOTAL</u>
1971*	-	-	-	-	-	0	0	0	0	1	1	0	2
1972*	0	0	0	1	0	0	0	0	2	0	1	0	4
1973*	0	0	0	0	0	0	0	0	0	1	2	1	4
1974*	0	0	0	0	0	0	0	0	0	0	1	0	1
1975	1	0	0	0	2	0	0	0	0	1	2	0	6
1976	0	0	0	1	0	1	0	0	1	1	0	1	5
1977	0	0	0	0	1	1	0	0	0	1	2	0	5
1978	0	0	0	0	1	0	0	0	0	1	2	0	4
1979	0	0	0	0	1	1	0	0	2	1	2	0	7
1980	0	0	0	0	0	0	0	0	0	0	1	1	2
1981	0	0	0	0	0	0	0	0	0	1	1	1	3
1982	0	0	0	0	1	1	0	0	0	2	1	0	5
1983	0	0	0	0	0	0	0	1	0	1	1	0	3
1984	0	0	0	0	1	0	0	0	0	1	2	0	4
1985	0	0	0	0	2	0	0	0	0	2	1	1	6
<u>1975-1985</u>	<u>.1</u>	<u>-</u>	<u>-</u>	<u>.1</u>	<u>.8</u>	<u>.4</u>	<u>-</u>	<u>.1</u>	<u>.3</u>	<u>1.1</u>	<u>1.4</u>	<u>.4</u>	<u>4.5</u>
<u>AVERAGE</u>													
CASES	1	0	0	1	9	4	0	1	3	12	15	4	50

\* JTWC warning responsibility began on 4 June 1971 for the Bay of Bengal, east of 90E. As directed by USCINCPAC, JTWC issued warnings only for those tropical cyclones that developed or tracked through that portion of the Bay of Bengal. Commencing with the 1975 tropical cyclone season JTWC's area of responsibility was extended westward to include the western portion of the Bay of Bengal and the entire Arabian Sea.





# TROPICAL CYCLONE 01B

Tropical Cyclone 01B was the first of two cyclones to form in the North Indian Ocean during the Spring transition season. Although only reaching an intensity of 60 kt (31 m/s), it was one of the most noteworthy storms of 1985 due to the tremendous loss of life the cyclone caused in Bangladesh. An estimated 6,000 people died from the storm, with an additional 300,000 people left homeless. Most of the deaths were due to the storm surge, estimated at 15 ft (5 m), which completely inundated many of the low-lying islands (DeAngelis, 1985).

By late May, the Spring transition season was well underway in the North Indian Ocean. The southwest monsoon had moved into the southern Bay of Bengal and was creating a large amount of convection across the region. Late on the 20th of May, an area of convection began to show some organization in the southwest Bay of Bengal. This prompted the Signifi-

cant Tropical Weather Advisory (ABEH PGTW) to be reissued at 202030Z to include mention of this disturbance. During the following nine hours satellite imagery showed the disturbance continuing to improve in organization. As a result, the potential for significant tropical cyclone development was upgraded to "fair" on the 210600Z Significant Tropical Weather Advisory. Subsequent data continued to show slow development. An upper-level anticyclone was forming over the disturbance and a Dvorak analysis of satellite imagery estimated surface winds of 25 to 35 kt (13 to 18 m/s). This resulted in the issuance of a TCFA at 222100Z as the disturbance moved into the central Bay of Bengal.

Since the disturbance was developing in the monsoon trough (Figure 3-01B-1), there was some uncertainty as to whether a closed surface circ-

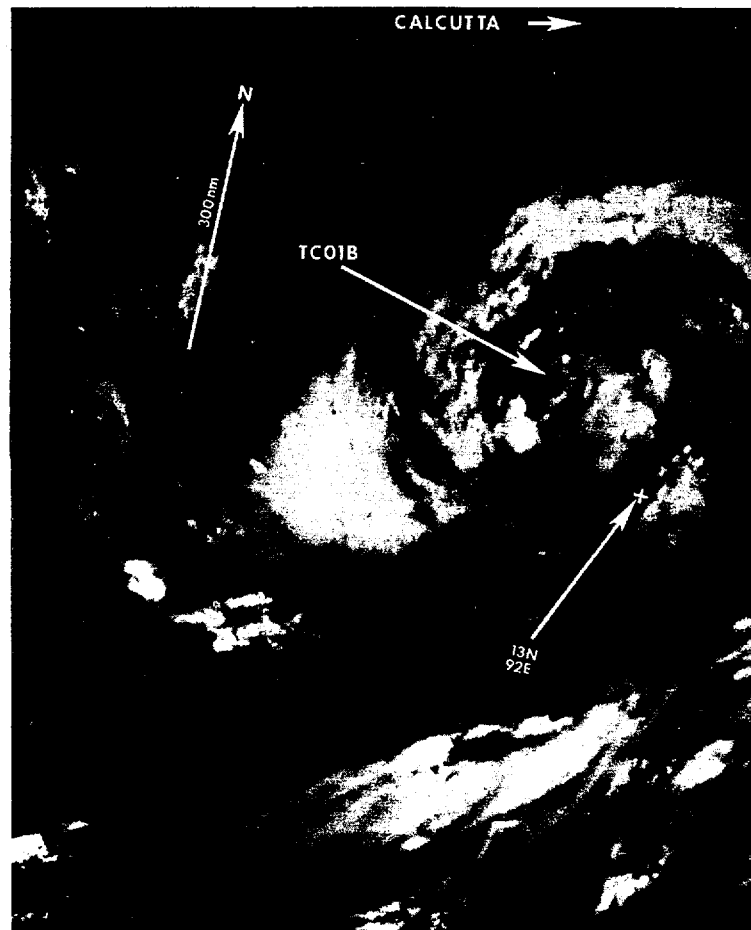


Figure 3-01B-1. The tropical disturbance, which became Tropical Cyclone 01B is consolidating in the Bay of Bengal. Estimated surface winds at this time are 25 kt (13 m/s) (220432Z May DMSP visual imagery).

lation existed or the disturbance was still a broad trough. Analysis performed by the Air Force Global Weather Center (AFGWC) on satellite imagery at 230442Z quickly settled the question by estimating surface winds of 45 kt (23 m/s), which supported a closed surface circulation. Based on this information, the first warning on Tropical Cyclone 01B was issued at 231200Z.

The forecast reasoning for Tropical Cyclone 01B centered on the presence of the monsoon trough. The initial forecast called for the storm to remain in the trough and move to the north-northeast. This forecast philosophy proved to be correct, and remained unchanged throughout the lifetime of Tropical Cyclone 01B. As a result, Bangladesh received nearly a 36 hour warning of the cyclones arrival. The only forecasting difficulty with Tropical Cyclone 01B was predicting its speed. Based on satellite fixes of the poorly defined circulation center from nighttime infrared imagery, the first three warnings indicated a slower forward speed than was actually taking place. This was corrected early on the 24th, when visual satellite imagery revealed the location of the low-level circulation center (Figure 3-01B-2).

Tropical Cyclone 01B continued to intensify, reaching a peak intensity of 60 kt (31 m/s) at 241800Z. This intensity was maintained until land-

fall at 250200Z just west of Chittagong, Bangladesh (WMO 41977). The cyclone lost organization fairly rapidly as it moved inland, but still brought torrential rains and extensive flooding to the higher elevations of Bangladesh and eastern India. The final warning was issued at 250600Z.

The fact that Bangladesh was given advance warning of the cyclones approach was responsible for the saving of thousands of lives. Tropical Cyclone 01B inflicted the greatest damage and death in the delta region of the Ganges. Several low-lying islands were completely submerged due to the 15 ft (5 m) storm surge which accompanied the storm at landfall. In several cases the only structures left standing were concrete multi-story shelters built after the 1970 cyclone (In November 1970, a tropical cyclone hit Bangladesh and killed an estimated 300,000 people). The islands of Sandwip, Urir Char and Bhola were among the most heavily damaged. Further inland, heavy rains caused severe flooding along Bangladesh's northeastern border with India. Overflowing rivers affected tens of thousands of people, with the Tripura and Manipur States of India being among the hardest hit regions.

Reference: DeAngelis, Dick, 1985: Under the Bangladesh Cyclone. Mariners Weather Log, Vol 29, No. 3, pp. 141-143.



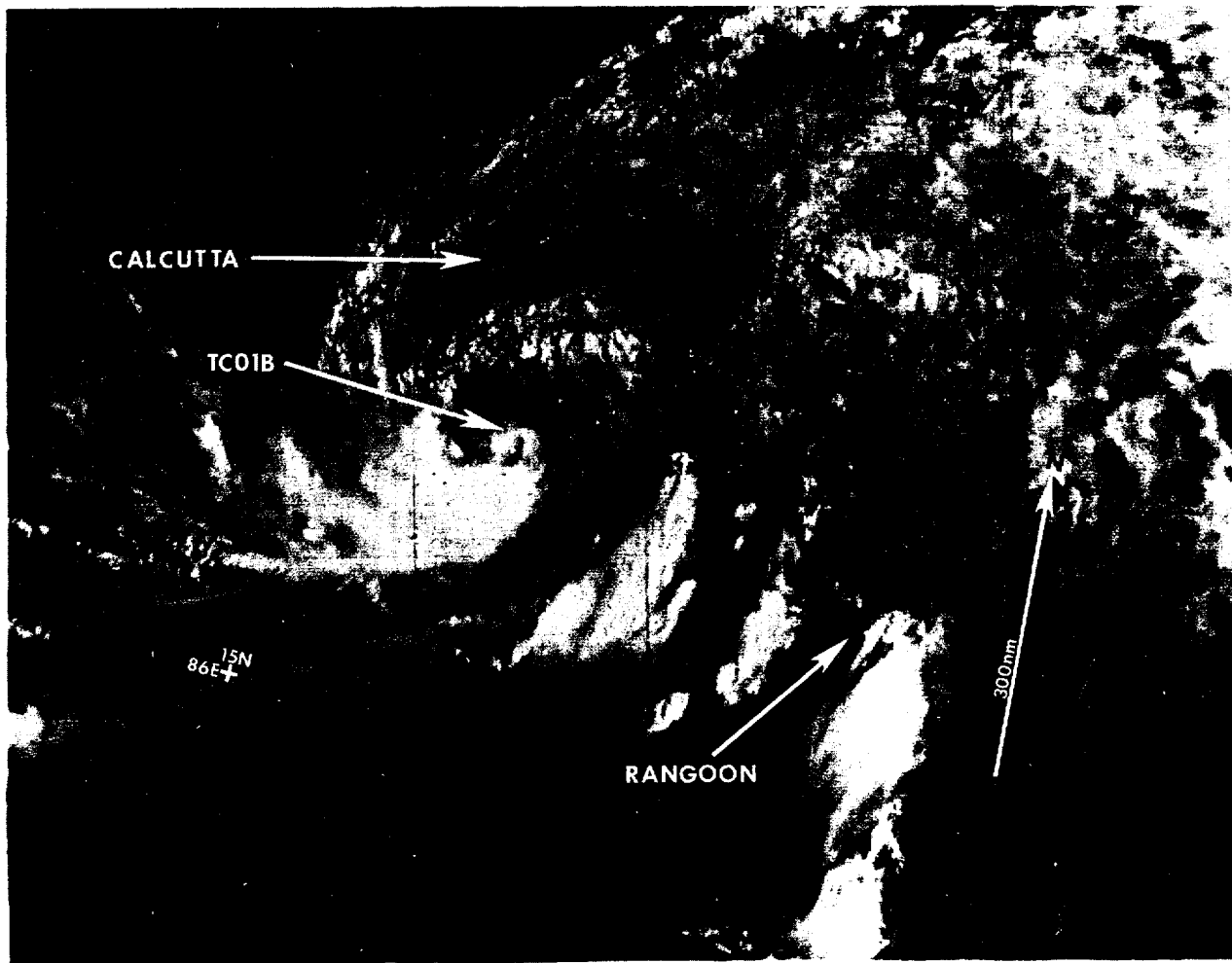
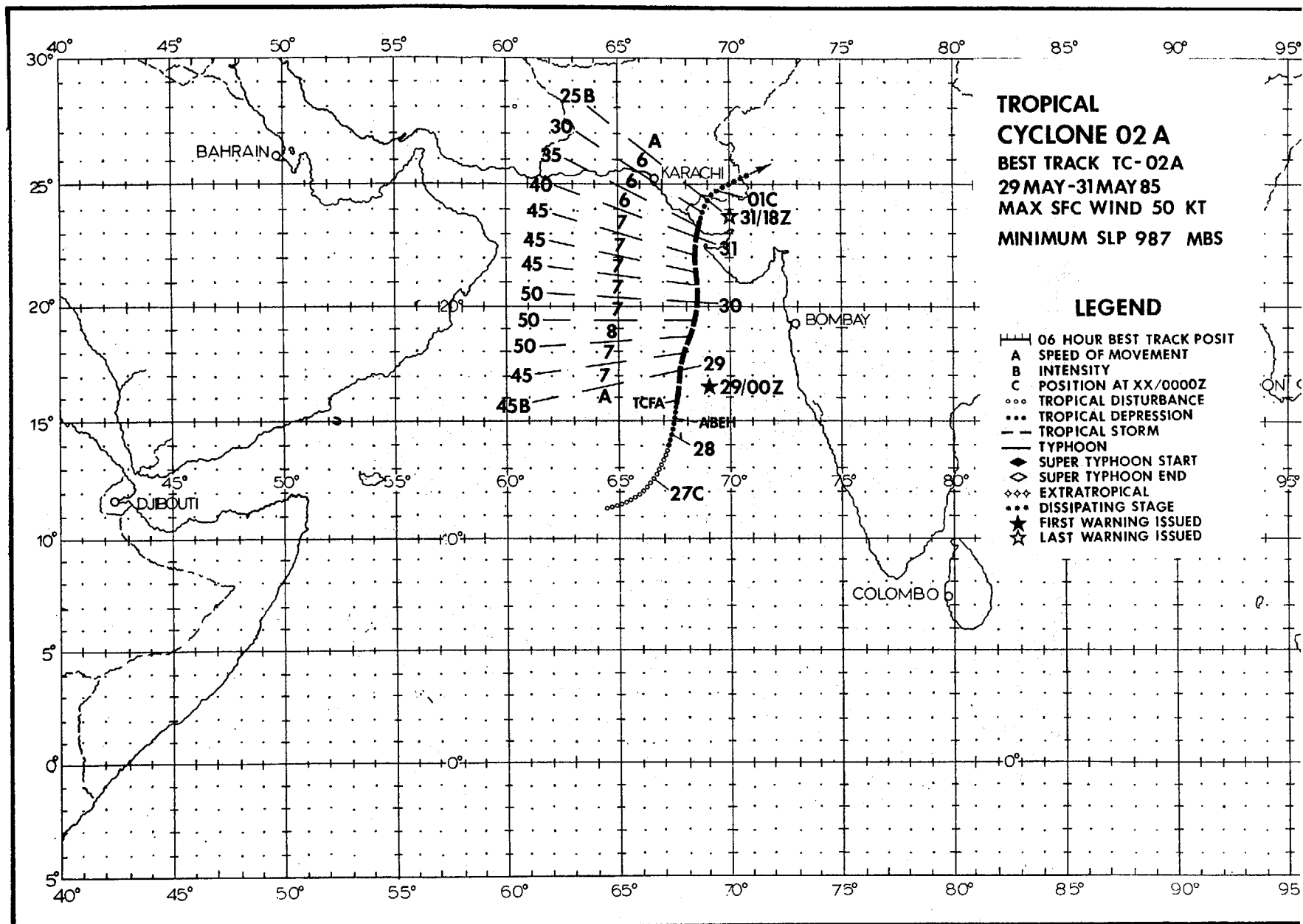


Figure 3-01B-2. Tropical Cyclone 01B less than one day prior to making landfall over Bangladesh (240351Z May DMSP Visual Imagery).



TROPICAL CYCLONE 02A

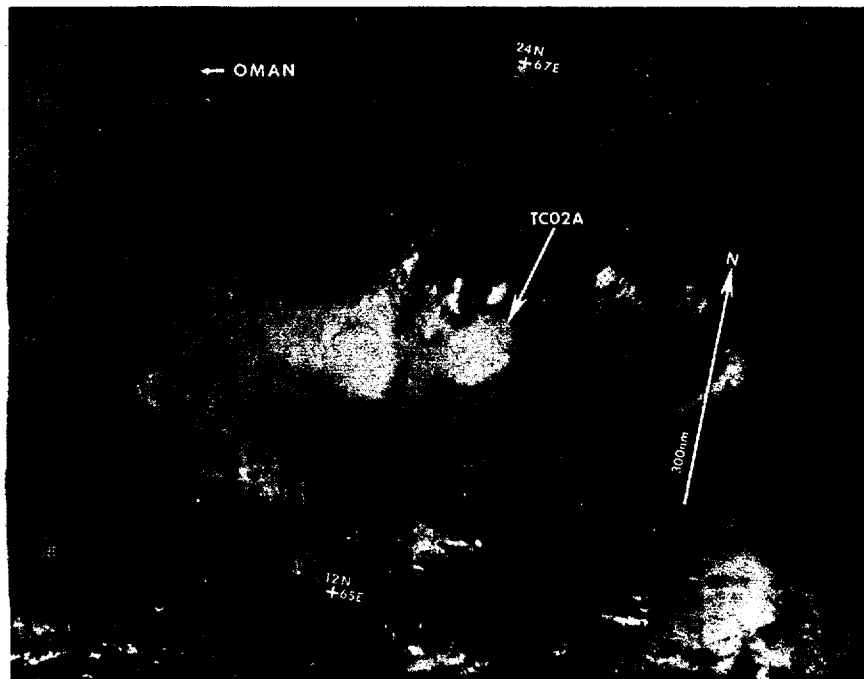


Figure 3-02A-1. Tropical Cyclone 02A near peak intensity. The low-level circulation center is just at the edge of the central cloud mass (290533Z May DMSP visual imagery).

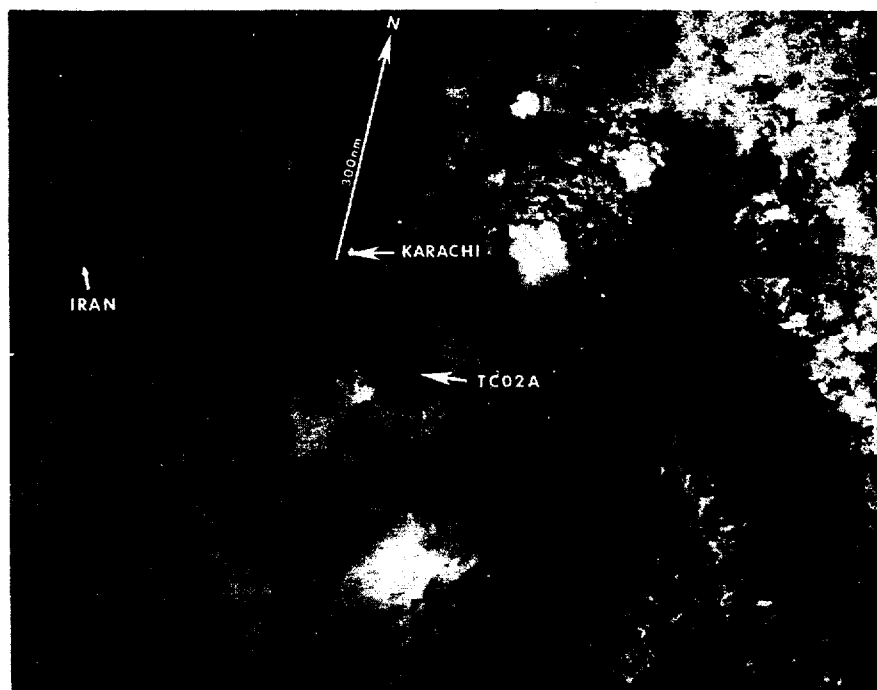
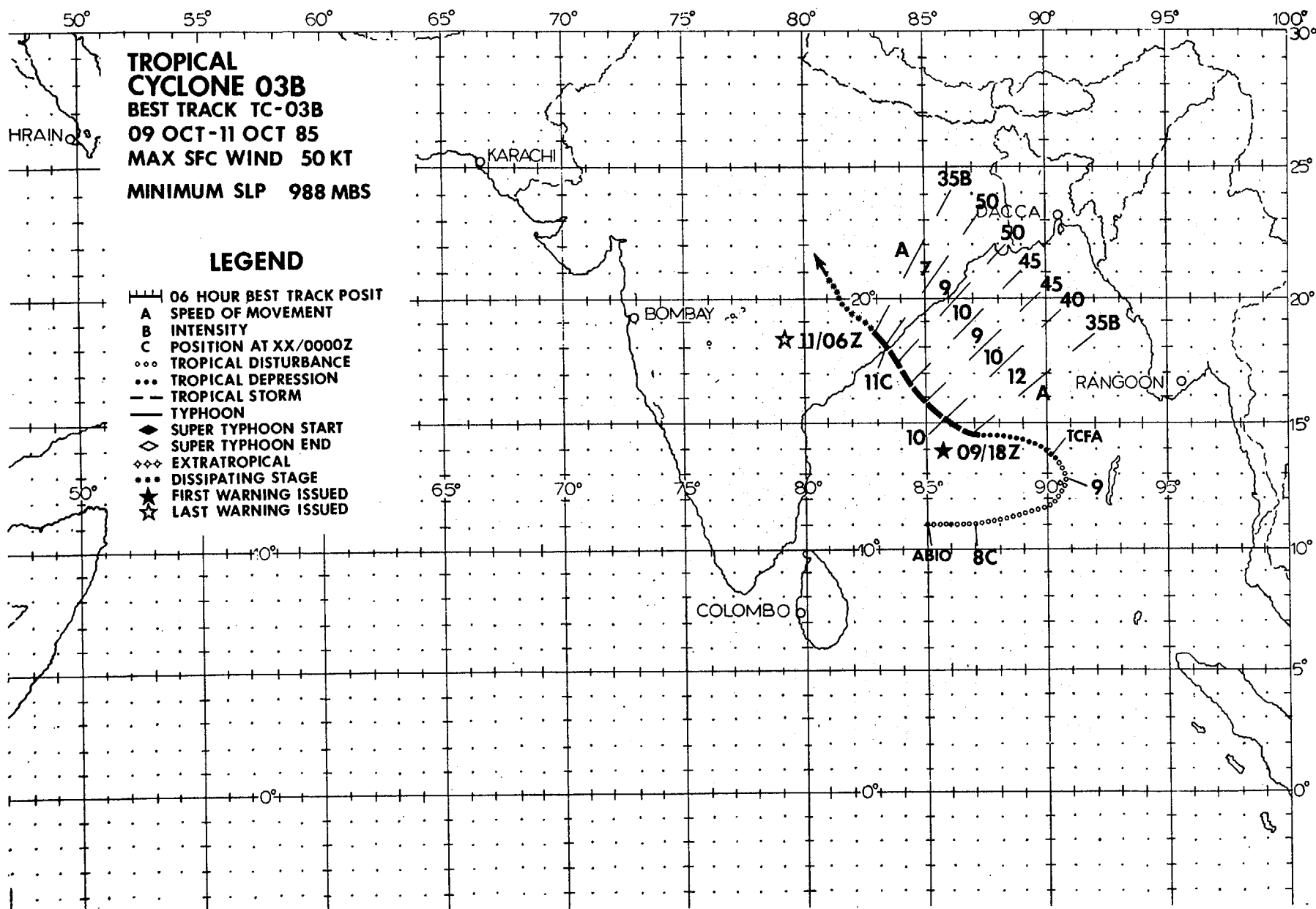


Figure 3-02A-2. Nighttime moonlight image of 02A weakening off the west coast of India. The low-level circulation center is completely exposed (301753Z May DMSP visual imagery).



TROPICAL CYCLONE 03B

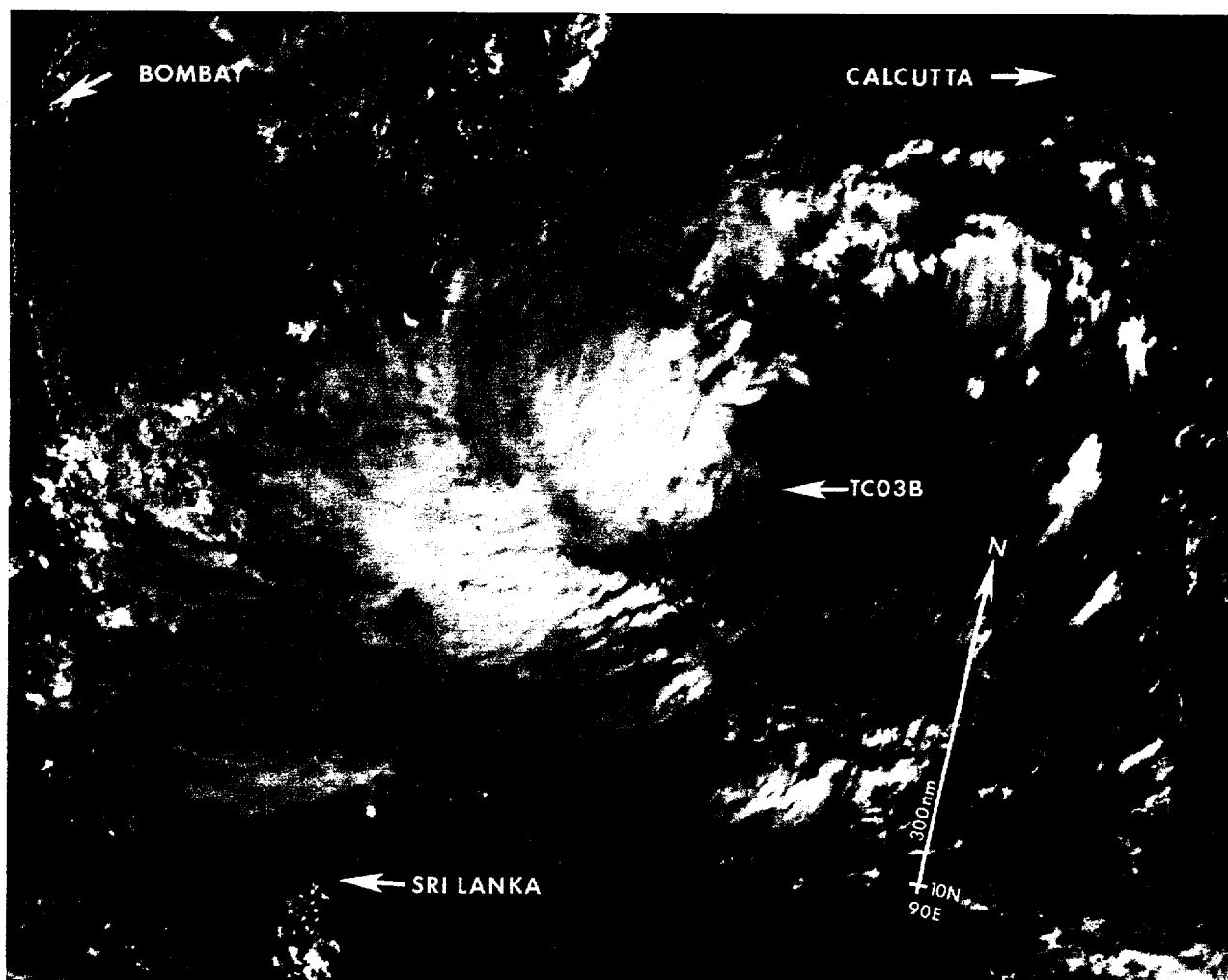
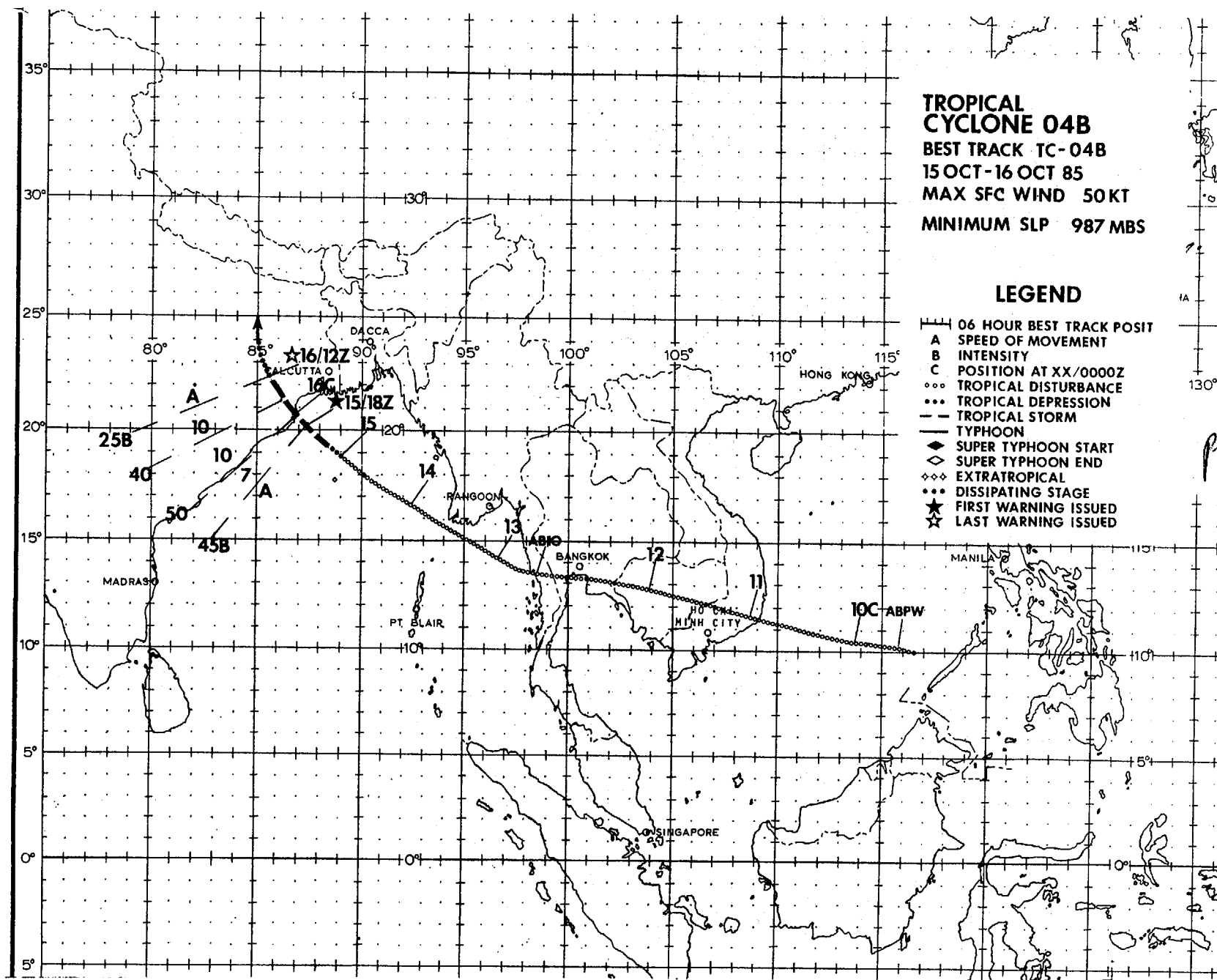


Figure 3-03B-1. Developing in early October, Tropical Cyclone 03B was the first of four tropical cyclones to develop during the Fall transition season. After an initial movement to the east during its formative stage, Tropical Cyclone 03B turned and followed a climatological track to the northwest. The Tropical Cyclone reached a maximum intensity of 50 kt (26 m/s) just prior to making landfall near Visakhapatnam, India (WMO 43149) at 102200Z. There were no reports of damage or injuries from this cyclone. The [above] imagery shows Tropical Cyclone 03B as it consolidated in the Bay of Bengal. At this time the intensity was 40 kt (21 m/s) (100409Z October DMSP visual imagery).



# TROPICAL CYCLONE 04B

Despite being in warning status for only 18 hours, Tropical Cyclone 04B had a long life. It was first detected on 9 October, almost a week before the initial warning was issued, as an area of poorly organized convection in the South China Sea. The Tropical Disturbance was developing in the active monsoon trough, midway between Tropical Cyclone 03B in the Bay of Bengal, and a disturbance in the Philippine Sea that would soon develop into Typhoon Cecil.

Satellite fixes of an upper-level circulation center, based on the extrapolation of cirrus and convective curvature, followed the progress of the system as it moved closer to Vietnam. For the next two days, the system continued to move west-northwestward across the Southeast Asian Peninsula. It emerged in the Andaman Sea late on the 12th, still a poorly organized area of convection. The disturbances westward progress was also reflected at the surface, where a 10 to 15 kt (5 to 8 m/s), 1004 mb low pressure center was present.

During the 13th and 14th, the disturbance turned to the northwest, crossed the northern Andaman Sea and entered the Bay of Bengal. Upper-level support remained relatively weak and diffuse. Positioning by satellite imagery, hampered by mid- to high-level cloudiness, was accomplished on these two days mostly by analysis of spiral band curvature and extrapolation of a poorly defined low-level circulation center. With conditions favorable for slow intensification, the minimum sea-level pressure dropped from 1004 mb on the 12th to an estimated 1000 mb late on the 14th. Surface winds showed a corresponding rise, increasing to 25 kt (13 m/s). Early forecasts on the 14th predicted the system would cross the North Orissa-West Bengal Coast late on the 15th.

Early on the 15th, available data showed little change. Synoptic data at 150000Z showed a 30 kt (15 m/s) surface circulation in the north central Bay of Bengal with an upper-level anticyclone located approximately 80 nm (148 km) to the northeast. Since earlier positions had indicated greater separation between the upper- and lower-level systems, this may have signaled the beginning of increased organization. Still, available synoptic data showed no further decrease in pressure nor significant increase in surface winds. On satellite imagery, the system remained broad and diffuse, showing little improvement in organization over the past 24- to 48-hours (Figure 3-31-1). Meanwhile, coastal Bangladesh, with fresh memories of Tropical Cyclone 01B, which killed

over 6,000 people in May, braced for the current cyclone still expected to hit the coast late on the 15th. Port cities like Chittagong (WMO 41978), Khulna (WMO 41930) and others were advised to raise cautionary signals and fishing boats were advised to stay near the coast.

As 151200Z data became available, it was obvious that the system had, indeed, developed over the past 6- to 12-hours. Synoptic data from ships located a rapidly developing cyclone about 180 nm (333 km) south of Calcutta (WMO 42809). Minimum sea-level pressure was estimated to be near 990 mb and winds had increased to 45 kt (23 m/s). At 151555Z, an abbreviated Tropical Cyclone Warning Bulletin was issued by JTWC to reflect the latest data which indicated a cyclone had formed. By then, more port cities had hoisted warning signals, low-lying areas were preparing for a possible storm surge of 4 to 7 ft (1 to 2 m) above sea-level, and more fishing boats and trawlers had sought shelter.

At 151800Z, JTWC issued the first complete warning on Tropical Cyclone 04B. Subsequent ship reports had indicated a continued fall in the mean sea-level pressure and confirmed surface winds of 45 kt (23 m/s). Satellite imagery at 151649Z showed a dramatic increase in organization and convection over the past 12-hours. The strongest convection was already onshore, but the low-level circulation center remained offshore and was located on the northeast edge of the strong convection.

By 160000Z, Tropical Cyclone 04B had reached maximum intensity as it made landfall on the coast of India approximately 55 nm (102 km) south of Balasore (WMO 42895) and about 140 nm (259 km) southwest of Calcutta. A large area of strong convection remained associated with the system (Figure 3-04B-2). However, shearing conditions had already begun to disrupt vertical organization and, as the system continued to track inland, more and more convection and organization were lost. The final warning was issued at 161200Z.

At least 38 people were killed, with over 200 reported still missing as late as six days after the storm struck the coast. Most of the missing were from the east Indian state of Orissa where a village was completely washed away by flood waters. Heavy rain-induced flooding combined with storm-induced high tides to swamp offshore islands cutting-off access to more than 500 villages.

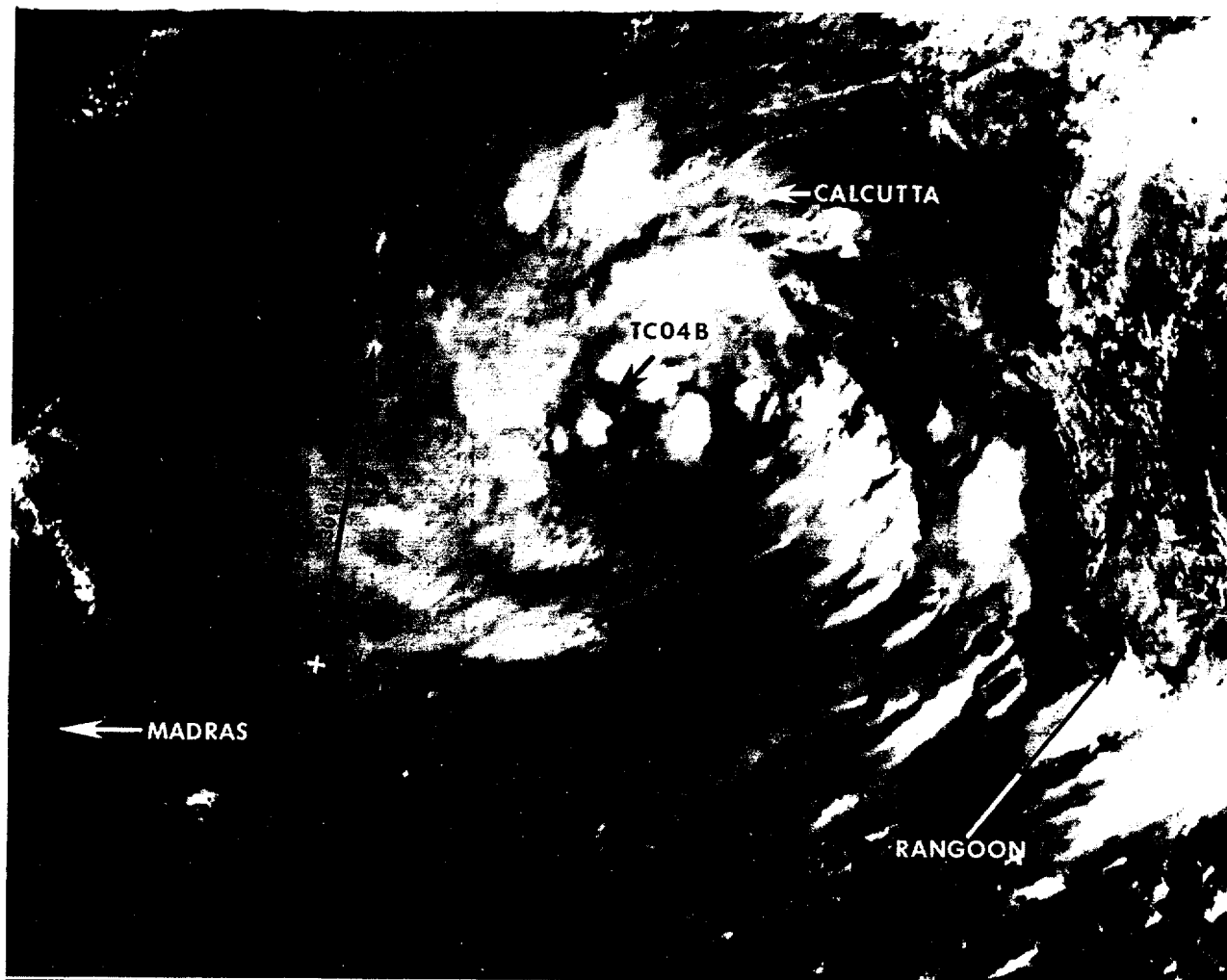


Figure 3-04B-1. The Tropical Disturbance in the Bay of Bengal just prior to undergoing rapid development. The Dvorak intensity estimate is 25 kt (13 m/s) (150408Z October DMSP visual imagery).



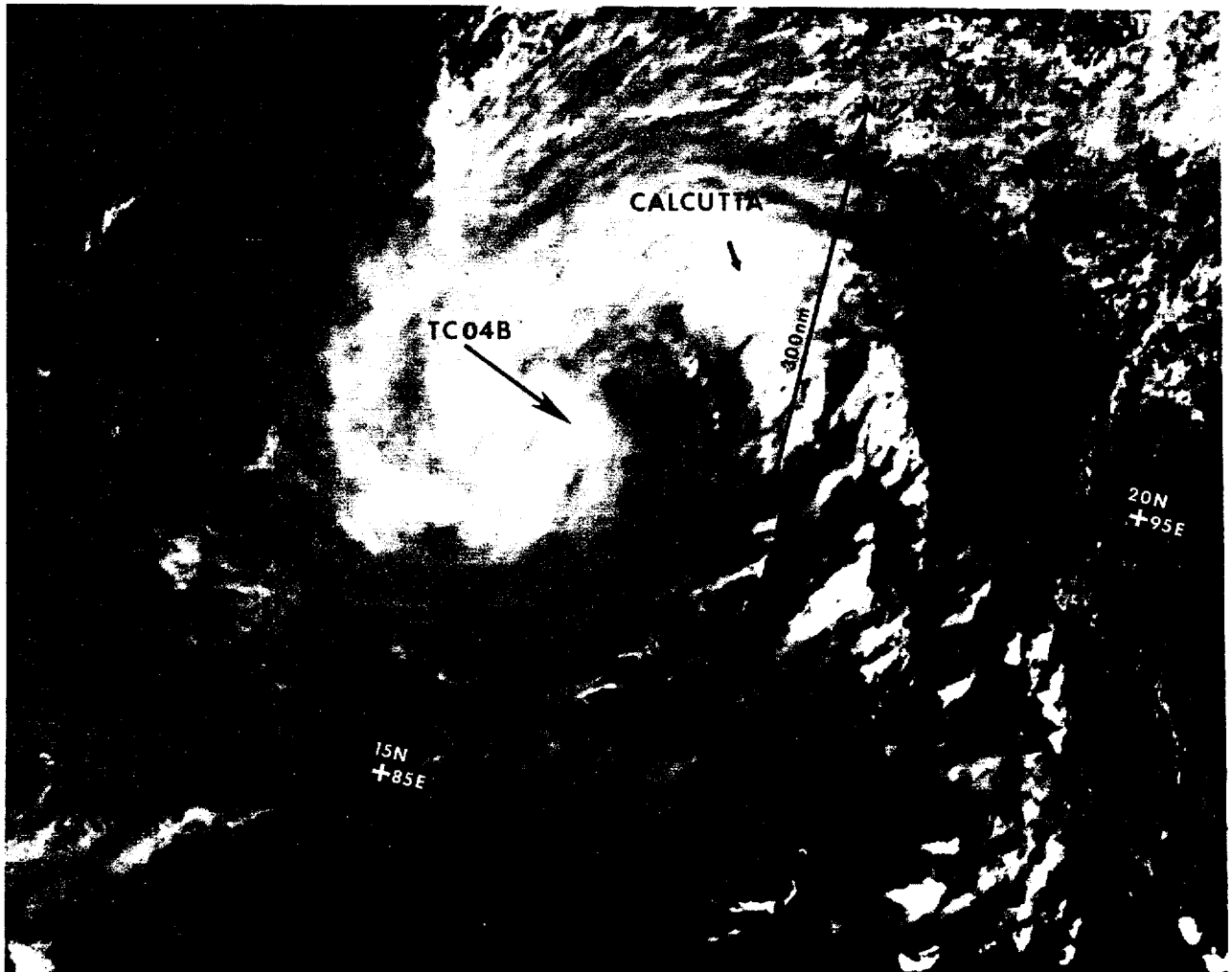


Figure 3-04B-2. Tropical Cyclone 04B just after it made landfall over eastern India. There is a dramatic increase in organization as compared to the imagery in Figure 3-31-1 (160348Z October DMSP visual imagery).

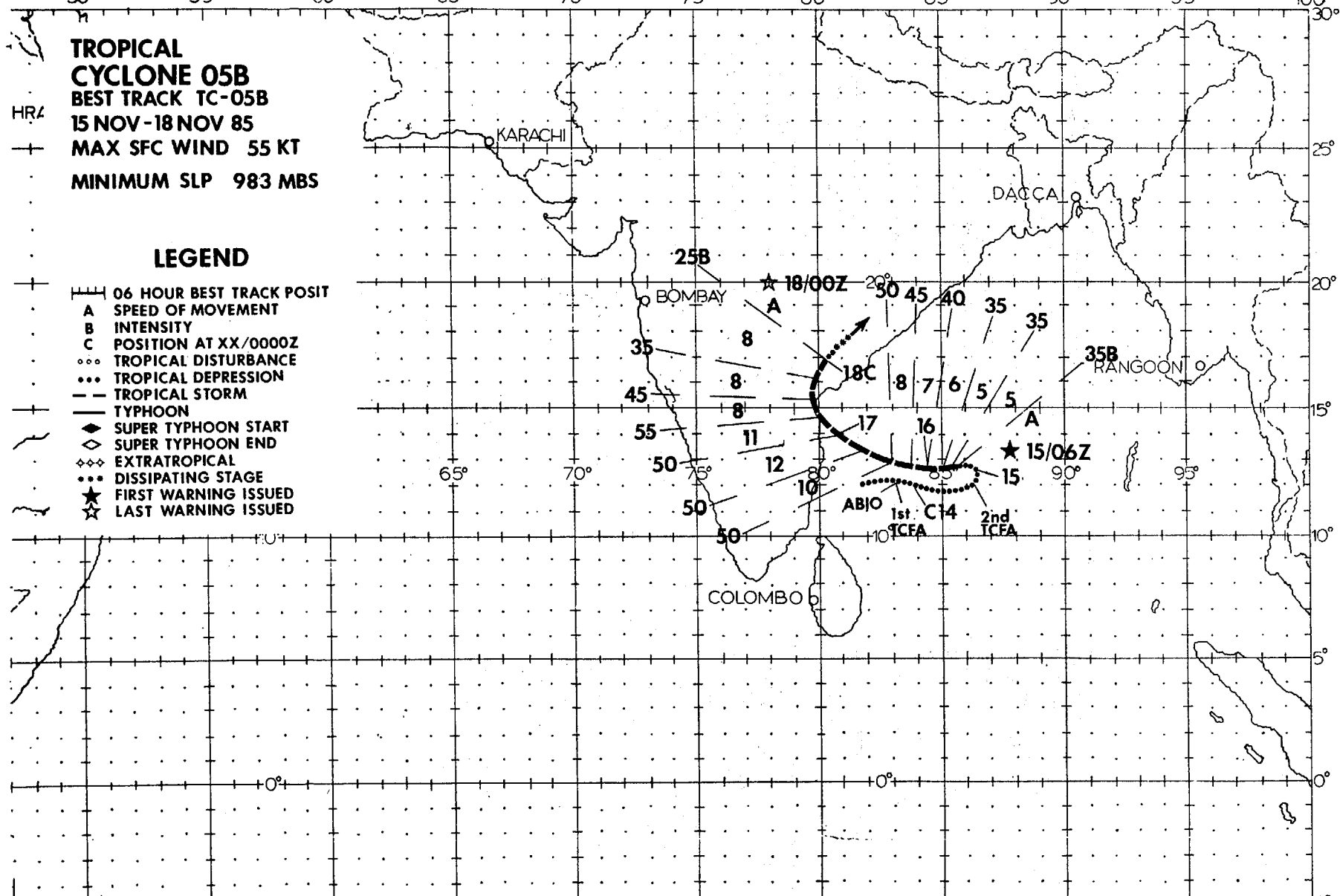
50° 55° 60° 65° 70° 75° 80° 85° 90° 95° 100°

**TROPICAL  
CYCLONE 05B**  
BEST TRACK TC-05B  
15 NOV-18 NOV 85  
MAX SFC WIND 55 KT  
MINIMUM SLP 983 MBS

### LEGEND

- 06 HOUR BEST TRACK POSIT
- A SPEED OF MOVEMENT
- B INTENSITY
- C POSITION AT XX/0000Z
- ... TROPICAL DISTURBANCE
- ... TROPICAL DEPRESSION
- TROPICAL STORM
- TYPHOON
- ◇ SUPER TYPHOON START
- ◇ SUPER TYPHOON END
- ◇◇ EXTRATROPICAL
- ... DISSIPATING STAGE
- ★ FIRST WARNING ISSUED
- ☆ LAST WARNING ISSUED

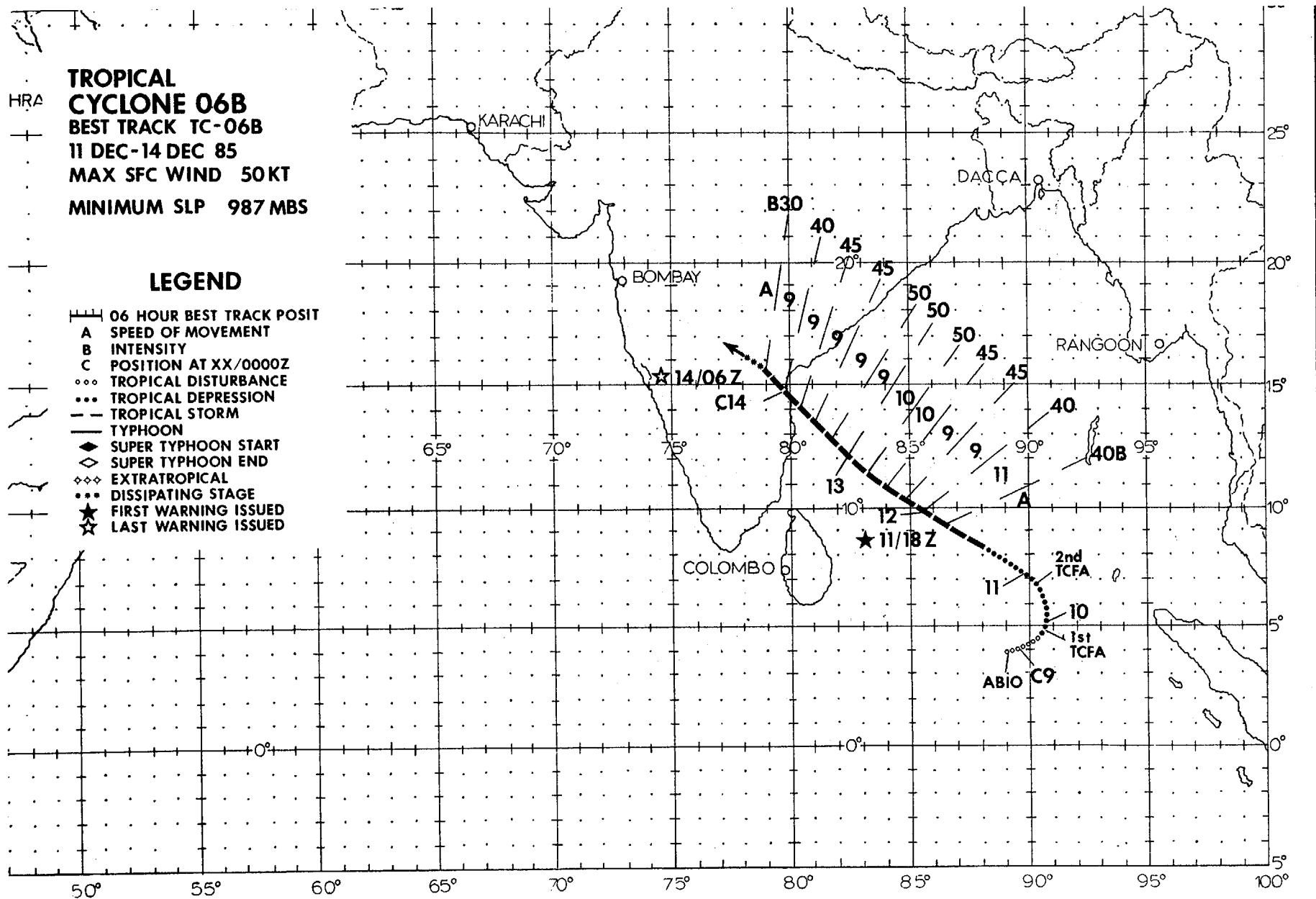
134



#### TROPICAL CYCLONE 05B

Tropical Cyclone 05B formed as a monsoon depression on the southern periphery of the monsoon trough approximately 120 nm (222 km) east-southeast of Madras, India. The system was initially thought to be associated with a disturbance that formed on the east Indian coast near Madras. However, post-analysis of satellite fixes and imagery indicate that the first disturbance formed near the western extent of the monsoon trough on 111200Z, then went ashore on about 120600Z. Therefore, it was determined that the first system was not part of the disturbance that eventually became Tropical Cyclone 05B. At 130600Z, a small area of convection on the southern extent of the monsoon trough developed into a cyclone of about 25 kt (13 m/s). A TCFA was issued at 131800Z as the system remained at 25 kt (13 m/s) and moved east along the southern periphery of the monsoon trough. A second TCFA was issued at 141800Z as the cyclone remained at the same intensity and continued to move east at about 9 kt (5 m/s). Tropical Cyclone 05B finally began to intensify slightly when it reached the eastern extent of the monsoon trough at about 150000Z. Subsequently, the system slowed to about 6 kt (3 m/s), began to move north, and intensified to 35 kts (18 m/s), prompting the issuance of the first warning at 150600Z.

At 151200Z, it was apparent that Tropical Cyclone 05B had begun to move west toward India under the influence of low- to mid-level easterlies to the north of the monsoon trough. At this point, the system continued to intensify slowly and began to accelerate, turning to the west-northwest. Tropical Cyclone 05B reached a maximum intensity of 55 kt (28 m/s) just prior to landfall at 170600Z, 90 nm (167 km) north of Madras. No reports of damage or loss of life due to Tropical Cyclone 05B were received.



TROPICAL CYCLONE 06B

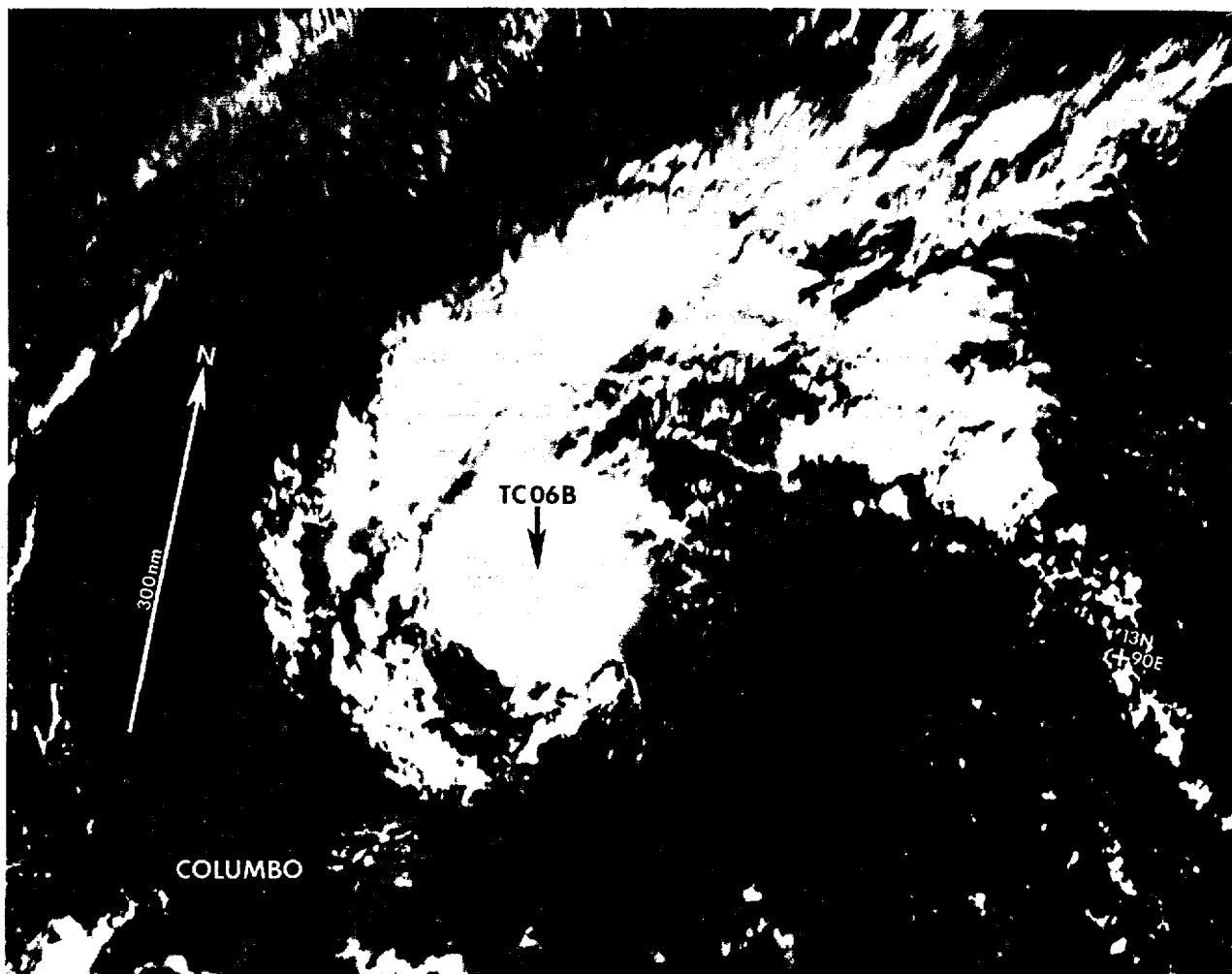


Figure 3-06B-1. Tropical Cyclone 06B formed in the monsoon trough, intensified, and moved northwestward across the Bay of Bengal. In the satellite image, the low-level cumulus lines that are spiralling into the circulation center can be seen along the southern edge of the central dense overcast (130426Z December DMSP visual imagery).